

# Liquid Particle Size Measurement Techniques

**Tishkoff/Ingebo/Kennedy**  
editors

**ASTM STP 848**

# LIQUID PARTICLE SIZE MEASUREMENT TECHNIQUES

A symposium  
sponsored by ASTM  
Committee E-29 on  
Particle Size Measurement  
Kansas City, MO, 23–24 June 1983

ASTM SPECIAL TECHNICAL PUBLICATION 848  
J. M. Tishkoff, Air Force Office of Scientific Research,  
R. D. Ingebo, NASA Lewis Research Center,  
and J. B. Kennedy, United Technologies  
Research Center, editors

ASTM Publication Code Number (PCN)  
04-848000-41



1916 Race Street, Philadelphia, PA 19103

## Library of Congress Cataloging in Publication Data

Liquid particle size measurement techniques.

(ASTM special technical publication; 848)

Includes index.

1. Particle size determination—Congresses. 2. Spraying equipment—Congresses.  
3. Drops—Measurement—Congresses. I. Tishkoff, J.M. (Julian M.) II. Ingebo,  
Robert D. III. Kennedy, J. B. (Jan B.) IV. ASTM Committee E-29 on Particle Size  
Measurement. V. Series.

TA418.8.L57 1984 620'.43 83-73515

ISBN 0-8031-0227-5

Copyright © by AMERICAN SOCIETY FOR TESTING AND MATERIALS 1984  
Library of Congress Catalog Card Number: 83-73515

### NOTE

The Society is not responsible, as a body,  
for the statements and opinions  
advanced in this publication.

Printed in Ann Arbor, MI  
September 1984

## Foreword

The symposium on Liquid Particle Size Measurements was held in Kansas City, MO, 23–24 June 1983. The symposium was sponsored by ASTM Committee E-29 on Particle Size Measurement. Julian M. Tishkoff, Air Force Office of Scientific Research, Robert D. Ingebo, NASA Lewis Research Center, and Jan B. Kennedy, United Technologies Research Center, presided as symposium chairmen and editors of this publication.

## Related ASTM Publications

Stationary Gas Turbine Alternative Fuels, STP 809 (1983), 04-809000-13

Pesticide Formulations and Application Systems: Second Conference, STP 795  
(1983), 04-795000-48

Compilation of ASTM Standard Definitions, Fifth Edition, 1982, 03-001082-42

## A Note of Appreciation to Reviewers

The quality of the papers that appear in this publication reflects not only the obvious efforts of the authors but also the unheralded, though essential, work of the reviewers. On behalf of ASTM we acknowledge with appreciation their dedication to high professional standards and their sacrifice of time and effort.

*ASTM Committee on Publications*

# ASTM Editorial Staff

Janet R. Schroeder  
Kathleen A. Greene  
Rosemary Horstman  
Helen M. Hoersch  
Helen P. Mahy  
Allan S. Kleinberg  
Susan L. Gebremedhin

# Contents

<b>Introduction</b>	1
INTRODUCTORY TOPICS	
<b>Droplet Analysis Techniques: Their Selection and Applications—</b> W. D. BACHALO	5
<b>Investigating the Commercial Instrument Market—</b> H. C. SIMMONS	22
PARTICLE SIZING BY OPTICAL, NONIMAGING TECHNIQUES	
<b>Particle Sizing by Optical, Nonimaging Techniques—</b> E. D. HIRLEMAN	35
<b>Measurement of Drop-Size Distribution by a Light-Scattering Technique—</b> N. K. RIZK AND A. H. LEFEBVRE	61
<b>Extending the Applicability of Diffraction-Based Drop Sizing Instruments—</b> L. G. DODGE AND S. A. CERWIN	72
<b>Liquid Rocket Injector Atomization Research—</b> A. J. FERRENBURG	82
<b>A Review of Ultrahigh Resolution Sizing of Single Droplets by Resonance Light Scattering—</b> T. R. LETTIERI AND W. D. JENKINS	98
PARTICLE SIZING WITH IMAGING TECHNIQUES	
<b>Droplet Characteristics with Conventional and Holographic Imaging Techniques—</b> B. J. THOMPSON	111
<b>An Instrumentation System to Automate the Analysis of Fuel-Spray Images Using Computer Vision—</b> L. M. OBERDIER	123
<b>Sizing Study of Drops Produced by High Diesel Fuel Injection Pressure Sprays—</b> D. M. POPA AND K. S. VARDE	137
NONOPTICAL PARTICLE SIZING	
<b>Hot-Wire Technique for Droplet Measurements—</b> D. S. MAHLER AND D. E. MAGNUS	153
CLOSURE	
<b>Comparative Measurements Using Different Particle Size Instruments—</b> N. CHIGIER	169
SUMMARY	
<b>Summary</b>	189
<b>Index</b>	195

# Introduction

---

Ten years ago the sizing of liquid particles in sprays was confined to a handful of research and development laboratories. Since that time there has been a veritable explosion in the number of measurement methods proposed. Some of these methods have been developed into commercially available instruments which sell at costs of tens of thousands of dollars. Furthermore, drop-size measurement has moved from the realm of research into process and quality control for such diverse application areas as agriculture, spray drying, and gas turbine manufacturing. The associated investment in money, manpower, and facilities has become very extensive and continues to grow.

In a technological sense, ten years represents a very short period of time. The drop sizing practices which have been adopted are relatively untried with respect to requirements such as accuracy and limitations on use. The major theme of this symposium is that the progression from a method to size individual particles based on well understood physical principles to the characterization of a spray is neither straightforward nor simple. Since 1976 ASTM Subcommittee E29.04 has been engaged in formulating definitions and procedures for the characterization of liquid particles, including the sizing of droplets in sprays. We encourage interested individuals and organizations to become involved in our activities. This symposium provides a benchmark for the current capabilities and limitations of techniques for sizing liquid particles. In particular, the five invited survey papers, by Drs. Bachalo, Chigier, Hirtleman and Thompson, and Mr. Simmons, offer unique, comprehensive introductions to the techniques for and applications of liquid particle sizing.

The papers which follow have been divided into five subject areas: introductory topics; particle sizing by optical, nonimaging techniques; particle sizing with imaging techniques; and nonoptical liquid particle sizing and closure. Reader comments on this symposium and topics for future symposia are welcome.

*Julian M. Tishkoff*

Air Force Office of Scientific Research, Bolling  
Air Force Base, Washington, DC 20332;  
symposium cochairman and coeditor.

# **Introductory Topics**

W. D. Bachalo<sup>1</sup>

## Droplet Analysis Techniques: Their Selection and Applications

---

**REFERENCE:** Bachalo, W. D., "Droplet Analysis Techniques: Their Selection and Applications," *Liquid Particle Size Measurement Techniques, ASTM STP 848*, J. M. Tishkoff, R. D. Ingebo, and J. B. Kennedy, Eds., American Society for Testing and Materials, 1984, pp. 5-21.

**ABSTRACT:** Drop size measurement instrumentation is being developed to provide a reliable and accurate means for obtaining drop size data with a minimum expenditure of time. The physical principles involved in the measurement concepts are relatively complicated. Thus, the instrument selection process becomes difficult without at least a general knowledge of the selection criteria, available concepts, and their inevitable limitations. At the same time, there are a broad range of applications with specific measurement goals to be met. The measurement requirements include drop size range, spatial and temporal resolution, and the determination of mass flux. Drop shape can be also an important factor when measuring large droplets that may distort under the prevailing aerodynamic forces. Measurements are further complicated by the need to obtain the results in difficult environments.

In this paper, a general review of drop size measurement applications is given with discussions of the associated conditions affecting the measurements. The descriptions of the measurement conditions and requirements are then related to the corresponding instrument capabilities. An overview of the measurement concepts most commonly used is given and the respective capabilities discussed. Techniques based upon both optical and material probe concepts are considered. The information outlined is intended to provide a guide to the evaluation and inquiries that should be made during the selection of a drop size measurement instrument.

**KEY WORDS:** drop sizing, sprays, particle counters, light scatter detection, drop size instrumentation

The need to form droplets with controlled size distributions, spray patterns, and flow rates, and to correlate this information with the associated phenomena, spans a broad range of applications. These applications include fuel spray combustion, pulverized coal combustion in the form of coal-oil and coal-water slurries, agricultural sprays, meteorology, and a variety of industrial and medical uses. A growing consciousness of our limited energy and water resources has

<sup>1</sup>Senior scientist, Aerometrics, Inc., Mountain View, CA 94022.

raised a spectre of concern in utilizing these resources efficiently with minimum damage to the environment. Such concerns will continue to motivate the research in these and related areas and, consequently, will place increased demands on the diagnostic techniques.

Driven by the need to accurately and rapidly perform spray measurements, instrumentation based on all possible concepts has been developed, and new techniques are continuing to evolve for this purpose. These methods incorporate a variety of physical principles. Techniques include methods for the measurement of actual droplets or of substitute liquids, indirect physical determination, photographic methods, and optical methods. As may be expected, the systems based on the assortment of concepts also have a broad range of performance characteristics. Unfortunately, evaluation criteria and standards for assessing the accuracy of the measurements have not been established. However, efforts are being made (for example, by the E29.04 Committee of the ASTM) to set up such standards of evaluation.

At the present time, a potential user in search of a system to fulfill his measurement goals may experience some considerable frustration while shopping for the ideal spray diagnostics instrument. The importance of making the best choice is heightened by the presently tight research budgets and high costs. Because of the multitude of physical principles used, the instrument designs, and the availability of microcomputers for data acquisition and reduction, it is virtually impossible for a potential user to thoroughly comprehend and evaluate all of the available measurement techniques.

In this presentation, an effort will be made to assist the potential user of a droplet analyzer in choosing the right system for a specific application. To do this, a brief description of some areas of application along with the measurement constraints and required results will be given. Although all of the applications cannot be reviewed, these discussions should apprise the user of pitfalls and considerations that need to be made. The desired characteristics of a droplet sizing device will be discussed to provide a guide in the selection inquiries. Finally, a review of some of the concepts commonly used and their positive and negative characteristics is given.

## **Areas of Application**

### *Agricultural Sprays*

The use of sprays in agriculture can be separated into categories involving irrigation and the application of pesticides. Each application requires a specific droplet mean diameter and size standard deviation measurement capability. For irrigation alone, a broad range of nozzle types from moderately small area coverage sprinklers generating small droplets to large rain guns covering distances of over 60.8 m are used. Such nozzles generate droplets up to the order of a millimetre in diameter at very high flow rates. In all cases, the goal is to apply

the water uniformly and efficiently. If a large number of small droplets is produced significant water loss due to drift and evaporation can occur. More recently, efforts have been devoted to designing nozzles that maintain the spray size distributions while operating at lower line pressures. The reduced pressures require less energy to pump the water. Where millions of acres fall under irrigation, this savings can be substantial.

Herbicides are typically applied using deflector or conical spray nozzles situated in a spray bar that is towed at levels just above the crop or flown on small aircraft. Droplet drift can be very critical, since spraying to kill broad-leaved weeds in a crop from the grass family can destroy the neighboring broad-leaved crops. Undoubtedly, range conflicts have occurred because of such indiscretions. If the droplets are too large, an excessive volume of herbicide will be required and adequate surface coverage may not be attained.

The application of insecticides is even of greater concern [1]. One need only to recall the public uproar generated by the spraying of Malathion in efforts to eradicate the Medfly to realize this. Insecticides function on several principles in order to deal the fatal blow. Some sprays require the droplets to impact the insect and attach to the setae or setal hair which are the nerve endings of the insect. Other sprays operate on the bait and kill principle in which the poisonous chemical is mixed with a liquid bait. This mixture is applied with airborne sprayers generating relatively large droplets that fall upon surfaces and attract the subjects to the bait.

Spraying with both fixed wing and rotor aircraft can create problems in attaining uniform coverage. [2]. The down draft and vertical motions induced cause the spray to collect and roll up in the wake vortices. Size segregation and evaporation frustrate the efforts to deposit uniform concentrations of the spray. In some cases the horizontal vortices produced by fixed wing aircraft actually aid the deposit of the pesticide beneath the leaves where some pests dwell. Research is being conducted in this area utilizing research aircraft with on-board spray diagnostics equipment to improve the application of airborne sprays.

In the foregoing applications, some general instrument requirements can be identified. It is apparent that the instrument would have to cover a broad size range; probably a range from a few micrometers to millimeters in diameter. The instrument could operate in selectable size range increments, but the range selection may have to be set automatically. Selectable range settings may be preferable since, as we will learn later, it is virtually impossible to produce measurements with acceptable sensitivity over a size range much greater than a decade. The size measured should include the Sauter mean diameter (SMD) and the distribution measured directly. Whether the size is obtained optically, through aerodynamic selection, or photographically is not particularly relevant but should be relatable to data obtained by other means. Because the spatial uniformity of the spray deposition is required, the instrument should have adequate spatial resolution. But in most agricultural applications this is not a difficult requirement to meet since the spatial scales are often as large as several meters.

Frequently, the mass flow rate obtained by measuring the numbers of droplets of various sizes that have passed a known cross section in a given amount of time is required. This requires a means of measuring the individual droplet velocities as well as their size. However, one should not overlook the possibility of using the simpler method such as collecting the droplets while using the instrument to determine their size. The additional velocity measurement capability would be of value to determine the droplet flight velocities to assess their potential for breakup and to determine drift characteristics of the spray.

The measurement of large droplets traveling at high velocities can be an expected requirement. These droplets will be deformed by the aerodynamic forces. Therefore, the instrument should be able to measure the size and shape of the droplet or at least the equivalent spherical diameter.

In terms of the instrument design, the instrument will undoubtedly be required to operate out of doors, in large-scale wind tunnels (greater than 0.5-m test section) and on aircraft. Hence, the instruments must be rugged, waterproof, and reasonably portable. The instrument may be also required to operate in remote areas so reliability will be more important than in the case of laboratory systems.

#### *Spray Combustion and Energy Systems*

Research in fuel spray combustion has been very active over the past years [3] and promises to continue as the cost of energy increases and the emission control requirements become more stringent. The work has covered the entire range of droplet combustion from the burning of individual droplets to the atomization of coal-derived fuels and the measurement of the complex dynamics in highly turbulent spray combustors. Measurement of the droplet size distribution in these environments is important in that the drop size correlates with the formation of  $\text{NO}_x$  and other pollutants. It has also been found that a decisive factor of soot formation is the relative velocity between the larger droplets in the fuel spray and the combustion air. This relative motion also affects the fuel heat release by providing a mechanism for combustion product removal and supply of oxygen to the droplet. The relative velocity between the droplets and the gas phase turbulence is a result of the droplet inertia causing it to lag in the turbulent fluctuations.

Most of the work in the characterization of fuel sprays has been carried out on cold or nonburning sprays and on the burning of individual droplets. These data are useful in correlating the performance of nozzle type and fuel flow parameters with the combustor performance. However, if the scientific understanding of liquid-fuel spray combustion is to emerge, then in situ measurements within the combusting spray must be made. Fuel spray combustion which is an extremely complex process is dependent upon the fuel type, droplet size distribution, ambient gas composition, temperature, and pressure. These parameters affect the heat, mass and momentum transfer, and the chemical reactions. Data on the droplet size at various regions in the spray flame, droplet flight angle, velocity, and the gas phase velocity would be useful.

Droplet size measurements in cold or nonburning sprays present similar requirements as do other spray characterizations. Some additional problems occur when measuring fuels like number 6 fuel oil or SRC-II (solvent refined coal) [4,5]. These heavy fuels cover all surfaces they contact with a film of black. Skin contact with SRC-II is also hazardous because of the irritations it produces and the fact that it is a carcinogen. Thus, the measurement techniques considered should be nonintrusive. That is, laser light scatter or photographic techniques or both will prove to be most satisfactory.

The burning of heavy oils shows some unique characteristics that are not observed when burning gasoline and light diesel oil sprays. For example, the heavy oils do not burn at a rate proportional to the droplet diameter squared. Heavy oil combustion is also characterized by droplet swelling and disruptive boiling. Disruptive boiling occurs when the lower vapor pressure volatiles within the parent droplet flash to a vapor and cause the droplet to literally explode forming much smaller droplets.

Thus, the technique applied to the study of these phenomena must be able to make in situ measurements with a large size range capability and high speed. Holographic and shadowgraph recordings using a ruby laser light source have been used to effectively quantify these phenomena.

The need to nebulize alternate liquid fuels has introduced new parameters for the nozzle manufacturers to contend with. For example, SRC-II has a very high viscosity at room temperature; so, it must be heated before nebulizing. Fortunately, because of the disruptive boiling that occurs, it may not be necessary to form small droplets with the injector. Spraying coal-oil and coal-water slurries, which consist of mixtures of as much as 75% finely-ground coal and have the consistency of paint, present their own problems of injection. These slurries have reduced surface tension and unusual viscosity characteristics. The usual spray formation processes may be altered. Thus, careful characterization of these injectors operating on the specific liquids is desired.

Methods used in measuring the sprays formed with alternate fuels and slurries will obviously have to be independent of the liquid or slurry composition. Material probes or optical methods that are not isolated from the fuels cannot be expected to operate satisfactorily. Traditionally, droplet size and velocities have been measured using impaction onto magnesium oxide-coated slides or high-speed photography [6]. These techniques were useful in single-drop or very diffuse spray investigations but are of limited utility in investigations involving dense sprays. Laser light scattering techniques including small angle diffraction and the interferometry are diagnostic techniques that have promise in producing the measurements needed to advance the understanding and verify the theoretical predictions of the combustion of these fuels.

In general, for combustion spray measurements, an instrument should produce the droplet size distribution and mean diameters including the  $D_{32}$  and also information on the droplet ballistics. The size measurements should be obtainable with relatively good spatial resolution, since the complex aerodynamics involved

will produce localized zones where droplet collisions and segregation by weight occur. Also, regions of high droplet evaporation and burnout will need to be identified. Because of the need to measure the burning sprays, the instrument should be nonintrusive and have a sufficient range such that the optics may be located outside of the facility.

When using optical methods, either light scatter detection or imaging, the instrument accuracy will be affected by the density gradients produced by the turbulent hot gases in the flame. Some methods are more seriously affected by turbulence in the optical paths than others. It is rather difficult to quantify the errors caused by the beam wander and phase front degradation that will result. Although theoretical analyses have been carried out, careful experimentation is needed on controlled environments before attempting measurements in combustors. Contamination of the optical access ports can be also expected so the instrument concept used should be relatively independent of light beam attenuation.

The need to measure the droplet and gas phase velocities in the combustor can be realized with a conventional laser Doppler velocimeter (LDV) with some modification. A means is required to discriminate signals from the various droplets or particles that are too large to respond to the turbulent fluctuations. This can be achieved by the measurement of the integrated signal amplitude for gross discrimination or the signal visibility for more refined size measurements. An LDV with such size discrimination can be then used to reliably measure the mean velocity, turbulence intensity, Reynolds shear stress, and turbulent kinetic energy in spray combustors. Velocity measurements utilizing LDVs have been made in swirl stabilized combustors, dump combustors, and in internal combustion engines to name a few examples.

### *Atmospheric Measurements*

Research in the area of fog formation, visibility, aircraft icing, cloud studies, and the formation of rain and snow is of vital interest to commercial, general, and military aviation, and to meteorologists. As in the agricultural applications, these areas of droplet studies are generally involved with measurements in large-scale facilities or in situ in the atmosphere by carrying instruments aloft on balloons and other aircraft. The droplet size range can be expected to vary from a few micrometres to millimetres in diameter. Some specific requirements are the need to make real time and time resolved measurements and the need to discriminate liquid droplets from ice crystals.

In clouds, the size distribution of droplets is not only controlled by the micro-physical process of droplet growth by condensation and coalescence, but also by the cloud dynamics [7]. The cloud dynamics determine the degree of mixing with the environment, the vertical velocity and scale, intensity of the turbulence, and the amount of time that the individual droplets remain in the cloud. Observed cloud droplet spectra indicate that the growth of droplets up to 40  $\mu\text{m}$  in diameter

can be accounted for by condensation on observed nuclei. Once the droplets have reached sizes greater than  $50 \mu\text{m}$  in concentrations of  $10^2$  to  $10^3/\text{cm}$ , further growth proceeds rapidly by coalescence, and showers soon occur.

When the rain falls, droplets with diameters greater than about 2 mm undergo distortion in shape. This distortion continues until the droplet breaks up. Experiments on droplets suspended in vertical airstreams have shown that breakup generally occurs when the droplet diameter exceeds about 6 mm. Thus, droplets greater than 6 mm rarely occur in rain. Droplets larger than 5 mm are extremely sensitive to the degree of small-scale turbulence in the air. Breakup will also follow the collision of two droplets. The size and number of the fragments formed depends upon the size, shape, and the phase of oscillation of the parent droplet at the moment of breakup.

The measurement of these phenomena, needed to verify the theories, places some specific requirements on the instrumentation. Observation of the droplets at the point of nucleation to when they fall as rain requires a size range of approximately  $20 \mu\text{m}$  to 6 mm in diameter. Because of the distortion in shape, the instrument should be able to measure the equivalent spherical diameter or preferably, the droplet size and shape at high speeds. Since the release of showers can also occur by the growth of ice particles, the measurement of particle shape takes on added importance.

Considerable research has been devoted to the subject of aircraft icing involving the identification of atmospheric conditions conducive to ice formation and the correlation of these variables with expected icing severity and the types of ice formations produced [8]. The three parameters generally associated with aircraft icing are liquid water content (LWC), temperature, and the droplet size distribution. Different combinations of these parameters affect the type of ice formation on the aircraft component. The amount of water impinging onto the aircraft surfaces is affected by the droplet diameter and the shape and size of the component. Smaller droplets will tend to follow the airflow streamlines, whereas the larger droplets having greater inertia will cross streamlines and impact on the component surfaces.

Icing research involves not only the measurement of naturally occurring cloud droplets but also using the simulations. The simulations involve both wind tunnels and artificial icing clouds produced by spray tankers. Proper simulation requires the formation of droplet size distributions and number densities (or LWC) that are similar to those occurring in natural clouds.

Thus, it is important that instrumentation required for these applications be capable of measuring the droplet size distribution and liquid water content. The droplets are expected to have a mean volume diameter ( $D_{v,5}$ ) in the range of 10 to  $30 \mu\text{m}$ . In this size range, the droplets can be expected to be spherical. To measure the LWC, the measurement cross section of the device must be known, and a means to determine the average velocity must be available. If droplet impact studies are to be performed to correlate droplet size with probability of

impact on the airfoil, then a system which is able to measure the droplet size and velocity simultaneously would be very useful.

### *Industrial Applications*

Industrial applications of sprays obviously span a great number of specific processes that cannot be covered here. Some of the applications that are of interest will be briefly discussed to complete this section.

One application that is of importance because of the potential environmental disaster that could occur with the extensive use of coal is the development of scrubbers. Wet scrubbers are used in the control of particulate and dry scrubbers in the control of sulfur dioxide ( $\text{SO}_2$ ).

When a gas stream approaches a spherical droplet the fluid streamlines curve around the droplet. Particles in the gas stream have a much greater inertia than the gas molecules and, hence, approach the droplet surface. Particles impinging on the surface of the droplet attach and are removed with the liquid. The collection of particulate by the droplets is dependent upon three factors: the velocity distribution of the gas flowing around the droplets; the particle trajectory (which is dependent upon factors such as the aerodynamic forces on the particle, the particle mass, the droplet diameter, and the gas velocity with respect to the droplet); and the adhesion of particles to the droplet once it has impacted upon the droplet surface.

An effective instrument would be one that measures the diameters and velocities of individual droplets in relatively high number density environments. Simultaneous measurements of the particle velocities would even be more useful. The combined droplet sizing and LDV techniques have the foregoing capabilities.

In the case of dry scrubbers, the requirement is that as large a surface area of the sorbent chemical as possible should come in contact with the flue gas containing  $\text{SO}_2$ . The injectors used must handle high flow rates, yet atomize the liquid to mean diameters of the order of  $100\ \mu\text{m}$  or less. Turbulent mixing and recirculation can be used to effectively increase the period of contact between the dirty gas and the droplets. Because relative velocities of the droplets and the gas phase are required, the process and measurement requirements are similar to wet scrubbers.

### **A Review of Spray Diagnostic Techniques**

This section was originally planned to include the description of an ideal sizing instrument. Unfortunately, having a knowledge of the physics involved in the available techniques and having reviewed the diversity of applications led to what we should have suspected. Only a ludicrous combination of techniques would satisfy all the requirements outlined. Such a monstrosity would fail on the requirements of reliability and ease of operation. Instead, this section shall outline general characteristics of the instrument that need to be considered. These characteristics will include what the instrument must measure, what it should be able

to measure, and what features are desirable, but are not necessary to the acquisition of the results. A summary of instrument categories and concepts will follow along with a brief description of the physics involved.

### General Requirements

The requirements stated here cover the physical concepts used and how they are utilized but do not treat the specific engineering of the instrument. For example, two manufacturers may use a similar concept but one instrument may be more rugged, reliable, and portable than the other. Such selections must be made by the potential user.

#### *"Must Have" Category*

*Size Measurement Range* — The instrument concept selected must be capable of measuring the anticipated droplet size range involved. Generally, light scattering techniques will cover a range from submicron to hundreds of microns. Imaging techniques will be suitable for particles in the range of 5  $\mu\text{m}$  and larger. Probe methods such as the hot-wire technique claim a size range of 1 to 600  $\mu\text{m}$ .

*Droplet Shape* — Depending upon the size of the droplets to be measured and the aerodynamics involved, the droplets may be distorted. Some methods, although not specifically stated, may produce measurements that are relatively unaffected by the droplet shape, whereas others will produce significant measurement errors if the droplets are not spherical. In some cases, information on the droplet shape and size may be required which would suggest the use of an imaging or shadow detection technique.

*Size Resolution and Accuracy* — The system should have adequate precision or size resolution to characterize the spray and draw the desired conclusions from the results. Generally, a size resolution that is uniform over the measurement range is preferred. Manufacturers often quote accuracy as well as size resolution. However, because there is, as yet, no accepted measurement standard or method for assessing the measurement accuracy, these claims are without basis. If a monodisperse stream or particle field was used, then the accuracy only pertains to monodisperse particle measurements in a particular environment. Information on instrument validation measurements should be always requested and examined carefully.

*Compatibility with the Test Environment* — The concept must be capable of operating in the particular test environment. Some constraints will be obvious but others may result in marginal performance. For example, certain optical techniques are very sensitive to window contamination whereas others are not. Most techniques have a limitation on the physical size of the test chambers in which they can operate reliably. Imaging techniques requiring that the optics be introduced into the spray will be precluded from use in combustions or heavily contaminating sprays.

*Size Type Measured* — The available measurement techniques utilize different qualities of the droplet to determine its size. That is, light scattering interferometry measurements are based on the relative index of refraction of the droplet and its radius of curvature. Small angle forward scatter detection devices base the measurement on the projected cross section of the droplet. These measurements are often referred to as the optical diameters. Measurements obtained by such methods as cascade impactors produce the aerodynamic diameter. The hot-wire method obtains a droplet size which is dependent upon its capacity to cool the hot wire. Only under ideal conditions and with the relevant parameters known will all of these diameters agree.

*Spatial and Temporal Resolution* — A prior decision must be made as to whether the size distribution in a small region of space is required or whether a spatial average taken over a large region of the spray is sufficient. In the case of rainfall measurements this is, in fact, desirable.

Some instruments are able to produce size distributions averaged over almost any length of time. Other methods such as photographic and holographic techniques obtain an image in essentially an instant. Presumably, a time average could be obtained from a collection of images taken at fixed time intervals, but this would be tedious.

*Number Density Capabilities* — The high droplet number densities (particles/cm<sup>3</sup>) involved has frustrated many attempts at measuring sprays with most optical single particle counter techniques. Light extinction by the large numbers of droplets in the optical paths also reduces the signal-to-noise ratio of most optical instruments. When using absolute light scatter detection methods large errors can be produced because of the indeterminate light intensity incident on the droplets.

On the other hand, in environments wherein the droplet number densities are low, the small angle forward scatter detection methods have low signal-to-noise ratios, because these methods obtain measurements based upon light scattered by the collection of droplets located in a collimated laser beam. Too few droplets in the beam will not scatter enough light nor smooth the diffraction patterns at the detector. Imaging techniques would require the acquisition of a large number of recordings to obtain a sufficient number of droplets for a representative statistical distribution.

*Liquid Water Content (LWC)* — Some concepts used are incapable of measuring the LWC or number density of the spray. If these data are required, information should be obtained from the manufacturer as to how the LWC is determined and what verifications, if any, have been carried out.

#### *Desirable Characteristics Category*

*Nondisturbing* — Although the ideal situation is to have a nonintrusive device, the size of the environment and the need for greater accuracy may require introduction of the measurement head into the spray. Caution is required when

using intrusive devices to measure droplets in a moving airstream, since the smaller droplets will follow streamlines whereas the larger ones will migrate across the streamlines. This can cause a size bias in the measurements. Intrusive instruments also can become fouled while in the spray environment which can cause significant measurement errors.

*Data Management* — The system should have automated data acquisition and processing to accumulate results in a matter of seconds. When the number density is required, the system must be fast enough to record every droplet passing the measurement volume. Since the droplet arrivals will be random, the individual droplet recording time must be much less than the average droplet arrival time (typically on the order of 100  $\mu$ s).

A real time display of the size distribution is useful but not necessary. However, the data management system should be able to rapidly reproduce the distribution in histogram form and the various mean diameters and standard deviation.

The system should provide for adequate data storage and a hard copy printout of the tabular results.

*Size Range* — The instrument should have a size range capability of at least a factor of 10 but a factor of about 30 is desirable. Some techniques have continuously selectable or adjacent size ranges that can cover the complete droplet size distributions. Because of nonlinear instrument response curves, some instruments have a greatly reduced size sensitivity or ambiguities at the small size end of their response curves. A size range that is too large may have required a compromise in resolution.

*Velocity Measurement* — In a significant number of applications, either the average velocity or the size and velocity of individual droplets is required. If only the average droplet velocity is sufficient, several devices are available that can provide that information. The light scattering techniques that may be combined with LDV can produce the droplet velocity and the size velocity correlations. Other methods coupling the LDV technique with absolute light scattering methods have been used, but, as aforementioned, these systems are limited to relatively low droplet number densities.

## Categories of Techniques

The measurement concepts most commonly used shall be briefly reviewed in this section along with the measurement capabilities.

### *Light Scatter Detection*

When particles greater in diameter than the wavelength of light pass through a light beam, they scatter light in proportion to their diameter squared. The intensity and angular distribution of the scattered light can be described accurately using the Mie theory. This theory describes the light scattered by homogeneous spheres of arbitrary size passing through a light beam located in a

homogeneous medium. For droplets much larger than the wavelength of light, the simplified theories of Fraunhofer diffraction, reflection, and refraction may be used. These theories have been shown to be in good agreement with the results of the Mie theory under the appropriate conditions and are much easier to use.

The intensity of light scattered by a droplet and the angular distribution in the near forward direction can be related to the droplet diameter. Instrument concepts have been developed to measure droplet sizes based on the measurement of either the scattered light intensity or the angular distribution. These concepts fall into two general types: the single particle counters and the multiple particle detection systems.

As their name implies, the single particle counters measure individual particles or droplets that pass through a focused laser beam or incandescent source. Because the single particle counters must "see" only one droplet at a time, the size of the measurement volume sets the limitation on the particle number densities in which they will operate accurately. The measurement volume is controlled by the diameter of the focused beam, the receiver  $f$ /number and its angle to the transmitted beam, and the aperture on the photodetector.

The single particle counter methods, although limited to moderate number density environments, make measurements with high spatial resolution and produce the size distribution directly by accumulating a large number of individual droplet measurements and sorting them into size classes. By counting all of the particles passing the measurement cross section, single particle counters also have the potential of measuring the number density.

The light scattering interferometry technique [9] is a unique single particle counter since it can operate in high number density environments. This is made possible by using large off-axis light scatter detection angles which are very effective in reducing the size of the measurement volume.

Multiple particle detection systems base the measurements on the average light scatter distribution produced by a large number of droplets passing a collimated laser beam [10,11]. The Fourier transform of the forward scatter distribution is obtained and analyzed to produce the SMD. Recently, systems based on this concept have incorporated analyses to perform a deconvolution on the measured intensity to extract the size distribution without relying on a specific distribution function [12].

Instruments based on this concept have the advantage of being able to operate in very high droplet number density environments. However, they have low spatial resolution and cannot measure the droplet flux or number density directly. The low spatial resolution is due to the fact that particles along the entire beam path are detected.

In general, the light scatter detection methods are able to make in situ non-intrusive measurements with relatively little effort or time. These concepts are usually accompanied by high speed signal processors and data management systems that use microprocessors to provide fully automated data handling. The

size range capability of systems based on light scatter detection covers droplets from submicron to several millimetres in diameter. The light scatter detection methods, unlike imaging techniques, can resolve particles that are on the order of the wavelength of light ( $\sim 0.5 \mu\text{m}$ ) or smaller at distances of up to a meter or greater.

### *Imaging Techniques*

The old adage “seeing is believing” has always been a significant factor in the ready acceptance of imaging techniques, especially by those unfamiliar with the physics. However, these methods can produce erroneous results if they are used in marginal applications, where, for example, the droplet number densities are very high or the optics are not of the highest quality. Also, the data reduction or particle counting can be biased by inexperienced or impatient workers when handling the data manually and by image analyzer systems that cannot properly discriminate out-of-focus images.

Perhaps, the most limiting characteristic of the conventional imaging systems is that the resolution is inversely proportional to the distance from the droplet. That is, the usual Rayleigh criterion for the minimum distance between points on an object that can be resolved with a diffraction limited (highest resolution possible) lens is given by

$$d = \frac{1.22f\lambda}{D} \quad (1)$$

where

- $d$  = dimension of the object,
- $f$  and  $D$  = focal length and diameter of the imaging lens, and
- $\lambda$  = wavelength of light.

High quality lenses required to approach the diffraction limited criteria at small  $f$ -numbers ( $f/\text{no.} = f/D$ ) are very difficult to fabricate except for moderate ( $\leq 50$  mm) focal lengths. When receiving the image through windows or through turbulence with density gradients, the image will be significantly degraded from the diffraction limited case. This will be also true when imaging through a dense spray.

Despite the above difficulties, droplet images have been obtained using still photographs, video recordings, and photodiode arrays. The extraction of the data from the recordings by manual counting can be extremely time consuming. Fortunately, automated image analyzers have been developed for this purpose. Recently developed systems utilize standard television equipment with the image sizing performed by a fast microprocessor interfaced directly to the camera. These systems can produce real time data on the droplet size and shape without need of peripheral storage. Algorithms which reject out-of-focus droplets by

evaluating the threshold and density gradient at the edge of the image have been incorporated in these systems.

With the use of specialized illumination optics, a train of double pulses has been used to obtain the droplet velocity and flight angle.

The obvious advantage of imaging or shadowing systems is that the projected shape of the droplets is available. Also, with real time imaging, such dynamic events as droplet breakup and spray formation can be recorded and studied in detail. Other events such as droplet collisions and coalescence may be also detectable with imaging systems.

Because of the relatively short working distances of the conventional imaging systems, there will be instances wherein the optical head may have to be submerged in the spray. The size of the hardware introduced should raise concern about the possibility of aerodynamic deflection of the smaller droplets. Problems may also occur as a result of contamination of the optics with fog and droplets. Attempts have been made to shield the optical components or automatically wash them but without much reliability.

The use of holography relieves some of the constraints of conventional imaging techniques [13]. Holography is interesting in that the information obtained from the light scattered by the particles is recorded and used to reconstruct the images. Thus, holography can be used to record images with good resolution at much greater distances than with conventional photography. Since the droplet distribution in a volume of the spray can be reconstructed, a single hologram contains several orders of magnitude more information than a photograph. High resolution can be achieved by premagnifying a region of the spray before recording it holographically. A penalty is paid in that the size of the image field is reduced.

Holography has been used to characterize sprays, but, unfortunately, the image analysis systems have not been developed to the point where large numbers of spray distributions can be obtained with sufficient confidence. The very short exposures ( $\sim 20$  ns) available with ruby and ND:YAG lasers make this technique most effective in observing the mechanisms of atomization and transient phenomena such as disruptive boiling. The measurement size range for this technique is about  $5 \mu\text{m}$  and greater.

A significant source of error in imaging systems is in the determination of the size of the detectable or viewing volume to be assigned given droplet sizes. Droplets are classified on the basis of the number per unit volume in each size class. Larger droplets will be detectable and appear to be in focus over a larger volume than the smaller ones, so the number of droplets counted must be normalized to a unit area if an accurate distribution is to be obtained. Thus, a careful determination of the viewing volume should be carried out by placing test spheres in the field of view and adjusting their positions to map the limits of detectability. Although this procedure can be carried out with good accuracy, the calibration can change due to reduced signal-to-noise rates in the presence of a spray and drift in the electronics because of sensitivity to the environment.

### *Material Probes and Sampling*

Several simple but expedient methods have been used to characterize sprays. For example, the so-called patternator probes have been used to measure the spatial distribution of the mass flow rate from nozzles. The patternator consists of an array of sampling tubes arranged in an arc along the radius of the spray. The liquid collected by each tube is measured to establish the nozzle spray angle and flow characteristics.

The hot-wire probe [14] method has been also developed to obtain the size and concentration of liquid droplets present in a gas stream. This device, based on the heat transfer to the droplet, measures the cooling caused by a droplet attaching to the hot wire. Without a droplet present, the resistance of the wire is high and essentially uniform along its length. When a droplet attaches to the wire, local cooling by the droplet reduces the resistance in proportion to the droplet size. This reduction in resistance appears as a voltage drop across the wire supports. The constant current electrical energy supplied to the wire subsequently evaporates the fluid, leaving the device ready for further measurements.

Although this is an intrusive technique, its actual operation appears to be relatively simple. The wire which is platinum, 5  $\mu\text{m}$  in diameter and 1 mm long, should not cause a sensible disturbance to the flow. Measurement of the gas phase velocity is also available, since the device is identical to the hot-wire anemometer. The technique is apparently not applicable to the measurement of droplet materials that can leave a residue on the wire, since this will affect the calibration. There is also some question about the effect of liquid collected on the needle support leaking onto the wire and of droplets hitting the ends of the wire. The device can only operate at flow velocities of order 10 m/s when measuring large droplets because of droplet shattering on the wire.

### **Summary and Conclusions**

It should be apparent that a careful selection of a measurement technique is required for a specific application if satisfactory droplet field characterizations are to be attained. Because there is such a wide range of applications with some very specific constraints and data requirements, no single instrument concept can be expected to cover all possible situations. Thus, the measurement concepts that can be used must first be established by outlining the data requirements for the intended application and then comparing these with the instrument capabilities. The criteria to be considered include:

1. Size range.
2. Droplet shape.
3. Size resolution and accuracy.
4. Test environment limitations.
5. Spatial and temporal resolution.
6. Number densities.

7. Mass flow rate.
8. Nonintrusive or intrusive.
9. Droplet and gas phase velocities.

Although some of the criteria will exclude the use of certain concepts, others may be a matter of choice. The instrument cost was not discussed, but obviously this is a factor in the selection. When weighing the relative costs and the compromises that may be necessary, it is very important to consider not only the purchase price of the instrument but also the time involved in learning how to use it and the relative time needed to obtain and process the data.

When trying to assess the relative accuracies of the instruments, remember that there is no standard established for this purpose. Also, the relative accuracies of the various measurement techniques will also depend upon the test conditions. Insist upon a demonstration of the instrument on a spray or other droplet field that is similar to the one to be measured and preferably one that has been characterized by other means. If the results agree, then some confidence in the method has been earned. When they do not agree, which device was in error cannot be concluded. Also, obtain detailed information on how the instrument capabilities were verified. It is also useful to seek out other customers using the instrument. However, this information is only useful in the evaluation of the general features of the instrument and how it has been engineered. Unfortunately, agreement of results between users of the same type of instrument is sometimes misconstrued as a determination of its measurement accuracy.

The knowledge of the available concepts acquired in this symposium should be of value in not only the selection of a droplet sizing instrument but also in evaluating the published data. As new sophisticated measurement techniques evolve and are applied to complex spray characterizations, a certain amount of erroneous data can be expected.

Finally, it is normal for manufacturers to expound the capabilities and virtues of their instruments and overlook the limitations; caveat emptor.

## References

- [1] Spillman, J. and Sanderson, R., "A Disc-Windmill Atomiser for the Aerial Application of Pesticides," *Proceedings*, 2nd International Conference on Liquid Atomization and Spray Systems, June 1982, Madison, WI, p. 169.
- [2] Yates, W. E., Cowden, R. E., and Akesson, N. B., "Procedure for Determining In Situ Measurements of Particle Size Distribution Produced by Agricultural Aircraft," *Proceedings*, 2nd International Conference on Liquid Atomization and Spray Systems, June 1982, Madison, WI, p. 335.
- [3] Chigier, N. A., "Instrumentation Techniques for Studying Heterogeneous Combustion," Central States Section, The Combustion Institute Technical Meeting, Fluid Mechanics of Combustion Processes, NASA Lewis Research Center, Cleveland, OH, March 1977.
- [4] Black, C. H., Chiu, H. H., Fischer, J., and Clinch, J. M., "Review and Analysis of Spray Combustion as related to Alternate Fuels," Report ANL-79-77, Argonne National Laboratory.
- [5] Oeding, R. G. and Bachalo, W. D., "Synthetic Fuel Atomization Characteristics," *Combustion of Synthetic Fuels*, William Bartok, Ed., Symposium Series 217, American Chemical Society.

- [6] Zinn, S. V., Eklund, T. I., and Neese, W. E., "Photographic Investigation of Modified Fuel Breakup and Ignition," Report No. FAA-RD-76-109, U.S. Department of Transportation.
- [7] Mason, B. J., *The Physics of Clouds*, 2nd edition, Clarendon Press, Oxford, 1971.
- [8] Belte, D., and Ferrell, K. R., "Helicopter Icing Spray System," presented at the 36th Annual Forum, The American Helicopter Society, Wash. DC, 1980.
- [9] Bachalo, W. D., Hess, C. F., and Hartwell, C. A., "An Instrument for Spray Droplet Size and Velocity Measurements," Winter Annual Meeting, Paper No. 79-WA/GT-13, American Society of Mechanical Engineers, 1979.
- [10] Swithenbank, J., Beer, J. M., Taylor, D. S., Abbot, D., and McCreath, G. C., "A Laser Diagnostic Technique for the Measurement of Droplet and Particle Size Distributions, 14th Aerospace Sciences Meeting, Washington, DC, Paper No. 76-69, American Institute of Aeronautics and Astronautics, Jan. 1976. Also published in *Experimental Diagnostics in Gas Phase Combustion Engines, Progress in Aeronautics and Astronautics*, by B. T. Zinn, Ed., Vol. 53, 1977, p. 421.
- [11] Hirtleman, E. D., this publication, pp. 35-60.
- [12] Weiner, B. B., "Particle and Droplet Sizing Using Laser Diffraction," Particle Sizing, Wiley, NY, 1982.
- [13] Trolinger, J. D., "Particle Field Holography," *Optical Engineering*, Vol. 14, No. 5, 1975, pp. 383-387.
- [14] KLD, Associates, Inc., Huntington Station, NY.

Harold C. Simmons<sup>1</sup>

# Investigating the Commercial Instrument Market

---

**REFERENCE:** Simmons, H. C., "Investigating the Commercial Instrument Market," *Liquid Particle Size Measurement Techniques*, ASTM STP 848, J. M. Tishkoff, R. D. Ingebo, and J. B. Kennedy, Eds., American Society for Testing and Materials, 1984, pp. 22-32.

**ABSTRACT:** The characteristics of instruments that are available commercially for the measurement of liquid particle sizes are examined critically in relation to the varied needs of users. Deficiencies in the methods employed are discussed, and examples are given of potential sources of error. Recommendations are made to improve the situation.

**KEY WORDS:** liquid particle, measurements, commercial instruments

The object of this paper is to review the important considerations involved in choosing an instrument for the purpose of making measurements of liquid particles and to discuss in general terms what is currently available commercially. The investigation is primarily concerned with the suitability of instruments for use with sprays produced by nozzles or atomizers and capable of being used in a routine manner.

The author's experience with this subject started in the 1940s with fuel nozzles for the first aircraft jet engines, a field which provided both incentive and adequate funding for research.

## Background

Dealing briefly with the history of liquid particle sizing it is worth noting that the 1940s were what may be termed "precomputer" days. At that time there were no instruments available commercially for the purpose of measuring and counting liquid drops because this is one area in which the computer's capabilities are vitally necessary. Any serious attempt at characterizing the properties of a cloud of drops or a spray is going to require the measurement, counting, and classi-

<sup>1</sup>Director of Engineering, Research and Development, Gas Turbine Fuel Systems Division, Parker Hannifin Corporation, Cleveland, OH 44112.

fication of very large numbers of drops which can become both tedious and time consuming if it has to be done manually.

A classification of the methods that can now be used is given in Table 1, which shows a broad distinction between sampling (intrusive) techniques and non-intrusive optical methods. Initially, the first two techniques were all that was available. The problem with the first was that the liquids involved were all relatively volatile, and it was necessary to collect them in special ways such as immersion in a nonmiscible liquid to preserve them for the sizing and counting operations. The great difficulty of making such measurements inevitably resulted in very little data being published, and, since the time to analyze a single test condition could take days or weeks, it was very difficult to carry out parametric studies of any sort.

Workers with solid particles, of course, do not have these difficulties and much very important work was achieved 50 years ago, including in particular the work done by Rosin and Rammler which led to the establishment of their equation for the distribution of particle sizes which has been of considerable use to this day. The solid particle workers, in addition to being able to retain particles indefinitely for microscopic or photographic examination, are also able to obtain data in a direct manner by the process of sieving through wire mesh screens. The author's earliest introduction to the sizing of liquid particles was the method of spraying molten wax which then solidified so that the drops would be treated and handled as solid particles. A considerable amount of work was done using this method, but little was published due to the needs of military secrecy. As a technique, however, it was time consuming and had severe limitations in dealing with small

TABLE 1—*Classification of drop-sizing methods.*

Sampling Liquid Drops (intrusive)
Collection on slides etc. as liquid Microscope, photography
Solidification Sieving, weighing
Momentum effects Cascade impacters
Heat transfer effects Hot wire anemometer
Optical (nonintrusive)
Photographing individual drops <i>in situ</i> (imaging) Holography, automated sizing
Light-scattering effects (nonimaging) Individual drops Ensembles of drops
Laser-doppler etc.

drop sizes. Cascade impacters, which are widely used for solid particles, were found to be unsuitable for nozzle sprays and their use was discontinued.

The use of photographic methods began to benefit during the 1950s from the first efforts at electronic counting which were of tremendous value in saving time especially when the photographic plate was replaced by the television camera. Such "imaging" methods are valuable when the spray characteristics are not known *a priori*. More recently very considerable use has been made of the large number of optical phenomena exhibited by particles which can be generically described as "light-scattering" techniques, and these "nonimaging" systems are particularly useful with sprays of known characteristics.

At the present time there is a large body of literature on the subject of liquid particle sizing including several excellent recent surveys typified by Ref 1, but these do not indicate what is actually commercially available. We are dealing with a very broad subject, and so it is not surprising to find that different industries or scientific interests have worked along almost unrelated lines and that the instruments and methods which they developed exhibit a wide variety of methods of data acquisition, recording, and analysis. Probably each of the commercially available instruments was evolved initially in response to a specialized problem.

If the methodology suitable for a particular purpose can be identified from the literature, there are two alternative possibilities: one can either build an apparatus oneself from the information available or determine if such an instrument is commercially available.

Table 2 outlines the most important characteristics to be investigated by a potential user and purchaser of an instrument, and these are discussed next under each heading.

### Imaging Versus Nonimaging

The choice between imaging and nonimaging techniques depends both on the needs of the liquid particle measurement project and also the knowledge previously obtained on the subject. If it is known for example that an atomization process is essentially complete, then it is usual to assume that the drops are spherical, and a nonimaging system may be appropriate. On the other hand if

TABLE 2—*Instrument characteristics.*

---

Imaging versus nonimaging
Drop-size range
Drop-size distribution
Size-class intervals
Spatial versus temporal data
Accuracy and precision
Calibration
Life
Cost

---

there is reason to believe that the liquid particles are nonspherical then an imaging technique may be necessary. There are obvious advantages to using both techniques in parallel.

### Drop Size Ranges

The next most important question is the range of sizes which can be measured by the instrument. Two orders of magnitude appears to be the limit of any commercially available instrument with a single setup of optics, but, as Fig. 1 shows, instruments can be obtained to cover all sizes from submicron to several millimetres. The lower limit of size for imaging devices is about  $2\ \mu\text{m}$ . Many sprays exhibit a range of drop diameters greater than two orders of magnitude; so, if it is desired to obtain the fullest possible data, it may be necessary to use two instruments (or change the optics of a single instrument) and then deal with the problem of combining the data.

The subject of required instrument range raises some difficult questions, the importance of which depends entirely on the use to which the observed data is put. In studying the combustion of sprays, for example, it is well known that the presence of a very few large size drops can have a dominating effect on the completeness of combustion and hence on the composition of the exhaust, leading to smoke and other forms of air pollution. In this case one needs an instrument which is designed to ensure that large drops are correctly evaluated and recorded. On the other hand, in many cases concerned with health hazards, the "inhalable particulates" for example, it is more important to know the proportion of a spray

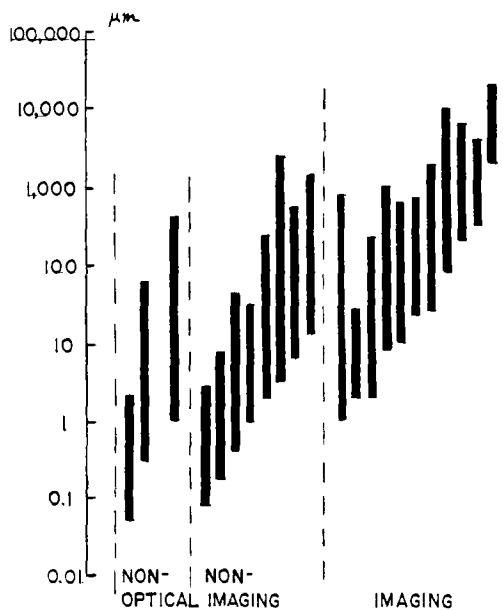


FIG. 1—Advertised ranges of instruments.

TABLE 3—*Effect of truncating data on SMD<sup>a</sup>*

Range of Measurement, $\mu\text{m}$	Number of Classes	SMD,	Error %
8 to 512	12	133.9	...
8 to 362	11	130.5	-2.5
16 to 512	11	134.3	+0.3
32 to 512	9	137.8	+2.9
32 to 362	8	134.3	+0.3
45 to 256	5	136.4	+1.9
64 to 181	3	130.3	-2.7

<sup>a</sup>For spray having drop-size distribution as given in Ref 2 and "maximum" drop diameter = 512  $\mu\text{m}$ .

which falls below a given drop size limit so the instrument must have a suitable capability at the other end of the size scale.

For many purposes, however, an "average" size is adequate and one or other of the various statistical means as defined in ASTM Practice for Determining Data Criteria and Processing for Liquid Drop Size Analysis (E 799-81) can be determined from the observed data, assuming that all the drop sizes are within the size range of the instrument. Even if they do not, it is possible in some cases to ignore the fact that either larger or smaller drops exist and go unrecorded. This is reasonably safe if the observed drop size distribution follows some well-defined mathematical expression such as Rosin-Rammler. For example, Table 3 shows the results of truncating either or both ends of a set of data representative of the performance of fuel spray nozzles. These data were reduced [2] to an empirical equation for the continuous distribution of numbers of drops with drop size from which figures can be calculated for any postulated size class limits. It will be seen that the Sauter mean diameter (SMD), for example, is surprisingly insensitive to loss of data at either end. However, if the drop size distribution is not fully known, the calculated mean may be incorrect and misleading. This problem is of particular concern if the instrument or its associated data reduction process present only a computed mean result.

### Drop Size Distributions

The subject of drop size distributions in relation to the design of the instruments deserves more study than it has received so far. If one can be sure *a priori* that the instrument will only be used to make measurements on sprays produced by a given type of device and there is sufficient background or history to show that the overwhelming majority of the data can be fitted to a particular mathematical expression, then one is justified in designing the instrument on this basis and recording results in simple terms such as the 2 or 3 variables which characterize the distribution. Otherwise there is much to be said in favor of instruments which simply record the observed data in size classes with no attempt to curve-fitting

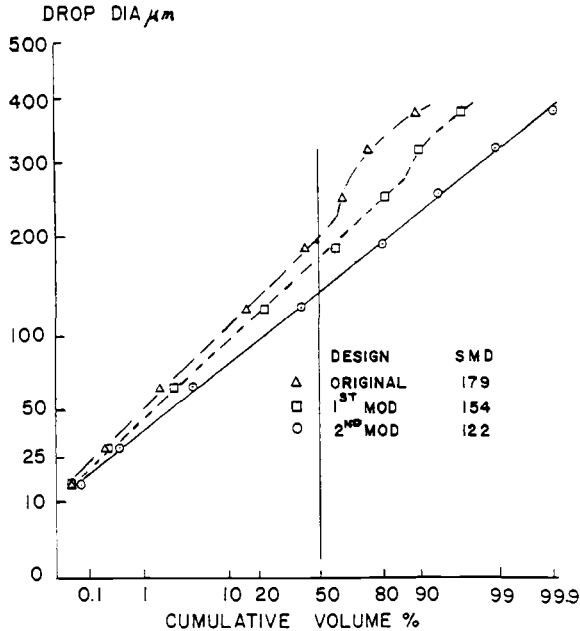


FIG. 2—Changes in drop-size distribution due to improvements in nozzle design.

or interpretation. The ability of fully computerized instruments to display these data in graphical or histogram form on a cathode ray tube (CRT) is particularly useful in making judgments on the data while a series of tests is in progress.

As an example of the value of using observed data rather than an assumed distribution, the following case is presented. One very important use of a spray-analyzing instrument is to evaluate improvements in design or manufacturing techniques for products such as fuel nozzles; this is illustrated by Fig. 2. The data [3] are presented (by manual plotting) on a graph of cumulative volume (mass) of drops less than stated values of the drop diameter, using a normal probability scale for the volume and a square root scale for the diameter. The three curves show the improvement in atomizing performance obtained by design changes on a given fuel nozzle at given conditions. It is important to note that the size classes used for the top end of the size scale were linearly spaced which allowed the instrument to show the abnormal number of large drops obtained with the original design and how, as these were reduced, the average drop size (SMD) in this case was significantly lowered. Experience over many years has shown that the distributions for this class of atomizing device plot close to straight lines on this graph when the spray performance has been optimized. It is also worth noting that this result was demonstrated clearly although the number of size classes available on the equipment at that time is smaller than modern capabilities. The point that is being made here is that it is not always necessary to collect large amounts of data (once the background has been established) to serve a practical purpose.

TABLE 4—*Effect of size class intervals and number on SMD\**<sup>a</sup>

Size Class Interval, $\mu\text{m}$	Number of Classes	SMD, $\mu\text{m}$	$\Delta\%$
Linear			
...	$\infty$	130.7	...
5	101	130.5	-0.15
10	51	130.4	-0.2
20	26	130.3	-0.3
50	11	129.0	-1.3
100	6	123.5	-5.5
Geometric Ratio			
1.04	100	131.0	+2.0
1.09	50	131.2	+0.4
1.20	20	131.8	+0.8
1.41	11	133.9	+2.4
1.70	7	138.3	+5.8
2.0	6	143.3	+9.6

<sup>a</sup>For spray having drop-size distribution as given in Ref 2 and "maximum" drop diameter = 512  $\mu\text{m}$ .

### Size Class Intervals

The choice of class size intervals deserves some consideration. Although there is a natural inclination to use logarithmic or geometric scales particularly for comparative purposes, it has been suggested that the larger drops need a linear scale to obtain sufficient accuracy. If the purpose of a test is to determine an average diameter such as SMD, however, it is not obvious which is better. Using the same drop size distribution as for Table 3, a comparison can be made of the effect of using different size class intervals (both linear and geometric) and hence the number of size classes on the computed SMD. The results are shown in Table 4 and Fig. 3. It will be seen that there is a definite advantage in using linear spacing of the size classes, especially if the number of classes is small. It is also noteworthy that the gain in accuracy by using a very large number of classes is negligible in either case. However, there are certainly cases of sprays or clouds of drops which do not exhibit continuous or unimodal distributions either by design or accident and, if this is suspected, then the use of a large number of size classes is justified.

It is perhaps necessary to point up that we have been talking about the number of classes which the instrument can discriminate, that is, the raw data, and not the display of the data in hypothetical classes which is a trivial matter for modern computers.

The conclusion to be drawn from the preceding illustrations is that one should try to choose an instrument with a size range which is somewhat greater than the drop size distribution to be examined, especially at the upper end of the scale, and that a linear size-class scale may be preferable.

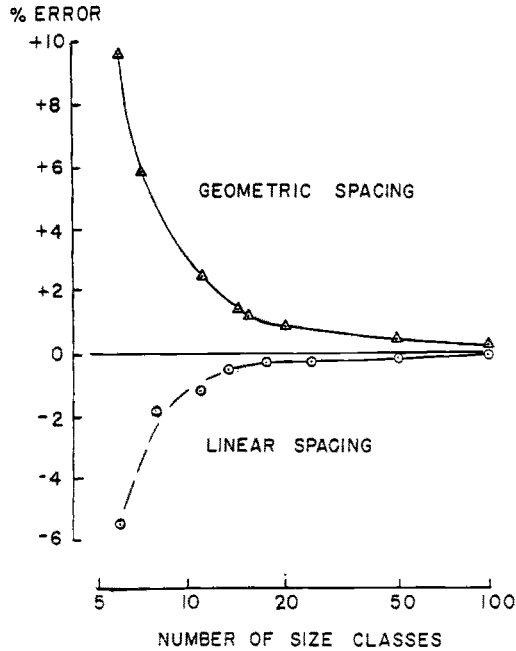


FIG. 3—Effect of number and spacing of size-classes on accuracy.

### Spatial Versus Temporal

For many purposes it is important to know the velocities of the individual drops and to include this information in the final analysis so as to derive the “temporal” distribution rather than the “spatial” distribution (which is the accepted term for an instantaneous “stop-action” measurement as defined in ASTM E 799-81). In observing sprays very close to their point of formation [25.4 to 50.8 mm (1 to 2 in.) is typical for gas turbine fuel nozzles for example] there is probably little difference and the error is not serious but at greater distances and in other situations the differences are very noticeable as Fig. 4 [4] shows. Certain types of instrument collect data from continuous observations and thus will automatically take account of differing drop velocities to report a “temporal” distribution. In other instruments simultaneous measurement of both size and velocity of each particle is possible allowing both types of distribution to be determined. A disadvantage of all systems which count individual drops, however, is that they necessarily observe only a small volume sample of a spray. It has been shown that the distributions of both drop size and flux vary sharply from point to point in typical sprays produced by nozzles, and therefore a large number of observations at different stations is required followed by some form of averaging such as area-weighting to obtain a representative result. In contrast, those methods which rely on optical effects produced by an ensemble of drops may be able to obtain a representative “average” by a single test, which is a great time saver especially in parametric studies.

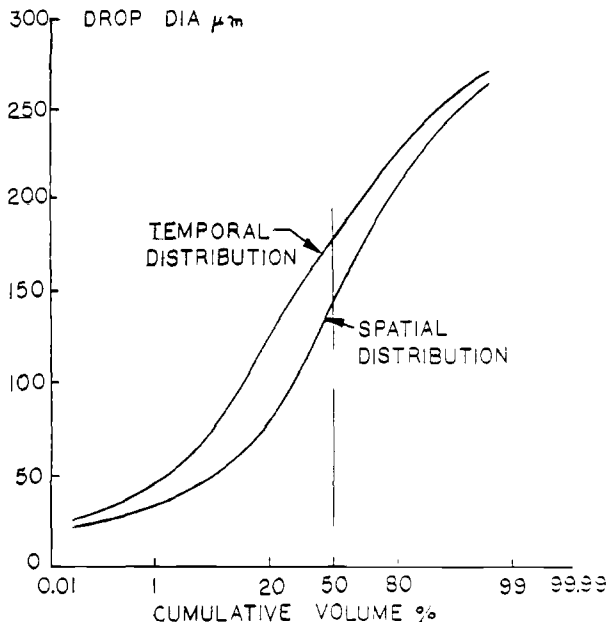


FIG. 4—Comparison of spatial and temporal drop-size distribution.

### Accuracy

We must now turn to the most difficult question for both the intending purchaser and the instrument maker. What “accuracy” can we expect? It is necessary to distinguish here between the fundamental accuracy of the method and the ability of the instrument to perform its function, that is, between “accuracy” and “precision” as defined by ASTM.

For imaging instruments such factors as magnification are calculable, and errors in measurement are most likely to be due to judgment of sharpness of focus and the manufacturing tolerances associated with reticules or equivalents (spaced light-sensing diodes, video-scanning, etc.). Nonimaging systems depend more heavily on theoretical relationships but are also considered as calculable from first principles. In most cases, therefore, the error limits can be estimated with reasonable accuracy ( $\pm 5\%$  is the figure typically used). Furthermore, since generally a large sample of drops is involved, it is customary to assume that the errors tend to cancel out, and thus the statistical means will be of the same order of accuracy or better. This conclusion, however, rests on the further assumption that the instrument is in good condition.

### Calibration

There are many possible causes of inaccurate results being obtained. Optical systems, for example, can be very sensitive to alignment and to lens fouling, while the electrical components including light sources, sensors, and computers

are certainly not yet trouble free. The classic answer to this problem is to use some standardized method of "calibration" both in the initial manufacture of the equipment and as a routine periodical check on its behavior. It is surprising that this subject has not received more attention from instrument designers; some rely on the claim that their machines work on "first principles" while other suggest the use of solid particle standards, since there are no liquid standard reference materials (SRMs). In the author's experience, the use of "standard" spray nozzles has been a successful substitute for an SRM, provided that they are handled carefully to prevent damage and are regularly checked against a "master" nozzle. Imaging instruments can also use simulated drop silhouettes of known size. A recent extension of this technique [5] produces an ensemble of images which simulates a spray of known drop size distribution and is particularly useful for some nonimaging instruments. It would clearly be an advantage for a commercial instrument to have a built-in capability for some kind of calibration check.

The use of a standardized calibration technique is particularly necessary in determining the consistency or reproducibility of measurements made by different instruments of the same nominal design. The word "nominal" is used advisedly: even instruments carrying the same model or type designation may vary with respect to the components employed, particularly the electronic and computer parts, and these may affect the end result. There is some excuse for this in that these fields are still developing very rapidly and there is a great temptation to use newer components especially if they offer advantages in efficiency (reduced power consumption or time), life or cost; but, in the author's opinion, the manufacturer has a duty (in the scientific sense) to keep his previous customers and operators of the equipment informed of these changes by service bulletins or newsletters. Planned obsolescence may be a legitimate marketing device for the general public, but it has no place in the field of continuing search for knowledge.

## Life

In the present context "life" refers to the time period before a significant loss of accuracy or capability occurs with an instrument. It may be defined as the number of hours of operation or even the number of test sequences which are performed. It would be useful to know in advance how many times a flash unit can be flashed or how many hours will a laser or vidicon or photo-diode perform satisfactorily, but such data are rarely given.

There is also a need for information on the most suitable operating environment and any limitations on ambient pressures, temperatures, or humidity. The operating and maintenance manual should provide information relative to setting up and alignment procedures, need for anti-vibration mountings, and safety precautions.

If the instrument is to be used routinely, it is essential to stock recommended spare parts to prevent unnecessary down time. Such a list should be provided by the manufacturer and should also describe diagnostic procedures.

## Cost

The complexity of the liquid particle measuring problem virtually predicates the use of expensive equipment, and the market for instruments does not appear to be sufficiently large for any substantial degree of standardization. It is unlikely, therefore, that there can be any significant cost savings due to manufacturing economies. Under these circumstances, it is necessary to consider the operating, maintenance, and spares costs over the useful life of the equipment as well as the first cost in evaluating the return on investment. This subject has not yet received sufficient attention.

## Summary and Conclusions

The conclusions reached under the previous headings are:

1. Imaging versus nonimaging — Instruments of both types are available; users may need both to obtain sufficient data.
2. Drop size range — The whole of the size range of interest is covered by available equipment but individual instruments tend to have a limited range.
3. Drop size distribution — In most cases, it is preferable that the instrument design is not based on any assumed distribution.
4. Size class intervals — This subject needs more study by users and instrument designers.
5. Spatial versus temporal — The choice of method depends on the usage of the data: both types are available.
6. Accuracy — The instrument's capability is not clearly stated in most cases; but neither are the needs of the user.
7. Calibration — There is an obvious need for frequent calibration checks which has not been foreseen by most instrument designers.
8. Life — Generally insufficient data are provided to evaluate the life of instruments.
9. Cost — Both instrument manufacturers and users need to study the return-on-investment aspect of costs if equipment is to be used routinely.

In summary, there is an obvious need for better communication between the instrument manufacturer and the potential user to define the scope and needs of the instrumentation problem.

## References

- [1] Azzopardi, B. J., *Journal of Heat and Mass Transfer*, Vol. 22, 1979, p. 1245.
- [2] Simmons, H. C., *Journal of Engineering for Power*, Vol. 99, July 1977, p. 315.
- [3] Simmons, H. C., "Air-blast Fuel Nozzle Spray Analysis and Drop-Size Distributions," paper presented at meeting on Multi-fuel Capability of Gas Turbine Engines at U.S. Army Tank-Automotive Command, Detroit, MI, 9 July 1975.
- [4] Tate, R. W., "Some Problems Associated with the Accurate Representation of Droplet Size Distributions," *Proceedings*, 2nd International Conference on Liquid Atomization and Spray Systems, Madison, WI, June 1982, p. 341.
- [5] Hirtleman, E. D., "Calibration Studies of Laser-Diffraction Droplet Sizing Instruments, Combustion Institute, Western States Section, Livermore, CA, 11-12 Oct. 1982.

# **Particle Sizing by Optical, Nonimaging Techniques**

*E. Dan Hirleman*<sup>1</sup>

## Particle Sizing by Optical, Nonimaging Techniques

---

**REFERENCE:** Hieleman, E. D., "Particle Sizing by Optical, Nonimaging Techniques," *Liquid Particle Size Measurement Techniques, ASTM STP 848*, J. M. Tishkoff, R. D. Ingebo, and J. B. Kennedy, Eds., American Society for Testing and Materials, 1984, pp. 35-60.

**ABSTRACT:** Optical, nonimaging techniques for sizing liquid particles of diameters greater than 1  $\mu\text{m}$  are reviewed. Nonimaging optical diagnostics separate into two classes, ensemble or multi-particle analyzers and single particle counters (SPC). A discussion and analysis of the theoretical basis, performance characteristics, and calibration considerations for the various methods in each class is presented. Laser diffraction ensemble techniques, crossed-beam dual-scatter interferometric SPC, and finally single beam SPC based on the measurement of partial light-scattering cross sections of the particles are considered in detail.

**KEY WORDS:** liquid particles, particle sizing, nonimaging techniques, light scattering, optical techniques

The myriad of methods for sizing liquid particles (droplets) presents a significant problem for both the potential user and one trying to review the technology as well. The scope of this paper includes optical, nonimaging diagnostics for liquid particles with diameters greater than 1  $\mu\text{m}$ . These particle dimensions also correspond to the nominal sizing range of photographic and holographic imaging techniques. The reader is referred to previous reviews [1-3] for a discussion of optical diagnostic techniques outside the scope of this paper.

The techniques for sizing particles and droplets can be divided into two generic approaches: optical in situ (or in vivo to use medical terminology) methods; and batch sampling, with subsequent in vitro or external analysis. In the latter a hopefully representative sample of the aerosol is extracted from the original environment and transported to a remote artificial site for either on-line or off-line size analysis. Quite often a laser/optical particle sizing instrument is used for the remote size analysis. With batch sampling the possibility of size segregation or

<sup>1</sup>Associate professor, Mechanical and Aerospace Engineering, Arizona State University, Tempe, AZ 85287.

biasing in the sampling process and condensation, deposition or coagulation in the sampling lines are always of utmost concern. In contrast, in situ methods attempt to perform the sizing in place without removing an aerosol sample.

The significant advantages accruing from the nonintrusive nature of in situ methods must be discounted to varying degrees as the measurements are generally less direct and more equivocal. For example, a solid particle sample might be extracted, analyzed by optical microscopy, and then stored with the possibility for analyzing it again at a later time. In contrast an in situ laser light-scattering single particle counter (SPC) collects scattered light from individual particles which traverse an illuminated optical sample volume in microseconds. If the scattered light deriving from the particle is significantly larger than the background noise level during the transit time across the sample volume the sizing instrument will recognize it as a particle and attempt a size classification based on the amplitude or the time dependence of the scattered light signal. Unfortunately several potential sources of error are present since pulses at the output of a photodetector can derive from a number of phenomena other than scattering from particles or droplets in the sample volume. Despite some potential and demonstrated problems optical in situ methods are desperately needed in those applications where batch sampling techniques are impossible due either to lack of probe access, for example between blades in a steam turbine, or due to survivability problems as in gas turbine combustors.

Laser/optical methods for particle sizing can be subdivided into three main classes:

1. Ensemble or multi-particle techniques.
2. Single particle counters (SPC).
3. Imaging techniques, photographic or holographic.

The former two do not involve the formation of optical images of the particles or droplets and will be discussed here. For a discussion of imaging methods the reader is referred to the paper by Thompson [1] in this volume.

Ensemble techniques analyze the aggregate effect that a distribution of particles or droplets has on incident laser radiation. In contrast to SPC a large number of droplets are in the optical sample volume at any particular time. Since a multitude of droplet sizes contribute to the interaction of radiation with the aerosol, several properties of the radiation exchange process must be studied to determine a droplet size distribution. For example, the attenuation of radiation by the aerosol as a function of wavelength (dispersion quotient) might be measured [2]. For useful precision with these dispersion quotient methods probe wavelengths which bracket the size distribution of interest are generally required. In the case of sprays where droplet sizes may be several hundred microns it becomes very impractical to utilize such methods. Generally for sprays the light scattering pattern as a function of scattering angle  $\theta$  (measured from the forward or light beam propagation direction) is utilized for size distribution measurements. The maximum information content of the scattering from an ensemble

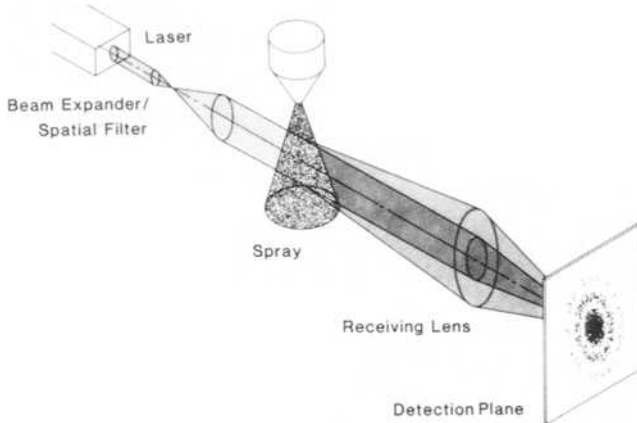


FIG. 1. — *Schematic of laser diffraction particle sizing instrument.*

of particles larger than several microns is in the near-forward scattering angles, and since the dominant contribution to forward scattering is diffraction, laser diffraction techniques have become the most common diagnostic for multi-particle size analysis in this size range. The optical configuration (less detector) for a laser diffraction droplet sizing instrument is shown in Fig. 1. This technique will be described in detail later; at this time note that the optical sample volume comprises the entire collimated beam between the exit lens of the spatial filter and the receiving lens, and the technique is an ensemble, line-of-sight diagnostic.

Single particle counters serve a complementary purpose to ensemble methods. A generalized schematic of an SPC is given in Fig. 2. In SPC the characteristic dimension of the optical sample volume is made small compared to the mean particle spacing by using focused probe beams and by optically limiting the axial extent of the sample volume with the detector field(s) of view. Thus only one particle at a time is present in the optical sample volume, and these are sized individually. A statistically significant number of particles is then analyzed as the aerosol flows through the probe volume. Either a single beam or two intersecting probe laser beams can be used, and one advantage of SPC over ensemble methods derives from the fact that particle velocity can be measured simultaneously with size. Particle size analysis using SPC for sizes  $>1 \mu\text{m}$  has generally been performed using one of two light scattering properties. First, a partial light scattering cross section can be measured and related to particle size, and, secondly, the phenomenon of interference between the two scattered waves produced by a particle traversing the intersection region of two crossed laser beams can be used. Regardless of the specific analysis technique an SPC must accomplish two things in order to measure a meaningful size distribution. First and rather obviously, those particles "seen" by the instrument must be sized correctly, and, second, all particle sizes must either be sampled in an unbiased (with respect to size) manner or a correction for size-selective sampling bias must be made. In the following

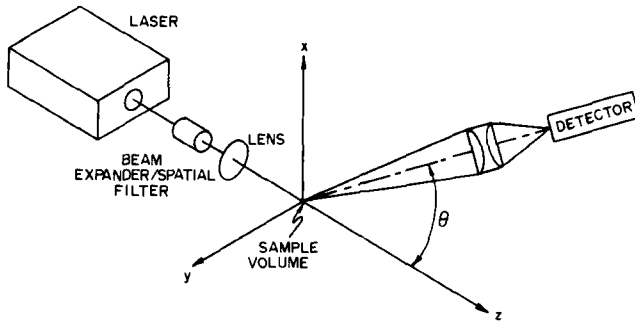


FIG. 2—Generalized schematic of a laser-based single particle counter.

paragraphs a discussion of the specific SPC methods used in particle sizing applications will be presented. A recent and somewhat more comprehensive review directed solely toward SPC has been published elsewhere [3].

The balance of this paper addresses the theoretical basis of the laser diffraction and SPC techniques most commonly used for sizing liquid particles  $>1 \mu\text{m}$ . In addition, calibration methods and the absolute accuracy of the various techniques are discussed.

### Laser Diffraction Particle Sizing Techniques

The generalized schematic of a laser diffraction droplet sizing apparatus is shown in Fig. 1. The beam from a laser, typically a several mW He-Ne model, is spatially filtered, expanded, and collimated to several millimetre diameter at the  $1/e^2$  intensity points. This collimated probe beam is directed through the aerosol of interest, and the transmitted (unscattered) portion is focused to a spot at the back focal plane of the receiving lens. Light scattered by particles in the probe beam which passes through the aperture of the receiving lens is directed to off-axis points on the observation or detection plane. A monodisperse ensemble of spherical particles with diameter  $d$  significantly greater than the wavelength  $\lambda$  would produce the characteristic Airy diffraction pattern shown in Fig. 1 as described by Fraunhofer diffraction theory

$$I(\theta) = I_{\text{inc}} \frac{\alpha^4 \lambda^2}{16\pi^2} \left( \frac{2J_1(\alpha\theta)}{\alpha\theta} \right)^2 \quad (1)$$

where

$I_{\text{inc}}$  = intensity incident on the particles (assumed constant),

$\alpha = \pi D/\lambda$  the size parameter,

$J_1$  = first order Bessel function of first kind, and

$\theta$  = scattering angle measured from the incident beam propagation direction.

A small angle approximation has been invoked in Eq 1 by dropping sin functions and the obliquity correction. The receiving lens in Fig. 1 converts angular scattering information into a spatial distribution at the detection plane as

dictated by  $\theta = r/f$  where  $r$  is radial distance measured from the center of the diffraction pattern and  $f$  is the receiving lens focal length. The diffraction signature is independent of droplet position for all scattered light which actually passes through the receiving lens (that is, neglecting vignetting). However, the fraction of diffracted light truncated by the receiving aperture is a function of particle position, and the diffracted light actually detected is biased toward larger particles as distance from the receiving lens increases.

In practical systems a distribution of droplet sizes or a polydispersion is generally encountered. The composite scattered intensity profile is a linear combination of the characteristic profile of each droplet size with a weighting coefficient equal to the number of particles of that size in the sample volume. The diffraction signature of a polydisperse spray is given by

$$I(\theta) = \int_0^{\infty} n(\alpha) I_{\text{inc}} \frac{\alpha^4 \lambda^2}{16 \pi^2} \left( \frac{2J_1(\alpha\theta)}{\alpha\theta} \right)^2 d\alpha \quad (2)$$

where  $n(\alpha) d\alpha$  is the number of droplets with sizes between  $\alpha$  and  $\alpha + d\alpha$  and the small angle approximation has been made. A primary effect of broadened size distribution is elimination of the contrast in the diffraction pattern.

A common two-parameter size distribution form which often adequately describes liquid sprays is the Rosin-Rammler distribution given by

$$F = e^{-(D/\bar{x})^N} \quad (3)$$

where

- $F$  = cumulative volume fraction greater than the particle diameter  $D$ ,
- $\bar{x}$  = mean diameter such that 36.8% of volume is in sizes greater than  $\bar{x}$ , and
- $N$  = width parameter.

As  $N$  increases the distribution becomes more monodisperse, and typical fuel nozzles produce sprays with  $N$  in the range 2 to 3. The scattering signatures  $I(\theta)$  for Rosin-Rammler distributions with some representative parameter values are plotted in Fig. 3.

The basic task in laser diffraction droplet sizing is to detect and analyze the diffraction signature  $I(\theta)$ , and then mathematically invert Eq 2 to determine parameters of the particle size distribution. Chin et al in 1955 [4] proposed several detection techniques, one of which was to traverse a pinhole/photo-detector assembly across the diffraction pattern. Due to the mechanical traverse this detection approach requires a significant amount of time to cover the entire diffraction pattern. Further, the large dynamic range of the diffraction signature seen in Fig. 3 is another difficulty for such systems. Thus application to transient sprays is not very practical although Peters and Mellor [5] have reported data using a multiplexing technique that assumes the transient spray injection characteristics do not change appreciably between injections.

The advantages of real time analysis of the entire diffraction signature as opposed to traversing a detector across either the diffraction pattern itself or a

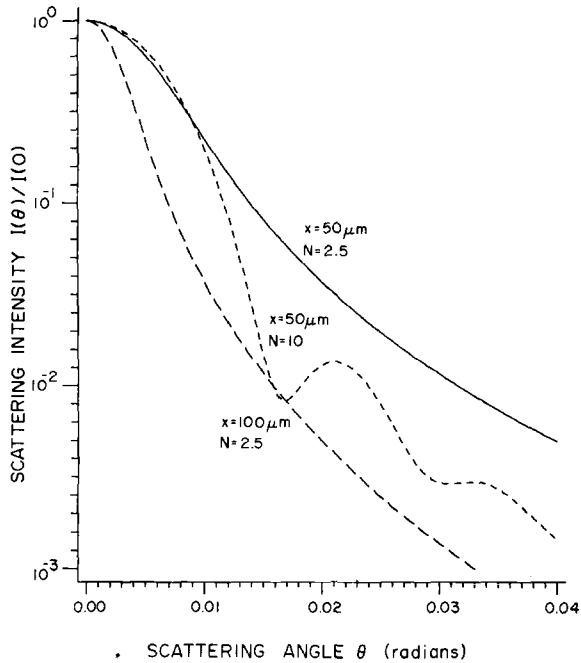


FIG. 3—Forward scattering intensity signatures calculated using Fraunhofer diffraction theory with  $\lambda = 0.6328 \mu\text{m}$  for three Rosin-Rammler particle size distributions  $\bar{x}$  is the Rosin-Rammler mean diameter such that 36.8% of the volume is in sizes greater than  $\bar{x}$ .  $N$  is a width parameter.

photographic image thereof are obvious. McSweeney and Rivers [6] developed an optical fiber faceplate assembly which collected the diffracted light in a number of annular concentric rings and transferred the energy from each ring to a separate photodetector using fiber optics. Cornillault [7] designed a rotating circular mask to be placed at the detection plane which had a series of apertures situated at various distances from the center of rotation. The optical system of Wertheimer et al [8] involved an additional field lens behind a detection plane mask which directed the diffracted light onto a single stationary photodetector. A second mask was also used [8] to effectively time multiplex the diffraction contributions at the various angles onto the photodetector. A commercial instrument based on this concept is available [9].

Developments in monolithic solid state multi-element detector arrays in the 1970s improved the situation by allowing the entire diffraction signature to be analyzed instantaneously. The detector designed by Recognition Systems, Inc. [10] for parts recognition applications was utilized by Malvern Instruments Ltd. [11] in a commercial diffraction particle sizing instrument based on the work of Swithenbank et al [12]. The original circular detector [10] was comprised of 31 semicircular annular ring detector elements on one half, 32 wedge elements on the other half, and a small circular detector in the center. The dimensions of the annular detector elements of this detector are given in Table 1. Note the in-

TABLE 1—Dimensions of the annular ring detector elements on the Recognition Systems Inc., Model WRD 6400 photodiode array [10]. These dimensions are virtually identical (within 0.001 mm) to those for the Malvern Instruments Ltd. detector as reported [54]. The only discrepancy is the inner radius of Ring No. 1 which has been reported [54] as 0.124 mm. However, the corresponding elements of the scattering matrix used in the Malvern 2200 instrument [11] are consistent with the value of 0.149 mm shown here. Note however that the area correction factors (ratio of photosensitive area to geometric area) due to the conductor leads are different for each element of the two detectors.

Detector Ring No.	Inner Radius, mm	Outer Radius, mm
1	.149	.218
2	.254	.318
3	.353	.417
4	.452	.518
5	.554	.625
6	.660	.737
7	.772	.856
8	.892	.986
9	1.021	1.128
10	1.163	1.285
11	1.321	1.461
12	1.496	1.656
13	1.692	1.880
14	1.915	2.131
15	2.167	2.416
16	2.451	2.738
17	2.774	3.101
18	3.137	3.513
19	3.549	3.978
20	4.013	4.501
21	4.536	5.085
22	5.121	5.738
23	5.773	6.469
24	6.505	7.282
25	7.318	8.184
26	8.219	9.185
27	9.220	10.287
28	10.323	11.501
29	11.537	12.837
30	12.873	14.300
31	14.336	15.900

creasing thickness of the annular detector elements which, when coupled with increasing circumferential length, result in a significant increase in detector area as radius increases. This effect compresses the dynamic range of the scattering measurements as indicated in Fig. 4.

A number of data processing methods have been used to extract particle size information from measured diffraction patterns. Chin et al [4] utilized the integral transform derivation of Titchmarsh [13] to analytically invert Eq 2 to obtain

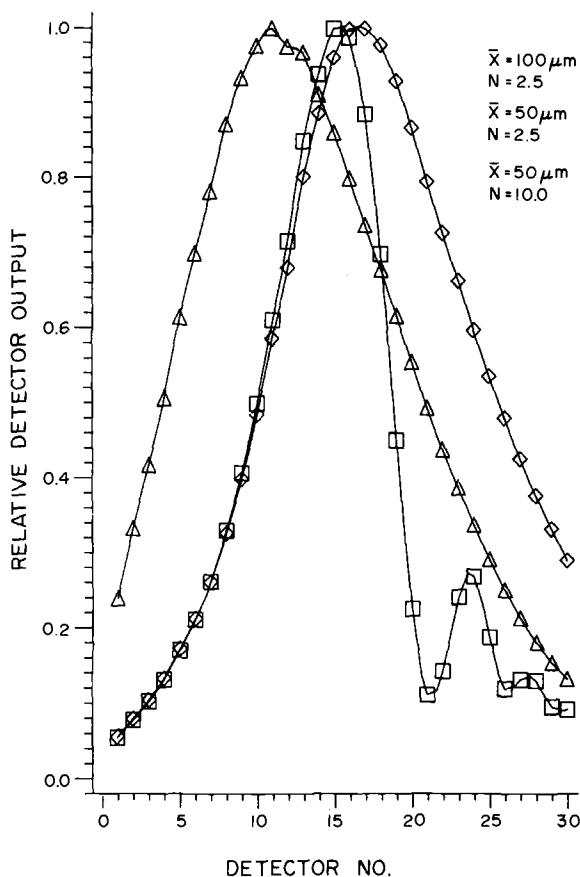


FIG. 4—Forward scattering signature as indicated by relative outputs of the annular ring detector geometry of Table 1. The data were calculated using Fraunhofer diffraction theory with  $\lambda = 0.6328 \mu\text{m}$  for Rosin-Rammler particle size distributions with the indicated parameters.

$n(\alpha)$ . Dobbins et al [14] somewhat paradoxically observed that the diffraction signatures were relatively independent of the form of the droplet size distribution and depended primarily on the volume to surface area mean diameter  $D_{32}$  (Sauter mean) defined as

$$D_{32} = \frac{\int_0^{\infty} n(D)D^3 dD}{\int_0^{\infty} n(D)D^2 dD} \quad (4)$$

The authors [14] utilized a single parameter of the diffraction pattern, the angle at which the scattered light is down to 10% of the on axis value, to determine  $D_{32}$ .

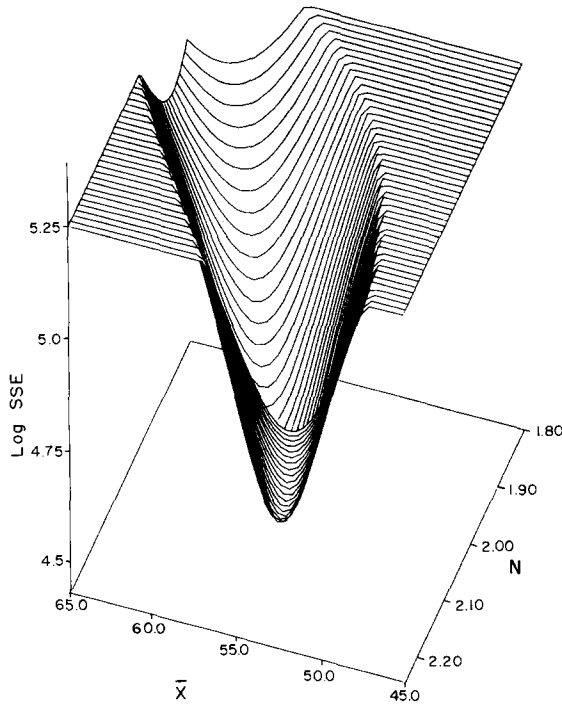


FIG. 5—Typical plot of sum square error (SSE) between measured diffraction signature and that calculated assuming Rosin-Rammler distributions with parameter values shown for Malvern 2200. The SSE is calculated after normalizing the relative detector outputs to a maximum of 2047.

Others [15,16] have since modified slightly this approach and it is still in use today.

Swithenbank et al [12] analyzed the diffracted pattern with the annular ring detector just discussed and subsequently did a numerical inversion (as opposed to integral transform) of a discretized form of Eq 2 to obtain the volume distribution in 7 discrete size bins. There were some problems with that approach, and the authors [12] also assumed that the size distribution was of the Rosin-Rammler form of Eq 3 and estimated the two parameters. The early commercial instruments of Malvern Instruments Ltd. [11] adopted the same data processing algorithm where the  $\bar{x}$  and  $N$  parameter values which produced the best least squares fit between the measured and calculated diffraction pattern were determined. An example of the error surface for a calibration run from the present study on a Malvern 2200 instrument is given in Fig. 5. For each value of  $\bar{x}$  and  $N$  the annular detector scattering signature predicted from the Rosin-Rammler distribution was compared with the measured scattering signals at each of 15 detector pairs and the sum square error calculated. This was repeated for the range of parameter values indicated in Fig. 5, and the values  $\bar{x} = 56$  and  $N = 2.04$  were

TABLE 2—Size class limits for Malvern 2200  
laser diffraction particle sizing instrument  
with 300 mm focal length receiving lens.

Size Class No.	Lower Size Limit, $\mu\text{m}$	Upper Size Limit, $\mu\text{m}$
1	5.8	7.2
2	7.2	9.1
3	9.1	11.4
4	11.4	14.5
5	14.5	18.5
6	18.5	23.7
7	23.7	30.3
8	30.3	39.0
9	39.0	50.2
10	50.2	64.6
11	64.6	84.3
12	84.3	112.8
13	112.8	160.4
14	160.4	261.6
15	261.6	564.0

found to minimize the error. Note that the scattering data are normalized to a maximum value of 2047 [11] and minimum log error in Fig. 5 was 4.38. Recent developments in “model independent” software [11] do not require an assumption of the form of the size distribution but provide a 15 parameter least squares fit to the scattering data using the 15 discrete size bins of Table 1.

One unfortunate property of the Malvern instruments is the poor resolution for the large particle sizes as shown in Table 2. The size limits in Table 2 are determined [11,12] by the detector geometry of Table 1 and the property that a given particle size  $\alpha$  has a maximum in the function  $I(\theta)\theta$  (the so-called “energy distribution” [12]) at  $\alpha\theta = 1.357$ . To improve the resolution in Table 2 for large particles would require a redesign of the detector.

A series of papers [17–19] have focused on the integral transform suggested by Chin et al [4]. One problem with inverting Eq 2 is the fact that the diffracted intensity  $I(\theta)$  can be measured only for a finite range of scattering angles, and the inversion integral is truncated. The authors [17–19] have addressed some of the theoretical and experimental problems in this general inversion approach.

In practical applications of laser diffraction particle sizing, two phenomena often lead to erroneous results. First, if either the particle number density or the optical path length become too large multiple scattering becomes important and Fraunhofer diffraction theory no longer applies. The importance of multiple scattering effects is indicated by the obscuration or attenuation of the incident laser beam. The second problem arises in systems with refractive index gradients due to evaporation or thermal gradients present, for example, in combusting sprays. In this situation significant steering of the probe laser beam can occur causing the diffraction pattern to shift off-center at the detection plane and

thereby invalidating the scattering data for the smallest angles. In order to extract meaningful data under either of these conditions it is necessary to first detect the problem and then hopefully correct the data accordingly. The calibration reticles discussed below offer the potential for on-line detection and correction for these effects.

### Laser/Optical Single Particle Counters (SPC)

A generalized schematic of an optical SPC is presented in Fig. 2. The output beam from a laser or other source of radiation is directed (and typically focused) into the optical sample volume. This sample or probe volume can be thought of as that region of space where a single particle can generate a sufficient detector signal to be discriminated or "seen" over the background noise. As individual particles pass through the sample volume they interact with the incident radiation beam (that is, scatter, absorb, or fluoresce light or all three) and are observed by detection optics oriented at some angle(s)  $\theta$  with respect to the beam propagation direction. The single particle signal obtained at the photodetector(s) are processed to provide information on the size of each particle.

#### *Light-Scattering Cross-Section Measuring Techniques*

The most common approach to particle sizing in the range of interest here involves the principle that the magnitude is a nominally monotonic increasing function of particle size; hence, measurement of a scattering cross section can be used to infer particle size. The SPC signal response  $S$  to a particle in an incident radiation field (uniform over the particle) of intensity  $I_{inc}$  is given by

$$S = kI_{inc}C_i \quad (5)$$

where

$k$  = system gain in transducing radiant energy to voltage using a photodetector, and

$C_i$  = appropriate partial light-scattering cross section for the radiation process under study.

The partial cross sections, as opposed to total light-scattering cross sections, depend on the specific finite aperture detector configuration in use. For light scattering and extinction by spherical particles the cross sections are functions of the particle diameter  $D$ , the complex refractive index  $n$ , and the radiation wavelength  $\lambda$  as predicted by the Lorenz-Mie theory [2]. Thus, a response function  $S(D)$  relating measured signal levels to the diameters of spherical particles of known refractive index passing through a SPC sample volume of known incident intensity  $I_{inc}$  and given  $k$  can be determined from theoretical calculations of  $C_i(D)$ .

A plot of partial light-scattering cross section for spherical particles illuminated by a coherent uniphase wave calculated using a Lorenz-Mie theory computer code [2] is given in Fig. 6. The calculations are for an off-axis  $f/1.96$  collection

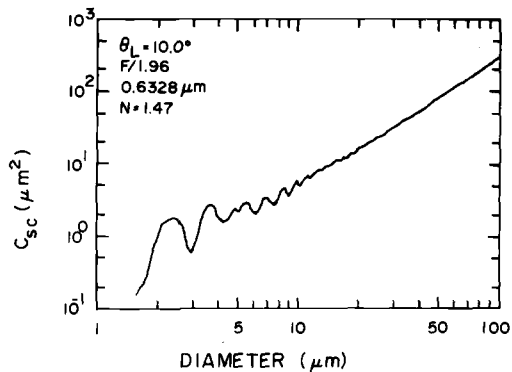


FIG. 6—Partial light scattering cross sections for spherical particles with refractive index  $n = 1.47$  for an  $f/1.96$  receiving lens oriented for  $10$  deg off axis collection in the plane normal to the direction of polarization of the incident beam. The Mie theory calculations used  $\lambda = 0.6328 \mu\text{m}$ .

lens centered at  $\theta = 10^\circ$  from the incident radiation propagation direction (forward scattering). The oscillatory nature of the plot is a result of resonance interactions in the scattering process and results in ambiguities in particle size determination. Another problem inherent in using the laser as a SPC radiation source is the nonuniform intensity profile across the beam [3]. Unfortunately, an ambiguity in signal levels arises for in situ SPC since the particles are free to traverse the sample volume at any position. Thus, particles will experience different peak incident intensities  $I_{\text{inc}}$  depending on the trajectory and even a monodisperse (uniform size) aerosol will generate a broad distribution of signal amplitudes  $S$ .

A number of methods have been devised to eliminate the unknown incident intensity effect in cross section measuring techniques. The basic approaches include: (1) analysis of only those particles which pass through a selected portion of the beam of known and constant intensity, (2) analysis of all particles and later correction of the distribution of particle trajectories and corresponding incident intensities, (3) use of the ratio of scattering signals at two or more angles to cancel the incident intensity effect. The ratio technique, which has been reviewed elsewhere [3,28,29], is difficult to apply for particles larger than several micrometers and will not be discussed here. The early laser light-scattering SPC of Heyder et al [20] aerodynamically focused the aerosol sample through a small region at the center of the laser beam of known and constant intensity. For in situ measurements various optical methods of discriminating those particles which pass through a control portion of the beam have been used, including coincidence detectors at  $90^\circ$  by Hirleman [21] and Chigier et al [22] and in the forward direction by Knollenberg [23].

A second general approach to the ambiguous incident intensity problem is to correct after the fact. One implementation of this approach demonstrated by Holve and Self [24] is to first consider the peak signal height distribution generated by particles of one size passing with equal probability through all portions

of the laser beam focus region. The signal height distribution from a polydispersion is then a linear combination of the monodisperse particle response distributions. A numerical scheme was developed [24] to invert the resulting system of equations and solve for the linear coefficients which are proportional to concentrations in the discretized particle size intervals.

Another somewhat similar approach proposed by Hirleman [25] involves the use of signals generated by particles traversing two adjacent laser beams. The dual peak signature is used to determine two velocity components and the trajectory of each particle. Given known laser beam properties the incident intensity history for a particle is then completely determined which permits a real-time correction for the intensity ambiguity. After  $I_{\text{inc}}$  in Eq 5 is determined a calibrated response function prediction such as Fig. 2 would be used to relate signal amplitude to particle size. This technique [25] has been proposed for light-scattering, extinction, and fluorescence cross-section measurements although experiments to date have used only light scattering.

### *Particle Sizing Interferometry*

Another approach which can provide particle size information independent of incident intensity is particle sizing interferometry (PSI). As a single particle passes through the intersection region of two nonparallel laser beams, Doppler-shifted scattered light waves from each beam emanate from the particle. Heterodyning the two contributions of scattered light at a detector will produce the Doppler-difference frequency which is directly related to the particle velocity and the angle between the laser beam propagation vectors. This principle underlies the laser Doppler velocimeter (LDV). A particle crossing the LDV beam intersection region will produce an approximately Gaussian signal (pedestal) with the modulated Doppler-difference component written on the pedestal [30]. The ratio of the modulated signal amplitude to the pedestal amplitude (that is, the visibility or contrast) provides a measure of particle size as shown in Farmer [30] and others [31,32] who used a scalar description of the process. For large apertures which collect all of the forward scattered (diffracted) light the visibility  $V$  as a function of particle diameter  $D$  and fringe spacing  $\delta$  was shown by Robinson and Chu [32] to be

$$V = \frac{2J_1(\pi D/\delta)}{\pi D/\delta} \quad (6)$$

A plot of  $V$  is given in Fig. 7.

Calculations considering the complete problem of scattering by a sphere simultaneously in two coherent, collimated laser beams [33] predicted a strong dependence of the visibility on particle refractive index, the detector aperture, and detector position relative to the beams. A number of experimental studies have confirmed the importance of careful receiving optics design [33,34] although conflicting observations have also been made [35].

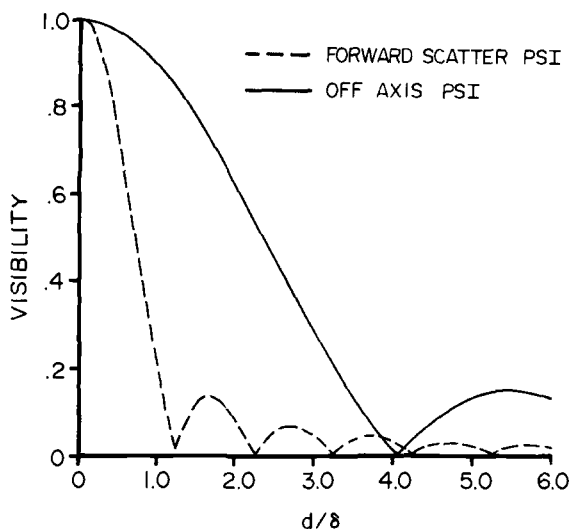


FIG. 7—Calculations for the fringe visibility  $V$  as a function of particle diameter to fringe spacing ratio  $d/\delta$  for particle sizing interferometers (PSI). The data apply to a PSI collecting all of the forward scattered light and to an off-axis PSI with an  $f/2$  collection lens oriented at  $\theta = 20$  deg.

Another related approach is the off-axis PSI proposed by Bachalo [36] which utilizes the interference of refracted or reflected light-scattering contributions rather than the diffractive scatter of a conventional PSI [30]. This method is applicable to particles significantly larger than the wavelength and is based on the difference in optical path length traveled by refracted rays from the two crossed beams which pass through the particle and arrive coincidentally at the detector. The visibility response function for a commercial [37] off-axis PSI with a collection angle [36] of  $20^\circ$  is also shown in Fig. 7, and the expanded  $D/\delta$  sizing range for this concept is apparent.

One problem with PSI type instruments is the limited applicable particle size range. It has been suggested to utilize the amplitude of the Doppler bursts from PSI instruments to size particles in what basically is a scattering cross section measurement approach. The incident intensity ambiguity is then reintroduced and a correction must be made. Those particles traversing the center of the intersection region can be discriminated using coincidence detection with small aperture detectors or using an additional, tightly focused pointer beam. Unfortunately the latter approach merely shifts the trajectory ambiguity problem from the PSI beams to the Gaussian pointer beam.

## Calibration

Optical nonimaging techniques for measuring droplet sizes are inherently indirect and without exception require calibration in some form. As the terms

calibrate or calibration can be somewhat ambiguous we quote the three applicable definitions from the ASTM Standards Compilation [40]:

1. *Calibrate* — General — to determine the indication or output of a measuring device with respect to that of a standard.

2. *Calibration* — Determination of the values of the significant parameters by comparison with values indicated by a reference instrument or by a set of reference standards.

3. *Calibration* — The process of comparing a standard or instrument with one of greater accuracy (smaller uncertainty) for the purpose of obtaining quantitative estimates of the actual value of the standard being calibrated, the deviation of the actual value from a nominal value, or the difference between the value indicated by an instrument and the actual value. These differences are usually tabulated in a “Table of Corrections” which apply to that particular standard or instrument.

Now to define the term introduced previously we refer to the same source [40]:

1. *Calibration Standard* — Any of the standards of various types having accepted parameters. The calibration standard may be used to adjust the sensitivity setting of test instruments at some predetermined level and for periodic checks of the sensitivity.

Now there are a number of unknowns and uncertainties in optical, nonimaging particle sizing instruments including relative detector sensitivities in multiple detector instruments, absolute detector sensitivities in single detector SPC, and the background noise level which determines the lower threshold or sizing limit of the instrument, to name but a few. Since these are generally very difficult if not impossible to quantify independently, calibration with particles of known size is the necessary approach.

Single particle counters must perform two operations correctly, (1) sizing of particles in the sample volume, and (2) counting of particles in an unbiased manner to provide valid concentration data. Thus, primary calibration of a single particle counter requires both size and concentration calibration standards, the latter of which appears to be often overlooked. Ensemble analyzers have somewhat different requirements as concentration calibration is less critical. Finally, imaging techniques are relatively easy to calibrate for size determination, but it is considerably more difficult to account for sample volume effects due to depth-of-field variations with particle size.

The fundamental problem in calibration is the generation of monodisperse, spherical particles or droplets of known and preferably controllable size and concentration. As an alternative, one might utilize a polydisperse particle system of known concentration and size distribution as a primary calibration standard for droplet sizing instruments. Unfortunately, in the words of an ASTM Standard Test Method for particle sizing and from the experience of this author and countless other researchers, there is no totally acceptable particle size and

concentration standard available. There are however some possibilities which include:

1. *Polystyrene Latex Spheres*—These polystyrene spheres are generally very monodisperse for sizes below about  $5\ \mu\text{m}$  (0.1% relative standard deviation typical) but have significantly broader distributions for larger sizes. Polystyrene spheres are subject to size changes with age and steps must be taken to prevent agglomeration. Polystyrene spheres larger than about  $5\ \mu\text{m}$  cannot be reliably atomized and must be used in suspension which requires a mechanical pumping or stirring system [42]. Polystyrene spheres are commercially available [43].

2. *Glass Microspheres*—Distributions of glass microspheres are commonly used as sedimentation standards and in other industrial applications. A sample of these spheres could be size analyzed using a calibrated imaging system, and then in turn used to calibrate SPC or ensemble analyzing optical instruments. These microspheres have been utilized for calibration while attached to glass slides [8] and in liquid suspension as well [42]. The difficulties of differential settling, deposition, and differential separation in flow systems and associated problems in reproducibility make glass microspheres in suspension a very poor candidate as a primary calibration standard. Glass microspheres deposited on a glass slide would appear better suited, but the difficulties of manufacturing calibration slides with thousands of glass spheres of identical sizes and positions are formidable.

3. *Photomask Calibration Reticles*—An interesting property of light scattering is that near-forward scattering or diffraction signatures from spherical particles, opaque disks, and circular apertures of the same diameter are equivalent. Thus it has been suggested that carefully designed arrays of circular apertures photoetched into a chrome on glass substrate be used to calibrate optical non-imaging instruments which utilize diffractively scattered light or optical imaging. These calibration reticles, which [44,45] have been used successfully in both types of instruments, provide a stable, practical, and highly reproducible calibration standard. Unfortunately the reticles cannot be used to calibrate systems which utilize reflective or refractive (off-axis) scattering. The applicability of reticles for calibrating instruments for particle sizes below several microns is questionable.

4. *Droplet Generators*—Mechanical approaches for generating a stream or a cloud of nearly monodisperse droplets involve the systematic breakup of cylindrical or planar liquid jets. The natural frequencies or instabilities of the cylindrical jets are synchronously excited using a piezoelectric crystal to break the liquid stream into a series of droplets of constant diameter (to within typically 1%). This concept has been exploited using a jet forced through an orifice in a vibrating thin plate [46,47] and a syringe jet [48]. The vibrating orifice technique [46,47] is theoretically capable of producing droplets ranging from  $10\ \mu\text{m}$  to about  $150\ \mu\text{m}$ , and syringe jets have reported [48] to be capable of generating droplets in the  $15$  to  $500\ \mu\text{m}$  diameter size range. Spinning disk droplet generators have been also utilized but generally are limited to relatively small droplets. Un-

fortunately there have apparently been no developments which allow generation of specified distributions of droplet sizes as would be useful for the calibration of ensemble scattering instruments. The possibility of utilizing a vibrating plate with an array of orifice sizes to generate controlled droplet size distributions has been discussed, although this author is not aware of published results on this approach.

Droplet generators based on the breakup of cylindrical liquid jets can theoretically be used to calibrate both single particle and ensemble analyzers. For SPC the optical sample volume has been placed very near the jet breakup point to provide a spatially constrained stream of droplets with constant size and velocity. In this way it is possible to map out the SPC response as a function of droplet trajectory and size. Although this mapping exercise would satisfy both the size and concentration calibration requirements, most instrument manufacturers using this technique have only reported results obtained by directing the droplet stream through the center of the sample volume which constitutes only a size calibration. The potential for droplet deposition and coagulation introduce some uncertainties into the concentration calibration.

Another powerful calibration application would be to disperse monodisperse droplets of low vapor pressure by diluting the stream with known and controlled amounts of air to generate practical 2-D flows with monodisperse droplets of known concentration. This flow stream could then be used to calibrate either SPC or ensemble instruments. Unfortunately the very low droplet concentrations produced by these generators make calibration of laser diffraction instruments rather impractical. Some problems with jet breakup droplet generators concern questions about long term droplet size stability, the susceptibility to orifice clogging, and difficulty in day-to-day reproducibility of stable operation conditions.

5. *Polydisperse Sprays*—A final approach to droplet size calibration is to standardize on a particular spray nozzle or other spray source. Presumably manufacturing tolerances could be maintained so that the spray characteristics could be at least as good as the instrumentation. This concept has been tested with mixed success by the ASTM Subcommittee E29.04 on Droplet Sizing. Problems concerned with the liquid supply system reproducibility and test position definition must be addressed in the future.

### *SPC Calibration*

As an example of SPC calibration some work performed by this author and co-workers on the Multiple Ratio Single Particle Counter (MRSPC) will be discussed. Calibration studies by numerous other researchers could have been discussed as well (see for example [24] and [27]) but are not in the interest of brevity.

The details of the MRSPC have been exhaustively covered elsewhere [3,28], for our purposes here it is an instrument in the general form of Fig. 2 but with multiple detectors. A focused laser beam of typically 50 to 200  $\mu\text{m}$  diameter is

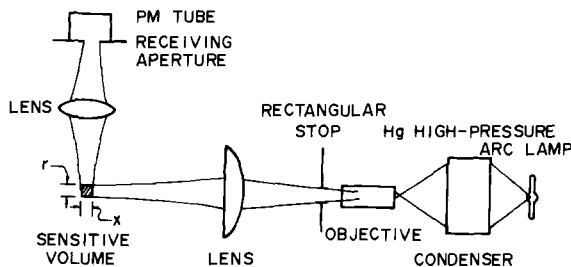


FIG. 8—Schematic of 90 degrees white (incoherent) light particle counter.

used to illuminate individual particles. The ratios of scattered light signals at three or more detectors oriented in the near-forward direction are used to determine particle sizes in the nominal range 0.1 to 10  $\mu\text{m}$ . Since incident laser beam has a Gaussian radial intensity profile which drops off well inside the detector fields of view, the optical sample volume is a function of particle size. A large droplet passing through the shoulder of the Gaussian beam may still scatter enough light to be detected above the noise, but a significantly smaller particle must pass through the very center of the Gaussian intensity peak to be detected over the same noise level. For this reason SPC typically have a bias toward large particle sizes, that is, since the optical probe volume is larger for large particles they are preferentially sampled. This size-selective sampling bias can be predicted analytically, but it was necessary to perform some concentration calibrations to validate the model.

The MRSPC calibration was performed using polystyrene microspheres which were atomized from a dilute ethanol suspension and then dried before passing through the sample volume. Size calibration was done using the polystyrene particle sizes provided by the manufacturer, but concentration calibration was a problem as a significant but unknown fraction of the particles in the solution never reached the sample volume due to deposition or other losses. For that reason it was necessary to design an independent sizing instrument to characterize the size-selective sampling bias. This was done by overlapping the sample volumes from the 90° scattering white-light particle counter shown in Fig. 8 and the MRSPC. The intensity profile at the optical sample volume of the 90° white-light particle counter is shown in Fig. 9. The approximately "tophat" profile eliminates the incident intensity ambiguity for all but the edges of the sample volume which comprised a relatively small portion of the cross section. Thus the 90° SPC provided an on-line measurement of absolute concentration of the particles used to calibrate the MRSPC. Data for the sensitive area (projection of the sample volume) of the MRSPC are given in Fig. 10, where experiment and theory agree reasonably well. Unfortunately the sensitivity of the 90° counter was not sufficient to permit concentration calibration for particles sizes smaller than 1.011  $\mu\text{m}$ . This experiment provided both the size and concentration calibrations necessary to validate all single particle counting and instruments.

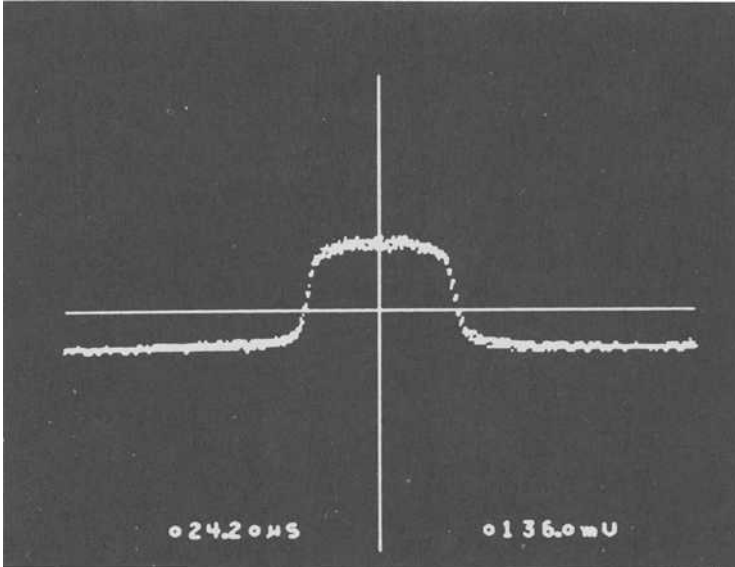


FIG. 9—Scan of the output from 1024 element linear photodiode array facing the incident beam at the sample volume of the SPC of Fig. 8. The diodes are on  $25.4\ \mu\text{m}$  centers and the incident beam width shown is about  $1.27\ \text{mm}$  (after Ref. 49).

### Calibration of Laser Diffraction Instruments

We consider here laser diffraction instruments which utilize multiple detector elements to measure the diffraction pattern including commercial instruments by CILAS [50], Malvern Instruments Ltd. [15], and Leeds and Northrup [9]. It has been incorrectly stated by some manufacturers that laser diffraction instruments need no calibration. This statement is true only for instruments which traverse a single detector across the diffraction pattern, but even then it is rather ill-advised to trust data from an instrument whose performance has never been verified. With respect to the commercial instruments which have detector arrays the statement concerning unnecessary calibration is incorrect. Clearly any variation in the detector responsivities or pre-amplifier gains will change the measured scattering signature, and there is no rational justification for assuming *a priori* that these quantities are constant. Even manufacturers of solid-state photodiode arrays specify  $\pm 10\%$  variation in responsivity between detector elements on a monolithic array [10,51]. Further, the potential problems of detector contamination, optical element contamination, thermal degradation, and amplifier drift should not be ignored. A laser diffraction instrument user should request calibration data from the manufacturer and periodically verify the instrument performance using one of the secondary calibration techniques just discussed.

Most users have tried one or more of these calibration methods to verify the performance of laser diffraction particle sizing instruments. Published data com-

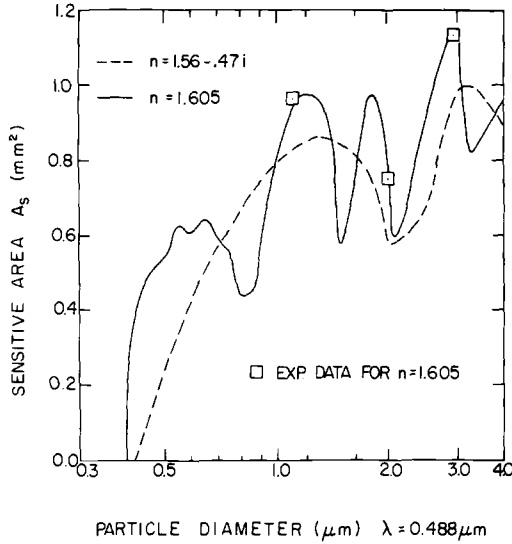


FIG. 10—Plot of sensitive area  $A_s$  versus particle size for the 12/6 deg ratio pair of the MRSPC [53]. Plotted with the theoretical predictions are experimental data for polystyrene latex spheres ( $n = 1.605$ ) taken at  $\lambda = 0.4416 \mu\text{m}$ . One undetermined calibration factor for the experimental data (the same factor for all 3 data points) was fixed by optimizing the fit between theory and experiment (after Ref 49).

paring the performance of several instruments on the same particle field are scarce, but some data for comparison between instruments have been obtained [45] using photomask calibration reticles on Malvern 2200 instruments [11] as shown in Fig. 11. The commercially available reticles [52] were fabricated by photoetching arrays of randomly positioned opaque circles of chrome thin film on a glass substrate. This reticle configuration is designated clear field (CF), and the photographic negative thereof with circular apertures in an opaque background is designated dark field (DF). The calibration sample area of the reticles was 8 mm diameter and provided a discrete approximation (using 23 different circle sizes) to a Rosin-Rammler droplet sizes distribution with nominal mean diameter of  $50 \mu\text{m}$  and nominal Rosin-Rammler exponent of 2.0. The standard Rosin-Rammler software supplied by the manufacturer was used in the size distribution inversion. Results from a series of runs on three different commercial instruments are plotted in Fig. 12. The data points in Fig. 12 are independent as both background and scattering signature measurements were taken each time. The elliptical patterns of the data points for each reticle on a particular instrument are consistent with normally distributed fluctuations (noise) in scattering measurements with standard deviations in the range of 1 to 2% of the peak signal level. The curves in Fig. 12 correspond to equal error contours at 1, 2, and 3% of peak signal level RMS from Fig. 5, which was calculated using the scattering signature averaged over all runs for the clear reticle on Instrument A. The

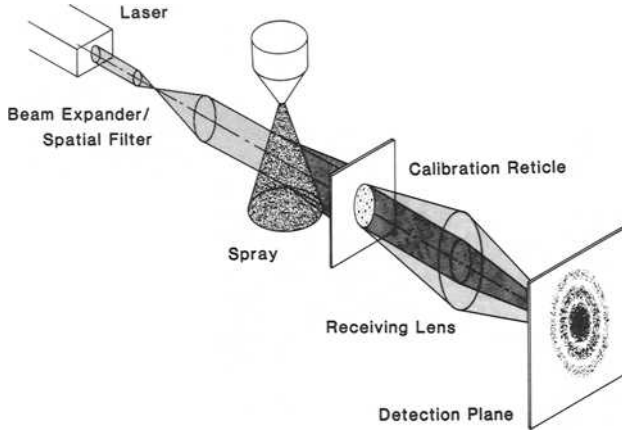


FIG. 11—Schematic of laser diffraction particle sizing instrument with clear field calibration reticle.

instrument-to-instrument variations are statistically significant when compared to the run-to-run variations discussed previously. Differences between instrument responses appears to be on the order of 20% as expected from sensitivity variations between monolithic detector elements. In order to obtain absolute accuracy better than 20% with the Malvern 2200 or similar laser diffraction instruments the sensitivity of each element in the photodiode detector array must be calibrated using reticles or uniform illumination.

### Optical Sampling: Spatial (Concentration) Versus Temporal (Flux)

Optical sizing instruments operate in one of two basic sampling modes. In the first mode an optical instrument samples all droplets in a volume of space, and therefore might be considered a concentration-sensitive diagnostic. Laser diffraction droplet sizing instruments in which the detector resolving time is much less than a typical droplet residence time in the laser beam operate in this concentration diagnostic mode. Size distribution parameters determined with these techniques would be volume-weighted, for example, a  $D_{32}$  consistent with Eq 4 could be obtained. There is, however, another weighting technique of interest in sprays, that of flux weighting.

Define here a particle-flux-weighted mean diameter  $D_{32, f}$

$$D_{32, f} = \frac{\int_0^{\infty} n(D) U(D) D^3 dD}{\int_0^{\infty} n(D) U(D) D^2 dD} \quad (7)$$

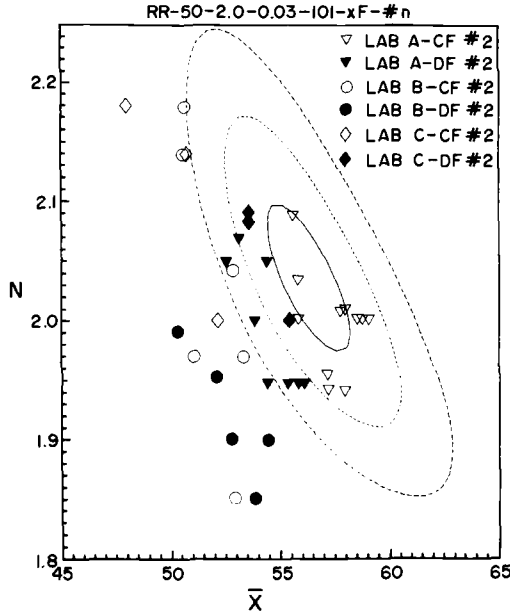


FIG. 12—Experimental data from three different labs with Malvern 2200 instruments analyzing the same two calibration reticles RR-50-2.0-0.03-101-CF-#2 (clear field) and RR-50-2.0-0.03-101-DF-#2 (dark field). Each data point represents a separate background and signal run. Also shown are equal error contours from Fig. 5 corresponding to 1, 2, and 3% of peak signal RMS error for the averaged scattering signature for the clear field reticle at Lab A.

where the additional subscript  $f$  indicates a quantity determined by a flux-sensitive diagnostic, and  $U$  is the velocity of particles of diameter  $D$ . Note that this  $D_{32}$ ,  $f$  may be the most relevant one in some situations, say for example in the idealized case of thin, one-dimensional spray flame front. In that case the important quantity controlling the combustion would be the flux or  $n(D)U(D)$  product rather than just the concentration or number density.

The second mode of instrument operation is one which actually measures this flux of particles across a surface during some finite measurement time. Optical single particle counters which utilize input beam focusing, and the detector field of view to optically define a relatively small optical probe volume are an example of a flux-sensitive diagnostic. The sensitive surface or sensitive area would be the projected area of the optical sample volume (projected into the direction of the droplet velocity vectors).

Results obtained with concentration-sensitive and flux-sensitive diagnostics are related through the velocity, which may be a function of droplet size. The rate  $J(D)$  at which particles with diameters between  $D$  and  $D + \Delta D$  are sampled by an SPC is given by

$$J(D) = n(D)U(D)A_s(D) \Delta D \quad (8)$$

where  $A_s$  is the optically sensitive area. The sensitive area  $A_s$  is a function of droplet diameter as controlled by the light-scattering properties and the threshold or droplet signal validation electronics.

It is seen from Eq 8 that for velocities independent of droplet size both concentration and flux-sensitive devices measure equivalent quantities. However, for typical sprays where velocity is a function of droplet size the differences in the two diagnostics can become quite significant. Data from flux-sensitive diagnostics such as single particle counters which do not simultaneously measure droplet velocity as well as size cannot be used to determine particle concentration or number density. Such instruments would directly measure  $J$  and have a known sensitive area correction factor  $A_s$ , so that

$$\frac{J(D)}{A_s(D)} = n(D)U(D) \Delta D \quad (9)$$

where the left-hand side would be measured/known in order to determine the right hand side of Eq 9. Then since  $n$  and  $U$  cannot be separated mean quantities would be calculated using  $J(D)/A_s(D)$  or equivalently  $n(D)U(D)$  as in Eq 8.

The similarity between these effects and velocity bias in laser velocimetry (LV) should be noted. Considering Eq 6, the rate of particle events or observations by SPC and counter-based LV systems is biased toward high velocities, or in other words particles with high velocities are sampled proportionally more often than particles travelling at low velocities. Several methods have been used in LV to correct for velocity bias and obtain an unbiased velocity estimator. One method is to sample LV signals at equal time intervals rather than sample every particle event and thereby perform time-averaged rather than particle averaged statistics. Similar methods might be adopted for droplet sizing instruments which measure velocity in addition to size, but again it depends on where spatial-averaged or flux-averaged information is more relevant.

Note also that as the velocity field changes so does the concentration in a spray with differential velocities and a constant initial droplet size distribution. Therefore, assuming that a concentration measure is of interest, measurements of droplet size distributions on a laboratory spray into a stagnant gas will in general not be indicative of concentration-size distributions present under other conditions where the dependence of droplet velocity on size has changed due for example to a change in the velocity of the gas surrounding the spray as discussed by Wittig et al [53].

## Conclusions

Optical nonimaging methods for droplet sizing have been reviewed. Single droplet analyzing instruments as well as ensemble analyzing techniques using multi-angle scattering or diffraction were discussed. Calibration of single particle counters must include both size and concentration measurement standards. Laser

diffraction instruments, despite suggestions to the contrary, require calibration as demonstrated by a series of experiments using calibration reticles. Finally, detailed characteristics of each droplet sizing instrument concept must be considered before attempting to reconcile data obtained with different instruments. This is particularly true when comparing spatial or concentration-sensitive techniques such as laser diffraction with data from temporal or droplet flux-sensitive instruments such as single particle counters.

### *Acknowledgments*

The author's research in optical particle diagnostics has been supported by the National Science Foundation, Particulate and Multiphase Processes Program, Dr. Morris Ojalvo, Director, and by the Office of Naval Research, Dr. Albert D. Wood, Project Director.

Further, the author is grateful to Brookhaven Instruments, Garrett Turbine Engine Co., Parker-Hannifin Co., and Carnegie-Mellon University for assistance in providing data reported herein.

### **References**

- [1] Thompson, B. J., this publication, pp. 111–122.
- [2] Kerker, M., *The Scattering of Light and Other Electromagnetic Radiation*, Academic Press, NY, 1969.
- [3] Hirtleman, E. D., *Optical Engineering*, Vol. 19, No. 6, pp. 854–860, 1980.
- [4] Chin, J. H., Sliepcevich, C. M., and Tribus, M., *Journal of Physical Chemistry Ithaca*, Vol. 59, 1955, p. 841.
- [5] Peters, J. and Mellor, A. M., *Journal of Energy*, Vol. 5, No. 1, 1981, pp. 57–59.
- [6] McSweeney, A. and Rivers, W., *Applied Optics*, Vol. 11, 1972, p. 2101.
- [7] Cornillault, J., *Applied Optics*, Vol. 11, No. 2, 1972, pp. 265–268.
- [8] Wertheimer, A. L., Frock, H. N., and Muly, E. C. in *Effective Utilization of Optics in Quality Assurance*, Vol. 129, Society of Photo-Optical Instrumentation Engineers, Bellingham, WA, 1977, pp. 49–58.
- [9] Leeds and Northrup Co., St. Petersburg, FL.
- [10] Recognition Systems Inc., Van Nuys, CA.
- [11] Malvern Instruments Ltd., Malvern, England.
- [12] Swithenbank, J., Beer, J., Taylor, D. S., Abbot, D., and McCreath, C. G. in *Experimental Diagnostics in Gas-Phase Combustion Systems*, B. T. Zinn, Ed., Progress in Astronautics and Aeronautics, Vol. 53, 1977, pp. 421–447.
- [13] Titchmarsh, E. C., *Proceedings London Mathematic Society*, Series 2, Vol. 23, p. xxii. 1925.
- [14] Dobbins, R. A., Crocco, L., and Glassmann, I., *American Institute of Aeronautics and Astronautics Journal*, Vol. 1, 1963, pp. 1882–1906.
- [15] Roberts, J. H. and Webb, M. J., *Journal*, American Institute of Aeronautics and Astronautics, Vol. 2, No. 3, 1964, pp. 583–585.
- [16] Dieck, R. H. and Roberts, R. L., *Applied Optics*, Vol. 9, No. 9, 1970, pp. 2007–2014.
- [17] Shifrin, K. S., *Izvestiya*, USSR Academy of Sciences, Atmospheric and Oceanic Physics, Vol. 2, 1966, pp. 928–932 (English translation).
- [18] Shifrin, K. S. and Kolmakov, I. B., *Izvestiya*, USSR Academy of Sciences, Atmospheric and Oceanic Physics, Vol. 3, 1967, pp. 749–753 (English translation).
- [19] Perelman, A. Y. A. and Shifrin, K. S., *Izvestiya*, USSR Academy of Sciences, Atmospheric and Oceanic Physics, Vol. 15, 1979, pp. 66–73 (English translation).
- [20] Heyder, J., Roth, C., and Stahlhofen, W., *Journal of Aerosol Science*, Vol. 2, 1971, p. 341.

- [21] Hirleman, E. D., "An Optical Method for Exhaust Gas Particulate Sizing," Laboratory for Energiteknik Report RE-74-14, Technical University of Denmark, 2800 Lyngby, Denmark, Aug. 1974.
- [22] Ungut, A., Yule, A. J., Taylor, D. S., and Chigier, N. A., "Simultaneous Velocity and Particle Size Measurements in Two Phase Flows by Laser Anemometry," AIAA Paper #78-74, presented at the AIAA 16th Aerospace Sciences meeting, Huntsville, AL, 10-18 Jan. 1978.
- [23] Knollenberg, R. G., Vol. 92 in *Practical Applications of Low Power Lasers*, Society of Photo-Optical Instrumentation Engineers, 1977, p. 137.
- [24] Holve, D. and Self, S. A., *Applied Optics*, Vol. 18, 1979, p. 1632.
- [25] Hirleman, E. D., *Optics Letters*, Vol. 3, 1978, pp. 19-21.
- [26] Hodkinson, J. R., *Applied Optics*, Vol. 5, 1966, p. 839.
- [27] Gravatt, C. C., *Journal of the Air Pollution Control Association*, Vol. 23, 1973, p. 1035.
- [28] Hirleman, E. D., "Optical Technique, for Particulate Characterization in Combustion Environments: The Multiple Ratio Single Particle Counter," Ph.D. dissertation, Purdue University, Aug. 1977.
- [29] Bartholdi, M., Salzman, G. C., Hiebert, R. D., and Seger, G., *Optics Letters*, Vol. 1, 1977, p. 223.
- [30] Farmer, W. M., *Applied Optics*, Vol. 11, 1972, p. 2603.
- [31] Fristrom, R. M., Jones, A. R., Schwar, M. S. R., and Weinberg, F. S., *Faraday Symposia of the Chemical Society*, Vol. 1, 1973, p. 183.
- [32] Robinson, D. M. and Chu, W. P., *Applied Optics*, Vol. 14, 1975, p. 2177.
- [33] Chu, W. P. and Robinson, D. M., *Applied Optics*, Vol. 16, 1977, p. 619.
- [34] Yule, A. J. Chigier, N. A., Atakan, S., and Ungut, A., "Particle Size and Velocity Measurement by Laser Anemometry," Paper No. 77-214, American Institute of Aeronautics and Astronautics, 1977.
- [35] Farmer, W. M., "Measurement of Particle Size and Concentrations Using LDV Techniques," in *Proceedings of The Dynamic Flow Conference*, 1978.
- [36] Bachalo, W. D., *Applied Optics*, Vol. 19, 1980, p. 363.
- [37] Spectron Development Labs, Costa Mesa, CA.
- [38] Kratochvil, J. P., Lee, M. P., and Kerker, M. P., *Applied Optics*, Vol. 17, p. 1978, 1978.
- [39] Alger, T. W., *Applied Optics*, Vol. 18, 1979, p. 3494.
- [40] *Compilation of ASTM Standard Definitions*, ASTM Committee on Terminology, American Society for Testing Materials, Philadelphia, PA, Fourth Edition, 1979, pp. 88-89.
- [41] Dos Santos, R. and Stevenson, W., *Applied Physics Letters*, Vol. 30, 1977, p. 236.
- [42] Negus, C. and Azzopardi, B. J., "Malvern Particle Size Distribution Analyzer: Its Accuracy and Limitations," Report AERE-R 9075, U.K. Atomic Energy Authority, Harwell, Dec. 1978.
- [43] Duke Standards, Palo Alto, CA.
- [44] Hirleman, E. D., "Aperture Arrays for the Calibration of Droplet Sizing Instruments," in *CLEOS Conference Digest*, IEEE/OSA CLEOS, 1982.
- [45] Hirleman, E. D., "On-line Calibration Technique for Laser Diffraction Droplet Sizing Instruments," ASME Paper 83-GT-232, International Gas Turbine Conference, Phoenix, AZ, March 1983.
- [46] Berglund, R. N. and Liu, B. Y. H., *Environmental Science Technology*, Vol. 7, 1973, pp. 147-153.
- [47] Vibrating Orifice Droplet Generator, available commercially from TSI Inc., St. Paul, MN.
- [48] Mason, B. J., Jayaratne, O. W., and Woods, J. D., *Journal of Scientific Instruments*, Vol. 40, 1963, pp. 247-249.
- [49] Hirleman, E. D., and Moon, H. K., *Journal of Colloid and Interface Science*, Vol. 87, No. 1, 1982, pp. 124-139.
- [50] Compagnie Industrielle des Lasers (CILAS), Paris, France and Marco Scientific, Sunnyvale, CA.
- [51] Reticon, Inc., Sunnyvale, CA.
- [52] Wittig, S. L. K., Aigner, M., Sakbani, K., and Sattelmayer, T., "Optical Measurements of Droplet Size Distributions: Special Considerations in the Parameter Definition for Fuel Atomizers," Paper 13 in Proceedings of AGARD Conference on Combustion Problems in Turbine Engines, Oct. 1983, Chesme, Turkey.

[53] Laser Electro-optics, Ltd., Tempe, AZ.

[54] Felton, P. G., "Measurement of Particle/droplet size Distributions by a Laser Diffraction Technique," presented at the 2nd European Symposium on Particle Characterization, Nurnberg, West Germany, 24-26 Sept. 1979, available from Department of Chemical Engineering, University of Sheffield, England.

Nader K. Rizk<sup>1</sup> and Arthur H. Lefebvre<sup>1</sup>

## Measurement of Drop-Size Distribution by a Light-Scattering Technique

---

**REFERENCE:** Rizk, N. K. and Lefebvre, A. H., "Measurement of Drop-Size Distribution by a Light-Scattering Technique," *Liquid Particle Size Measurement Techniques, ASTM STP 848*, J. M. Tishkoff, R. D. Ingebo, and J. B. Kennedy, Eds., American Society for Testing and Materials, 1984, pp. 61-71.

**ABSTRACT:** Although a light-scattering technique, using a single-element photomultiplier tube, has proved to be an accurate tool for determining the Sauter mean diameter (SMD) of a liquid fuel spray, it has been generally considered unsuitable for the measurement of drop-size distribution. Usually, a photomultiplier tube on the receiving side of the optical system is traversed in a direction at right angles to the optical axis, and the scattered light intensity due to the passage of a monochromatic laser beam through the spray is plotted against radial distance to provide a measurement of SMD. In the present study it is shown that this same light intensity profile can be also converted into an energy distribution which is uniquely related to drop-size distribution. Values of SMD obtained with this technique show good agreement with corresponding values as determined by a photographic method. Moreover, the drop-size distribution calculated by the proposed method is found to be almost identical to the distribution exhibited by a standard calibration reticle. Typical examples of SMD and drop-size distribution for sprays produced at various test conditions are presented.

**KEY WORDS:** atomization, drop-size measurement, fuel sprays

### Nomenclature

$E$	Light energy
$f$	Focal length of receiving lens
$J$	Bessel function
$K$	Constant in Eq 1
$M$	Number of size groups in Eq 1
$q$	Drop-size distribution parameter
$r_1, r_2$	Radii of rings
SMD	Sauter mean diameter
$T$	Matrix in Eq 2

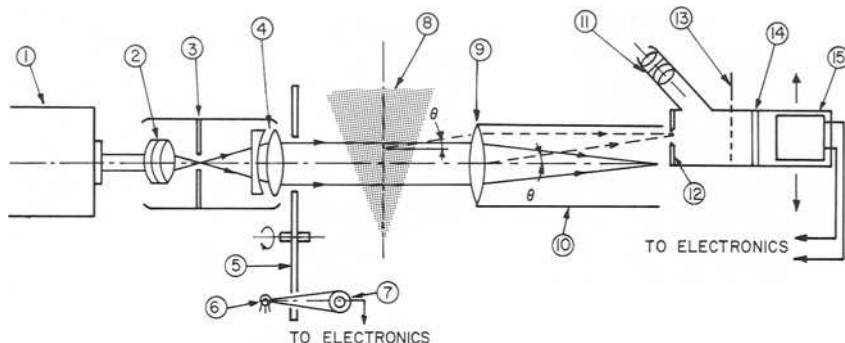
<sup>1</sup>Visiting professor and Reilly professor of combustion engineering, School of Mechanical Engineering, Purdue University, West Lafayette, IN 47907.

$V_i$	Volume or mass fraction
$v$	Volume or mass fraction of spray in drops of diameter less than $x$
$x$	Drop diameter
$\bar{x}_i$	Mean drop size in group number ( $i$ )
$x$	Drop-size parameter
$x_o$	Drop-size at maximum frequency of occurrence
$Y$	Parameter = $2\pi x_o r / \lambda f$
$\lambda$	Wave length

Knowledge of mean drop size and drop-size distribution in liquid sprays is a necessary step toward a proper understanding of combustion performance, and to the prediction of pollutant emission levels from both aircraft and industrial gas turbine engines. In their studies of the evaporation history of sprays, Dickinson and Marshall [1] and Chin et al [2] have shown that sprays having nonuniform drop-size distributions evaporate more rapidly in the initial phase than do sprays of uniform diameter with the same SMD, due to the presence of a larger number of small drops.

Although numerous methods of measuring drop sizes have been described in the literature, no standard method yet exists for measuring accurately the fine sprays produced by modern atomizers. In recent years considerable effort has been applied to research on optical methods for drop-size measurement which have an important inherent advantage in that they do not require the insertion of a sampling device into the flow. This is especially advantageous when measurements are required to be conducted at high pressures. One such method that has found widespread application is a light-scattering technique which is based on the scattering properties of small particles. It was first proposed by Dobbins et al [3], and a more sophisticated version was developed subsequently by Lorenzetto and Lefebvre [4]. To date, the technique has been applied only to the measurement of SMD, because it has been generally considered difficult to obtain drop-size distributions from measurements of light intensity, since the scattered light profile lacks the sensitivity necessary to determine the shape parameters uniquely [3]. To overcome this problem Swithenbank et al [5] have proposed a modification to the method which is based on measurement of the scattered energy distribution rather than the intensity distribution. This means that light is collected in entire annular rings, and the light energy contribution at any ring in the focal plane of the receiving lens represents the sum of the contributions from individual drops of all sizes. It can be shown that although any size of drop may diffract light to all radii, the energy distribution curve peaks at one particular radius [5]. Thus, if it is required to classify a drop-size distribution into a number of separate groups, it is preferable to make measurements at a number of radii.

In the present study a light-scattering technique is used to obtain a plot of light intensity versus radial distance which provides a direct measurement of SMD. This same plot is then converted into an energy distribution curve from which the drop-size distribution is evaluated.



- |                              |                                      |
|------------------------------|--------------------------------------|
| 1 He-Ne Laser Head           | 9 Receiver Lens (60 cm Focal Length) |
| 2 Condensing Lens            | 10 Stray Light Shield                |
| 3 Spatial Filter (Aperture)  | 11 Eyepiece                          |
| 4 Telescope-Collimating Lens | 12 Pin-Hole Aperture                 |
| 5 Rotating Disc (Chopper)    | 13 Shutter                           |
| 6 Small Lamp                 | 14 Neutral Density Filter            |
| 7 Photo Cell                 | 15 Traversing Photomultiplier        |
| 8 Spray Under Test           |                                      |

FIG. 1—The optical bench in diagrammatic form.

### Drop-Size Distribution Measurement

The light-scattering system shown in Fig. 1 employs a helium-neon (He-Ne) laser as a light source. After passing through the spray the light enters a photomultiplier tube which is placed at the focal plane of the receiving lens and is arranged to traverse in a direction at right angles to the optical axis. The signals from both the tube and a position transducer are fed simultaneously into an X-Y plotter to obtain the light intensity profile. Typical plots for sprays produced by a prefilming type of airblast atomizer are given in Fig. 2, while Fig. 3 shows the normalized light intensity profiles. The SMD is determined by measuring the radial distance from the optical axis to a point on the curve at which the light intensity is one tenth of its maximum value [6]. The SMD is then read off the curve shown in Fig. 4, which is based on a relationship between the relative light intensity and the scattered angle, as determined by Roberts and Webb [6].

Figure 5 shows values of SMD obtained by the light-scattering technique at different test conditions for a plain-jet airblast atomizer. Figure 6 compares values of SMD obtained by the photographic method described in Ref 7 and by the present method. The slightly higher values of SMD measured photographically may be attributed to the inability of this method to detect the smallest droplets.

Light intensity may be converted directly into light energy by determining first the relative light intensity at certain predetermined radial distances and multiplying these values by the corresponding distances [8]. The energy distributions shown in Fig. 7 were obtained in this manner from the light intensity profiles plotted in Fig. 3.

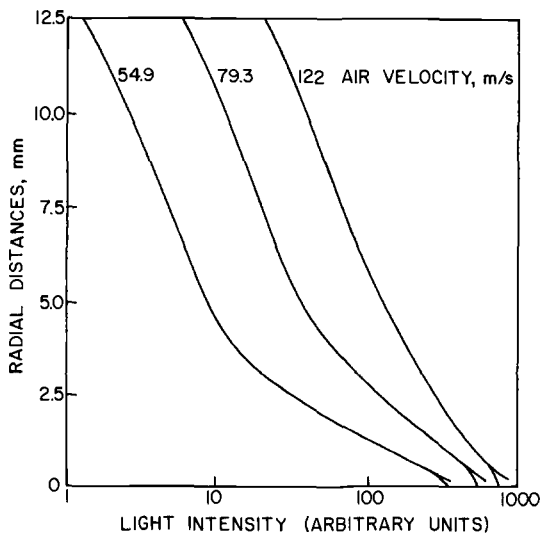


FIG. 2—Influence of air velocity on light-intensity distribution.

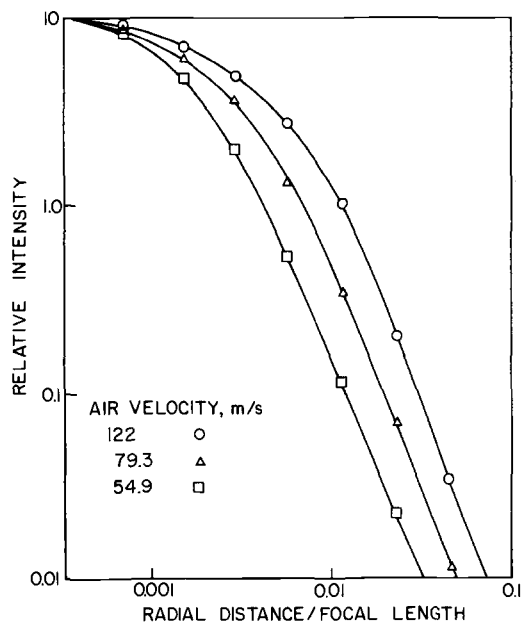


FIG. 3—Variation of relative intensity with radial distance.

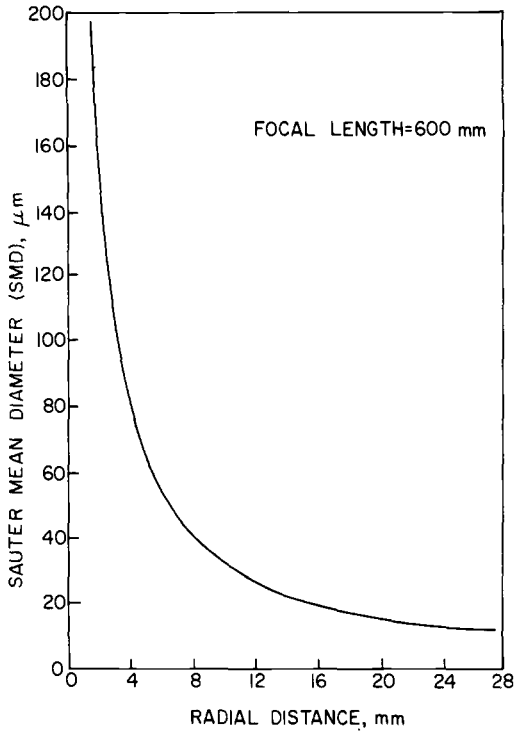


FIG. 4—Variation of SMD with radial distance.

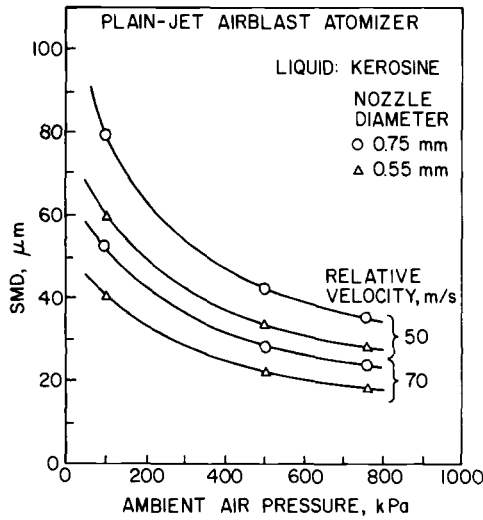


FIG. 5—SMD obtained by light-scattering technique at various test conditions.

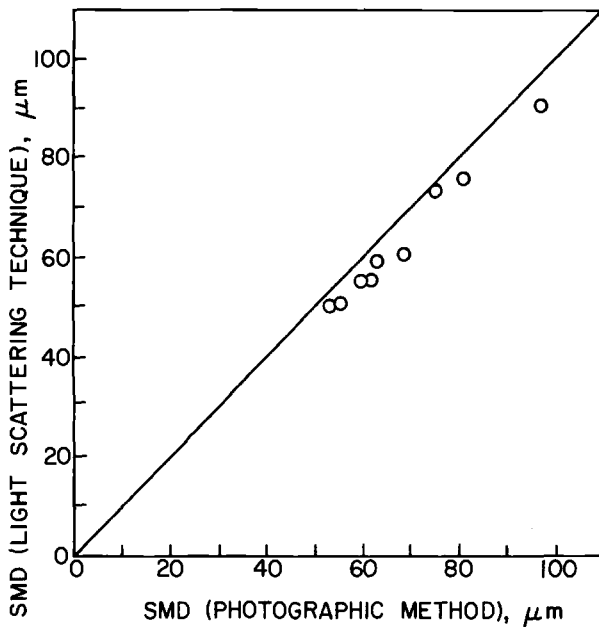


FIG. 6—Comparison of SMD values obtained by two different techniques.

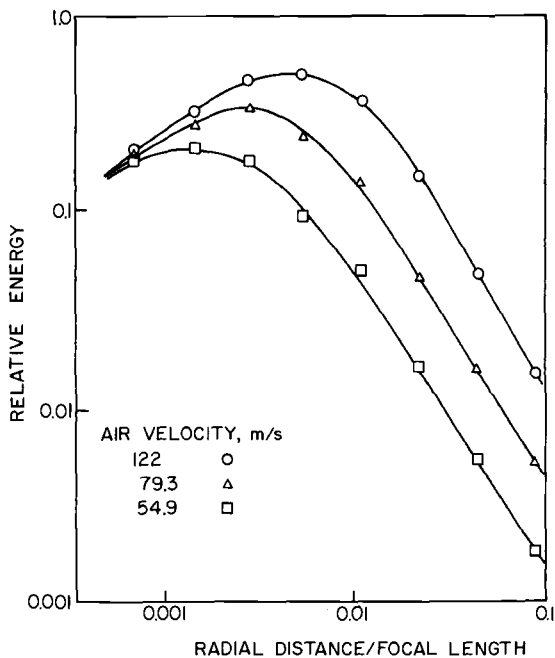


FIG. 7—Effect of air velocity on light energy distribution.

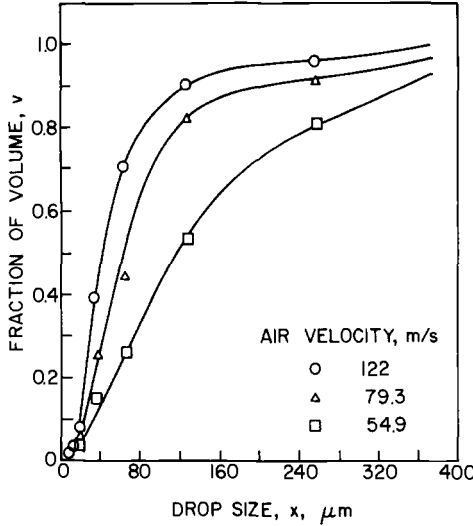


FIG. 8—Graphs illustrating the effect of air velocity on cumulative volume distribution.

The drop-size distribution as expressed by the volume or mass fraction ( $V_i$ ) in any size range is related to the energy distribution by the following relationship [5]

$$E_{r_1, r_2} = K \sum_{i=0}^M \frac{V_i}{x_i} [(J_0^2(Y) + J_1^2(Y))_{r_1} - (J_0^2(Y) + J_1^2(Y))_{r_2}] \quad (1)$$

where

- $J$  = Bessel function,
- $x_i$  = mean size of its group,
- $r_1$  and  $r_2$  = radii of rings,
- $Y = 2\pi x_i r / \lambda f$ ,
- $\lambda$  = wave length,
- $f$  = focal length of the receiving lens, and
- $K$  = a constant that depends on laser power and optical efficiency.

Equation 1 can be written in a matrix form as

$$E = VT \quad (2)$$

or, in terms of the inverted matrix

$$V = T^{-1}E \quad (3)$$

This inverted matrix  $T^{-1}$  consists of a set of coefficients which are arranged in a number of rows depending on the number of drop size groups chosen. It must be multiplied by the measured light energy vector to obtain the drop-size distribution. Examples of this inverted matrix are given in Refs 5 and 8.

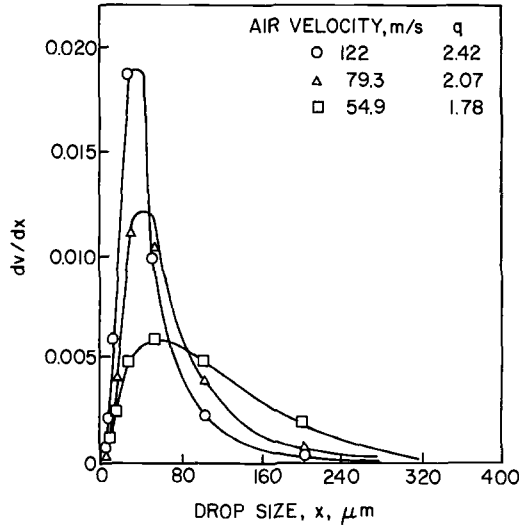


FIG. 9—Graphs illustrating the effect of air velocity on drop-size distribution.

Figures 8 and 9 contain drop-size distributions in cumulative form and general form, respectively, as obtained from the energy profiles shown in Fig. 7. Distributions of drop sizes in sprays produced by a pressure atomizer for different ambient air pressures are shown in Fig. 10.

These drop-size distributions were used to calculate the distribution parameter  $q$  for the Rosin-Rammler equation [9] which is expressed in the form

$$1 - v = \exp - (x/\bar{x})^q \quad (4)$$

where

$v$  = fraction of the total mass or volume contained in drops of diameter less than  $x$ , and

$\bar{x}$  = the size parameter.

Values of  $q$  at different test conditions are indicated in Figs. 9 and 10. It is, in fact, quite possible and very convenient to calculate the value of the distribution parameter  $q$  directly from the drop-size distribution curve. From the Rosin-Rammler equation it is seen that

$$x_o = \bar{x}[(q - 1)/q]^{1/q} \quad (5)$$

where  $x_o$  is the drop size at the maximum frequency of occurrence in the distribution ( $dv/dx_{\max}$ ).

Thus

$$\left(\frac{dv}{dx}\right)_{\max} = [(q - 1)/x_o] \exp - [(q - 1)/q] \quad (6)$$

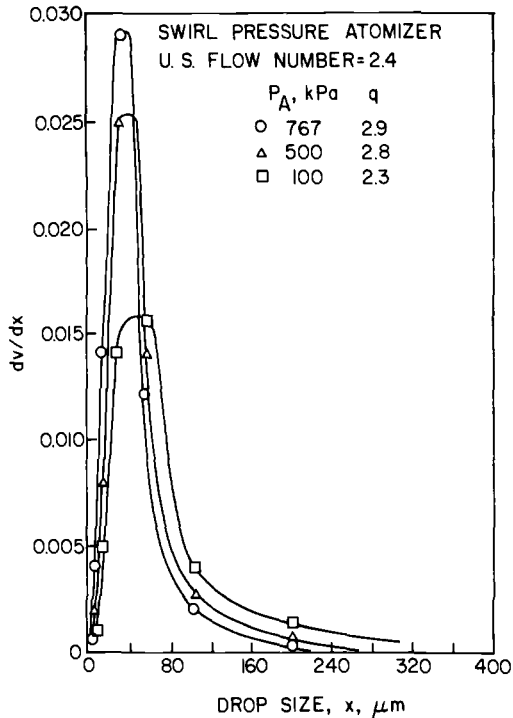


FIG. 10—Drop size distributions for a swirl pressure atomizer.

Clearly Eq 6 may be used to calculate the distribution parameter,  $q$ , from a knowledge of the maximum frequency and its corresponding drop size. To avoid the trial and error needed to find  $q$  from Eq 6 a simpler correlation is proposed as follows

$$q = 1 + 1.86 \left( \frac{dv}{dx} \right)_{\max} \cdot x_0 \quad (7)$$

Equation 7 has been found to provide directly a fairly good estimate of  $q$ , thereby avoiding lengthy computational procedures. This value of  $q$  could be used in conjunction with the size parameter  $\bar{x}$  to calculate SMD. However, the resulting value of SMD could differ appreciably from the corresponding value of SMD as determined by the light-scattering technique. This is attributed to differences in the temporal and spatial drop-size distributions in the spray which are now being investigated experimentally.

A calibration standard reticle of known drop-size distribution and SMD,<sup>2</sup> was used to check the accuracy of the light-scattering technique. The latter indicated

<sup>2</sup>Standard reticle manufactured by Laser Electro-Optics Ltd., P.O. Box 24717, Tempe, AZ 85282.

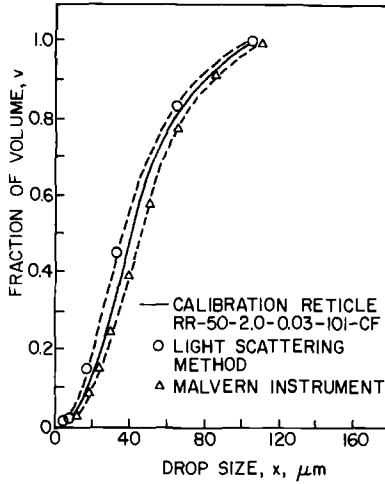


FIG. 11—Calibration of light-scattering technique.

a value of 35  $\mu\text{m}$  for the SMD of the calibrated reticle, as compared with the value of 33.1  $\mu\text{m}$  quoted by the manufacturer. A similarly close agreement was obtained for drop-size distribution, when plotted in cumulative form, as shown in Fig. 11. Also contained in this figure is the drop-size distribution curve for the calibrated reticle, as measured on the Malvern instrument [5]. The information required to plot this curve was supplied by the manufacturer of the reticle. Inspection of Fig. 11 shows that both the Malvern instrument and the light scattering give results that are quite close to the true values.

A further comparison of the values of distribution parameter,  $q$ , obtained by the light scattering technique with those of the calibration piece is provided by the

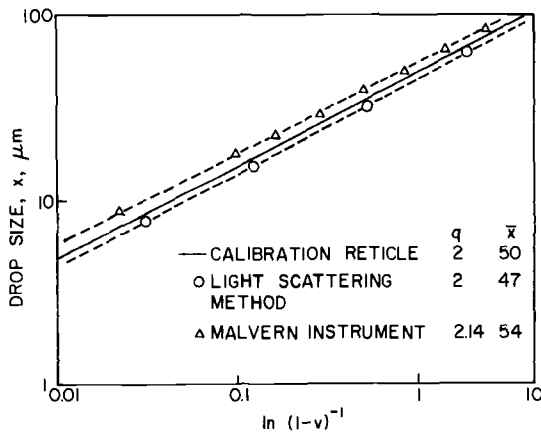


FIG. 12—Rosin-Rammler plot of calibration reticle distribution and results of light-scattering technique.

results plotted in Rosin-Rammler form in Fig. 12. The two sets of values are virtually the same, although there is a slight difference between the two values of size parameter  $\bar{x}$ .

## Conclusions

A proposed method for extending the use of the light-scattering technique to include measurements of drop-size distribution in addition to mean drop size is found to give results which exhibit close agreement with those obtained by other established techniques. The proposed method is simple and expedient. It has the advantage of recording the light intensity profile for inspection so that spurious results arising from imperfections in the spray can be discarded.

## References

- [1] Dickinson, D. R. and Marshall, W. R., *Journal of the American Institute of Chemical Engineering*, Vol. 14, No. 4, July 1968, p. 541.
- [2] Chin, J. S., Durrett, R., and Lefebvre, A. H., "The Interdependence of Spray Characteristics and Evaporation History of Fuel Sprays in Stagnant Air," to be presented at Gas Turbine Conference, Phoenix, March 1983, American Society of Mechanical Engineers.
- [3] Dobbins, R. A., Crocco, L., and Glassman, I., *Journal*, American Institute of Aeronautics and Astronautics, Vol. 1, No. 8, 1963, pp. 1882-1886.
- [4] Lorenzetto, G. E. and Lefebvre, A. H., *Journal*, American Institute of Aeronautics and Astronautics, Vol. 15, No. 7, July 1977, pp. 1006-1010.
- [5] Swithenbank, J., Beer, J. M., Abbott, D., and McCreath, C. G., "A Laser Diagnostic Technique for the Measurement of Droplet and Particle Size Distribution," Paper 76-69, 14th Aerospace Sciences Meeting, Washington, DC, 26-28 Jan. 1976, American Institute of Aeronautics and Astronautics.
- [6] Roberts, J. M. and Webb, M. J., *Journal*, American Institute of Aeronautics and Astronautics, Vol. 2, No. 3, 1964, pp. 583-585.
- [7] Rizk, N. K. and Lefebvre, A. H., *Journal of Energy*, Vol. 6, No. 5, 1982, pp. 323-327.
- [8] Marchionna, N., Watkins, S., and Opdyke, G. Jr., "Turbine Fuel Tolerance Study," Technical Report No. 12090, Avco Lycoming Division, Stratford, CT., Oct. 1975.
- [9] Rosin, P. and Rammler, E., *Journal of the Institute of Fuel*, Vol. 7, No. 31, Oct. 1933, pp. 29-36.

Lee G. Dodge<sup>1</sup> and Stephen A. Cerwin<sup>1</sup>

## Extending the Applicability of Diffraction-Based Drop Sizing Instruments

---

**REFERENCE:** Dodge, L. G. and Cerwin, S. A., "Extending the Applicability of Diffraction-Based Drop Sizing Instruments," *Liquid Particle Size Measurement Techniques*, ASTM STP 848, J. M. Tishkoff, R. D. Ingebo, and J. B. Kennedy, Eds., American Society for Testing and Materials, 1984, pp. 72–81.

**ABSTRACT:** Modifications to a commercial laser diffraction-based drop sizing instrument are described which allow the unit to be used for drop sizing in sprays evaporating in high-temperature air, and under conditions of very high ambient light levels. These modifications have permitted drop size measurements in sprays evaporating in air at temperatures and pressures as high as 700 K and 586 kPa.

**KEY WORDS:** sprays, drop sizing, evaporating sprays, fuel sprays

Efficient means of drop-size measurements in sprays in various environments are quite necessary for a better understanding of many physical problems. Of particular interest at this laboratory is the study of fuel sprays—both continuous (for example, gas turbine) and intermittent (for example, diesel) types, but the techniques described here may find application elsewhere. A number of instruments have been used at this laboratory to study sprays, including high-speed photography, single-shot high-resolution laser strobe photography, and drop sizing based on the forward-scattered diffraction pattern. Modifications to this last technique to extend its range of applicability form the subject of this paper.

In recent years, several techniques have been developed for the rapid determination of drop sizes in continuous sprays. Some of these are optical, including both imaging and nonimaging types. One type of instrument which has been widely used in the technical community is the Malvern Particle and Drop Size Analyzer.<sup>2</sup> Operation of this instrument is based on an analysis of the light scattered from collimated, coherent laser radiation by individual drops in a spray [1]. Scattered light is incident on a set of 30 detectors which are arranged as

<sup>1</sup>Senior research scientist and senior research scientist, respectively, Southwest Research Institute, San Antonio, TX 78284.

<sup>2</sup>Malvern, Ltd., Malvern, England.

concentric annular rings centered about the laser beam axis. Older units incorporate three small detectors arranged as the center spot of the detector system, with a balanced signal on the three detectors assuring proper alignment. Newer units use a photodiode/pinhole for center spot alignment. The annular detectors are coupled through a set of electronics to a dedicated microcomputer which converts the light distribution into a drop-size distribution. This instrument does suffer, however, from certain inherent limitations. The spray must be dense enough to scatter sufficient light (a few percent of incident intensity) to give a reasonable signal-to-noise ratio, while not being so dense as to have a significant number of individual photons scattered by more than one drop, an effect referred to as "multiple scattering." Also, the technique results in a line-of-sight average along the intersection of the laser beam with the spray, which is sometimes but not always an advantage. Although the instrument has some limitations, it provides a rapid and repeatable (for a single instrument) indication of the drop size distribution.

These drop-sizing instruments have been typically developed for operation at atmospheric temperature and pressure. However, it is of interest to the combustion scientist to know how sprays behave at actual injection and combustion conditions, that is, the drop sizes at initial atomization and through various stages of evaporation. Correlations have been developed to predict spray distributions upon initial atomization as a function of fuel and air properties, but experimental data at elevated temperatures and pressures are very limited. Computer models have been developed to predict evaporation of sprays, but, again, experimental confirmation is extremely limited. It would be of interest to document spray characteristics at elevated temperature and pressure both with and without combustion. In realistic combustion systems, the turbulence prevents an accurate knowledge of the temperature profile, limiting observations to qualitative ones. Therefore, evaporation experiments at constant temperature without combustion are necessary to evaluate spray models.

The purpose of this paper is to describe two sets of modifications to a commercially available Malvern drop sizer which allow measurements to be made under conditions where the standard unit is unusable. First, modifications will be outlined which permit data to be obtained at elevated temperature and pressure. Second, techniques will be described to overcome the interference caused by high ambient light levels, such as flame radiation.

### **Experimental Apparatus**

The principles of operation of the Malvern drop sizer have been explained by Swithenbank et al [1]. The angle at which light is diffracted by drops depends on their diameter with the smallest particles diffracting at the largest angles relative to the incident beam. The Malvern system employs a helium-neon (HeNe) laser as the light source with a beam expander to increase the beam diameter to about 9 mm. The light then passes through a Fourier transform lens with a (standard) focal length of 63, 100, or 300 mm. The corresponding  $f$  numbers are approxi-

mately 1.9, 2.3, and 7.3. The light diffracted by the drops is collected by a set of 30 detectors arranged as concentric annuli of rapidly increasing area with diameter. The light intensity decreases rapidly away from the centerline of the system, so a constant diode width would result in a very large signal on the inner rings and a very low, and hence noisy, signal on the outer rings. It can be shown that if the individual diode width is proportional to its midpoint radius, then the detector signals will be of the same order of magnitude. Such a log-scaled detector is used on the Malvern. The resulting detector signals for light scattered from simple sprays when plotted against detector ring number typically form a smooth single peaked function, as shown in Fig. 1a.

The peak signal tends to shift to the outer detector rings (to the right in Fig. 1a) as the spray is made finer, in agreement with the concept that smaller drops diffract light at larger angles relative to the laser axis. Although all the drops in the spray diffract some amount of light onto all the detectors, the peak signal due to drops of different sizes may be matched with the corresponding detector as shown in Table 1, for the 300-mm focal length lens. The 30 detectors are shown as 15 pairs because the computer averages adjacent detectors and then operates on the set of 15 intensity measurements. Evidently it was determined, after the detector was designed, that 15 intensity measurements were sufficient to determine the size distribution and were easier to handle than all 30 data.

Details about the data reduction procedure are proprietary to Malvern and the original paper by Swithenbank et al [1] is not especially enlightening in this area. Of importance to the work described here is the procedure used in the 2-parameter model, that is, to determine an "average" size and width of distribution necessary to specify any one of three preselected distributions—normal, log-normal, or Rosin-Rammler. In addition to the 2-parameter models, a model-independent program is available, but it has not been used with the technique described. Mathematically the 2-parameter model is equivalent to an overdetermined set of 15 data used to determine two parameters. A method for handling this problem is to assume a value for each of the two parameters specifying the drop-size distribution, calculate the corresponding signals at the detector, and compare those with the measured values. By establishing an iteration scheme, the error between the calculated and measured light distributions can be minimized, resulting in a best fit for the two parameters specifying the drop-size distribution. It is important to note that the 15 paired-detector data form an overdetermined set, and fewer data may be used to solve for the two parameters.

### *Evaporating Sprays*

Consider the problems associated with using a Malvern-type drop sizer in an elevated-temperature evaporating spray. Even with no spray present, thermal gradients in the hot air cause density gradients which refract the laser beam in a random high-frequency pattern (called beam steering) resulting in a spurious

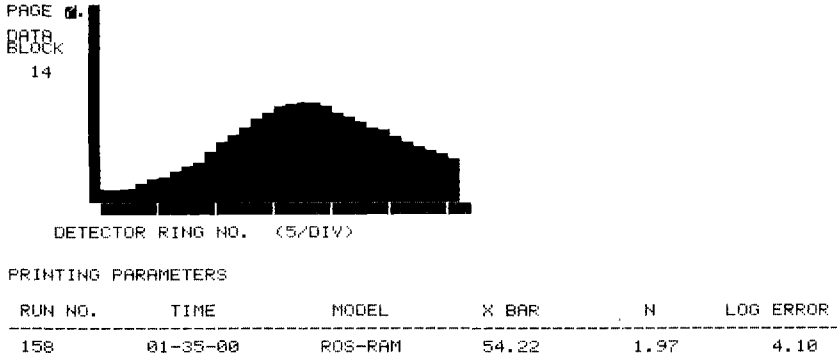


FIG. 1a — Normal light scattering intensity signal on detector array, and drop size data. Left side is for central detectors and right side for outer detectors.

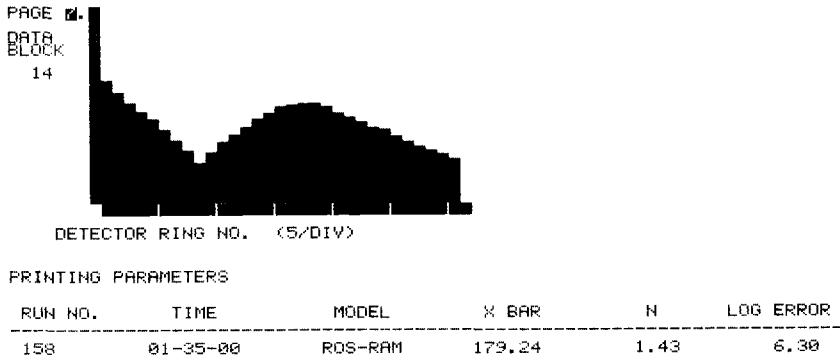


FIG. 1b — Same light intensity distribution as Fig. 1a except innermost eight channels artificially perturbed to simulate beam steering.

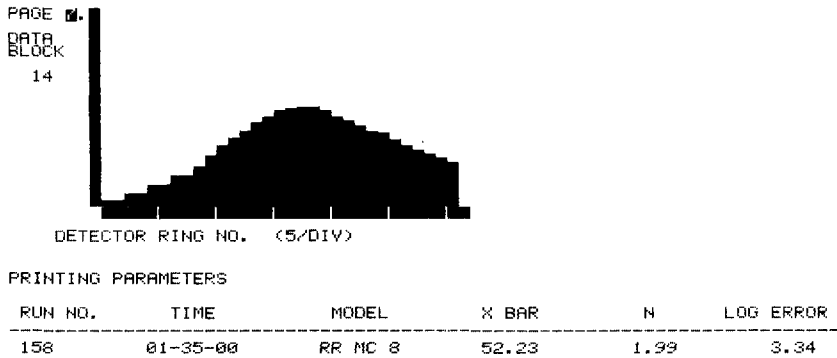


FIG. 1c — Corrected light distribution and drop size data after applying correction technique to data in Fig. 1b.

TABLE 1—*Correspondence between detector number and drop size (300 mm focal length lens).*

Detector Ring Number	Drop Size, $\mu\text{m}$	
	Lower	Upper
1,2	261.6	564.0
3,4	160.4	261.6
5,6	112.8	160.4
7,8	84.3	112.8
9,10	64.6	84.3
11,12	50.2	64.6
13,14	39.0	50.2
15,16	30.3	39.0
17,18	23.7	30.3
19,20	18.5	23.7
21,22	14.5	18.5
23,24	11.4	14.5
25,26	9.1	11.4
27,28	7.2	9.1
29,30	5.8	7.2

signal on the innermost detectors. When the spray is present, additional thermal and concentration gradients are created which result in the first few channels having abnormally large signals. It is not sufficient to subtract out the background when no spray is present to remove the unwanted signal from the inner detectors. The problem becomes more severe in going downstream from the spray nozzle where more of the inner channels are affected by the beam steering. However, the radii of the detectors increase rapidly in going away from the center spot, so the beam steering problems which are severe at any elevated temperature on the first couple of detectors must become much larger in magnitude to progress outward through the next few detectors.

Remembering that the 15 detector pairs form an overdetermined data set, the solution to the beam steering problem is obvious within certain limitations. If only the two or three innermost detectors are involved, their contribution can be ignored by appropriate changes to the software. As more detectors are affected it is still possible to achieve good results if the drop sizes are small enough so that the peak detector signal is located well outside the region of the disturbed channels. This is just a basic limitation from the physics of light-scattering. If the spray consists of many large drops which scatter light onto the inner detector channels, it is not possible to ignore those channels and still arrive at a reasonable drop-size distribution. Thus, the beam steering problems associated with thermal gradients limit the dynamic range of diffraction-based drop sizers on the high end.

This technique can be demonstrated by taking an actual light distribution from a spray, as shown in Fig. 1a, and artificially perturbing the signal in the first eight channels as shown in Fig. 1b. This is analogous to the perturbation caused by the beam steering. Note that the two parameters specifying the Rosin-Rammler

distribution,  $X$  BAR and  $N$ , are drastically altered and the indicated "LOG ERROR", which measures the goodness-of-fit, is significantly increased to an unacceptable value (greater than  $\sim 5.0$  is unacceptable). Hence, these results are useless. However, the original results can be almost duplicated by ignoring the data in the first eight channels and fitting the parameters in the same manner but using only the data from the remaining channels. The "corrected" light distribution and drop-size parameters shown in Fig. 1c are very comparable to that of Fig. 1a; the Sauter mean diameter (SMD) of Fig. 1a is  $30.1 \mu\text{m}$  and for Fig. 1c is  $29.3 \mu\text{m}$ . The Rosin-Rammler distribution has been used for all these measurements.

The same approach is used in cases where the perturbation is caused by beam steering problems associated with thermal gradients, rather than artificial manipulation as in Fig. 1b. It is necessary to make a judgment of how many channels contain spurious data based on the overall shape of the scattered light distribution and the jitter in the real time display of the signals. The jitter associated with beam steering on the inner detectors will be much larger than the normal jitter on the outer channels. An example of an actual light distribution which has been perturbed by beam steering is shown in Fig. 2a. When a drop-size distribution is computed from this light distribution which shows abnormally large contributions on the inner detectors (compare with Fig. 1a), the LOG ERROR is excessively large and the computed drop-size distribution is broad. After recomputing the light distribution based on data in the outer 24 channels, the new "corrected" light distribution is shown in Fig. 2b. For this case, the LOG ERROR is reduced, the computed drop size distribution is narrower (that is,  $N$  is larger), and the light distribution follows the shape expected for scattering from a spray.

There are three things to check to verify that the corrected light distribution is a reasonable one. First the corrected light distribution should show a smooth transition between the outer channels which were used to compute the drop-size distribution and the inner channels, in which the recorded data have been replaced by the new computed light distribution which best fits the overall pattern. Second, there should be at least four or five good detector signals to the left of the peak of the light distribution. When the perturbed detector signals approach the peak of the light distribution, this technique becomes invalid. Third, the LOG ERROR for the corrected light distribution should be less than 5.0.

Obviously the uncertainties associated with this correction scheme increase with the number of detector signals which have to be ignored. Best results are achieved with fairly fine sprays in which the light intensity signal reaches a maximum in the outer half of the detector channels.

#### *Burning Sprays or Sprays in High Ambient Lighting*

In addition to the correction technique for beam steering problems associated with sampling sprays in hot gases, a very effective set of modifications have been developed for discriminating against background radiation, such as flame radi-

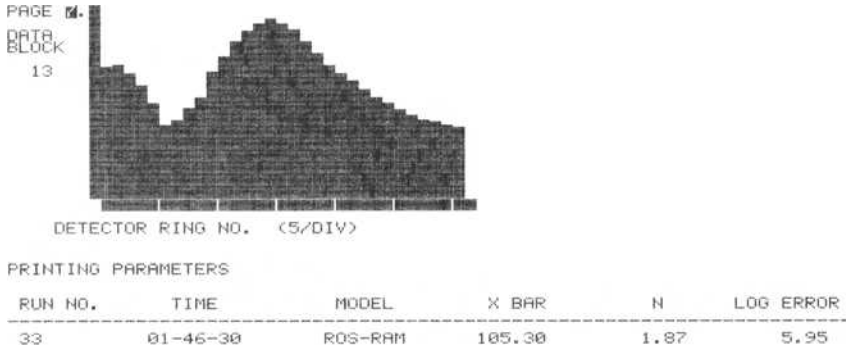


FIG. 2a—Light scattering intensity signal showing beam steering perturbation on inner five or six detectors.

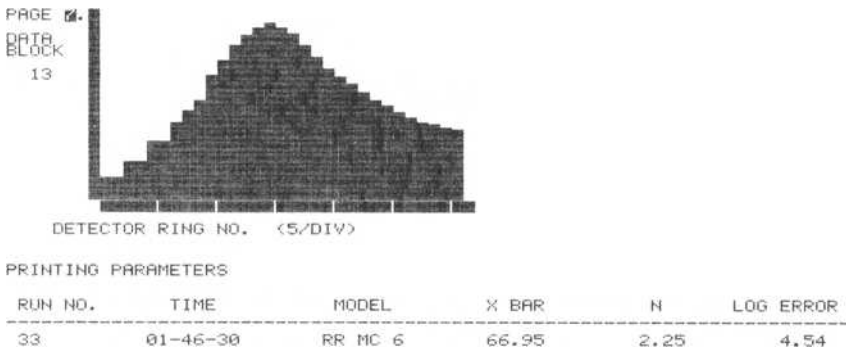


FIG. 2b—Corrected light distribution and drop size data after applying correction technique to data in Fig. 2a.

ation, which may be orders of magnitude more intense than the scattered light from the spray. However, in the case of burning sprays, although flame radiation has been successfully discriminated against, severe beam steering problems have precluded high quality drop-size measurements. A combination of three things has proved necessary to block out high intensity ambient light. First, the laser beam has been chopped and synchronously detected. Note, however, that the edge of the chopper blade produces large spurious signals, due to diffraction, so that it is necessary to sample the detector signal only when the beam is completely blocked or completely transmitting. Alternatively, the laser may be modulated by other methods than mechanical chopping. With the chopping frequency used for this study (667 Hz), it was necessary to slow the multiplexing rate of the electronics (controlled by the computer) so that a reasonable signal could be built up for each channel. That is, the individual detector channels are normally sampled at about 650 to 1200  $\mu$ s intervals in the standard instrument, depending on the

display mode. In order to allow the electronics time to average 20 specimens of the difference between the blocked and unblocked laser scattering signals (on a given channel) which are being sampled at a rate of 1.5 mS per pair of signals (667 Hz), it is necessary to slow the multiplexing rate to 30 mS (1.5 mS  $\times$  20) per detector channel. Thus, an electronic hardware approach is used to integrate the difference signal rather than a software technique, although repetitive scans are software averaged as in the standard instrument. This extends the total time for scanning and displaying the 30 channels of data from 20 or 38 mS to 900 mS, but provides an acceptable signal with fewer scans and eliminates most of the interfering background radiation.

The second modification was the use of a narrow band interference filter centered at the laser wavelength (632.8 nm). The bandpass of the filter is chosen as narrow as possible consistent with the maximum acceptance angle of the lens and detector system. The radiation transmitted by an optical interference filter depends on the angle of incidence of the light. Since the receiving lens must accept light over a range of angles without modifying the intensity, the bandpass must be much wider than the shift of the central wavelength at the maximum acceptance angle. The maximum acceptance angles for the three possible Fourier transform lenses standard to the Malvern are approximately 2.7° for 300 mm focal length, 8.1° for 100 mm focal length, and 12.8° for the 63 mm focal length. (These angles are determined from the maximum detector size rather than the lens apertures.) The effective central wavelength of the interference filter is shifted to a shorter wavelength at angles other than normal incidence according to the relation [2]

$$\lambda_i = \lambda_0(n^2 - \sin^2 i)^{1/2}/n$$

where

- $\lambda_i$  = central wavelength at angle  $i$  measured relative to normal incidence,
- $\lambda_0$  = central wavelength at normal incidence, and
- $n$  = refractive index.

For a refractive index of 2.0, the central wavelength for a 632.8-nm filter is shifted by 0.18, 1.57, or 3.89 nm for the 300, 100, and 63-mm focal length lenses, respectively. The attenuation at 632.8 nm for these higher angles of incidence must not be more than 5% relative to normal incidence or the outer detector rings will suffer too much attenuation relative to the central detectors, and the resultant computed size distribution will be in error on the high side. For an interference filter constructed of two or more periods, the transmission as a function of displacement from the central wavelength drops off to 95% of the central wavelength value at about 0.15 or greater times the full-width half-maximum (FWHM) bandwidth [2]. Thus, the minimum FWHM bandwidths for the interference filters may be calculated as (1/0.15) times the central wavelength shifts calculated above, or, 1, 10, and 26 nm for the 300, 100, and 63-mm focal length lenses, respectively. A 3-nm FWHM bandwidth filter has been used with the 300-mm lens, and an example of the amount of error which is introduced is

as follows. Without the filter the parameters were measured as  $\bar{X} = 41.4$ ,  $N = 1.83$ ,  $SMD = 21.2$ ,  $LOG\ ERROR = 3.95$ , while with the filter in place  $\bar{X} = 40.0$ ,  $N = 1.79$ ,  $SMD = 19.9$ ,  $LOG\ ERROR = 4.80$ . These values are within the precision of the basic instrument, except that the  $LOG\ ERROR$  does substantially increase due to reflections introduced by the filter. Caution must be also used in aligning the filter.

Similar geometrical optical analyses show that the detectors may "see" much radiation that originates outside the area of interest, that is, the intersection of the laser beam and the spray. An aperture of the minimum possible size should be inserted as close to the spray as possible. That size may be computed from the expanded laser beam size ( $\sim 9$  mm), and the acceptance angle of the lens/detector system, as given previously. The aperture size depends on its distance from the lens according to the relationship

$$D_A = D_L + 2(X_0 - X)\tan \theta_{\max}$$

where

$D_A$  = aperture diameter,

$D_L$  = laser beam diameter ( $\sim 9$  mm),

$X_0$  = maximum permissible distance between the lens and any part of the spray before vignetting occurs (336 mm for 300-mm  $f$ , 122 mm for 100-mm  $f$ , and 55 mm for 63-mm  $f$ ),

$X$  = distance from the lens to the aperture, and

$\theta_{\max}$  = maximum acceptance angle given previously.

Even a smaller aperture may be designed if necessary which accounts for the fact that the detectors are semicircles, but the aperture is no longer circular, and its location is not centered on the laser beam axis.

## Conclusions

The usefulness of the Malvern is greatly extended by using the modifications described which allow drop-size measurements in sprays evaporating in hot air. At some location downstream from the nozzle, the techniques described become ineffective due to the degree of evaporation which results in drastic beam steering problems, but useful information may be obtained in many sprays before that point. This allows initial drop-size measurements to be made at conditions much closer to those found in actual combustion systems as opposed to atmospheric conditions. These modifications have permitted drop size measurements in sprays evaporating in air at temperatures and pressures as high as 700 K and 586 kPa.

The modifications described to discriminate against background radiation have proved effective against bright flame radiation. However, severe beam steering problems have prevented the acquisition of reasonable data under these conditions.

### *Acknowledgments*

These techniques were developed under several programs, but principally the Office of Naval Research Contract No. N00014-80-K-0460, technical monitor M. K. Ellingsworth, and Southwest Research Institute Internally Sponsored Research Project No. 10-9172. It is a pleasure to acknowledge the help of technical monitor Mr. M. K. Ellingsworth of ONR and the supervisory role of Dr. C. A. Moses of Southwest Research Institute (SwRI). The electronics were assembled by Mr. H. F. Donoho.

### **References**

- [1] Swithenbank, J., Beer, J. M., Taylor, D. S., Abbot, D., and McCreath, G. C., "A Laser Diagnostic Technique for the Measurement of Droplet and Particle Size Distribution," in *Experimental Diagnostics in Gas Phase Combustion Systems*, B. T. Zinn, Ed., *Progress in Astronautics and Aeronautics*, Vol. 53, p. 421, American Institute of Aeronautics and Astronautics, 1977.
- [2] "Optical Filters, Designers Guide and Catalog," Infrared Industries, Thin Film Products Division, 1973.

Allan J. Ferrenberg<sup>1</sup>

# Liquid Rocket Injector Atomization Research

---

**REFERENCE:** Ferrenberg, A. J., "Liquid Rocket Injector Atomization Research," *Liquid Particle Size Measurement Techniques, ASTM STP 848*, J. M. Tishkoff, R. D. Ingebo, and J. B. Kennedy, Eds., American Society for Testing and Materials, 1984, pp. 82–97.

**ABSTRACT:** This paper describes the need for, application of, and state of the art of rocket engine atomization studies and droplet size measurement techniques that have been applied to liquid rocket engine propellant injectors. In addition, the capabilities of droplet sizing techniques required or desired or both for such atomization studies are discussed. Finally, the results of tests to evaluate droplet sizing interferometry employing the visibility technique and a technique involving both visibility and intensity are discussed.

**KEY WORDS:** atomization, droplet size measurements, droplet size distributions, combustion modelling, droplet sizing interferometry, visibility, liquid rocket engine injectors

## Nomenclature

$A$	Area
$D_{10}$	Number mean droplet diameter
$D_{30}$	Volume mean droplet diameter
$D_{32}$	Sauter mean droplet diameter
$N$	Rate of droplet flow
$V$	Velocity
$X$	Spatial coordinate
$\rho$	Droplet concentration

## Subscripts

$i$  Droplet size group

The design and development of future advanced liquid rocket engines requires the application of improved scientific methods of analysis. Foremost among

<sup>1</sup>Senior combustion specialist, Rockwell International/Rocketdyne Division, Canoga Park, CA 91304.

the analysis methods is the variety of computer codes that model or simulate the various processes that occur. However, the computer codes require that the physical phenomenon being considered be well enough understood to allow the phenomenon to be confidently reduced to a set of mathematical equations.

Liquid rocket combustor codes are utilized to assess various aspects of transient and steady-state performance, spacecraft contamination by ejected propellant droplets, feed system coupled and acoustic combustion stability, and wall effects (for example, propellant accumulation on combustion chamber walls and heat transfer). When properly applied they provide the best available description of these effects. However, there is considerable need for improvement. Modelling of many of the physical processes relies heavily on empirical correlations, and there is considerable extrapolation of test data to conditions very far from those at which the data were obtained.

In liquid rocket engines, the combustion process is generally considered to be primarily evaporation limited, that is, the evaporation of the propellants is the slowest step in the combustion process and, therefore, very important to model correctly. Droplet evaporation rate is a strong function of droplet size and velocity relative to the gas phase. It is possible to write the equations governing the motion and evaporation of a droplet. The forms of these equations and most of the parameters are known fairly well over many operating regimes of interest. The equations are ordinary differential equations that can be readily solved. However, as with all differential equations any such solution requires knowledge of the initial or boundary conditions. And this is the problem—these initial conditions are not well enough known. These conditions are the droplets' size and velocity at the locations where the droplets are formed. Given these initial conditions, the governing equations can be solved, and this is precisely what the combustor codes do. However, errors in the initial conditions produce corresponding errors in the predictions.

This problem has long been recognized, and a number of experimental programs have been performed to establish these initial conditions. Due to the complexity of the physical processes occurring during atomization, these critical initial droplet sizes cannot be predicted a priori. Thus, the experimental results concerning initial droplet conditions are generally characterized by empirical correlations. There is good reason to suspect the quality or applicability of these correlations.

The problem is further complicated by: (1) the inability to perform tests under the extreme conditions existing in a rocket combustor, (2) the need to perform tests with, or simulate, or extrapolate test data to, highly combustible fluids that are often cryogenic (for example, liquid oxygen), (3) the need to simulate and predict the local combustion gas velocity, and (4) the need to often discriminate between droplets of different compositions formed by impingement of streams of two different liquids.

The utilization of such atomization data and correlations in the combustor analysis codes is a major source of difficulty and error. All the major performance

codes in use attempt to use such correlations. In all these cases, it has been found necessary to modify the experimental correlations to force the codes into agreement with large-scale, rocket engine performance tests. Such “calibration” of computer models with the actual hardware they attempt to model is a standard procedure when dealing with complex unknown phenomena—although it is obviously a technique of last resort. The poor performance of these drop size correlations indicates that something is wrong with the measurement techniques, the correlations developed from the measurements, or the manner in which they are applied or all three. The findings of the literature survey described herein provides reasons to suspect all of these. The droplet size measurement capabilities required to support liquid rocket atomization studies and the experience to date with droplet sizing interferometry are also discussed.

### **Survey of Rocket Engine Injector Atomization Studies**

Liquid rocket engine propellant injectors are generally simple, pressure-fed, orifices through which the two reactants separately are introduced into the combustion chamber. Although single stream atomization is occasionally employed, the more common injector elements are of the impinging stream-type or coaxial gas/liquid injectors. The impinging elements consist of two to five impinging streams which may have the same fluid in each stream, or unlike fluids. At least one of the propellants will be liquid. Coaxial injectors consist of a central stream of liquid surrounded by an annular, high-velocity gas stream. The space shuttle main engine (SSME) employs coaxial injectors with a liquid oxygen center stream and an outer stream of hot hydrogen and steam. In general, the environment into which propellants are injected is one of high-temperature combustion at pressures ranging from vacuum to over 30 MPa.

During the period 1955 to 1975, there were a number of experimental programs designed to establish the atomization characteristics of rocket engine injectors. A bibliography and more detailed synopsis of these programs is contained in Ref 1. Since 1975, there has been little support for such research. The great majority of these efforts studied doublet injectors (that is, two impinging streams), especially like doublets (that is, the same liquid in each stream). Nearly all of this work was performed with one of three types of droplet sizing techniques—imaging techniques (for example, photography and holography), droplet freezing techniques (primarily hot wax), and droplet capture techniques (on slides or in immiscible fluids).

All three of these droplet sizing techniques are subject to inaccuracies and questions associated with the basic assumptions employed, their manner of use, or the quantities of data usually obtained. The following discussion is limited to the two techniques most widely used in past rocket engine injector studies—imaging techniques and the hot wax technique. More details can be found in Ref 1.

### *Imaging Techniques*

These include photography and holography and have been the most extensively employed methods for droplet sizing. They offer the advantage of actually "seeing" the droplets as they exist at the point and time where knowledge of their size is desired. Although multiple exposure techniques can be employed to obtain velocity data, none of the experimental efforts surveyed did so. As will be discussed shortly, this velocity information is essential to the determination of temporal droplet size distributions when imaging techniques are employed. Imaging techniques have been employed to measure droplet sizes in reacting flows. This is an important and valuable feature that has apparently been rarely employed in the studies of liquid rocket engine combustors.

A major problem with the use of these early imaging techniques has been the need for human analysis of the images. Although computerized techniques have been recently developed for analysis of photographic images, all of the rocket injector atomization work employed at least some degree of human involvement in the analysis of the droplet images. It is necessary for someone to determine which droplets are to be counted (that is, which droplets are in focus), and in most cases, to manually measure the droplet sizes. This causes errors in two ways—human judgment and insufficient droplet counts to define the spray.

First, at the lower limits of resolutions, the small droplets are less likely to be counted than the larger ones. The smaller droplets are more often out of focus or outside the depth of the field being viewed. Another problem associated with imaging techniques is the time (that is, cost) required to manually identify, count, and measure the droplets. This often prevents the counting of a sufficient number of droplets. The number of small drops may be over 1000 times as great as the number of large ones, and yet these large drops are often the most important to include. In Ref 2, it is calculated that it is necessary to count 5500 droplets to be 95% confident that the Sauter mean diameter (SMD) is correct to within 5%. Rarely are so many droplets counted. More recent imaging techniques have been developed which are automated and count large numbers of droplets.

Perhaps the most important problem associated with past imaging techniques employed for rocket injector atomization studies is that these techniques only measure the concentrations of each size of droplets in a given volume of space (that is, spatial distribution) rather than the temporal droplet distribution. This problem appears to have been neglected in many rocket engine atomization studies.

Many new atomization researchers are unaware of this problem, and the magnitude of the difference between temporal and spatial size distributions is somewhat controversial. ASTM Practice for Determining Data Criteria and Processing for Liquid Drop Size Analysis (E 799-81) defines and describes these two types of measurements and the following may further aid someone attempting to assess the importance of this issue.

In a steady-state, one-dimensional flow of droplets, the number of droplets (and the number of droplets of each size) entering a particular region in space per unit time must be constant. It is possible to write this as a droplet number conservation equation (analogous to a mass conservation equation) as follows

$$N_i = \rho_i A V_i \quad (1)$$

where

$N_i$  = rate of droplets of size group  $i$  entering a region or control volume (drops/s),

$\rho_i$  = local concentration of droplets of size  $i$  (drops/cm<sup>3</sup>),

$A$  = cross sectional area of region perpendicular to the direction of flow, (cm<sup>2</sup>), and

$V_i$  = velocity of the droplets of size group  $i$  (assuming all drops in size group  $i$  are travelling at the same velocity) (cm/s).

Now, the temporal distribution of droplets produced by an injector can be obtained by counting the droplets per second of each size group  $i$  crossing  $A$ , that is, by measuring and comparing the values of the  $N_i$  terms. However, the older imaging techniques measure the local droplet concentrations, that is, the  $\rho_i$  terms, which change as the droplets' velocities change.

To assess the importance of this effect, a brief analytical study was conducted. It was assumed that a known distribution of droplets was being continuously injected axially into a constant and uniform velocity gas stream (Fig. 1). At  $X = 0$ , all droplets have the same velocity, and the temporal and spatial droplet size distributions are the same. However, as the droplets move downstream, aerodynamic drag forces begin to slow them (the gas velocity is less than the droplet injection velocity). Since the small droplets are more rapidly decelerated, and since Eq. (1) must apply at each axial location (this is a steady flow problem), the local droplet concentrations ( $\rho_i$  terms) must each change by different amounts.

A simple computer program was constructed to model this situation. This program computed the motion of each of approximately 20 size groups of droplets under the influence of the aerodynamic forces of the uniform gas velocity. Based upon this motion, the code also computed the droplet concentrations of

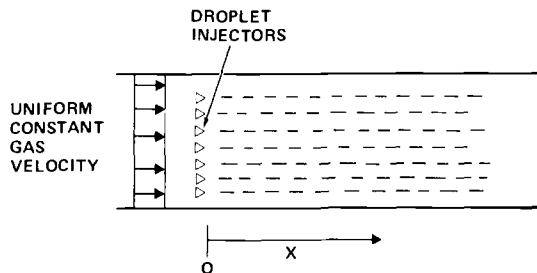


FIG. 1—Droplet distribution analysis—problem geometry.

each size group and the  $D_{32}$ ,  $D_{30}$ , and  $D_{10}$  (refer to ASTM Standard E 799 for definition) of the spray at specified axial locations. [The results of two representative cases are presented in Figs. 2 and 3 (Case 1) and Figs. 4 and 5 (Case 2).] At  $X = 0$ , the droplets all have the same velocity and temporal and spatial distributions, and their temporal and spatial  $D_{32}$ ,  $D_{30}$ , and  $D_{10}$  are the same. As the droplets travel downstream, the smaller droplets are more rapidly decelerated, thereby increasing their concentration. This effect causes the droplet concentrations and derived distributions and representative diameters to vary in the manners shown.

Case 1 models a uniform distribution of high density (for example, liquid oxygen) droplets injected into a gas whose density is comparable to that of a high pressure rocket engine combustor. The droplets injection velocity is 32.6 m/s and the gas velocity is 5 m/s. The smaller droplets are quickly decelerated and at a distance of only 1 cm from the injection point, their concentration has increased by almost an order of magnitude (Fig. 2). The larger droplets are more slowly decelerated. Even at a distance of 15 cm, the uniform droplet size distribution has not yet been restored. The effect on the representative diameters is greatest at about 1 cm and gradually diminishes with increasing  $X$ , as shown in Fig. 3.

Case 2 is a more familiar situation, which models the injection of a more realistic distribution of water droplets into 300 K, 1 atmosphere, air. The liquid injection velocity is 35 m/s and the gas velocity is 2 m/s. The injection rate droplet distribution (that is, the temporal distribution) would be the same as the spatial distribution at  $X = 0$  (Fig. 4). At other downstream locations, the effect of the nonuniform variations in droplet concentration causes the spatial distributions and the representative diameters to vary as shown in Figs. 4 and 5.

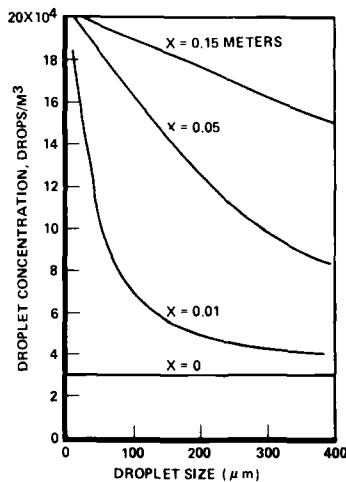


FIG. 2—Case 1 results—droplet concentration versus size at various axial locations.

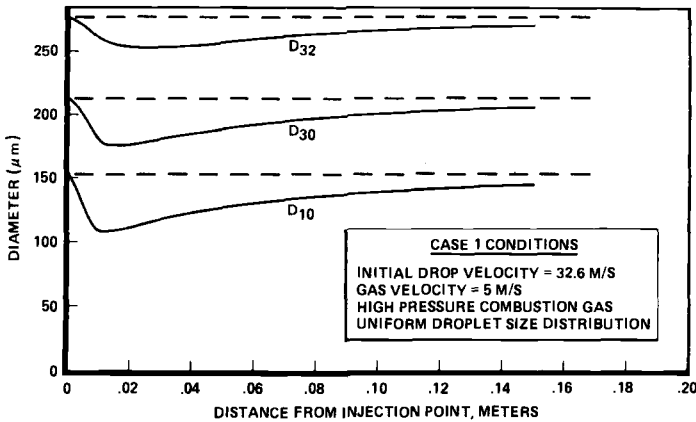


FIG. 3—Case 1 results—representative droplet diameters versus axial locations.

As shown in these two sample cases, spatial distributions and their derived representative diameters vary with the measurement location and may be considerably different than those of a temporal distribution. These different droplet size distributions and their derived representative diameters would be those obtained with a technique which only measured the spatial droplet size distribution. Of course, such idealized situations as these examples rarely occur in nature or experiments. However, this simple analysis indicates that the differences between temporal and spatial distributions can be significant and should be considered in atomization studies.

#### *Hot Wax Technique (Droplet Freezing)*

This technique has been extensively applied in the study of rocket engine injectors. Nearly all of this work directly related to rocket engine injectors was performed at Rocketdyne during the period 1967 to 1975 and utilized wax as the injected liquid. The liquid wax is injected into the atmosphere or a large pressure vessel where the droplets rapidly cool and solidify. They are then collected and sampled. The sample is then subjected to a sieving operation where the wax droplets are separated into size groups. Each size group is then weighed and a plot of droplet mass (volume) versus size is constructed. Thus, the cumulative volume, volume distribution, and mass median diameter are measured directly, without the great time and manpower associated with the sizing and counting of individual droplets. Also, the temporal distribution of droplets is measured, since all the droplets produced by the spray over a long period of time (several seconds) are collected. And finally, the number of frozen wax droplets included in the sample is on the order of millions. This technique does not suffer from a lack of sufficient sample size to be statistically accurate.

The manpower requirements for the hot wax testing, although considerably less than for imaging techniques, is still a significant expense. All the droplets

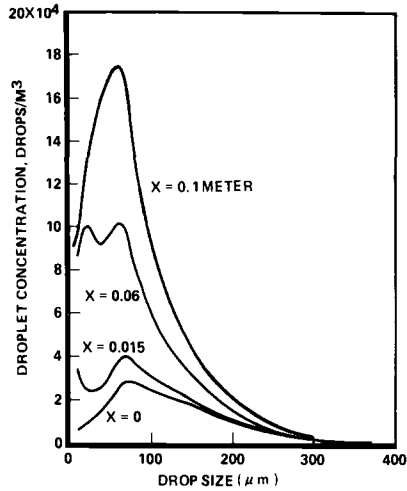


FIG. 4—Case 2 results—droplet concentration versus size at various axial locations.

must be collected, properly sampled, sieved, and the sieves weighed. In addition, the wax preparation facility and injector must be maintained at an elevated temperature (approximately  $95^{\circ}\text{C}$  for most of the Rocketdyne wax test programs). The facility required for the performance of hot wax tests is fairly large and moderately complex and requires a considerable effort to prepare and operate.

One serious disadvantageous feature of the hot wax technique is the limited choice of materials that can conveniently be applied. Since the properties of the actual propellants are different from the simulants, it is necessary to establish the effects of these properties (surface tension, density, and viscosity) on the atomization process. Thus, the capability to perform tests with different fluids having widely varying properties is important. Another feature of the wax technique that merits consideration is the density increase upon freezing. Because of this, some earlier investigators have corrected the wax droplet sizes by multiplying the measured droplets' volumes by the ratio of the solid to liquid densities. However, the physics of the freezing phenomenon indicates that the droplets should freeze on the outside first. If this is correct, then the frozen drops should be hollow and no density change drop size correction is required. Dickerson [3] has discovered that the droplets are indeed hollow, and that the volume of the central void is approximately equal to the size change due to freezing—at least for the larger drops.

One of the most serious criticisms of most of the hot wax investigations involves the problem of defining the temperature (and hence the properties) of the liquid wax during atomization. In most investigations, the hot liquid wax is injected into a relatively cold gas (for example, the atmosphere). For these cases, it is necessary to question whether the wax has cooled significantly prior to the completion of atomization. Zajac [4] presents data showing that the surface

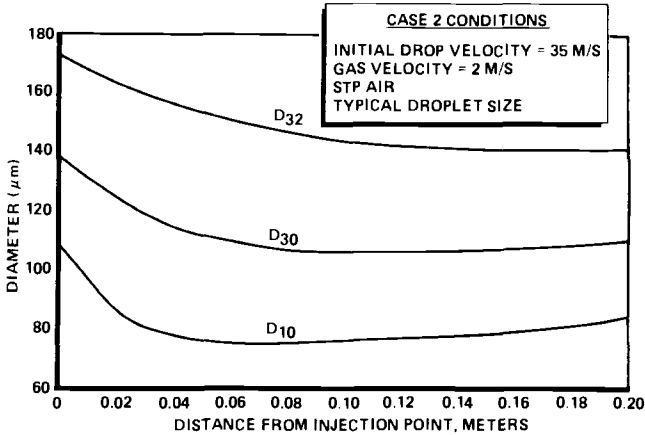


FIG. 5—Case 2 results—representative droplet diameters versus axial locations.

tension and viscosity of the particular wax utilized (Shell 270) increase by 12 and 83%, respectively, between 93°C (the nominal injection temperature) and 66°C (slightly above the wax fusion temperature). Certainly the surfaces of the wax ligaments and droplets must be cooler than the bulk wax injection temperature. Thus, the wax properties at the injection temperature may not be the same as those existing during atomization. Longwell [5] presents results suggesting that the wax technique may give erroneously large droplets due to viscosity increases as the liquid cools during atomization. However, Hasson and Mizrahi [6] present extensive data demonstrating that the wax technique produces significantly and erroneously small droplets.

### Desired Features in a Droplet Size Measurement Technique

To provide the critical droplet size information required by rocket engine combustor computer models, it is necessary to have the following measurement capabilities: First, it is necessary to measure the temporal distribution of droplets in the 10 to 500  $\mu\text{m}$  size range. The codes require the droplet temporal size distribution. The varying spatial distributions can then be computed at downstream stations as, and if, desired. The droplet sizing technique should be nonintrusive, perform satisfactorily when the droplet environment varies from vacuum to very high pressures, and work for droplets of various materials. It would be desirable to have a technique that also provides droplet velocity information, could be used in combusting flows, and has some capability to discriminate between droplets by composition (rocket injectors often employ two different liquid propellants). Also, it is highly desirable that the measurement technique provide the capability to examine the variations in droplet size at different locations within the spray. For studies of regions where droplets are forming or breaking, the capability to measure nonspherical droplets is required. It is also necessary to consider the droplet concentration in choosing a measurement technique.

One other aspect of rocket engine atomization studies that has been often neglected is the motion of the gas into which the liquid is being injected. The work of Ingebo [7] and Zajac [8] have clearly demonstrated the great effect of the gas velocity on droplet size. Representative droplet diameter variations by a factor of three or more have been observed as the gas velocity varies. In some instances, it appears that the local gas velocity is of greater importance than any other parameter, including the type and design of the injector. Unfortunately, this gas velocity is practically unknown in rocket engine combustors, and is rarely measured in atomization experiments. Finally, the gas motion (or lack of motion) existing prior to injection is not that which exists after spraying begins. The droplets transfer momentum with the gas and change the gas motion. There is no such thing as "spraying into still air." This great importance of the gas velocity field on drop size leads to an additional measurement requirement—the need to measure the local gas velocity within the spray.

The primary data desired are the number of droplets of each size versus droplet size. Although representative droplet size for a spray (that is,  $D_{32}$ ,  $D_{30}$ ,  $D_{10}$ , mass mean, etc.) are useful for characterizing sprays, current combustion models are already of sufficient complexity and capability to beneficially employ the greater information available in number versus size distributions. Also, cumulative volume (or mass) versus droplet size data should be very cautiously applied. Such representations of the data can be misleading—especially when the number of droplets counted is relatively small. For example Fig. 6 shows the cumulative volume distribution of data obtained using an imaging technique. The solid line is a "best fit" of a droplet distribution equation, and it appears to describe the data very well. However, the manner in which the data are to be employed in combustion models, and the manner in which the data were obtained, is the number of droplets of each size versus droplet size. That is, the form in which the data were obtained and in which it is most useful is the derivative of the cumulative distribution. If we differentiate the best fit curve of Fig. 6 and plot it against the normalized volume of the droplets of each size (that is, the numerical derivative of the data points shown in Fig. 6), we obtained the results presented in Fig. 7. Now the inaccuracies associated with these data are apparent. Cumulative distributions tend to mask these inaccuracies that are due to an insufficient number of droplets counted (in this example over 400 droplets were counted).

### **Evaluation of the Droplet Sizing Interferometry Visibility Technique**

One technique that offers, or has the potential for, most of the droplet size measurement capabilities previously discussed is droplet sizing interferometry (DSI). Tests were performed to evaluate the performance of this technique in late 1981. This technique is based upon a measurement of the visibility of the signal (the Doppler burst) created by the light refracted through a droplet passing through an interference region (the probe volume) formed by the intersection of two laser beams (Fig. 8). The scattered light is imaged onto a photomultiplier tube located 30 deg off the axis of the intersecting beams. Theoretical analyses,

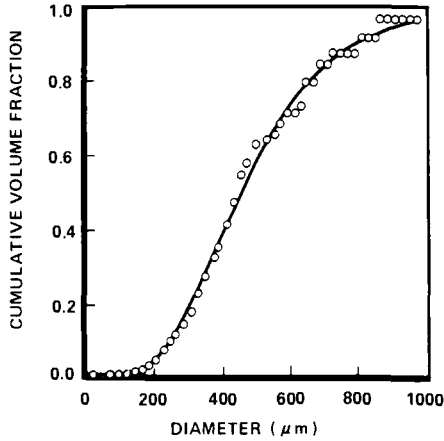


FIG. 6—Normalized cumulative volume distribution.

the particular equipment employed, and earlier work to evaluate this technique, are described in Refs 9 and 10.

To properly evaluate any measurement technique, it is desirable to have a reference or known standard. The measurement of this standard can be then compared with its known, actual value. Unfortunately, such a standard spray does not exist. Thus, this effort was limited to an evaluation of the repeatability and internal consistency of the technique.

A small (approximately 7 L/h) nozzle was set up and operated with low pressure (approximately 200 kPa) water. Measurements of the droplet size distribution were obtained at particular locations within the spray. Measurements designed to test the repeatability of the technique, including the ability to align the optical system, were performed. The results were characterized by the general shape and the mode of the number distribution. These tests indicated that highly repeatable results could be obtained without realignment and that the optical

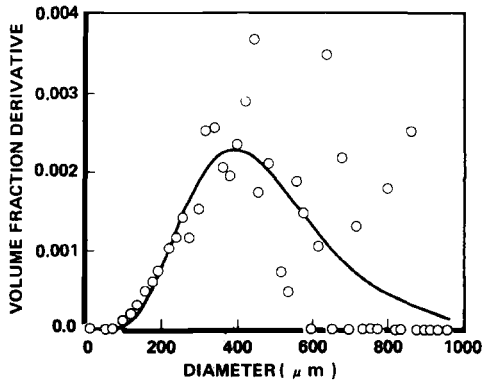


FIG. 7—Normalized volume distribution derivative.

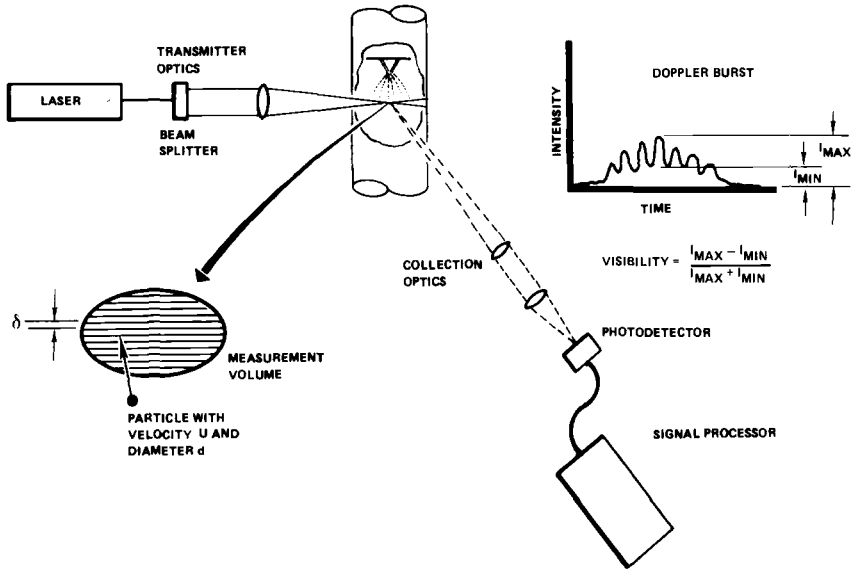


FIG. 8—Droplet sizing interferometry.

system could be realigned and still produce results having the same general shape and mode (to within less than 10%).

Additional tests were then performed to evaluate the effects of the interference pattern fringe spacing on the results. Since the visibility technique is based upon a theoretical relationship between the measured visibility and the ratio of the droplet size to the fringe spacing, it was believed that such a variation of fringe spacing would be a good check on the technique. Accordingly, a number of measurements of the droplet size distribution were made at a selected location within the spray and with several different fringe spacings. The results of these tests demonstrated that the shape and mode of the number distribution was dependent strongly upon the fringe spacing selected. More than twofold variations in the mode of the distribution occurred as the fringe spacing was varied from 6 to 20  $\mu\text{m}$ . Despite the great complexity of this technique, it was concluded that these results were not due to operator error.

Subsequent studies identified the cause of this failure as poor fringe contrast. That is, the fringes formed by the interference of the two intersecting laser beams were not perfectly dark or light. They had become "smeared," so that the dark regions were not totally dark and the bright regions had lower intensity than they should. The effect of poor fringe contrast is to always decrease visibility, that is, to make the droplets appear larger than they are. Although some equipment related problems can contribute to poor fringe contrast, the major cause of poor fringe contrast was found to be due to the passage of drops through the two laser beams prior to their intersection. These droplets attenuate the beams and effect polarization, which results in fluctuating and poorer fringe contrast.

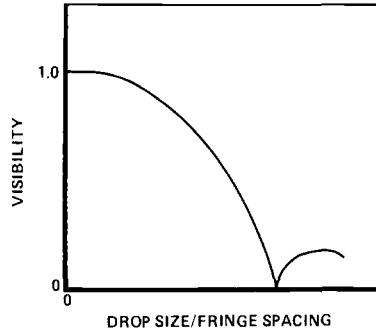


FIG. 9—*Visibility versus relative droplet size.*

### Evaluation of the Droplet Sizing Interferometry Visibility/Intensity Technique

The droplet sizing interferometry (DSI) visibility/intensity (V/I) technique employs a measurement of the intensity of the signal produced by the droplet to check the accuracy of the visibility measurement. Figure 9 depicts the relationship between visibility and droplet size (relative to fringe spacing) that is used to obtain droplet size from the measured visibility. Observe that any reduction in visibility (for example, due to poor fringe contrast) serves to increase the apparent droplet size. Also, in the high visibility region the curve is quite flat and small errors in visibility can cause large errors in measured droplet size.

Figure 10 depicts the relationship between the relative peak intensity of the light scattered from a droplet and the droplet size. This peak intensity is a strong function of droplet size, increasing as the droplet diameter squared. The DSI V/I technique employs a measurement of the relative peak intensity to “check” the visibility measurement. Although fringe contrast, and hence visibility, are occasionally and inconsistently reduced by other transparent droplets in the beams, the intensity of the signal is scarcely affected. As a part of the processing of each droplet’s signal, the measured peak intensity is compared with the measured visibility (that is, the apparent droplet size). If the droplet size was incorrectly measured, based on visibility, then its intensity measurement will be outside of an acceptable range for that visibility. That measurement will then be rejected.

Testing was performed at Rocketdyne to evaluate the capabilities and accuracy of this DSI V/I technique. The results of these tests should be considered preliminary. Considerable additional work is required and is planned. Problems were encountered during this testing that necessitated limiting the measurement ranges, flexibility of the equipment, and capabilities of this technique. The allowable number of fringes within the probe volume and the minimum sizes of the laser beams (and hence the probe volume size) were restricted. In addition, it now appears that the high visibility data (that is, in excess of about 0.95 visibility) is unreliable. This effectively reduces the size range that can be measured to about a factor of 6 for any given fringe spacing. Thus measurements

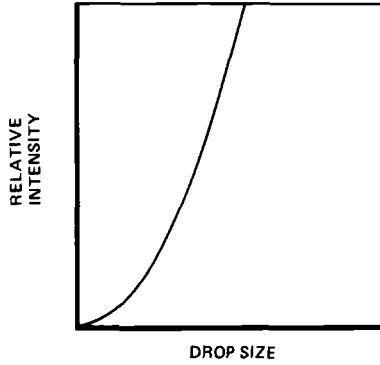


FIG. 10—Relative intensity versus droplet size.

at more than one fringe spacing will be generally required. Combining data for different fringe spacing is an important aspect of data processing. Alignment and operating procedures were developed. These currently require the use of a monodisperse droplet generator.

With proper consideration of the above limitations, very encouraging results have been recently obtained. One such set of results is presented in Fig. 11. These are plots of the time normalized droplet distribution function (droplets counted per unit time per micron of width of the “bins” into which the droplets were counted) versus droplet size. The two plots presented were each constructed from a number of different measurements taken over several different nonoverlapping velocity ranges. Over 4000 droplets were counted to obtain each plot, and droplets of all velocities are included. In comparing such distributions obtained with different bin widths and counted during different length time periods, it is necessary to normalize the results into a droplet distribution function as presented here.

The two plots in Fig. 11 were obtained at two different fringe spacings, each of which covered a different range of droplet sizes. In the overlapping region, the

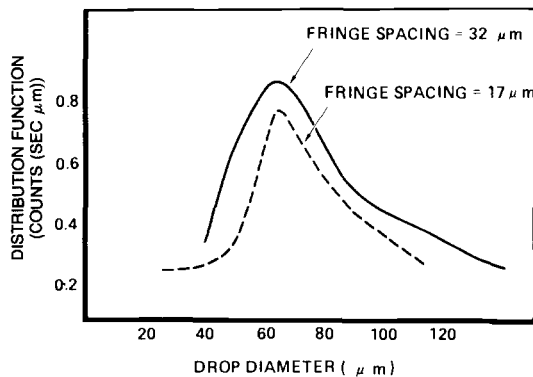


FIG. 11—Droplet distribution functions at two fringe spacings.

data can be compared. The mode of the distributions and the general shape of the overlapping portions of these curves are in good agreement. The rate at which droplets were counted was consistently higher at the larger fringe spacing. This difference is not considered to be of great importance, as only a portion of the droplets passing through the probe volume are counted in either case. These data indicate that the V/I technique does not discriminate against any particular sizes of droplets in choosing those to be counted.

Additional effort is still required before the viability of the DSI V/I technique is proven and the limitations and capabilities defined. Such efforts are underway at Rocketdyne. In addition, the capability to perform atomization testing in high pressure environments (up to 6.3 MPa) is being developed.

### Summary

The state of the art regarding the knowledge of liquid rocket engine injector atomization processes is generally limited. The physics is at best, only qualitatively understood. The available data and correlations are generally of questionable validity or utility or both. Many of the most critical parameters are unknown or are not simulated in tests or both (for example, real propellant fluid properties and combustion gas motion). Perhaps the most critical parameter affecting droplet size is the combustion gas velocity field. This is unfortunate since the detailed velocity field near the injectors in a rocket combustor and in atomization experiments is unknown. This parameter greatly complicates atomization studies and modelling efforts as it couples the processes (and the governing equations) of atomization, droplet combustion, and fluid motion. This poor status of rocket injector atomization studies appears to be attributable to two primary causes: the great complexity of atomization processes, and the inaccuracies, errors, and limitations associated with previous droplet size measurement techniques.

All of the droplet size measurement techniques applied to the study of rocket engine atomization processes have substantial limitations and potential or known sources of error or both. Most imaging techniques measure the spatial distribution that can vary significantly as droplet velocities change and can be significantly different than the temporal distributions. It is the temporal distributions that are required by the rocket engine combustor computer models, and which the droplet freezing (for example, hot wax) and the interferometric techniques attempt to measure.

An interferometric technique employing the principle of visibility was studied and found to be incapable of correctly measuring droplet sizes in a dispersed spray of reasonable density. An improved technique employing both signal visibility and peak intensity has been recently investigated. Some limitations in this technique have been identified, and test procedures have been developed. Preliminary results are limited but encouraging. Additional work is in progress.

### Acknowledgments

The work reported in this paper was performed under a Rocketdyne Independent Research and Development program, "Combustion Diagnostics," and under NASA Contract NAS8-34504, "Atomization and Mixing Study," under the direction of Fred Braam, NASA Marshall Space Flight Center. The evaluation of the DSI droplet sizing techniques was performed with the support and technical advice of Spectron Development Laboratories. Results and conclusions reported herein are only those of the author.

### References

- [1] Ferrenberg, A. and Jaqua, V., "Atomization and Mixing Study, Interim Report," Rocketdyne RD 83-170, Contract NAS8-34504, July 1983.
- [2] Bowen, I. and Davies, G., "Particle Size Distribution and Estimation of Sauter Mean Diameter," Report ICT 28, Shell (London), Oct. 1951.
- [3] Dickerson, R. et al, "Correlation of Spray Injector Parameters With Rocket Engine Performance," AFRPL-TR-68-147, Air Force Rocket Propulsion Laboratories, June 1968.
- [4] Zajac, L., "Correlation of Spray Droplet Distribution's and Injector Variables," Rocketdyne Report R-8455, Contract NAS7-726, Feb. 1971.
- [5] Longwell, J., "Fuel Oil Atomization," D.Sc. thesis, Massachusetts Institute of Technology, 1943.
- [6] Hasson, D. and Mizrahi, J., "The Drop Size of Fan Spray Nozzles: Measurements by the Solidifying Wax Method Compared with Other," Haifa, Israel, *Transactions of the Institute of Chemical Engineering*, Vol. 39, 1961.
- [7] Ingebo, R., "Drop Size Distributions for Impinging Jet Breakup in Airstreams Simulating the Velocity Conditions in Rocket Combustors," NACA TN-4222, National Advisory Committee for Aeronautics, 1958.
- [8] Zajac, L., "Droplet Breakup in Accelerating Gas Flows," NASA-CR-134478 (&9), National Aeronautics and Space Administration, Oct. 1973.
- [9] Bachalo, W., Hess, C., and Hartwell, C., "An Instrument for Spray Droplet Size and Velocity Measurements," ASME 79-WA/GT-13, American Society of Mechanical Engineers, 1979.
- [10] Bachalo, W., "Method for Measuring the Size and Velocity by Spheres by Dual-Beam Light-Scatter Interferometry," *Applied Optics*, Vol. 19, Feb. 1980.

# A Review of Ultrahigh Resolution Sizing of Single Droplets by Resonance Light Scattering

---

**REFERENCE:** Lettieri, T. R. and Jenkins, W. D., "A Review of Ultrahigh Resolution Sizing of Single Droplets by Resonance Light Scattering," *Liquid Particle Size Measurement Techniques*, ASTM STP 848, J. M. Tishkoff, R. D. Ingebo, and J. B. Kennedy, Eds., American Society for Testing and Materials, 1984, pp. 98–108.

**ABSTRACT:** Resonance light scattering as a means for ultrahigh resolution sizing of liquid droplets in the 5 to 50  $\mu\text{m}$  diameter range is reviewed. So far, the technique has been used to make relative size measurements with resolutions of 30 ppm on individual, non-evaporating droplets and 300 ppm on individual, evaporating droplets. The calculated existence of resonances sharper than those observed thus far offers the possibility of size resolutions approaching 0.1 ppm on highly transparent spherical droplets. The paper also reviews the relatively small amount of reported work on resonance light scattering from aerosols and from individual aspheres.

**KEY WORDS:** aerosols, dimensional measurement, drops (liquid), light scattering, particle size, resonance scattering

One of the most promising new techniques for ultrahigh resolution sizing of individual liquid droplets in the 5 to 50  $\mu\text{m}$  diameter range is resonance light scattering. The technique has been already used to make relative measurements of droplet size with resolution approaching 10 ppm [1] and has the potential for making absolute size measurements with comparable accuracy. This is at least two orders of magnitude better than that obtainable with conventional, intensity-versus-angle measurements of Mie light scattering [1].

This paper reviews the status of the technique up to the present, starting with a section on the theory of the resonance phenomenon in light scattered from dielectric spheres. It then reviews how the resonances have been used to determine experimentally the size of individual liquid droplets (both evaporating and nonevaporating) and the mean size of (growing) aerosol droplets. The final

<sup>1</sup>Physicists, National Bureau of Standards, Washington, DC 20234. W. D. Jenkins is also associated with Howard University.

section on resonance light scattering from aspherical droplets is brief, since little work, experimental or theoretical, has been done in this area.

### Spherical Droplets-Theoretical Background

The occurrence of sharp resonance peaks in calculations of light scattering cross sections of nonabsorbing dielectric spheres was first reported by Chylek, Kiehl, and Ko [2]. Using the well-known solutions for Mie scattering, Chylek et al calculated the radiation pressure cross section as a function of size parameter,  $X$  ( $= 2\pi a/\lambda$ , where  $a$  is sphere radius and  $\lambda$  is light wavelength in the surrounding medium). The radiation pressure, as well as all other scattering parameters, depends upon scattering amplitudes  $S_1$  and  $S_2$  defined as

$$S_1(\theta) = \sum_{n=1}^{\infty} \frac{2n+1}{n(n+1)} [a_n \pi_n(\cos \theta) + b_n \tau_n(\cos \theta)]$$

$$S_2(\theta) = \sum_{n=1}^{\infty} \frac{2n+1}{n(n+1)} [b_n \pi_n(\cos \theta) + a_n \tau_n(\cos \theta)]$$

where  $\pi_n$  and  $\tau_n$  are angular functions and  $a_n$  and  $b_n$  are functions of size parameter and refractive index. The calculations of Chylek et al, done with far higher resolution than earlier calculations, revealed several orders of sharp resonances in the scattering spectra. The sharpest resonances, defined as first order, have a halfwidth of  $10^{-7}$  to  $10^{-8}$  for  $X$  about 40, while second-order resonances have a halfwidth of about  $10^{-5}$  in the same size parameter range. Figure 1 shows a plot of the calculated radiation pressure cross section for  $X$  about 60. The dotted lines indicate the positions of the extremely narrow first-order resonances, and the broader second- and third-order resonances are also shown. Note that these calculations were done assuming a perfectly nonabsorbing dielectric; Chylek et al have shown that even a small amount of absorption quickly damps out the resonances [2].

These peaks are the results of resonances which occur only in the individual partial wave scattering amplitudes  $a_n$  and  $b_n$  and not in the  $\pi_n$  and  $\tau_n$  coefficients. The peaks, therefore, do not appear as a function of angle. Also, since the  $a_n$  and  $b_n$  coefficients appear in all scattering cross sections, (for a fixed refractive index) resonances occur at the same values of size parameter in, for example,  $90^\circ$  scattering, backscattering, and the absorption cross section, as well as in the radiation pressure cross section. Experimental measurements of resonance spectra for various output parameters thus can be obtained and compared with calculated results. It should be noted that the size parameter can be varied in these experiments by either changing the incident light wavelength while holding the droplet radius fixed, or by varying the radius (by allowing the droplet to evaporate or grow) while using fixed-wavelength light.

A particularly useful output parameter is the polarization ratio, which is the ratio of the intensity of the light scattered with polarization in the scattering plane to that scattered with polarization perpendicular to the scattering plane. Taking

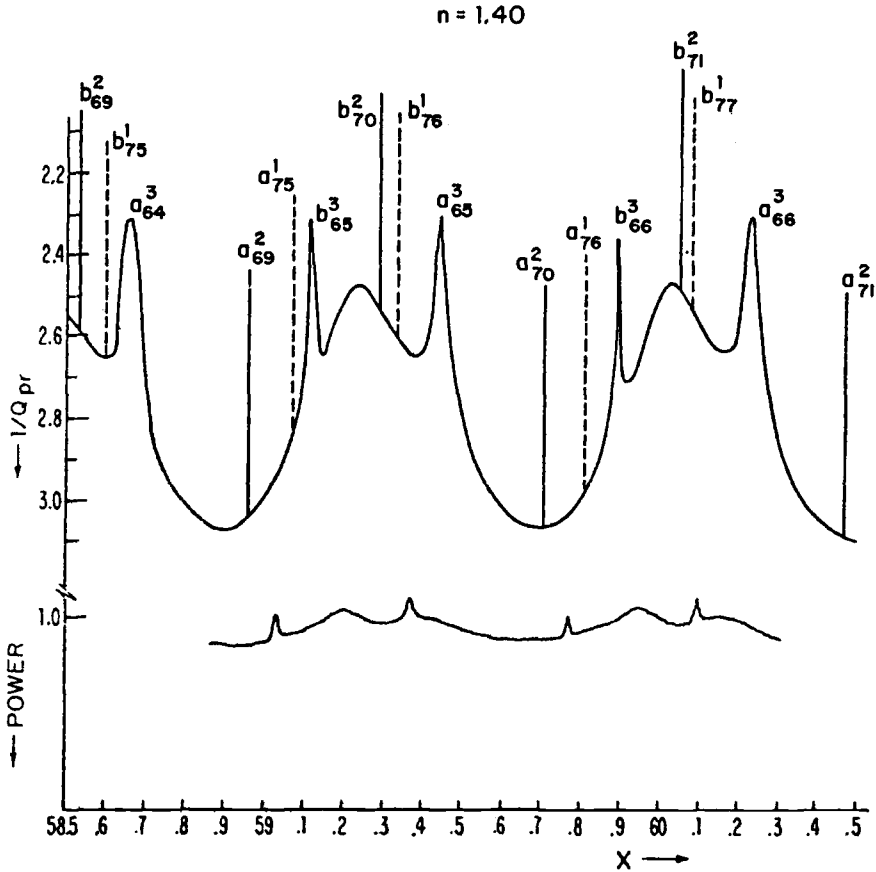


FIG. 1—Upper curve: Calculated radiation pressure cross section for nonabsorbing dielectric sphere of refractive index 1.40. The subscripts and superscripts on the a and b labels refer to the mode and order of the resonance. Lower curve: Experimental results of Ashkin and Dziedzic. The size parameter  $X$  is defined as  $2\pi a/\lambda$ , where  $a$  is the sphere radius and  $\lambda$  is light wavelength in the surrounding medium. Note that the experimental curve is shifted relative to the calculated curve because an inexact diameter was used in the calculations. After Ref. 2.

the ratio of these two intensities makes the appearance of each resonance peak distinctive and facilitates their identification [3].

### Spherical Droplets—Experimental Work

#### *Levitated Single Droplets*

*Optical Levitation*—In order that the resonances may be clearly seen, single droplets must be stably suspended away from the substrate. This is necessary for two reasons: (1) to eliminate the shape-distorting effect of the substrate and (2) to eliminate background light scattering from the substrate. In all of the work reported in this section, the droplets were suspended by optical levitation, which

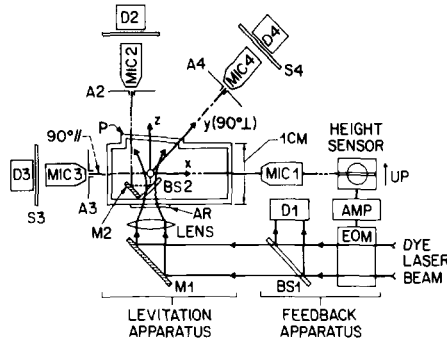


FIG. 2—Schematic diagram of optical levitation apparatus and feedback apparatus, which locks the droplet height. MIC = microscope, D = detector, EOM = electrooptic modulator, AR = antireflection coating, A = aperture, and S = screen. After Ref 1.

uses the radiation pressure of a vertical, focused laser beam to trap and stably hold the droplet near the focus [4,5]. Only a few milliwatts of continuous-wave laser power are required to levitate the smaller droplets (about 5  $\mu\text{m}$  in diameter) and approximately one watt is required for the larger ones (about 50  $\mu\text{m}$  in diameter). The resonances can be then detected in the light scattered from the same beam which suspends the droplet. Alternatively, a laser beam could be scattered from a droplet suspended by the radiation pressure of a second laser beam or by electrostatic levitation. The latter scheme avoids one of the drawbacks of optical levitation, namely, that the locally intense electric fields can heat even a slightly absorbing droplet, causing it to become unstable and, possibly, fall out of the beam.

*Nonevaporating Droplets* — The first experimental observation of resonance light scattering from individual liquid droplets was reported by Ashkin and Dziedzic [6]. Their study showed the existence of sharp resonances in the radiation pressure cross section of silicone oil and index-matching oil droplets ranging in diameter from 4 to 30  $\mu\text{m}$ . A schematic diagram of their experimental instrumentation is given in Fig. 2. An important feature of the instrumentation is the feedback apparatus, which keeps the droplet locked at a fixed height. Since the amount of laser power necessary to levitate a droplet at fixed height is inversely related to the radiation pressure cross section, a plot of radiation pressure as a function of wavelength can be obtained as the dye laser wavelength is continuously varied.

Figure 3 shows their results for a (nominal) 8  $\mu\text{m}$  diameter silicone oil droplet. Since the diameter is constant, the wavelengths at which resonances occur will give the absolute droplet size if high resolution Mie scattering calculations are available. Such calculations were not available to Ashkin and Dziedzic at the time of their experiment. Even without them, however, the relative sizes of two droplets could be very precisely determined by comparing the wavelengths of equivalent resonances. In this way, Ashkin and Dziedzic were able to distinguish diameter differences of 30 ppm (0.4 nm) between two droplets. In addition,

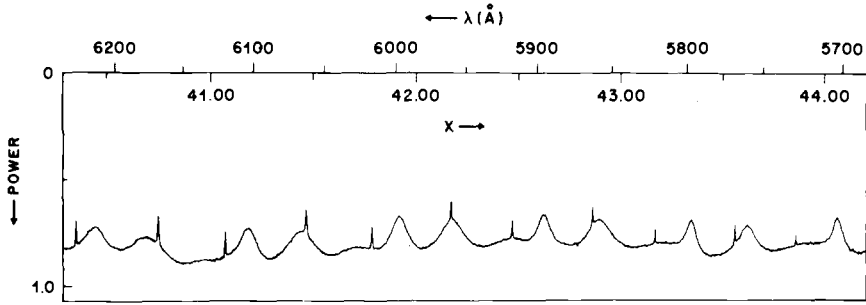


FIG. 3—Measured laser power for levitation versus wavelength ( $\lambda$ ) and size parameter ( $X$ ) for a nominal  $8 \mu\text{m}$  diameter silicone oil droplet. After Ref 6.

without calculations, very small changes in diameter (about 2 ppm) of a nominally fixed-diameter droplet were measured by tuning the laser wavelength to an edge of a resonance and then monitoring the output parameter (radiation pressure,  $90^\circ$  scattering, etc.) as a function of time.

The previously mentioned computer calculations of Chylek et al [2] were later compared with the experimental results with good qualitative agreement. However, the experimental resolution was not sufficient to show the two sharpest orders of peaks appearing in the calculations (see Fig. 1).

In addition to radiation pressure cross-section resonances, Ashkin and Dziedzic have also observed backscattering and  $90^\circ$  scattering resonances in light scattered from fixed-diameter silicone oil droplets as a function of laser wavelength. Typical data are shown in Fig. 4 [1].

In all of the previously mentioned experiments with nonevaporating droplets, only qualitative matches between calculated and experimental resonances were made as a way to determine the (approximate) droplet size. A more accurate determination would involve finding a value of droplet diameter which minimizes the error between calculated resonance values obtained as a function of size parameter and those obtained from experimental data as a function of wavelength.

*Evaporating Droplets* — As mentioned in the theory section, resonances can be also observed in light scattered from evaporating or growing droplets, the laser wavelength in this case being held constant. Results of Lettieri, Jenkins, and Swyt for evaporating glycerol droplets are shown in Fig. 5 [3]. Here, the experimental resonances which occur in the polarization ratio as a function of time can be matched with the calculated resonances which occur as a function of size parameter. The instantaneous droplet diameter can then be obtained with very high resolution; for the droplets of Fig. 5, the instantaneous resolution was about 300 ppm (3 nm). An expanded view of a section of Fig. 5 is given in Fig. 6, and a schematic diagram of the experimental apparatus is shown in Fig. 7.

Note that the technique could be also used to measure the droplet evaporation rate if the effects of the laser beam (heating, etc.) are taken into account. The evaporation rates of glycerol droplets reported by Lettieri et al ranged from 3 to

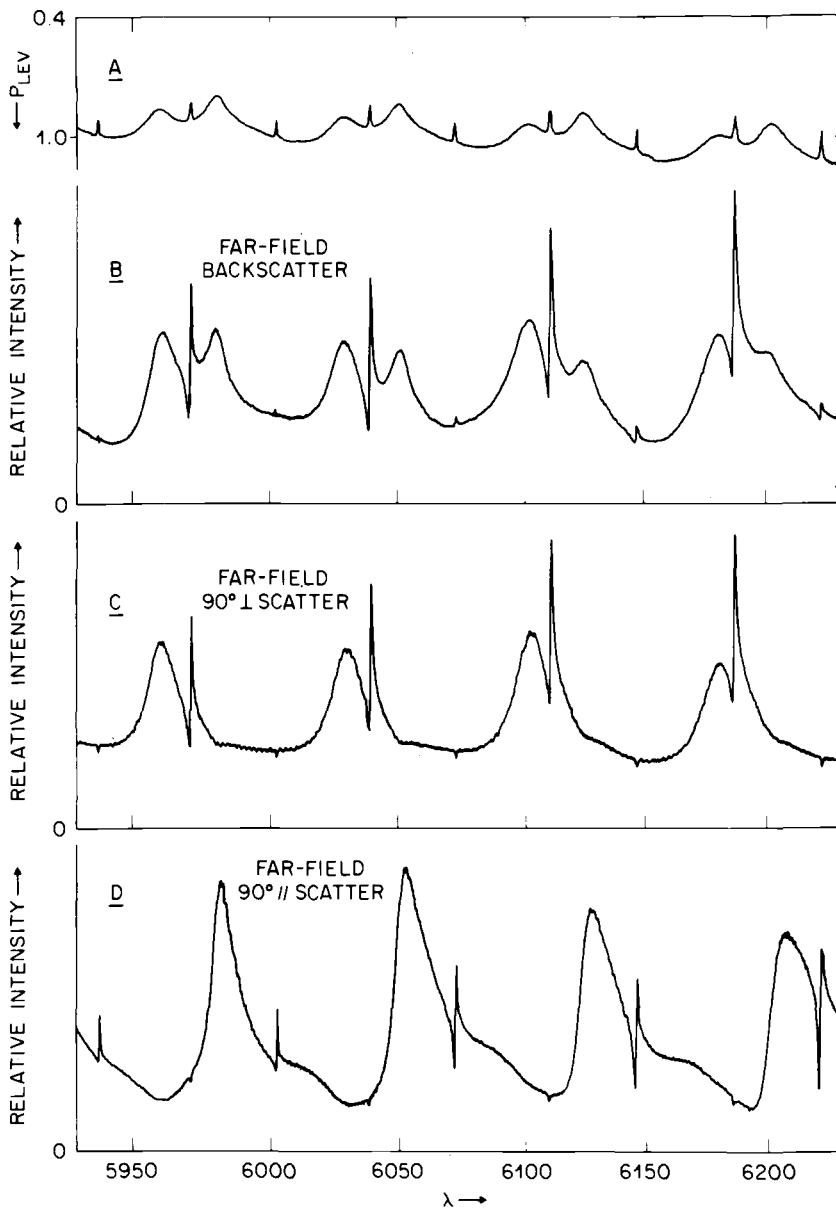


FIG. 4 — Wavelength dependence of four light scattering parameters: (A) laser power for levitation, (B) far-field backscattering, (C) far-field  $90^\circ$  perpendicular scattering, and (D) far-field  $90^\circ$  parallel scattering. Nominal diameter for the silicone oil droplet is  $11.4 \mu\text{m}$ . After Ref 1.

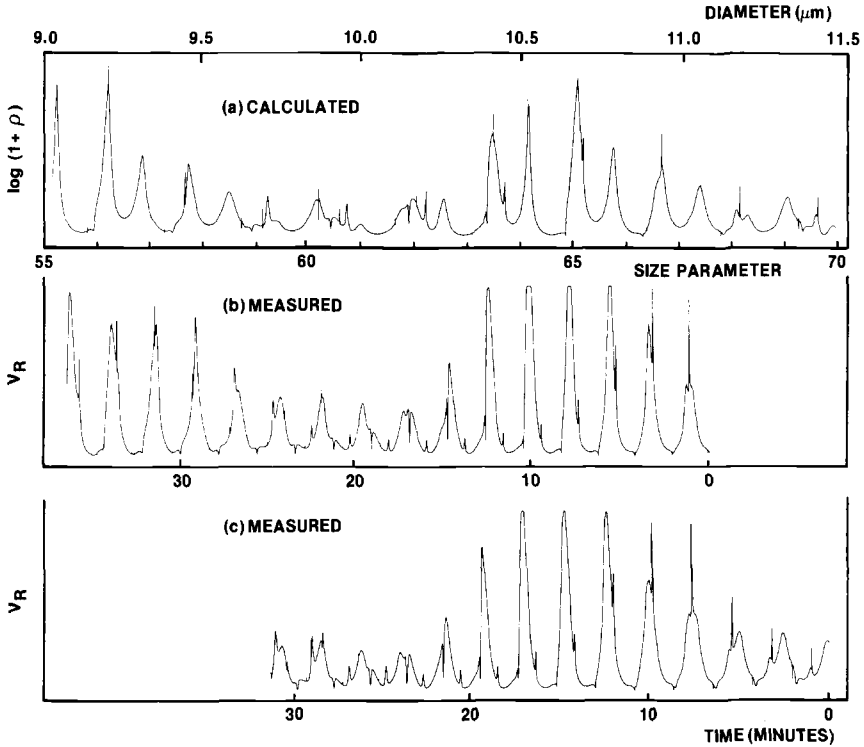


FIG. 5—Polarization ratio plots for two droplets in the 9.0 to 11.5  $\mu\text{m}$  diameter range. (a) calculated curve for lossless dielectric sphere of refractive index 1.47; (b) and (c) experimental curves for two different evaporating glycerol droplets. After Ref 3.

5  $\mu\text{m}/\text{h}$  under normal atmospheric conditions to as slow as 0.6  $\mu\text{m}/\text{h}$  in a saturated atmosphere.

Resonances from evaporating droplets have been also observed in the radiation pressure cross section [1]. Figure 8 shows the experimental results for a droplet of index-matching oil which decreased from 11.9 to 9.8  $\mu\text{m}$  in diameter in about one hour.

### Aerosols

Most of the resonance light-scattering work reported so far has been done with individually levitated liquid droplets. However, one recent paper by Szymanski, Pohl, and Wagner has reported the experimental observation of light-scattering resonances from a narrow-distribution aerosol of growing water droplets [7]. A plot of the light flux scattered at  $15^\circ$  from the forward direction by the aerosol is shown in Fig. 9.<sup>2</sup> The lower, calculated curve can be compared with the upper,

<sup>2</sup>Note the millisecond time scale for the water droplets as compared to the tens-of-minutes time scale for the glycerol droplets of Fig. 5.

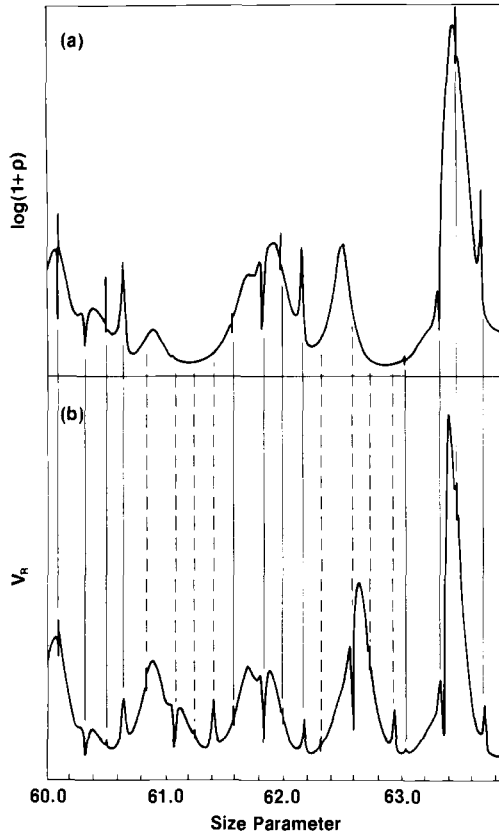


FIG. 6—Expanded view of Fig. 5 in region from  $X = 60$  to  $64$ . (a) calculated; (b) measured. Solid lines indicate resonances which appear in both sets of data. Dotted lines indicate resonances which appear only in experimental data. After Ref 3.

experimental curve and an unambiguous assignment made between the two sets of resonance features.<sup>3</sup> The mean size of the distribution as a function of time can be then obtained. It should be noted that in order to observe the resonances, the droplet size distribution must be kept very narrow. In the present case, distribution width varied between 0.6 and 2.4%.

**Aspherical Droplets**

Because an exact solution is available for scattering from spherical droplets, a comparison of calculated and experimental resonance spectra can be made. For aspherical particles, such exact solutions do not exist; however, two methods are frequently used to calculate scattering for particular nonspherical shapes. The

<sup>3</sup>The fact that the abscissa scales are not aligned is a result of the nonlinear growth with time of the mean droplet diameter.

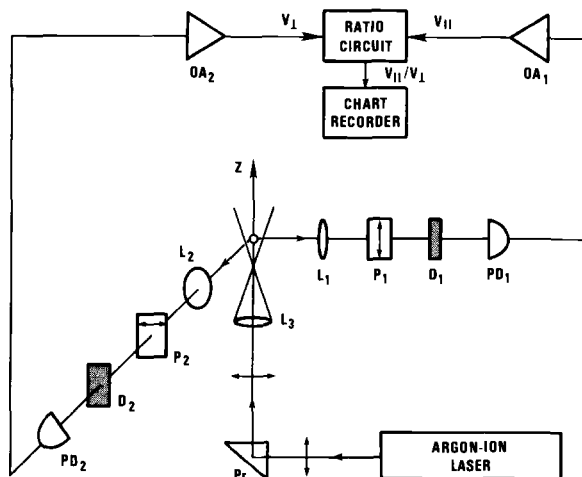


FIG. 7—Experimental apparatus for droplet sizing by detection of polarization ratio resonances. Arms 1 and 2 collect and detect scattered light polarized, respectively, parallel and perpendicular to the scattering plane.  $L$  = lens,  $P$  = polarizer,  $D$  = diffuser,  $PD$  = photodiode, and  $OA$  = operational amplifier. After Ref 3.

first, the Extended Boundary Condition method [8], has been very useful for size parameters less than ten. In the resonance region, however, calculations using this method are prohibitively long, and the series convergence of the calculations is in doubt [9]. The second approach, the perturbation method [10], is appropriate for those shapes which vary only slightly from sphericity. A preliminary study by Kiehl, Ko, Mugnai, and Chylek [11] compared perturbation calculations with more accurate Extended Boundary Condition calculations for small values of size parameter. Agreement between the two sets of calculations was poor, particularly near resonances. In this study, however, no effort was made to optimize the selection of an unperturbed radius to improve agreement, and the calculations were done only to first order. A perturbation expansion chosen particularly to yield good results at resonance and carried out to higher order should be more accurate.

Experimentally, no work has been reported on resonance light scattering from aspherical droplets, although Ashkin and Dziedzic have unpublished results showing shifts in resonances from electrostatically distorted droplets [1]. In addition, they have been successful in optically levitating spheroidal particles which were assembled from quartz microspheres surrounded by index-matching oil [12]. No attempt was made, however, to observe resonance light scattering from these particles.

## Conclusion

Resonance light scattering affords to the researcher an opportunity for studying liquid droplets with unprecedented size resolution. This capability should prove

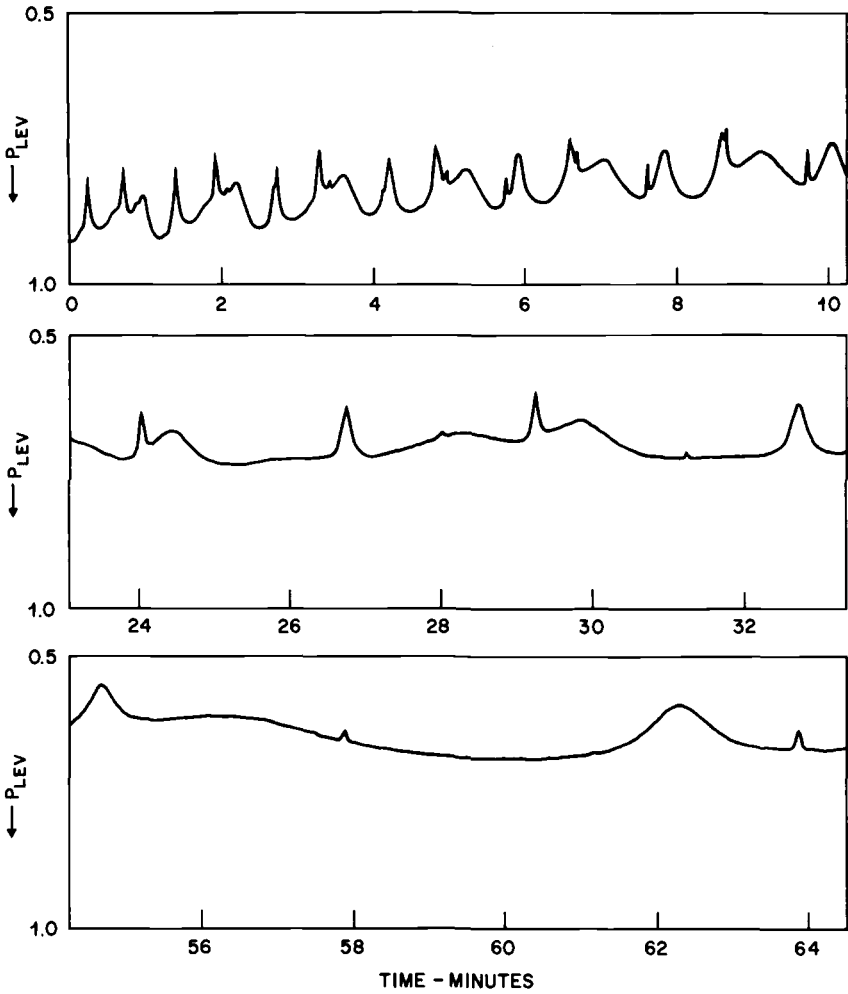


FIG. 8—Laser power to levitate versus time for an evaporating droplet of index-matching oil. After Ref 1.

useful in numerous studies of droplets and droplet physics, in the measurement of diffusion coefficients and in studies of aerosol growth and evaporation.

**References**

[1] Ashkin, A. and Dziedzic, J. M., *Applied Optics*, Vol. 20, No. 10, May 1981, pp. 1803–1814.  
 [2] Chylek, P., Kiehl, J. T., and Ko, M. K. W., *Physical Review A*, Vol. 18, No. 5, Nov. 1978, pp. 2229–2233.  
 [3] Lettieri, T. R., Jenkins, W. D., and Swyt, D. A., *Applied Optics*, Vol. 20, No. 16, Aug. 1981, pp. 2799–2805.  
 [4] Ashkin, A. and Dziedzic, J. M., *Science*, Vol. 187, March 1975, pp. 1073–1075.  
 [5] Ashkin, A. and Dziedzic, J. M., *Applied Physics Letters*, Vol. 30, No. 4, Feb. 1977, pp. 202–204.

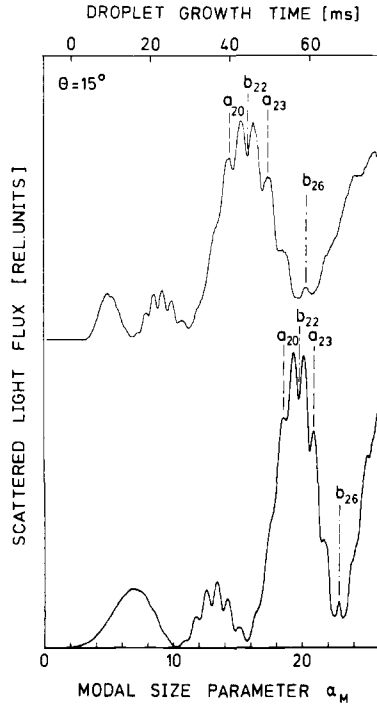


FIG. 9—Upper curve shows experimental results for light flux scattered at  $15^\circ$  from growing aerosol droplets versus growth time. Lower curve is calculated light flux for actual droplet size distribution as a function of modal size parameter. After Ref 7.

- [6] Ashkin, A. and Dziedzic, J. M., *Physical Review Letters*, Vol. 38, No. 23, June 1977, pp. 1351–1354.
- [7] Szymanski, W., Pohl, F. G., and Wagner, P. E., *Journal of Colloid and Interface Science*, Vol. 85, No. 1, Jan. 1982, pp. 289–301.
- [8] Barber, P. and Yeh, C., *Applied Optics*, Vol. 14, No. 12, Dec. 1975, pp. 2864–2872.
- [9] Mugnai, A. and Wiscombe, W. J., *Journal of Atmospheric Science*, Vol. 37, No. 6, June 1980, pp. 1291–1307.
- [10] Erma, V., *Physical Review*, Vol. 179, No. 5, March 1969, pp. 1238–1246.
- [11] Kiehl, J. T., Ko, M. W., Mugnai, A., and Chylek, P., in *Light Scattering by Irregularly Shaped Particles*, D. W. Schuerman, Ed., Plenum Press, New York, 1980, pp. 135–140.
- [12] Ashkin, A. and Dziedzic, J. M., *Applied Optics*, Vol. 19, No. 5, March 1980, pp. 660–668.

# **Particle Sizing with Imaging Techniques**

Brian J. Thompson<sup>1</sup>

## Droplet Characteristics with Conventional and Holographic Imaging Techniques

---

**REFERENCE:** Thompson, B. J., "Droplet Characteristics with Conventional and Holographic Imaging Techniques," *Liquid Particle Size Measurement Techniques*, ASTM STP 848, J. M. Tishkoff, R. D. Ingebo, and J. B. Kennedy, Eds., American Society for Testing and Materials, 1984, pp. 111-122.

**ABSTRACT:** The basic parameters of both single lens imaging and two-lens imaging systems are discussed with particular emphasis on resolution and depth of field. Holographic methods of imaging particulate volumes are described and illustrated together with some current examples. The extension of the holographic method to the simultaneous measurement of both size and velocity is included.

**KEY WORDS:** image formation, holography, total diffraction measurement

The various methods of image formation and detection have long been used in droplet size and cross-sectional shape analysis and can provide a satisfying result, since the image can be directly viewed and the size and cross-sectional shapes of individual droplets determined from these recorded images. In addition, with multiple frame recording, velocity information can be also obtained. Image forming methods are direct methods as opposed to the many other excellent techniques including diffraction, scattering, resonant scattering, interferometry, etc., which are all essentially indirect methods even though they may depend upon fundamental principles that do not require calibration except that the peripheral equipment used with these methods does, in fact, necessitate calibration. The human observer is always inclined to believe what is seen and is suspicious of what is inferred! With today's techniques that automate the imaging process, the human viewer is out of the loop, but nevertheless a visual image still can be retrieved in case you do not like the answer obtained by the automated methods. This may not be a problem for the next generation, since they will probably believe any number as long as it is given in eight or ten digits on a display!

<sup>1</sup>Dean, College of Engineering and Applied Science, University of Rochester, Rochester, NY 14627.

In this short review, some comments are made on the conventional imaging methods using both one- and two-lens systems with both incoherent and coherent incident illumination of the droplets. The properties of these systems, including resolution, depth of focus, depth of field, and field of view, are discussed. Automated readout systems that operate on the image produced by these imaging systems are now available from a variety of sources. Film is no longer necessarily the preferred recording medium, and recording with television (TV), vidicons, and computer-controlled display (CCD) cameras is becoming popular. However, it should be remembered that it is very hard to beat film as a storage medium because of the large number of resolution elements available per frame.

Diffraction (small angle forward scattering) systems are mentioned, since they can be used not only for near real-time measurement applications but also for readout techniques for holographic systems. The nonconventional imaging systems using in-line and off-axis holography have a valuable role to play in the field of liquid aerosol characterization; hence some attention will be given to these systems and the current state of the art. Finally, some comments are made on the possibilities of automated readout from the holographic record and the extension of the holographic method to simultaneous size and velocity distribution measurements using multiple pulse techniques and automated readout.

### **Conventional Imaging Systems**

Conventional imaging methods continue to be a major tool in liquid particle size measurement, particularly as new technology is added to the fundamental optical techniques of image formation. Direct photography, either still or movie, is the classical method used with either a camera lens or a microscope. This allows one plane at a time to be imaged with exposure times down to a microsecond with short duration flashlamps or a nanosecond or less with pulsed lasers. The high resolution and very large storage capacity of film is, of course, a major advantage. Current laser technology can provide even shorter durations of picoseconds. Chigier [1] has discussed a number of issues related to direct imaging and has commented upon the use of video recording and TV scanning methods of data analysis. Some fundamental comments about the optics of imaging subsystems are in order here, since the optics are a common component of such systems, which vary in how the image is recorded, stored, and analyzed. It is important to remember that the performance is determined by the optical subsystem, and the remainder of the system can only degrade that performance. The word performance will be interpreted to include such parameters as spatial and temporal resolution, depth of focus, depth of field, field of view, etc.

#### *Single Lens Imaging*

The basic parameters of a single lens imaging system are defined in Fig. 1. The lens is drawn here as a simple lens, but, in fact, it will really be a multi-element lens as in a camera. The comments to be made, however, do relate to these real

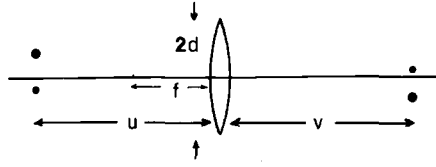


FIG. 1—Schematic diagram of a one-lens imaging system.

optical systems. The important parameters for a diffraction-limited system operating with incoherently transilluminated or front illuminated objects follow. It should be noted that aberrations will further degrade these parameters. Narrow band light is assumed and hence polychromatic light will again degrade the parameters unless the lens system is achromatic.

Resolution in image space	$R_i = \frac{1.22v\lambda}{2d}$
(half width of impulse response)	
Magnification (variable)	$m = v/u$
Depth of focus	$\Delta v = 2R_i^2/\lambda$
Resolution in object space	$R_o = \frac{1.22u\lambda}{2d}$
Depth of field	$\Delta u = 2R_o^2/\lambda$
Effective $f\#$ in object space	$f_o\# = \frac{u}{2d}$
Effective $f\#$ in image space	$f_i\# = \frac{v}{2d}$
Working range (magnified image)	
object space	$2f > u > f$
image space	$2f < v < \infty$

It will be noted that in this parameter set, the object and image space parameters are simply related by the magnification. The working range is defined by assuming that a system with magnification is desired.

Figure 2 shows a plot of the resolution as a function of effective  $f\#$ . The diagram can be interpreted as either  $R_i$  against  $f_i\#$  or  $R_o$  against  $f_o\#$ . The curves are for three different wavelengths of 600, 500, and 400 nm, respectively, and the curves are not plotted below the effective  $f\#$  of unity. Small  $f\#$ 's can be obtained, of course, with high power microscope objectives. It will be seen from the plot that while droplets of a micrometer or two can be detected, they cannot be sized accurately; but, a 5  $\mu\text{m}$ -diameter droplet can be measured with an accuracy up to  $\pm$  a micrometre. It will be also recognized that as the  $f_o\#$  gets smaller, the focal length will usually decrease; hence the working range becomes very small.

Figure 3 shows the depth of focus as a function of  $f_i\#$ . The working range, of course, is defined by the space under the curve. The diagram can be also used to

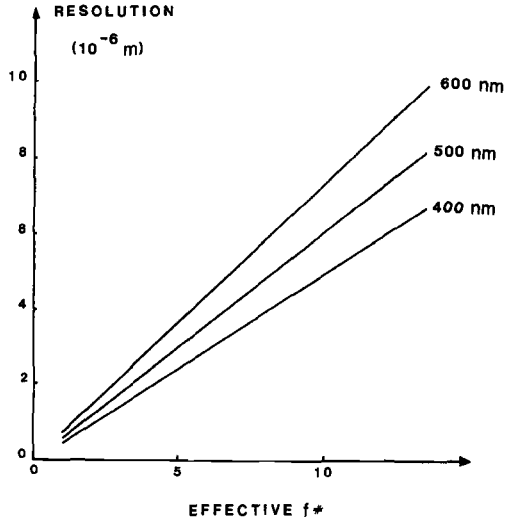


FIG. 2—Resolution as a function of  $f\#$ . This is a plot of  $R_0$  or  $R_1$  against  $f_{0\#}$  or  $f_{1\#}$ , respectively.

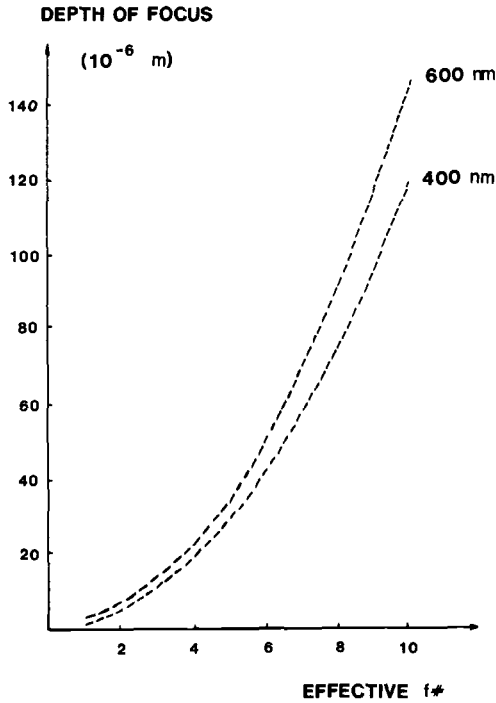


FIG. 3—Depth of focus as a function of  $f_{1\#}$ . The figure can also be interpreted as depth of field as a function of  $f_{0\#}$ .

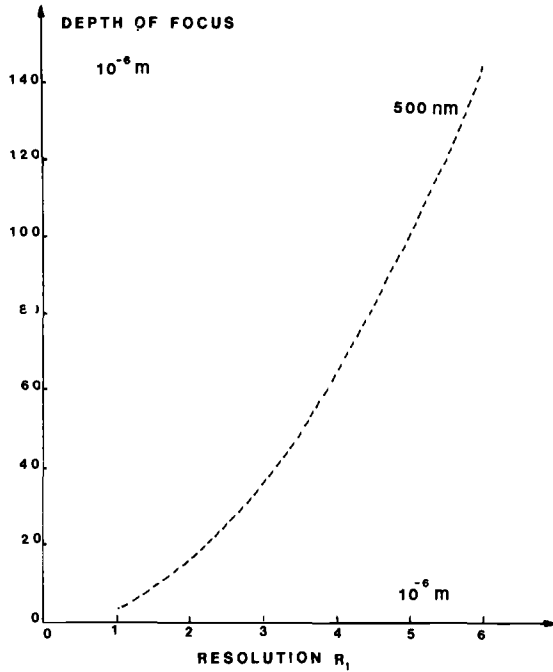


FIG. 4—Depth of focus as a function of resolution  $R_1$ .

determine the depth of field by merely relabeling the vertical axis as such and the horizontal axis as  $f_o\#$ . Finally, Fig. 4 shows the depth of focus as a function of resolution  $R_f$ . Again, the chart can be also used as a graph of depth of field as a function of  $R_o$ , and the working parameters lie in the space under the curve.

Since the depth of focus varies as the resolution squared, it provides an advantage in setting up imaging systems; however, that is a two-edged sword, since the exact image plane is, therefore, harder to determine and the magnification can be in error since it varies with the object, and hence the image, position. This error then becomes a systematic error in the size measurement.

*Two-Lens Imaging Systems*

Further magnification can be always added to the single lens system described previously, by adding a relay lens. However, the resolution, depth of field, etc., will be determined by the first lens. There is one particular system that has some special properties that make it worth consideration, and this system is shown in Fig. 5. The two lenses are separated by the sum of the focal lengths, and the system has the property that the magnification is constant over the range of object positions that produce a real image. This important property can remove the error associated with the single lens system. The parameters of this system where they

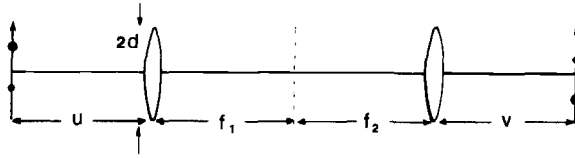


FIG. 5—Two-lens imaging system.

are different from the single lens system are:

<i>Resolution in image space</i>	$R_I = \frac{1.22v\lambda}{m2d}$
<i>Magnification</i>	$m = f_2/f_1$
<i>Working range</i>	
object space	$0 < u < f_1$
image space	$\infty > v > f_2$

### *Imaging Systems with Coherent and Partially Coherent Illumination*

Systems that use either coherent or partially coherent illumination have been studied in some detail for the diffraction limited case [2]. The edge sharpness (that is, acutance) is improved, which can be an advantage; however, mensuration errors can occur unless the square root of the image intensity is taken by controlling the effective  $\gamma$  of the recording process, where  $\gamma$  is the slope of the straight-line segment of the density versus the log exposure curve for the recording process. For systems other than completely incoherent, it is advisable to consider apodisation<sup>2</sup> of the aperture of the imaging system [3]; this technique ensures that the amplitude impulse response is real and positive and controls the edge ringing phenomenon that occurs when diffraction limited systems are used with coherent illumination.

The two-lens system shown in Fig. 5 is particularly important when used with coherent illumination of the input. It is the optical processing or spatial filtering system. The intermediate plane between the two lenses is the Fourier plane associated with the input (that is, the Fraunhofer diffraction plane). The intensity distribution in this plane is invariant with lateral or longitudinal position of the input and can be modified in amplitude and phase to change the nature of the final image. This method could have some value in droplet characterization but has not been used for that purpose.

### **Total Diffraction Measurements**

The total system of Fig. 5 has not found use as a spatial filtering system in droplet characterization, but the first half of the system is very important as a technique in size measurement. Figure 6 shows the preferred technique for using

<sup>2</sup>The process of apodisation comes from the Greek  $\alpha$ , to take away, and  $\pi\omega\delta\omicron\zeta$ , foot. Initially the process was used in incoherent systems to eliminate the side-lobe structures in the intensity impulse response. Today it refers to any modification of the transmittance function of a system.

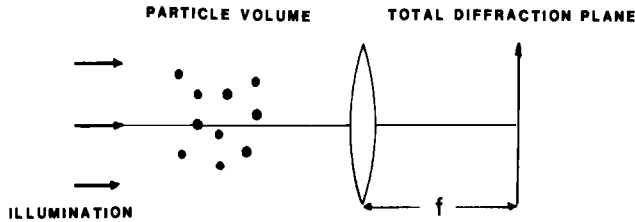


FIG. 6—Basic optical principle of the total diffraction technique.

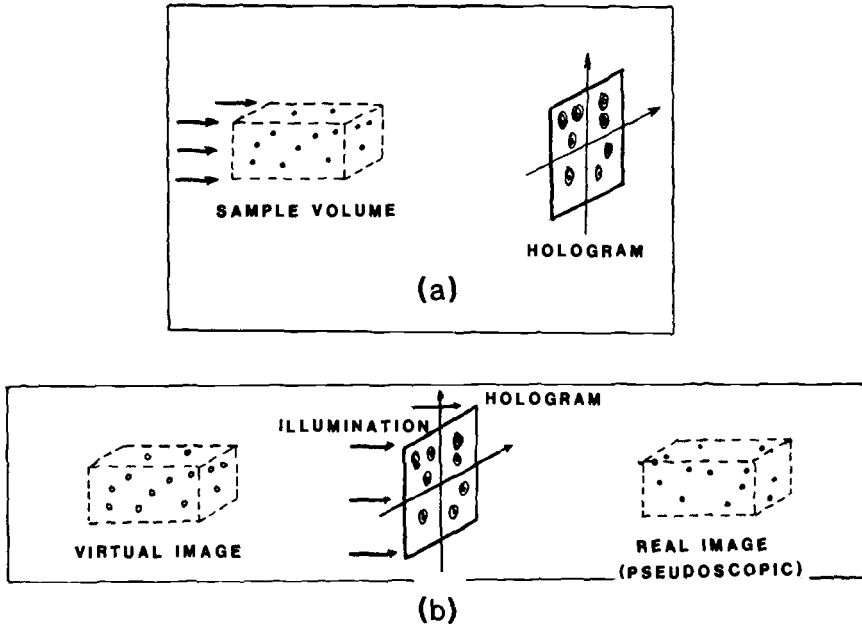
the diffraction method of size analysis as applied to a moving sample volume of droplets or particulates. The volume is illuminated with a collimated beam of coherent light, and each droplet produces its own diffraction pattern centered on the optical axis of the system in the rear focal plane of the lens. These diffraction patterns from all droplets overlap in this focal plane; hence, the total diffraction pattern of the sample volume can be detected. A reasonable terminology for this type of measuring system is perhaps a “total diffraction method.” The importance of the method is its independence to the movement of the particles. It should be also noted that the diffraction pattern formed is independent of the position of the particles in the volume.

The intensity distribution in the diffraction pattern has to be sampled and then that data “inverted” to get a histogram of size distribution. A variety of detection schemes have been used including single detectors and rotating masks, and segmented detectors of rectangular and specialized geometries. A number of systems have been described in the literature (Cornillault [4], Wertheimer and Wilcock [5], Swithenbank et al [6]). The systems described in these papers have been commercialized and instrumentation is available; a review of these techniques can be found in the literature (Thompson [1]). Another paper in this volume covers the current trends in this important technology (Hirleman [8]).

### Holographic Methods

Both in-line and off-axis methods of holography have been used in droplet measurements. Here we will concentrate on the in-line far-field method that has been particularly valuable in particulate and droplet size measurements. This method was first introduced 20 years ago with an initial set of papers describing the basic method. The development of the method occurred because of the desire to measure the droplet size distribution in naturally occurring fog; hence, application papers were published early in the history of the technology. Review papers cover the methods and applications contained in a rather extensive literature (Thompson [9], Trolinger [10], Thompson and Dunn [11], and Thompson [12]).

In the method of holographic particle size analysis, a sample volume of moving particles is illuminated usually with a coherent beam of light in the form of a short pulse. The hologram is then the record of the interference pattern formed between



(a) Formation of the hologram. (b) Formation of the image.

FIG. 7—The fundamental step in the holographic method of particle size analysis.

the light diffracted from each individual particle and the background or separate reference beam. The hologram contains information on both the cross-sectional geometry of each particle and its position. Thus complete information on the cross-sectional geometry and position of all the particles or droplets in the three-dimensional sample volume is obtained. The hologram can be then illuminated with a coherent beam of light to produce a stationary image of all the particles at their correct relative position in space. Since these images are stationary, they can be studied at leisure. Thus the holographic method is really a two-step imaging process that captures in a permanent form the cross-sectional shape and position of each particle in a moving sample of particles and produces a stationary three-dimensional image of each of the particles in the original volume. It is necessary to be quite precise about the three-dimensional nature of the image. It is meant here in the sense that each particle appears as a two-dimensional image of its cross-sectional shape in that plane, but each particle image is in the correct position in the three-dimensional space with respect to all other particles.

Figure 7 illustrates the two steps of this fundamental process. In this basic illustration, the simplest type of in-line far field holography is used. In Fig. 7a, a collimated beam of coherent light illuminates a sample volume containing several particles of different shapes. The hologram is recorded on a two-dimensional plane as shown. The second step is shown in Fig. 7b (sometimes called the reconstruction step); the hologram is illuminated coherently and

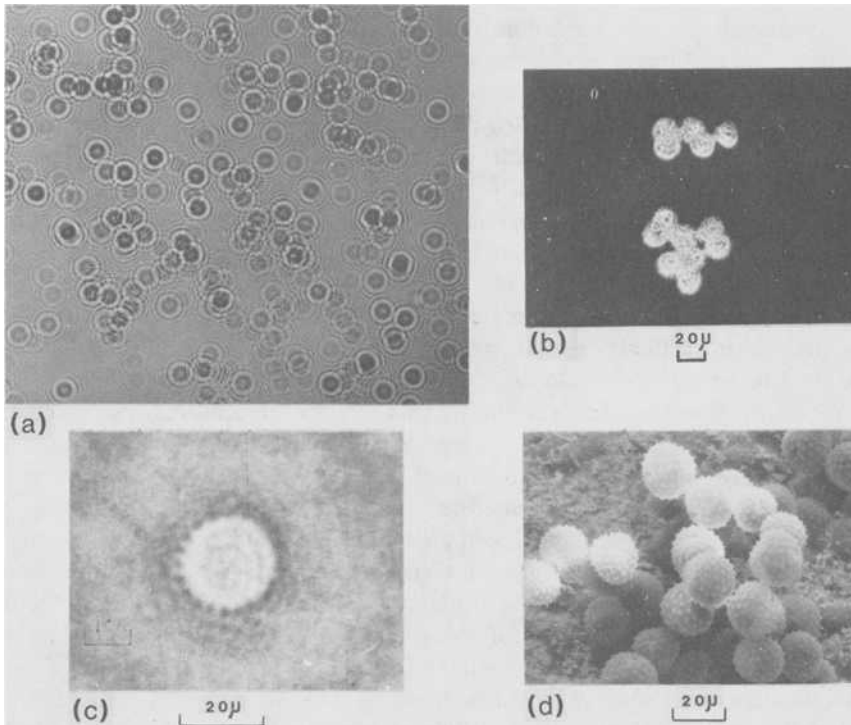
two volume images are formed as illustrated, one of which is real and the other virtual. The real image is pseudoscopic and the virtual image orthoscopic. An orthoscopic image has the same depth properties as the object volume, whereas a pseudoscopic image has inverted depth properties. It will be noted that in this illustration the whole process is carried out without the use of any imaging optics; however, lenses are often used to provide magnification (or demagnification) of the sample before the hologram is recorded. Naturally, the image, once formed, can be also magnified before a measurement is made and also detected—a particularly useful method employs a vidicon.

Clearly there are some distinct advantages to this method as well as some limitations. In the field of particle size analysis, there is no single method that can be used under all circumstances. Holography is important because, like direct imaging, it provides a fundamental method of measurement that, in principle, requires no calibration. This is very important since the calibration of many other techniques is more difficult (and perhaps more suspect) than the measurement itself. For example, in light scattering methods, it is particularly important to know the complex refractive index of the material to determine the exact formulation of the scattered field and even then it is only possible for a few selected geometries. The preparation of well characterized samples for empirical methods is a major problem; hence, even if holography was not a valuable method in its own right, it might well provide an input for calibration of other methods. (This is a problem under study at the moment, and it is too soon to tell whether this is a viable possibility.) Holography can be certainly used to record the same sample as the method to be calibrated and hence provide the necessary fundamental data.

The major limitation of this far-field holographic method is that it is used in transmitted light; that is, the particles are transilluminated. It cannot truly be used in reflected or scattered light, although some limited success can be achieved with the holographic method using a separate reference beam.

### *Applications*

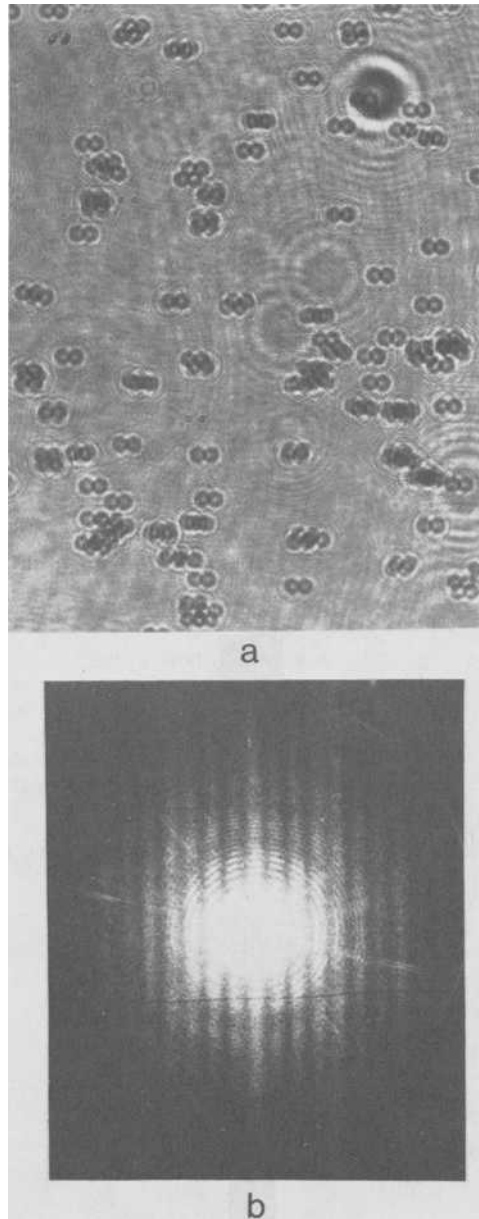
The method has been applied in a wide variety of circumstances, including fog droplets, cloud studies, dust erosion, agricultural sprays, combustion, drug vials, etc. The limit of resolution in the method is fundamentally set by the wavelength of light; hence, about  $1\ \mu\text{m}$  resolution can be obtained. Figure 8 shows that with some care, the ultimate resolution can be obtained. Figure 8*a* shows a hologram of a large number of particles of ragweed pollen. This pollen is about  $20\ \mu\text{m}$  in diameter and has an irregular surface. The image formed from a small portion of the hologram is shown in Fig. 8*b*; two clumps of pollen particles can be seen, the upper one consisting of four particles and the lower one of eight particles. Figure 8*c* shows the image of a single particle at high magnification, and the surface structure is apparent as a series of small spicules that protrude from the surface. For comparison, Fig. 8*d* shows an electron microscope photograph of some of these ragweed particles.



(a) Hologram of a large number of particles. (b) Image of a small section of the hologram showing two clumps of particles. (c) Image of a single pollen particle formed from the hologram. (d) An electron microscope photograph of the pollen [12].

FIG. 8—Holography of ragweed pollen.

There is considerable current interest in the simultaneous measurement of both particle size distribution and velocity. There are several possible techniques, but perhaps the most interesting one is that proposed by Ewan [13]. The interesting idea here is to record a double pulsed hologram so that there is a hologram associated with each of the two locations of each of the particles in the volume. The Fourier transform of this hologram is then formed optically using a lens in the conventional way; the velocity distribution can be then determined from the intensity distribution in the Fourier plane. Conceptually, the method can be understood by considering that all the particles in a field of view move with the same velocity; the two holograms formed with the double exposure are then basically the hologram and the hologram displaced. Upon Fourier transformation, cosine squared fringes are observed; the spacing of these fringes and their orientation give the velocity information. Figure 9 illustrates this concept and comes from our own current work on this topic [14]. Figure 9a shows a portion of a double exposure hologram in which a slide containing the particle has been translated horizontally through several particle diameters between expo-



(a) A portion of the double hologram. (b) Fourier transformer of (a).  
FIG. 9—Particulate velocity measurements using double exposure far field holography.

tures. Figure 9b shows the Fourier transform of the hologram of Fig. 9a, and the vertical fringe pattern crossing the field is readily apparent.

## Conclusions

This short review paper has attempted to deal briefly with both conventional and holographic imaging techniques. It is clear that both of these methods, with the current integration of new technologies, have a great deal to offer to the field of droplet characterization.

## References

- [1] Chigier, N., *Progress in Energy Combustion Science*, in press.
- [2] Thompson, B. J., *Progress in Optics*, E. Wolf, Ed., North Holland, Leyden, The Hague. Vol. VII, 1969, p. 169.
- [3] Thompson, B. J. and Krisl, M. E., *Photography Science and Engineering*, Vol. 21, 1977, p. 109.
- [4] Cornillault, J., *Applied Optics*, Vol. 11, 1972, p. 205.
- [5] Wertheimer, A. L. and Wilcock, W. L., *Applied Optics*, Vol. 15, 1976, p. 1015.
- [6] Swithenbank, J., Beer, J. M., Taylor, D. S., Abbot, D., and McCreath, G. C., *Proceedings*, 14th Aerospace Science Meeting (AIAA), paper number 70-69, 1976. See also in "Experimental Diagnostics in Gas Phase Combustion Engines," *Progress Aeronautics and Astronautics*, B. T. Zinn, Ed, Vol. 53, 1977, p. 421.
- [7] Thompson, B. J., *Proceedings*, 1978 International Optical Computing Conference, *Digest of Papers*, Institute of Electrical and Electronic Engineers, Vol. 139, 1979.
- [8] Hirtleman, E. D., this publication, pp. 35-60.
- [9] Thompson, B. J., *Journal of Physics E*, Vol. 7, 1974, p. 781.
- [10] Trolinger, J. D., *Optical Engineering*, Vol. 14, 1975, p. 383.
- [11] Thompson, B. J. and Dvnn, P., *Proceedings*, Society of Photo-Optical Instrumentation Engineers, Vol. 215, 1980, p. 102.
- [12] Thompson, B. J., *Proceedings*, 15th International Congress on High Speed Photography and Photonics (*Proceedings*, Society of Photo-Optical Instrumentation Engineers, Vol. 348, 1982, p. 626).
- [13] Ewan, B. C. R., *Applied Optics*, Vol. 18, 1979, pp. 623 and 3156.
- [14] Malyak, P., Crane, J. S., and Thompson, B. J., *Proceedings*, 15th International Congress on High Speed Photography and Photonics (*Proceedings*, Society of Photo-Optical Instrumentation Engineers, Vol. 348, p. 634).

Larry M. Oberdier<sup>1</sup>

# An Instrumentation System to Automate the Analysis of Fuel-Spray Images Using Computer Vision

---

**REFERENCE:** Oberdier, L. M. "An Instrumentation System to Automate the Analysis of Fuel-Spray Images Using Computer Vision." *Liquid Particle Size Measurement Techniques*, ASTM STP 848, J. M. Tishkoff, R. D. Ingebo, and J. B. Kennedy, Eds., American Society for Testing and Materials, 1984, pp. 123-136.

**ABSTRACT:** An intelligent instrumentation system is being implemented to analyze images stored during pulsed laser illumination of fuel sprays. Images are stored on magnetic video disk during the experiment and later analyzed with a system consisting of a commercial image processor and a minicomputer. The system employs computer vision algorithms to reduce the effects of shading and to segment candidate droplets from each image. Pattern recognition methods will be used to extract features from each droplet and to reject those which are not in the sample volume. The final output of the system is an accumulation of droplet size distributions at various sample points in the spray.

**KEY WORDS:** spray measurement, image processing, computer vision, video recording, lasers, image formation, optics, diffraction, pattern recognition, classification

In the field of spray research, photography remains a viable technique for measuring droplet size and velocity distributions. The test apparatus emits short pulses of light from a spark source or a laser through a section of the spray being studied. On the opposite side of the spray, images are stored on film or via a video camera on video storage. Some advantages of this method are:

1. With a video camera the system can be interactively adjusted for best image quality.
2. Spherical and nonspherical droplets over a large size range can be analyzed.
3. Two components of velocity can be determined by doubly exposing each image with a fixed time between light pulses.
4. Time resolved measurements can be made by synchronizing the light pulses to a related event such as a fixed time after injector firing.

<sup>1</sup>Staff research engineer, Instrumentation Department, General Motors Research Laboratories, Warren, MI 48090.

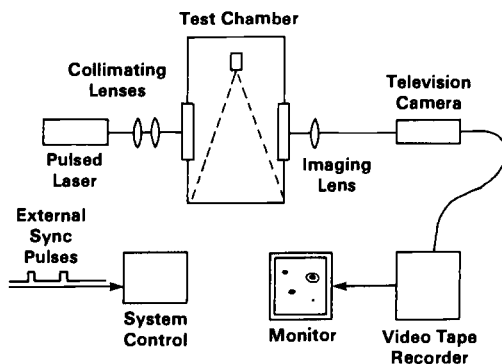


FIG. 1—Block diagram of existing laser-video system. Thousands of images are stored for analysis after the experiment.

Such a system [1-3] is now in use at the General Motors Research Laboratories as shown in Fig. 1. The spray is back illuminated with a pulsed nitrogen laser and focused onto a television camera on the opposite side. Thousands of images are stored on a surveillance type recorder for later analysis. A second laser is added and fired a fixed time later for velocity measurement.

The images which are stored by this method contain a mixture of in-focus and out-of-focus droplets. The analysis of the images involves deciding which droplets are in-focus and measuring their diameters. For velocity determination, multiple droplet images must be paired. The major disadvantage of photography for spray measurements is the effort needed to extract size and velocity information from the images and the errors associated with deciding which droplets are in-focus, that is, from the sample volume. Months of effort may be required to do this analysis for one point in the spray. A system to automate this analysis is desirable to increase accuracy and to allow more use of the measurement equipment.

To date several approaches have been taken to automate the analysis of fuel spray images. These can be grouped into two categories: (1) real-time compression of video signals and (2) off-line analysis of stored images. In the first category the work of Toner et al [4] involved real-time compression of video signals using three steps: high-pass filtering, a global threshold, and run length coding. The high-pass filtering was needed to eliminate shading, and the other steps greatly reduced the amount of data to be analyzed. The data were transferred into a microcomputer which grouped adjacent line segments into objects and computed size. The total analysis time is stated to be less than one second per image. A system described by Ow and Crane [5] stores images on film and analyzes the negatives using a television camera, digitizer, and a minicomputer. The resolution of the digitizer is 3-bits allowing the computer to reject out-of-focus droplets by measuring the width of the blurred region around their perimeter after Ramshaw [6]. The analysis time is 10 min per image.

The images produced by the General Motors Research (GMR) system have considerably more shading than the cited references. These images have come from two spray environments: the combustion chamber of a single cylinder engine and a high temperature flow facility. The shading combined with the need for analyzing thousands of images as reported by Tishkoff [1], has lead us to develop our own system for automating fuel spray image analysis. Our goal is to apply computer vision methods similar to those used in automatic cytology [7], as well as image analysis hardware which has recently seen dramatic cost reduction.

### **Description of Laser-Video System**

Referring again to Fig. 1, the laser-video system has three functions: image formation, image storage, and synchronization.

#### *Image Formation*

Spray droplets are illuminated with a 100- $\mu$ J pulsed nitrogen laser. Ten ns pulses of ultraviolet light are collimated and passed through the test section perpendicular to the spray. The imaging lens magnifies a 1.4 mm<sup>2</sup> sample area and focuses it on the face of the vidicon within the television camera. The images are formed by the creation of shadows by droplets in the object plane and by near-field diffraction from droplets which are on either side of the object plane. The result of choosing which droplets are in focus is to define a sample volume. The axial extent of that volume is a function of droplet diameter with larger droplets having a larger sample volume. Since the system treats large droplets preferentially, the size and velocity distributions must be deskewed. In the past, this has been accomplished using a curve supplied with the system by Laser Holography Inc., as shown in Fig. 2. Developing an automatic analysis system will formalize the criteria for rejecting droplets out of the sample volume and more accurately define the curve used to deskew the data.

#### *Image Storage*

Images are stored in the laser-video system with a Cohu camera and a Javelin surveillance recorder. The camera uses a vidicon imaging tube with standard raster scanning with the exception that the beam is blanked during one of the interlaced fields. The beam is blanked for two reasons: the bandwidth of the recorder is insufficient to warrant additional vertical resolution, and only one field may be viewed at a time during single frame playback. The camera was modified by Cohu to allow the blanking and to perform the test synchronization described next.

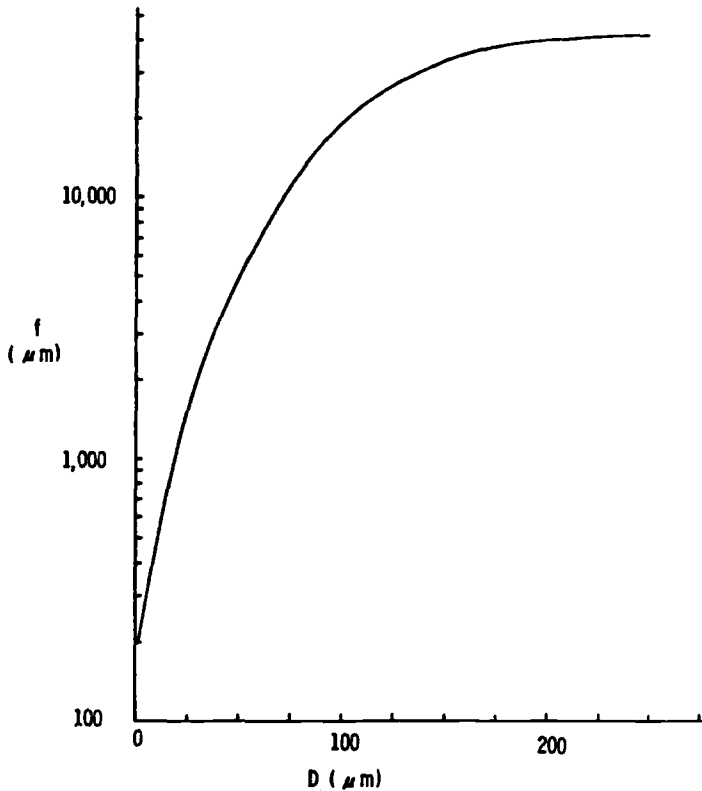


FIG. 2—Depth of field versus droplet diameter curve supplied by Laser Holography Inc., used to deskew size and velocity statistics.

### *Test Synchronization*

The laser, camera, and recorder are controlled by a board in the camera and a separate laser synchronized chassis. They monitor the readiness of the camera and recorder before allowing the laser firing. The system works in two modes: free running and externally synchronized. In the free running mode, laser firings occur at the end of video fields. This minimizes the latency time for images stored on the vidicon for best image quality. In the other mode, the laser fires when commanded by an external pulse. Normally this pulse is derived from an engine position sensor allowing time resolved spray analysis.

### *Velocity Measurements*

To allow the measurement of droplet velocity, a second laser is fired some fixed time (typically  $10 \mu\text{s}$ ) after the first laser. The result is a doubly-exposed image with the displacement of droplet subimages proportional to velocity. One problem with this technique is that the first laser exposes the vidicon at every point in the image field where a droplet shadow does not exist. These areas then are not able to

register shadows from the second laser. One solution is to reduce the laser intensities by 50%, allowing each laser to dilute the shadow from the opposite exposure. But this would mean that only half of the dynamic range of the camera would be used creating gray instead of black images of in-focus droplets. Another approach being developed is to reverse the contrast by placing a small optical block at the rear focal point of the imaging lens. The block only allows scattered light through to the camera creating a white on black image. Another way of viewing this method is that the block is located at a plane where the Fourier transform is formed by Fraunhofer diffraction and that it is eliminating low spatial frequencies [8]. The result is that the slow-varying background becomes zero (black). One problem with using contrast reversal is that the resulting images tend to have ringing at their edges due to Gibbs phenomenon [9]. This change in image will either have to be accounted for in the automatic analysis system or reduced by further development of the optical filter.

### Functions of the Automatic System

The automatic image analysis system will supplement and eventually replace the human involvement in extracting size and velocity data from stored spray images. Towards that end, we are developing a system with the following functions:

*Image Storage*—The system must store thousands of video frames with good fidelity during the test. During the analysis, the stored images must be retrieved frame by frame in a form which can be digitized.

*Image Processing*—The system needs to digitize each video frame and search the resulting integer array for in-focus droplets. Our goal is to analyze each image in 10 s. This corresponds to a rate of 8640 images/day. For velocity measurements, the system will search for paired images and compute the velocity.

*Compute Spray Statistics*—The size and velocity data will be accumulated for all of the images and printed after the analysis.

### Description of the Automatic System

As shown in Fig. 3, the system will consist of a magnetic video disk, time-base corrector (TBC), Vicom image analyzer, and minicomputer. The magnetic disk recorder was chosen because of its high bandwidth, low jitter, and an ability to store and retrieve whole video frames with remote control of frame advance. The time-base corrector is needed because the image analyzer requires the video being digitized to be synchronized to its clock. The TBC does this and also removes the jitter in the recorded video. The Vicom image analyzer performs the low level, pixel intensive computations on stored images with the minicomputer doing higher level work such as pattern recognition and test statistics generation.

Figure 4 is a block diagram of the image analyzer which was purchased in a stand-alone configuration to allow development of image analysis algorithms. The Vicom image analyzer [10], shown in Fig. 5, is built around a Motorola 68 000 microcomputer and includes a 16 Mbyte hard disk, data digitizing tablet,

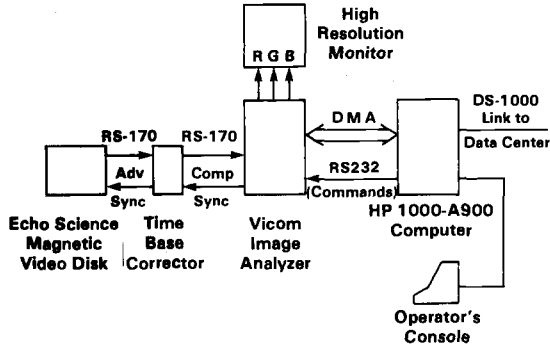


FIG. 3—Block diagram of fuel spray image analysis system.

a full screen editing terminal, and a high-resolution color monitor. Languages supported are Assembler, Fortran, Pascal, and C. Software from Vicom runs under Versados, the Motorola disk operating system. There is a 0.5 Mbyte of microcomputer memory and 2 Mbytes of image memory organized as four  $512 \times 512 \times 16$  bit planes. The image memory resides in the address space of the 68 000 microcomputer. This facilitates the development of image processing software by defining program arrays to exist in image memory. The four image planes are connected to digitizing, computation, and display boards over a high-speed pipeline. There are two processing boards: the point processor and the array processor. The point processor is used to perform arithmetic and logical opera-

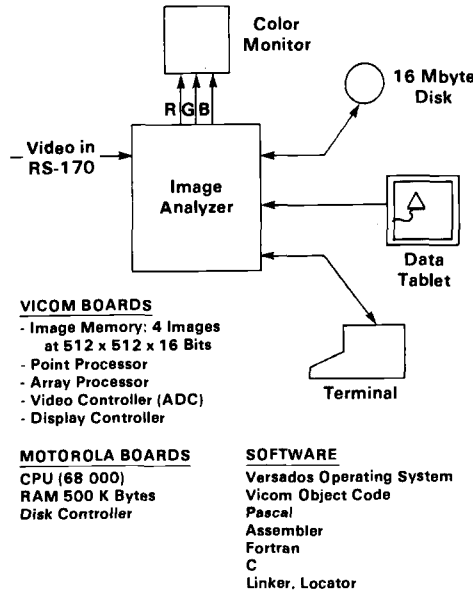


FIG. 4—Configuration of Vicom image analyzer.

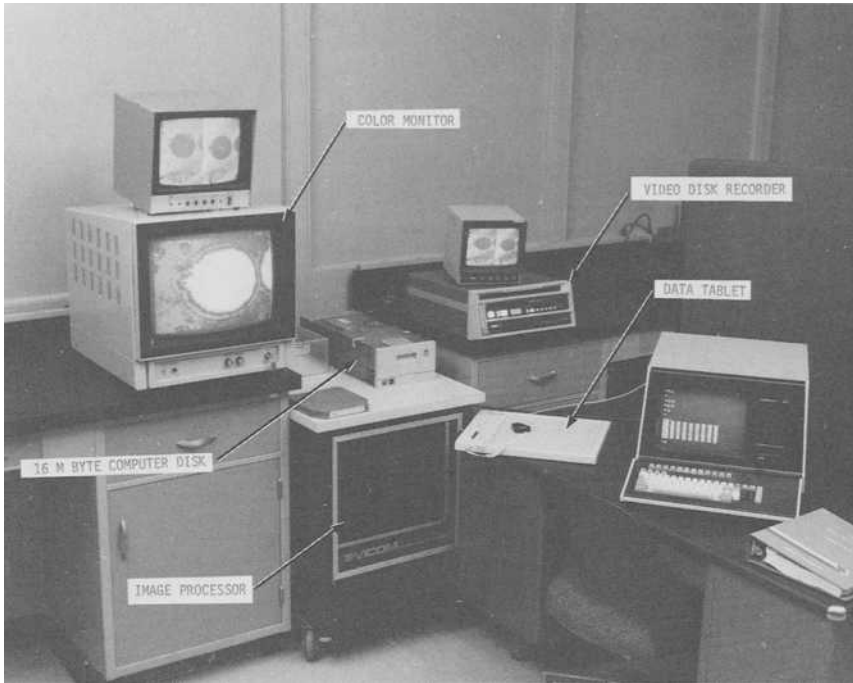


FIG. 5—*Photograph of Vicom image analyzer.*

tions on images such as gray level scaling, bit slicing, image addition, and thresholding. The array processor performs two dimensional convolutions of an image with an impulse response to achieve filtering, edge enhancement, or template matching.

### **Image Processing Steps**

To progress from a stored image of a fuel spray to a list of the in-focus droplets and their sizes will require several processing steps. The goal of each step is to reduce the amount of data for subsequent steps and to organize the data. Figure 6 shows the relationship of the following steps:

#### *Image Restoration*

Each image contains a considerable amount of shading from various sources such as laser, optics, and camera nonuniformities, and the accumulation of films on access windows. This shading often precludes the use of global thresholding as the first step to eliminate pixels which are not part of the objects of interest [11]. The goal of image restoration is to normalize each image by estimating a shading function and factoring it out of the data. The result will be an image which can be globally thresholded.

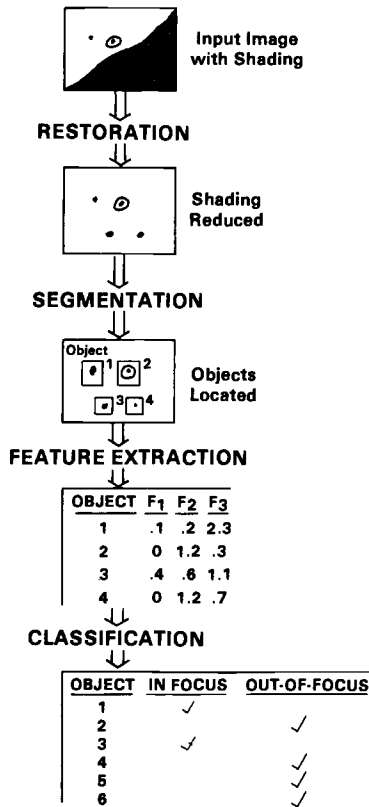


FIG. 6—Image processing steps.

### Segmentation

The result of thresholding is a binary (black and white) image where black pixels are part of objects. Although a binary image appears to be highly organized, the pixels in a binary image must still be organized by the computer [12]. This step is called segmentation. The output of segmentation is a list of objects and some characteristics such as location, area, perimeter, etc. Most segmentation methods can be grouped into one of the following types:

*Edge-Tracking*—Image data are scanned until an object pixel is located. Then the edge of the object is followed using a sequence of search templates until the starting location is again reached. More sophisticated methods use edge strength and direction information derived from the gray level image.

*Region Growing*—Adjacent pixels are assigned object numbers by passing an L-shaped template over the image and keeping track of intersecting objects in equivalence tables.

*Run Length Coding*—The image is processed line by line to generate a run length code (that is, start location and pixel count) for each segment which belongs to an object. The next step is to combine segments which are adjacent.

### *Feature Extraction*

Once objects are segmented from the binary image, we need to decide which ones are from in-focus (that is, from the sample volume) droplets. Our method will be to use the binary objects as a map to extract pertinent features from the gray level image and then to use these features to separate the objects into in and out-of-focus classes. Possible features are edge gradient, diffraction ring frequency, and interior gray level statistics.

### *Object Classification*

The output of the previous step will be a point for each object in  $n$ -dimensional feature space. If the point is within a previously defined volume, the object will be called in-focus. This volume will be determined by using statistical pattern recognition techniques [7].

### **Results of Image Restoration**

As discussed in the previous section, we need to restore images from the affects of shading so that global thresholding can be used to eliminate most pixels. Two methods which look promising are Log-Sobel edge enhancement and shading estimation by ensemble averaging. Figure 7 shows the result of applying a global threshold to a fuel spray image. The threshold was interactively chosen to be just low enough to include enough pixels to recognize object one. The threshold image is defined by

$$P_{\text{out}}(x, y) = \begin{array}{l} \text{white if } P_{\text{in}} > \text{threshold} \\ \text{black if } P_{\text{in}} \leq \text{threshold} \end{array}$$

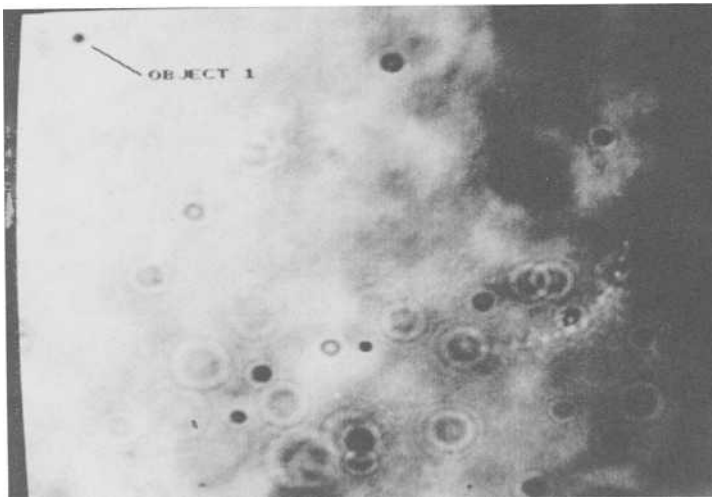


FIG. 7a—Fuel spray image with shading.

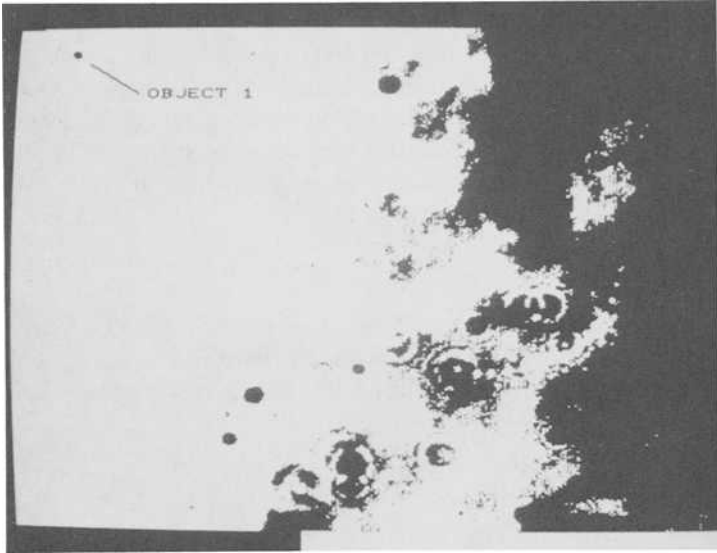


FIG. 7b—Result of applying a global threshold to Fig. 7a image.

where  $P_{in}$  is the input image and  $P_{out}$  is the result of thresholding. Note that this threshold separates object one from its neighboring background but does not reject background pixels from the darker side of the image.

*Shading Estimation and Correction*

As shown in Fig. 8, the fuel spray image can be considered to be the combination of an ideal image,  $P_I$  and a shading function  $P_S$  such that

$$P_R(x, y) = P_I(x, y) \cdot P_S(x, y)$$

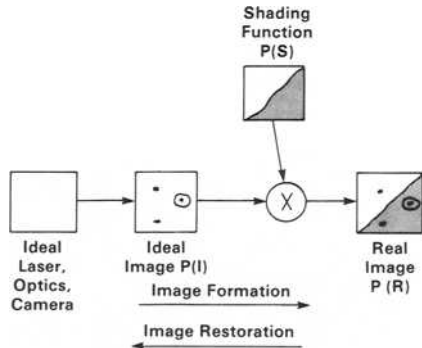


FIG. 8—Model for image restoration using shading estimation.



FIG. 9—Result of a point average of four images.

where  $P_R$  is the recorded image. This assumes that the shading is multiplicative and that it only modifies the amplitude of light without scattering. One approach to estimating the shading function takes advantage of the random nature of fuel droplets. Each image is of a different population of droplets, and it is assumed that their location is randomly distributed in the field of view. Then by averaging several frames, the droplets are attenuated and the resulting image will estimate that part of the shading function which is constant during the interval sampled. Figure 9 shows the result of averaging four frames. Figure 10a and b are the result of dividing an input image by the shading estimate and applying a global threshold.

#### *Log-Sobel Edge Enhancement*

Edge enhancement by spatial high-pass filtering is a common technique because object edges often occur at abrupt changes in gray level [13]. One popular method of edge enhancement is the Sobel edge operator which uses two  $3 \times 3$  templates which are separately convolved with the image to estimate the vertical and horizontal components of the gray level gradient. The two gradient images are combined to form the magnitude and direction images. These can be used as input to edge tracking algorithms or other segmentation methods. The vertical and horizontal gradient images  $G_V$  and  $G_H$  are computed by convolution of the input image with the respective templates

$$T_H = \begin{bmatrix} -1 & 0 & 1 \\ -2 & 0 & 2 \\ -1 & 0 & 1 \end{bmatrix}; \quad T_V = \begin{bmatrix} 1 & 2 & 1 \\ 0 & 0 & 0 \\ -1 & -2 & -1 \end{bmatrix}$$

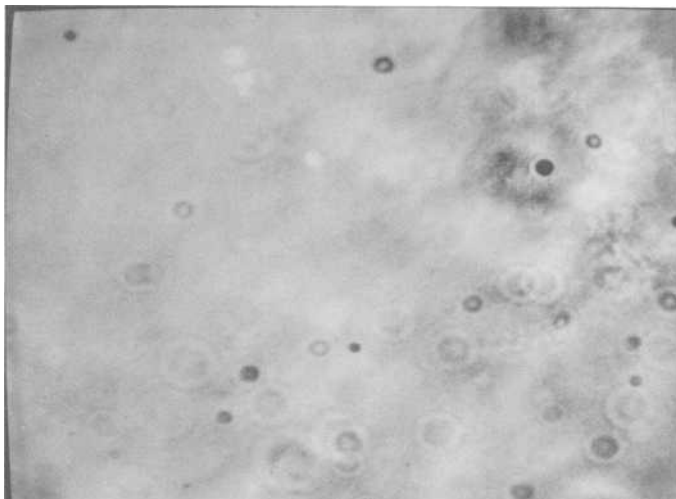


FIG. 10a—Restoration of Fig. 7a image by dividing it by Fig. 9 image and scaling.

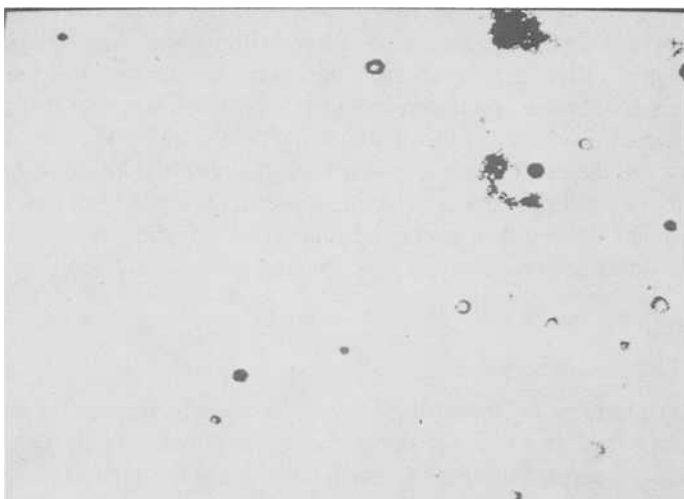


FIG. 10b—Threshold of Fig. 10a image.

The magnitude and direction images  $G$  &  $\theta$  are computed by

$$G = \sqrt{G_V^2 + G_H^2}; \quad \theta = \text{ARCTAN}\left(\frac{G_H}{G_V}\right)$$

The result of edge enhancement of the image from Fig. 7a is shown in Fig. 11a. Note that the edge strength of droplets in the darker part of the image

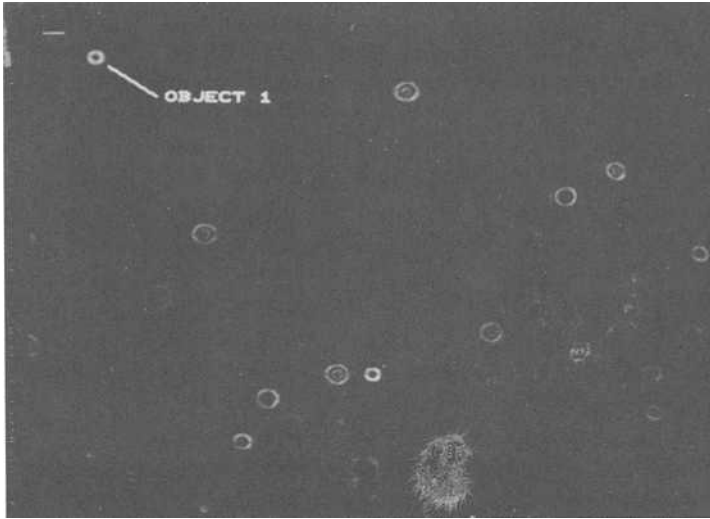


FIG. 11a—Sobel edge enhancement of Fig. 7a image.

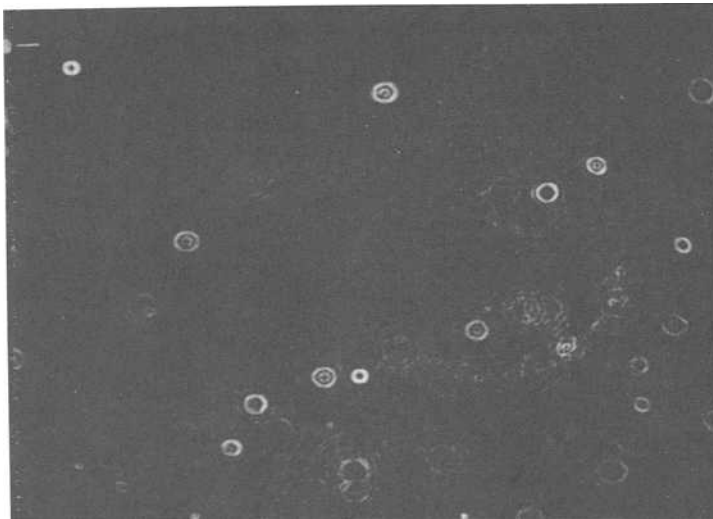


FIG. 11b—Log-Sobel edge enhancement of Fig. 7a image.

are reduced by the degraded local contrast. It was found that this degradation could be reduced if the input image is first log-compressed by the following

$$P_L = \ln(P_{in} + 1)$$

This method works because the edge operator subtracts adjacent columns and rows [13]. The result of subtracting the log image pixels is to compute the ratio

of gray levels. This ratio should be the same at edges in either the bright or dark areas of the image if the shading is multiplicative. Figure 11b shows the result of the Log-Sobel operator when used on the image from Fig. 7a.

## Conclusions

The images resulting from pulsed laser illumination of fuel sprays in operating engine or simulated engine environments have excessive shading and diffraction ring structure. These complications preclude the use of global thresholding for real-time data compression of video images and force the storage of all images during an experiment. To automate the analysis of the stored images requires the development and evaluation of methods for shading correction, object segmentation, feature extraction, and in-focus versus out-of-focus classification. The use of ensemble averaging of multiple images to estimate a shading function followed by the normalization of each image by that function works well on the images tested. Edge enhancement of log-compressed images using the Sobel operator is promising but needs more testing.

## Acknowledgments

The research for this project is also being conducted by G. Bertolini and Y. Lee of the General Motors Research Laboratories.

## References

- [1] Tishkoff, J. M., "Measurements of Particle Size and Velocity in a Fuel Spray," Second International Conference on Liquid Atomization and Spray Systems, Madison WI, 20-24, June 1982.
- [2] Tishkoff, J. M., Hammond, D. C., and Chraplyvy, A. R., "Diagnostic Measurements of Fuel Spray Dispersion," *Journal of Fluids Engineering*, Vol. 104, 1982.
- [3] Peters, B. D., "Laser-Video Imaging and Measurement of Fuel Droplets in a Spark-Ignition Engine," for presentation at Conference on Combustion in Engineering, Institution of Mechanical Engineers, April 1983, Oxford, England.
- [4] Toner, M. C., Dix, M. J., and Sawistowski, H., "A Television-Microprocessor System for High Speed Image Analysis," *Journal of Physics E: Science Instrumentation*, 1978, No. 11, P. 960.
- [5] Ow, C. S. and Crane, R. I., "A Simple Off-Line Automatic Image Analysis System with Application to Drop Sizing in Two-Phase Flows," *International Journal of Heat and Fluid Flow*, 1980, No. 2, p. 46.
- [6] Ramshaw, C., "A Technique for Drop-Size Measurement by Direct Photography and Electronic Image Size Analysis," *Journal of the Institute of Fuel*, No. 41, pp. 288-292.
- [7] Reinhardt, E. R., Erhardt, R., Schwarzmann, P., Bloss, W. H., and Ott, R., "Structure Analysis and Classification of Cervical Cells Using a Processing System Based on TV," *Analysis and Quantitative Cytology*, 1979, Vol. 1, No. 2, pp. 144-150.
- [8] Thompson, B. J. and Parrent, G. B., *Physical Optics Notebook*, Society of Photo-Optical Instrumentation Engineers, 1969.
- [9] Molk, J. G., *Digital Processing of Remotely Sensed Images*, National Aeronautics and Space Administration, Washington, DC, 1980.
- [10] "Vicomp Digital Image Processor User's Manual," Vicomp Systems, Inc., San Jose, Calif., April 1982.
- [11] Dahlberg, R. C., "Real Time Digital Image Filtering and Shading Correction," *Proceedings of the Society of Photo-Optical Instrumentation Engineers*, Vol. 207, 1979.
- [12] Ballard, D. H. and Brown, C. M., *Computer Vision*, Prentice-Hall, Englewood Cliffs, NJ, 1982.
- [13] Rosenfeld, A. and Kak, A. C., *Digital Picture Processing*, Academic Press, New York, 1976.

Daniel M. Popa<sup>1</sup> and Kesav S. Varde<sup>1</sup>

# Sizing Study of Drops Produced by High Diesel Fuel Injection Pressure Sprays

---

**REFERENCE:** Popa, D. M. and Varde, K. S., "Sizing Study of Drops Produced by High Diesel Fuel Injection Pressure Sprays," *Liquid Particle Size Measurement Techniques*, ASTM STP 848, J. M. Tishkoff, R. D. Ingelo, and J. B. Kennedy, Eds., American Society for Testing and Materials, 1984, pp. 137–149.

**ABSTRACT:** Experiments were conducted to measure droplet sizes and their distribution in high-pressure diesel fuel sprays. Fuel droplets were collected on glass plates which were treated with surface modifier. The droplets were photographed and subsequently analyzed on an image analyzer. The resultant information is used to calculate average diameter, Sauter mean diameter, etc. The degree of automation in the analysis process allows accurate measurement of a large number of photographed drops. It is estimated that the method used here allowed good measurements of small droplets on the order of 0.5  $\mu\text{m}$ . Typical output of the analysis together with the validity of the technique is presented in the paper.

**KEY WORDS:** high pressure sprays, droplet sizes, diesel fuel, droplet measurement, droplet analyzer

## Nomenclature

$D_i$  Droplet diameter

$N_i$  Number of drops of diameter  $D_i$ ,  $\mu\text{m}$

$N$  Total number of drops sampled  $N = \sum N_i$ ,  $\mu\text{m}$

$\bar{D}$  Average drop diameter,  $\bar{D} = \frac{\sum N_i D_i}{N}$ ,  $\mu\text{m}$

$\bar{D}_{32}$  Sauter mean diameter,  $\bar{D}_{32} = \frac{\sum N_i D_i^3}{\sum N_i D_i^2}$ ,  $\mu\text{m}$

As part of an overall program to study characteristics of fuel spray at high injection pressures, an investigation was undertaken to determine droplet size distribution in such sprays.

<sup>1</sup>Graduate student teaching assistant and professor of mechanical engineering respectively, Department of Mechanical Engineering, University of Michigan-Dearborn, Dearborn, MI 48128. Mr. Popa is presently with General Electric Company, Schenectady, NY.

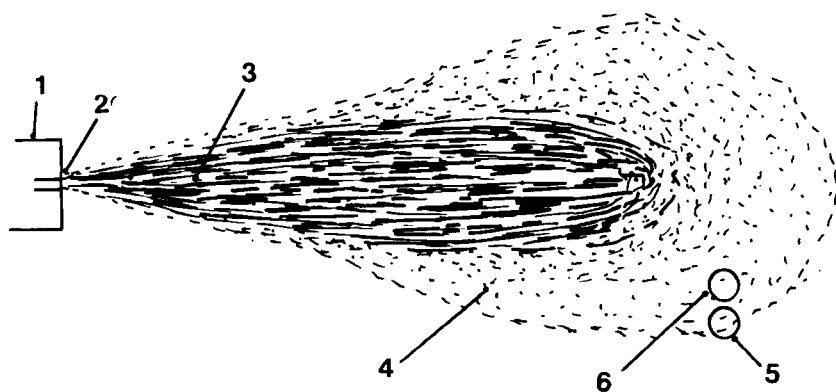


FIG. 1—Spray plume and locations of the sampling positions. 1: nozzle; 2: orifice; 3: main spray core; 4: mixing region; 5: sampling position #1; 6: sampling position #2.

The combustion process in a diesel engine is quite complex and its detailed mechanisms are not completely understood. Liquid fuel is injected at high pressure into the combustion chamber containing air at high pressure and temperature. The high velocity liquid jet interacts with the surrounding medium and breaks up into fine droplets. As these droplets continue to travel in the chamber with decreasing velocity they evaporate and form a combustible mixture. The success of the combustion process in a diesel engine and particularly in a direct injection engine, largely depends on the quality of the mixture formed in there, which, in turn, depends on the characteristics of the spray and how well they are matched with the aerothermodynamic conditions in the chamber.

One of the important characteristics is the fuel droplet size and the droplet size distribution in the spray. Sophisticated analysis of diesel combustion process has been difficult due to the lack of knowledge concerning the droplet size distribution in the diesel fuel spray.

High-pressure fuel sprays emerging through diesel fuel injection nozzles are characterized by a central core of highly dense liquid drops surrounded by a mixing region where droplet density is relatively low, as depicted in Fig. 1. A number of studies, dating as far back as 1920, have been made to measure droplet sizes in diesel sprays [1-6]. Generally, the following methods have been used to measure droplet sizes in diesel sprays:

1. Molten wax method.
2. Microscopic examination of collected drops.
3. Liquid immersion technique.
4. Optical methods based on absorption or scattering of light.
5. Impact method.

Each of these methods has its own disadvantages and limitations, and none of these is entirely satisfactory when applied to droplet sizing in a typical diesel

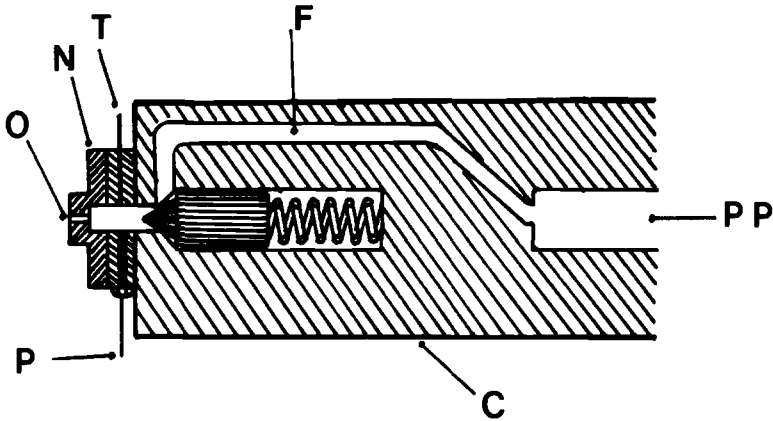


FIG. 2—Nozzle and the injector. C: cartridge; F: fuel passage; N: nozzle; O: orifice; P: fuel pressure transducer; PP: connection to plunger pump; T: fuel temperature sensor.

fuel spray. Some of these techniques and their limitations have been discussed in some of the recent review papers [7,8].

Generally, experimental investigations of droplet sizes in diesel sprays have been conducted up to an injection pressure of about 35 MPa. These investigations have shown droplet sizes to depend on the operating parameters such as injection pressure, orifice size, conditions of the surrounding medium, etc. However, in two recent studies [9,10] where an actual diesel fuel injection equipment was used, droplet sizes have been found to depend on the position in the spray and the sampling time. It was suggested that spatial and temporal dependence of droplet sizes may arise due to variations in injection pressure in a typical diesel fuel injection system. Our investigation was conducted to estimate droplet sizes at high diesel fuel injection pressures, since there are indications that such pressures improve performance of direct injection type engines [11]. To alleviate some of the problems associated with the variation in injection pressure, constant pressure fuel sprays were generated, and the measurements were made only in the mixing region. The design of the injection system, the chamber, and the method of generating high fuel pressures have been described in an earlier paper [12]. The injection nozzle had a single orifice as shown in Fig. 2. It was attached to a cartridge connected to a plunger pump capable of generating high injection pressures. This paper describes the technique and the equipment that was used in the quantitative droplet analysis.

### Experimental Apparatus and Procedure

The sprays under investigation were produced by a specially designed injector capable of generating fuel pressures as high as 150 MPa. The injector employed an intensifier system which was driven by nitrogen gas stored in an accumulator.

The injector had a single orifice, removable nozzle (shown in Fig. 2) so that nozzles with different orifice sizes could be used. Diesel fuel No. 2 (with cetane values between 44 to 46 and having a viscosity of  $3.6 \text{ mm}^2/\text{s}$  at  $22^\circ\text{C}$ ) at ambient temperature was used in all the experiments.

Fuel was sprayed into a chamber which could be pressurized up to 4.2 MPa and had access windows and sensors for visualizing and monitoring the sprays emerging from the nozzle. To avoid the effects of varying injection pressure, experiments were conducted at constant injection pressure ranging from about 25 to 150 MPa. The details of the experimental setup for generating sprays at constant injection pressure and the method used to measure some of the other spray parameters have been described elsewhere [12]. All of the experiments were conducted at atmospheric chamber pressure and both the fuel and the chamber gas, at room temperature. The injector was operated in a single pulse mode.

Because of the problems associated with the high density of drops in the main core of the spray, sampling was limited in the mixing region of the diesel fuel spray. To avoid droplet agglomeration as much as possible, drops were collected on glass plates which were treated with a fluorochemical surface modifier (3M-FC 723). Experiments conducted without treating the plate with the surface modifier showed a thin film of diesel fuel accumulated on the plate possibly due to agglomeration. When the collection system is used to sample drops there is a possibility of more than one drop adhering to the plate at the same location. To avoid this, a shutter type of mechanism was used to expose the plate to the spray for a short time interval, typically 0.3 to 0.4 ms.

The shutter mechanism was operated by a spring loaded solenoid which was activated by a current pulse generated from an electronic unit controlling the experiment. The electronic control unit had a pulse generator, similar to that used in activating and controlling electronic fuel injectors. The pulse generator supplied a boost current pulse of about 7 A to the solenoid for about 0.1 ms, followed by a holding current pulse of approximately 2 A. With this arrangement the start of droplet collection process and its duration could be independently controlled with respect to the arrival of the spray tip. In addition, by moving the plate assembly to a different location in the mixing region boundary, the effect of spatical variation in droplet sizes could be evaluated.

Most of the experiments were conducted by placing the assembly about 110 mm downstream from the nozzle and between 25 and 15 mm from the nozzle axis, as shown in Fig. 1. Except for the shutter opening period, the glass plate was completely sealed from the surroundings to prevent diesel fog particles from being deposited on the plate. The droplets were allowed to settle on the glass plate rather than blasting the spray on the slide. The design of the shutter mechanism was such that the boundary layer effect were considered not to be of great importance.

The droplets deposited on the collection plate were photographed using a Reichert metallographic camera capable of providing a suitable magnification.

Several photomicrographs were taken of each collecting plate so that the specimen size was at least 1000 drops. A fine grain 35 mm, black and white film (Kodak Tri-X 400) was used to photograph the collected drops so that the printed drops appeared to be very sharp. A number of precautions were taken to ensure that the droplet images were sharp. Internal reflections in metallographic camera adapter were eliminated by using internal tube. High quality lenses at low aperture opening were used during magnification. In addition, the Tri-X film was maintained at 22°C for at least a day before exposing in the camera.

A micron scale, supplied with the camera, was used in calibrating droplet sizes. After photographing the droplets for each run, a photograph of the calibration scale was made under identical conditions. The latter was used in calibrating the drop sizes. The overall magnification of the final printed drops were 150.

### **Data Reduction Technique**

The droplet photographs were analyzed electronically using an image analyzer unit (Quantimet 720). The Quantimet consists of an image analyzer interfaced with its own computer system and is designed to make certain kinds of measurements based on the information conveyed from the images. A television type vidicon camera converts the optical image of the droplets on a photograph into electrical signals. The images are then reproduced on a CRT display which is scanned continuously. During this process the entire image is digitized into 720 scan lines, each consisting of 1024 specimen points called pixels. Each pixel is assigned an integer value between zero and 63 based on a brightness gray scale with the white being 63 and complete dark being zero. The true optical density value can be then approximated from the gray level scale. The result is a digital matrix of 1040 by 720 with each element valued anywhere from zero to 63 depending on the brightness or the density scale. The size information, which is obtained from the density scale is then processed by the Quantimet computer and stored on a magnetic tape. The Quantimet used in this study required some editing when the specimen size was too large or when two or more drops were joined together. A digitized set of data can be edited by three distinct methods:

1. In the first method, a subset of the total image can be selected by framing the image, that is, by selecting a frame size less than the available 1040 by 720 pixel matrix. Thus, the results generated from this frame will include only the selected drops that lie within the frame. By moving the frame to a different location on the photograph, additional results can be generated until the entire photograph is covered. All of the results stored on the magnetic tape can be then combined to give droplet sizes and their distribution. This method of editing was used in the present work to cover a large sample of drops.

2. A digitized set also can be edited by a thresholding technique where images considered to be too bright or too dark are rejected. The threshold is specified with reference to the gray scale. Therefore, this method can be used to eliminate

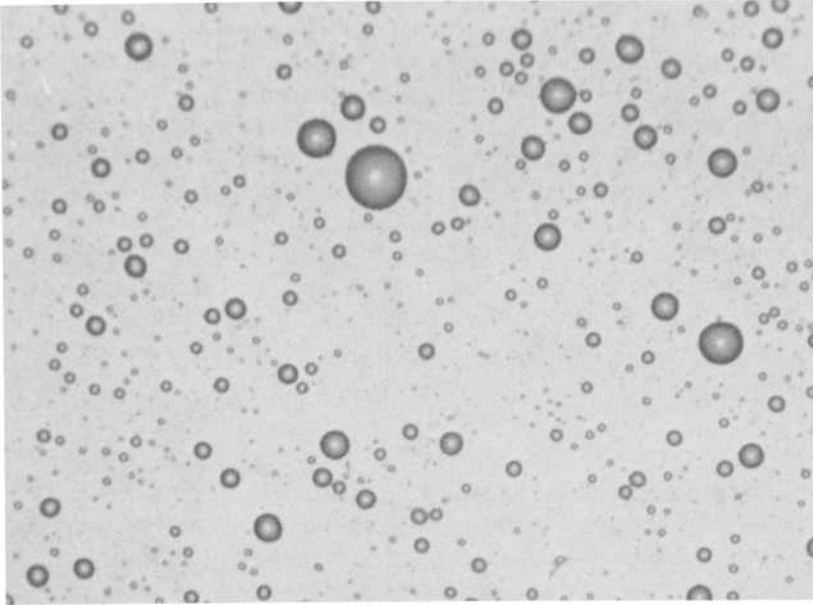


FIG. 3—*Droplet photograph. Orifice diameter 0.19 mm.*

undesirable patterns that may appear on the photographs. The thresholding levels can be set in such a way that complete drop is considered to be an image while the blank background can be considered to be undesirable patterns.

3. The third method uses an optical marker to discard defects on the photographs. Individual patterns not of interest can be circled by the marker thereby eliminating the encircled area from the computation. The marker also can be used to optically separate connected drops which otherwise would have been counted as one large drop. Thus, errors in identifying individual drops can be minimized. However, this method of editing is elaborate and time consuming particularly when the specimen size is large.

In our experiments the droplet photographs were generally of good quality but the specimen size was large. Hence, the framing technique of editing was used. Figure 3 shows a typical picture of some of the drops, at  $\times 150$  magnification, collected on the plate. The Quantimet considered a drop to be the area enclosed within the outer circular boundary, although some of the drops appeared to have a doughnut shape which was due to part of the drop being out of focus. Most of the drops were found to be spherical in shape.

The Quantimet has the capability of analyzing drops by measuring the following parameters:

1. Droplet cross-sectional area.
2. Droplet circumference of periphery.
3. Droplet volume (estimated).
4. Droplet diameter in four different directions: 0,  $\pi/4$ ,  $\pi/2$ , and  $3\pi/4$ .
5. Vertical projections.
6. Horizontal projections.

By using some of these parameters, it is possible to reject or include drops of any shape. In our size measurement, droplet diameters were calculated by averaging the four diameters measured in four different directions, as indicated previously.

Although the droplet photographs showed a few drops either joined together or connected to each other, no direct editing of the photograph was made on the image analyzer. Instead, editing was performed through the computer program, by comparing the diameters in the four different directions. If the measurement in one of the four directions exceeded the average drop diameter by 20%, then the particular image was deleted from the specimen. For drops of comparable size, where the contact length was appreciable compared to the diameter, the method served the purpose. In most of the instances the number of drops deleted from the specimen were less than 2%.

### Distortion and Resolution

The sizing technique employed in this work required droplets to be photographed. When the droplets are photographed, it is possible the droplet images may be distorted compared to their true shape. Fledderman and Hansen [13] have discussed droplet distortion during photographic process. To minimize distortions, a number of precautions were taken during processing of droplet photographs. No special developing process was used besides that recommended by the film manufacturer. During processing, however, all the chemicals were maintained at 22°C, and the prints were dried at the lowest temperature setting of the dryer. Based on the estimates given in Ref 13 and the precautions used, photographic distortions in our study were judged to be insignificant for drops of 1  $\mu\text{m}$  and over. However, there was some spreading effect on the collection slides. The correction factors were estimated by analyzing volumes of specimens of drops at high magnification ( $\times 500$ ) on the metallographic camera. For drops below 10  $\mu\text{m}$  the spreading factor was estimated to be 1.02, for drops between 10 to 30  $\mu\text{m}$  the corresponding factor was 1.05 and over 30  $\mu\text{m}$  it was 1.07. These factors were included in the final size analyses.

The second consideration in using the technique is its resolution. The total magnification of the droplets is of prime importance when small drops are to be sized. The vidicon system has some magnification, but the sizing technique requires an overall magnification of about 50 for a drop of about 1  $\mu\text{m}$  in size. The overall magnification used in our measurement technique was 150, thus allowing sizing even below 1  $\mu\text{m}$ .

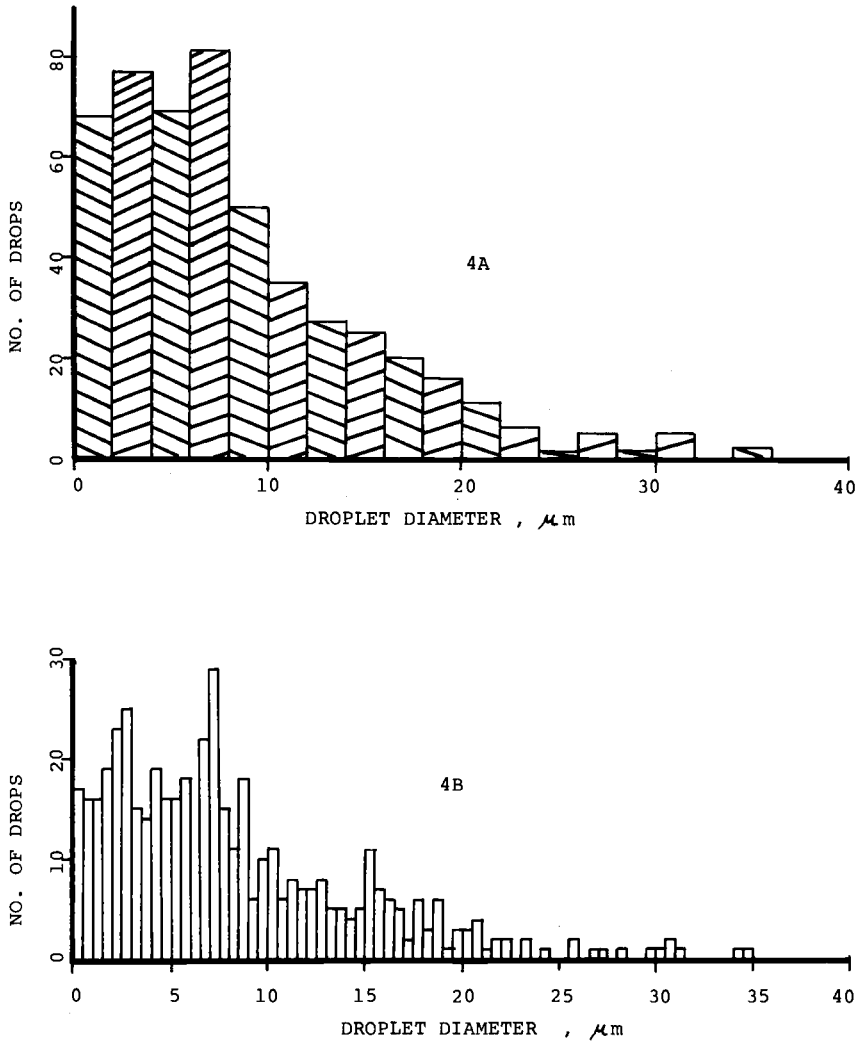


FIG. 4—Effects of size interval on distribution. 4A: size interval— $2\ \mu\text{m}$ ; orifice— $0.19\ \text{mm}$ ; injection pressure— $112\ \text{MPa}$ . 4B: size interval— $0.5\ \mu\text{m}$ ; orifice— $0.19\ \text{mm}$ ; injection pressure— $112\ \text{MPa}$ .

## Results

The system was programmed to give various droplet diameter, such as  $\bar{D}_{32}$ ,  $\bar{D}$ , and the size distribution. Figure 4a shows a typical histogram of about 500 droplets when the sizing interval was set at  $2\ \mu\text{m}$ . For the nozzle and the injection pressure used in this run, about 80% of the drops are below  $12\ \mu\text{m}$ . Figure 4b shows the histogram of the same experimental run when the sizing interval was reduced to  $0.5\ \mu\text{m}$ . It is clear that drops below  $1\ \mu\text{m}$  are detected by the analyzer as long as proper magnification is used.

It was indicated earlier that the particle density increases as sampling point is moved towards the axis of the spray jet. To evaluate if droplet sizes change accordingly, droplets were collected at different locations in the mixing region, as shown in Fig. 2. Figure 5a shows a photograph of the droplets collected at the periphery (Position 1 in Fig. 2), and Fig. 5b shows a corresponding photograph when the sampling point was moved about 10 mm towards the axis. The increase in the average droplet size as the sampling area is moved towards the axis is obvious from these photographs. Table 1 shows how  $\bar{D}$  and  $\bar{D}_{32}$  change when the sampling point is moved. It is not known if droplet sizes increase because of their agglomeration during their travel into the surrounding medium or because of poorer atomization around the main core of the fuel spray.

The accuracy of any droplet size measurement technique depends on the specimen size. To evaluate how specimen size may affect droplet diameters, the number of droplets in the specimen were varied from about 500 to 3500. Table 2 shows the variations in  $\bar{D}$  and  $\bar{D}_{32}$ . Also shown is the range of droplet sizes found in the specimen. It has been indicated that a specimen size of about 500 drops will yield an accuracy of  $\pm 15\%$ . Our results may show different accuracy since an increase in the number of drops in the specimen may also mean an increase in the collection area.

The vast number of experiments and the data generated from them have not been fully analyzed as yet. However, it is interesting to see some of the trends found in the constant pressure system. Figure 6 shows how  $\bar{D}_{32}$  at the periphery (Position 1) varied when the injection pressure was changed from about 50 to 140 MPa. Sauter mean diameter decreases as the injection pressure increases but the rate of change drops considerably when the pressure increases beyond about 100 MPa. This is important when designing a direct injection type diesel engine to operate on high fuel injection pressure.

### Validity of the Technique

An obvious and important question is : How valid are the results obtained with this collection method. No precise answer can be given at this stage. However, in an earlier research project in our laboratory, a similar technique was tried using an experimental diesel fuel injector. The latter was driven electronically so that the injection duration could be controlled independently. Experiments were conducted using an injection nozzle that delivered spray plume of about  $28^\circ$  cone angle; the amount of fuel injected per stroke was less than 0.5% of the amount of fuel injected in the constant pressure experiments discussed earlier.

In addition to the collection technique outlined in this paper, droplet sizes were measured by two other methods: direct photography and freezing of drops in liquid nitrogen. The number of measurements made with these alternative techniques were limited in nature. In the direct photography drops in the outer most mixing region (Position 1) were photographed at ambient temperature at magnification of 10. The droplets were forward illuminated for about 50  $\mu$ s. Since the

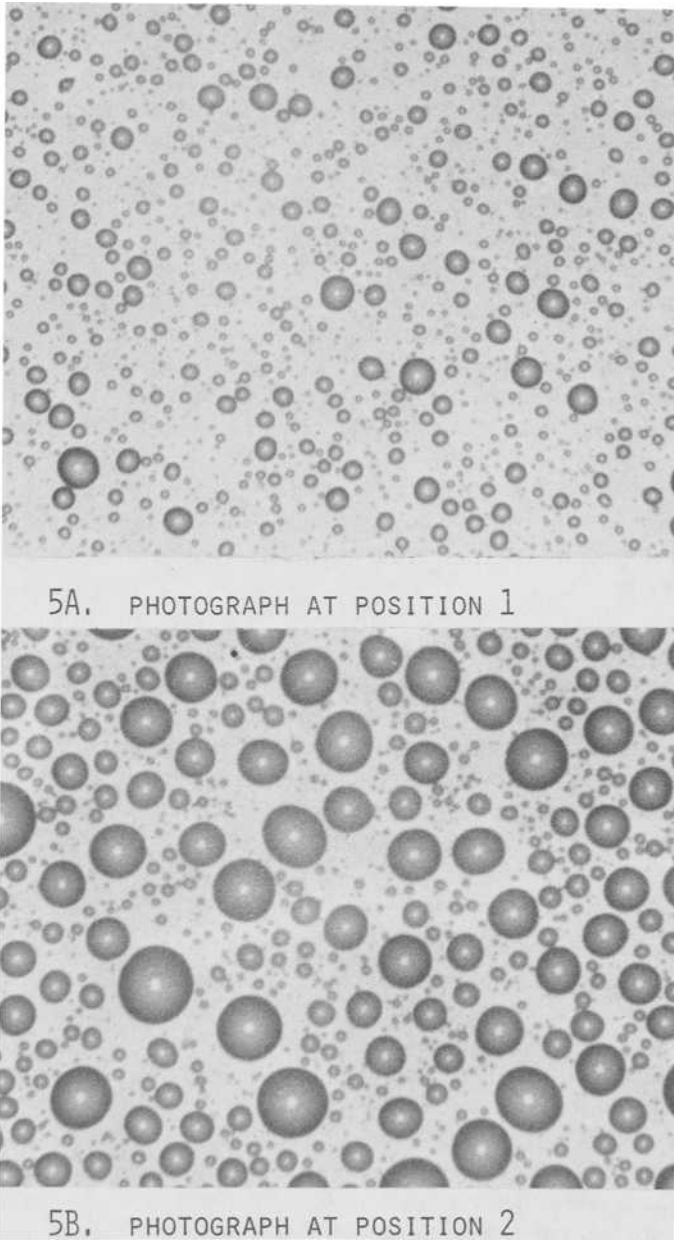


FIG. 5—Comparison of droplet photographs at two positions. 5A: position #1; 5B: position #2 and 10 mm from #1.

TABLE 1—Effect of sampling position on drop diameter (nozzle orifice 0.19 mm, injection pressure 112 MPa).

Specimen Position	$N$	$\bar{D}$ , $\mu\text{m}$	$\bar{D}_{32}$ , $\mu\text{m}$
Position 1 (outer periphery)	982	7.6	17.2
Position 2 (6 mm. from Position 1)	985	8.4	19.4

TABLE 2—Effect of specimen size on drop diameter (nozzle orifice 0.19 mm, injection pressure 112 MPa, sampling position: within 5 mm from the periphery).

Specimen Size, $N$	$\bar{D}$ , $\mu\text{m}$	$\bar{D}_{32}$ , $\mu\text{m}$	Droplet Size Range, $\mu\text{m}$
490	8.9	19.8	0.5 to 36
982	8.4	19.3	0.5 to 36
1982	8.1	18.5	0.5 to 38
3425	8.0	18.1	0.5 to 38

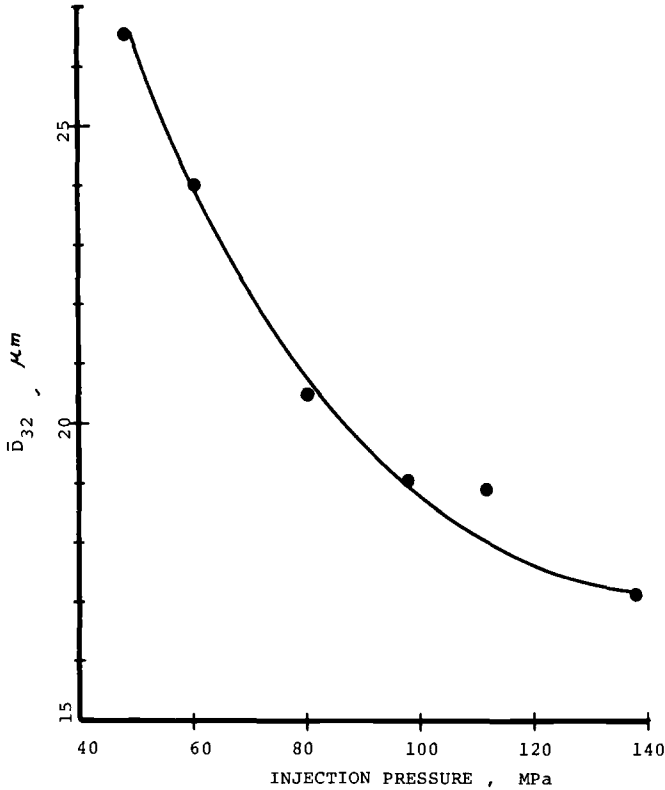


FIG. 6—Effect of injection pressure on Sauter mean diameter. Orifice: 0.19 mm; background density: atmospheric; injection rate:  $4.5 \times 10^{-3}$  to  $9 \times 10^{-3}$  kg/s.

TABLE 3—Comparison of droplet sizes by different methods (orifice size 0.36 mm).

Average Injection Pressure, MPa	Collection Method		Direct Photography		Freezing in LN <sub>2</sub>	
	$\bar{D}$ , $\mu\text{m}$ ( <i>N</i> )	$\bar{D}_{32}$ , $\mu\text{m}$ ( <i>N</i> )	$\bar{D}$ , $\mu\text{m}$ ( <i>N</i> )	$\bar{D}_{32}$ , $\mu\text{m}$ ( <i>N</i> )	$\bar{D}$ , $\mu\text{m}$ ( <i>N</i> )	$\bar{D}_{32}$ , $\mu\text{m}$ ( <i>N</i> )
14.0	24.8 (736)	58.3 (736)	23.9 (47)	55.6 (47)	25.3 (65)	61.4 (65)
26.2	20.2 (432)	43.1 (432)	19.3 (40)	41.4 (40)	20.9 (58)	45.2 (58)

droplets were moving, the photographs revealed small streaks from where droplet sizes were estimated. A maximum of about 50 drops were photographed since the depth of field was limited. In the freezing method, part of the spray was directed into a pool of liquid nitrogen. A shutter type of mechanism was used to control the amount of spray directed into the pool. The maximum number of drops frozen were less than 100. The frozen drops were photographed and later analyzed.

Table 3 shows the comparison of the diameters obtained by the three methods. The average injection pressure was calculated by integrating injection pressure over the entire injection duration. The peak injection pressure in each case was much higher than the average pressure. If direct photography is assumed to be more accurate then the collection technique over estimates both  $\bar{D}_{32}$  and  $\bar{D}$ . This can be attributed to the small specimen size used in the direct photography method. It appears that the collection technique, if used with great care, can give adequate droplet size measurement in the mixing region of a diesel fuel spray.

## Conclusions

Droplet sizes in the mixing region of a high-pressure diesel fuel spray have been measured by a collection technique where glass plates treated with a fluorochemical surface modifier were used. Using this method and an image analyzer specimen sizes containing large number of drops can be analyzed with the help of proper editing. The analyzer is capable of detecting droplets below 1  $\mu\text{m}$  if proper magnification is used in photographing the drops. Comparison of Sauter mean diameter (SMD) measured with the direct photography technique and the collection method shows good agreement at least in the mixing region. Droplet sizes measured in the mixing region of a constant pressure fuel spray showed spatical dependence.

## Acknowledgment

This work was funded by the U.S. Department of Transportation under Contract No. DTRS 5680-C-021. The authors would like to thank Dr. Thomas Connelly of the Department of Cell Biology, Ann Arbor Campus, for his assistance and in allowing us to use the Image Analyzer.

## References

- [1] Sauter, J., "Measurements of Fuel Particles in Fuel Sprays for Internal Combustion Engines" (in German), *Forsch ungsarbeiten auf dem Gebiet des Ingenieurwesens*, No. 279, 1926.
- [2] Sass, F., *Compressorless Diesel Engines*, Springer, Berlin, 1929.
- [3] Lee, D. W., "Measurements of Fuel Distribution within Sprays for Fuel Injection Engines," Report No. 565, National Advisory Committee for Aeronautics, Washington, DC, 1936.
- [4] Nukiyama, S. and Tanasawa, Y., *Transactions*, Japan Society of Mechanical Engineers, Vol. 4, No. 14, Feb. 1938, p. 86.
- [5] Joyce, J. R., *Journal of the Institute for Fuel*, Vol. 22, 1949, p. 150.
- [6] Hinze, J. O., *Applied Scientific Research*, Vol. A1, 1949.
- [7] Azzopardi, B. J., *Journal of Heat Mass Transfer*, Vol. 22, 1979, pp. 1245–1279.
- [8] Chigier, N., "Spray Combustion Processes—A Review," Paper 82-WA/HT-86, American Society of Mechanical Engineers, 1982.
- [9] Hiroyasu, H. and Kadota, T., "Fuel Droplet Size Distribution in Diesel Combustion Chamber," Paper 740715, Society of Automotive Engineers, 1974.
- [10] Takeuchi, K., Senda, J., and Shikuya, M., "Transient Characteristics of Spray Atomization and Droplet Size Distribution in Diesel Fuel Spray," Paper 830449, Society of Automotive Engineers, 1983.
- [11] Parker, R. F., "Future Fuel Injection System Requirements of Diesel Engines for Mobile Power," Paper 760125, Society of Automotive Engineers, 1976.
- [12] Varde, K. S. and Popa, D. M., "Diesel Fuel Spray Penetration at High Injection Pressures," Paper 830448, Society of Automotive Engineers, 1983.
- [13] Fledderman, R. G. and Hansen, A. R., "The Effects of Turbulence and Wind Speed on the Rate of Evaporation of a Fuel Spray," Report M604-3, U.S. Navy, Bureau of Ordnance Project, Washington, DC, 1951.

# **Nonoptical Particle Sizing**

David S. Mahler<sup>1</sup> and Daniel E. Magnus<sup>1</sup>

## Hot-Wire Technique for Droplet Measurements

---

**REFERENCE:** Mahler, D. S. and Magnus, D. E., "Hot-Wire Technique for Droplet Measurements," *Liquid Particle Size Measurement Techniques, ASTM STP 848*, J. M. Tishkoff, R. D. Ingelbo, and J. B. Kennedy, Eds., American Society for Testing and Materials, 1984, pp. 153–165.

**ABSTRACT:** An instrument using hot-wire technology to measure droplet size distributions in the 1 to 450  $\mu\text{m}$  size range is discussed. Such instrumentation has several advantages over present techniques which are dominated by a variety of laser light scattering approaches. The major advantages are: (1) the hot-wire instrument is readily portable; (2) no careful alignment is necessary; and (3) the instrument is available at a fraction of the cost of optical instruments.

The present paper discusses some details of the droplet/wire interaction, for example, effects of the wire mounting posts, "grazing" interactions, aerodynamic effects, and liquid variation. Also discussed are the means of raw data corrections to obtain a variety of mean droplet sizes, volume concentration, and volume flow rates.

Limitations will be discussed along with examples of where the instrument can best be utilized.

**KEY WORDS:** liquid, sprays, hot-wire, aerosols, particle size measurements

In recent years, the measurement of aerosols and sprays has been dominated by elaborate optical instruments based on a variety of laser light scattering principles or optical imaging approaches. Prior to such instrumentation, impaction techniques, or sensitized collection substrates, and a microscope were generally utilized. These latter techniques are time consuming, tedious, and subject to inaccuracies due to a limited statistical sample even with the use of digital computers. The optical instruments, on the other hand, are rather expensive and require careful alignment techniques.

The hot-wire method of droplet detection is an additional method which has received relatively little attention. This approach has been studied in laboratory environments [1] and has been independently researched [2–5]. A commercially available instrument has been produced by only one company<sup>1</sup> (Fig. 1). Though

<sup>1</sup>Physicist and president respectively, KLD Associates, Inc., Huntington Station, NY 11746.

<sup>2</sup>DC-2A manufactured by KLD Associates, Inc., 300 Broadway, Huntington Station, NY 11746.

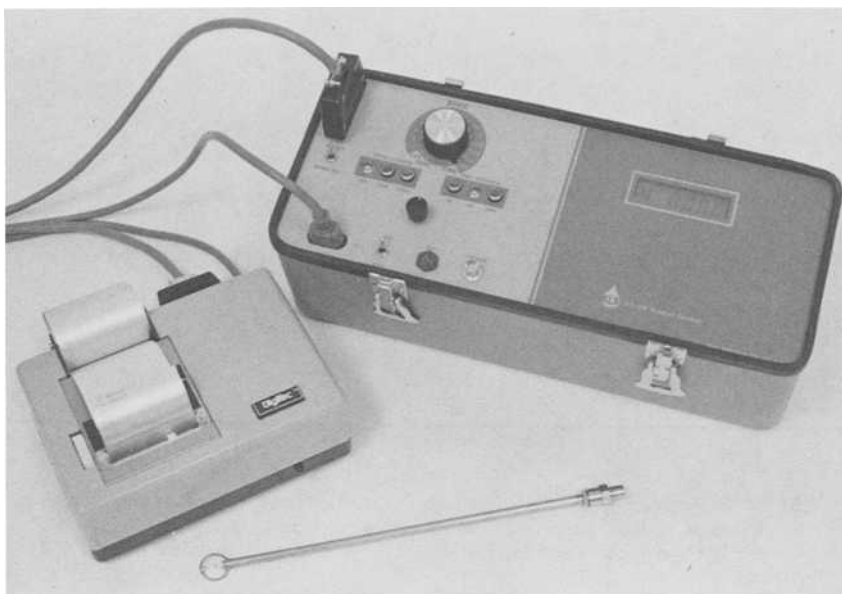


FIG. 1—*Model DC-2A, hot-wire droplet measuring instrument.*

the DC-2A has been used independently by a variety of industries, relatively little has been published in readily available media. One such independent report appears in Ref 6.

The work discussed in this paper is based on the research efforts which have led to the development of the DC-2A. The principle of operation of this instrument is based upon a constant temperature, 5- $\mu\text{m}$  platinum sensor. Figure 2 is an illustrative sketch. For purposes of the present discussion, the wire is heated to a uniform temperature.<sup>3</sup> A water droplet attaches to the wire, lowering its local temperature over a length of wire equivalent to the droplet diameter. The temperature drop causes the wire resistance to change in proportion to the droplet size. The sensor wire is part of a bridge circuit which generates a voltage pulse in response to the droplet. The bridge is initially balanced in order to take ambient temperature into account. A basic assumption in the instrument design is that the water droplets and air are at the same temperature. The overheat temperature of the sensor wire is set at 200°C above the ambient temperature. Using this setting, small variations of the droplet temperature will not have a significant effect on the electronic signals caused by the droplet/wire interaction.

Figure 3 is an illustration of an actual pulse. A droplet strikes the wire and is rapidly centered by surface tension forces. The leading edge of the signal is conditioned, and its droplet size determined within the first 20  $\mu\text{s}$ . The longitudinal conductive cooling of the wire then proceeds and the droplet begins to

<sup>3</sup>The actual temperature distribution is not uniform and a discussion of the real temperature distribution is presented in the section describing such effects.

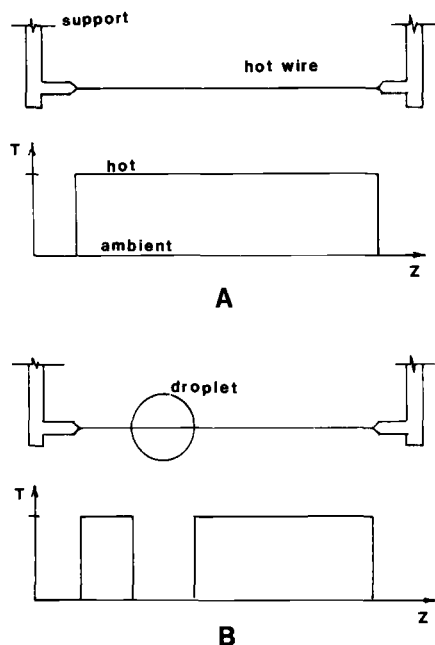


FIG. 2—Principle of operation of sensor. (a) Idealized longitudinal temperature distribution before droplet attachment. (b) After attachment.

heat up. When the droplet approaches the boiling point, evaporation takes place very quickly, and the wire is reheated to its initial overheated state. The entire process occurs within a maximum time of 2 ms, depending upon the droplet size.

The question of simultaneous collisions has been raised on several occasions and is best answered before proceeding. The term "simultaneous collision" has a relative meaning. A droplet is sized by the DC-2A within 20  $\mu\text{s}$  from its initial contact with the sensor. Therefore, a "simultaneous collision" must be defined as two or more droplets interacting with the wire within this time period. Such an occurrence has been shown to be unlikely. Tests performed with coarse sprays (SMD  $\approx 300 \mu\text{m}$ ) show that the DC-2A's bridge is rarely unbalanced for more than 2 ms, corresponding to the instrument's blanking period, even for counting rates approaching the instrument's upper limit. When pondering this point, the reader should consider that the sensing volume of even the largest droplet class (450  $\mu\text{m}$ ) is about  $1.3 \times 10^{-4} \text{cm}^3$ . Thus, even for dense sprays, the likelihood of "simultaneous collisions" is small.

The purpose of this paper is to discuss the methods used in calibrating the DC-2A and a variety of physical phenomena affecting the droplet/wire interaction. There will also be a brief discussion on how the raw data can be used to calculate various mean droplet sizes, volume concentrations, and volume flow rates. Finally, we will address some applications where hot-wire devices can be best used, and some of their advantages and disadvantages will be discussed in comparison to other techniques for droplet sizing.

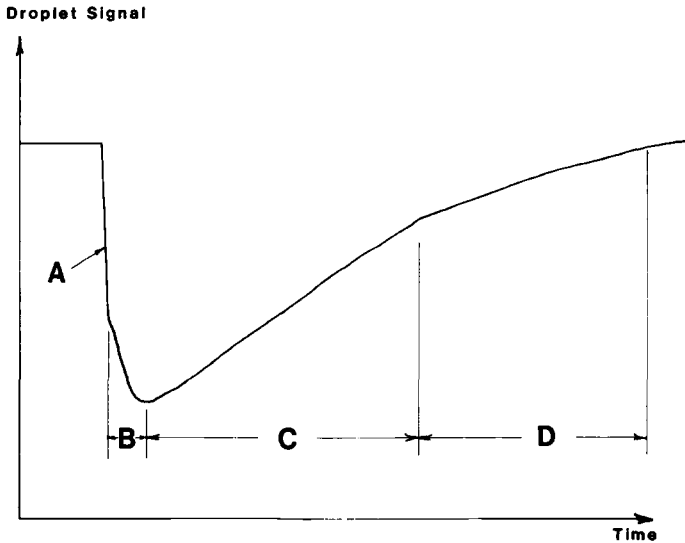


FIG. 3—Electrical droplet signal from sensor. (a) droplet/wire contact, (b) longitudinal heating, (c) droplet heating, and (d) droplet evaporation.

### Calibration

Any instrument using a secondary means of size determination requires a careful calibration. The apparatus used to calibrate the DC-2A is illustrated in Fig. 4. Here, a microscope is focussed onto the active portion of the probe. When a droplet interacts with a wire, the initial signal (in addition to being used for size determination) is used to trigger an electronic flash, thereby recording a photograph of the droplet during its initial attachment with the wire; and to trigger an oscilloscope, thereby displaying the electronic pulse created by the droplet/wire interaction.

Illustrations of both the droplet/wire photograph and the recorded pulse are shown in Fig. 5. The response time of the flash is kept within a microsecond so that no appreciable evaporation occurs before the acquisition of the calibration data. The flash duration is approximately  $4 \mu\text{s}$ .

An example of the calibration curve obtained for water is shown in Fig. 6. Here, the measured electronic pulse is plotted as a function of droplet size. The scatter in this data is discussed in the following sections.

### Droplet/Wire Interaction

The droplet/wire interaction is dependent upon numerous variables which cause the scatter indicated in Fig. 6. In addition, the nature of the droplet material will also alter the mean calibration line shown in Fig. 6. For example, the hot-wire technique for droplet detection is less sensitive for oils than for water.

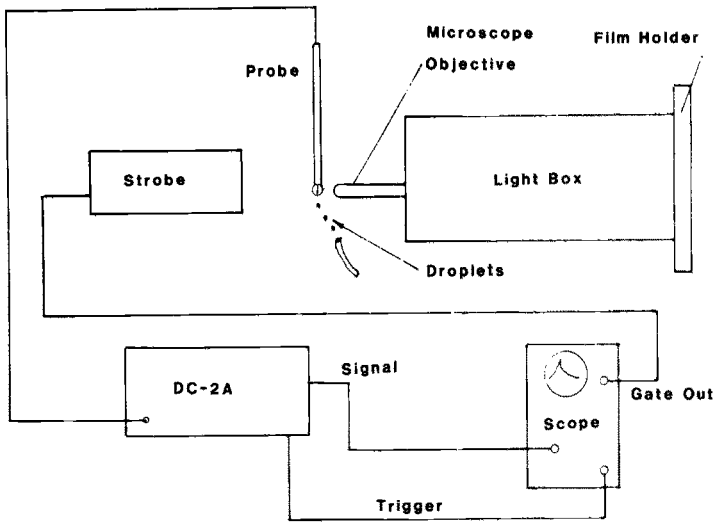


FIG. 4—Droplet calibration apparatus

In addition, various solutes in aqueous solutions may alter the data. For example, salts, such as exist in limestone, may coat the wire, thereby degrading the sensitivity of the probe. More of these material effects are discussed later. The present section is devoted to the actual physical interaction taking place between the droplet and the wire.

### *Aerodynamic Effects*

As a droplet approaches the vicinity of a hot wire, it will attempt to follow the altered stream lines around the cylinder. Such theories are presented in detail in discussions of filter technology [7]. Such corrections are only significant in the case of the smallest droplets. The aerodynamic corrections range from a theoretical value of 2.5 for droplets approaching  $1\text{-}\mu\text{m}$  and quickly approaches 1 for  $5\text{-}\mu\text{m}$  droplets, at which point the droplets are too massive to follow the stream lines or are large with respect to the flow alteration. The actual factor used to correct data gathered by the DC-2A is greater than the theoretical results as shown in Table 1. These correction factors were established by comparing data from the DC-2A with data from a Brink impactor [3] under carefully controlled laboratory conditions.

In addition to the corrections due to alterations of the stream lines caused by the presence of the wire, a second condition needs to be discussed. The specification of the DC-2A limits the droplet velocity (or the air stream velocity for fully entrained flow) to 10 m/s. This limitation is imposed for the larger droplets which can shatter upon striking the wire. Such events produce spurious signals which are interpreted by the instrument's signal conditioning circuits as being

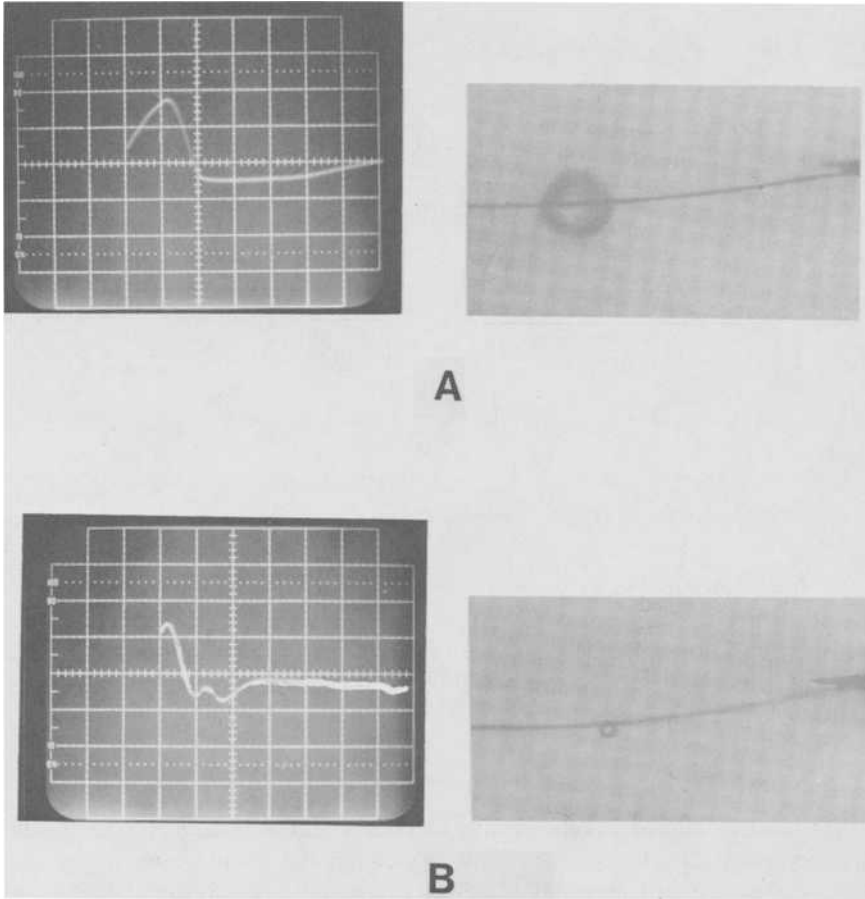


FIG. 5—Sample calibration data. (a) 98  $\mu\text{m}$ -diameter water droplet, 1 v/div, 10  $\mu\text{s}$ /div, (b) 24- $\mu\text{m}$  mineral oil droplet, 50 mv/div, 5  $\mu\text{s}$ /div.

numerous small droplets. In fact, the hot-wire technique can be used for velocities greater than 10 m/s provided that large drops are not present. Under these conditions, the operator should interpret the data with care.

#### *Eccentric Collision Effects for Various Liquids*

An eccentric collision occurs when a droplet strikes the wire off center. The extreme case of an eccentric collision is when a “grazing collision” occurs. A mathematical expression for the eccentricity is given by

$$\varepsilon = \frac{2x}{D} \quad (1)$$

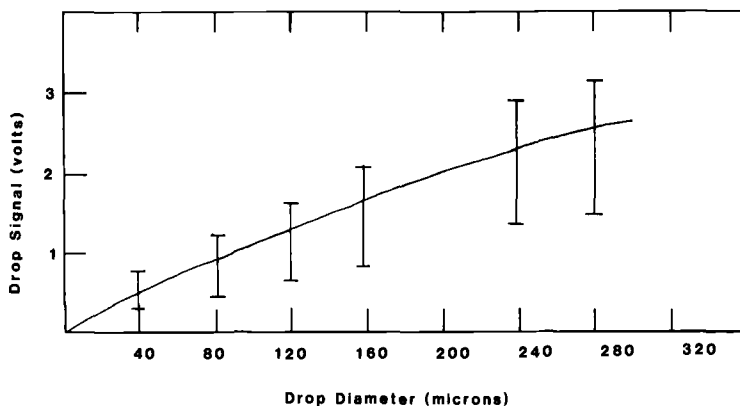


FIG. 6—Calibration curve for water.

As shown in Fig. 7,  $d$  is the droplet diameter and  $x$  is the distance between the center of the wire and the center of the drop at the moment of collision. In Fig. 7, the wire is assumed to be stationary with its longitudinal axis perpendicular to the plane of the paper. Thus, for a "head-on" collision,  $\epsilon = 0$ , while for a "grazing" collision,  $\epsilon = 1$ . The limits for eccentricity are, therefore, established as  $0 \leq \epsilon < 1$ .

Using the calibration apparatus described previously and a source of mono-disperse droplets, data were collected to establish the relationship between the electronic droplet signal and eccentricity. Figure 8 shows plots of the droplet signal as a function of eccentricity for water and for mineral oil.

The droplet signal for water has relatively little degradation as  $\epsilon \rightarrow 1$  when compared to the results for mineral oil. This difference is due to the relative

TABLE 1—Aerodynamic correction factor.

Bin No.	Size Range, $\mu\text{m}$	$K_{\text{Aero}_i}$	$K_i$
1	1 to 1.6	2.5	5.0
2	1.6 to 2.6	1.8	2.8
3	2.6 to 4.1	1.2	2.0
4	4.1 to 6	1.0	1.6
5	6 to 10	1.0	1.2
6	10 to 17	1.0	1.0
7	17 to 27	...	...
8	27 to 43	...	...
9	43 to 69	...	...
10	69 to 110		
11	110 to 176		
12	176 to 282		
13	282 to 450		
14	>450		

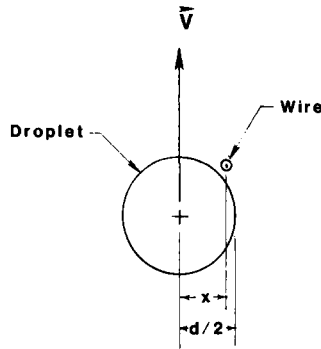


FIG. 7—Eccentricity geometry.

values of the surface tension for these two materials. The surface tension of water is more than twice that of mineral oil. Because of its large surface tension, water droplets are very quickly centered about the wire for eccentric collisions. This centering occurs so rapidly for the case of water, that very little effect is noticed on the droplet signals in the majority of cases. For the case of mineral oil, the droplet signals display a pronounced degradation for  $\epsilon > 0.7$ .

#### *Effects Due to Wire Temperature Distribution*

Another aspect influencing the calibration curve is the longitudinal position of the droplet with respect to the wire. Figure 2 depicts an idealized, constant longitudinal temperature distribution. For such a case, the droplet signals for a prescribed droplet size would only be altered if the longitudinal location of the collision partly included the support structure at the moment of impact. However, the longitudinal temperature distribution is not constant, but obeys the expression

$$\frac{T(z) - T_f}{T_\infty - T_f} = 1 - \frac{\cosh(z/l_c)}{\cosh(l/2l_c)} \quad (2)$$

where

$T(z)$  = local wire temperature at point,  $z$ , along the wire, here,  $z$  is measured with respect to the center of the wire;

$T_\infty$  = temperature of an infinitely long wire with the same current;

$T_f$  = temperature of wire supports which is assumed to be that of the fluid;

$l$  = wire length;

$l_c = \frac{d}{2} \left[ \frac{R_w k_w}{R_a k_f} \frac{1}{Nu} \right]^{1/2}$  = cold length;

$d$  = wire diameter;

$R_w$  = wire resistance at overheat temperature;

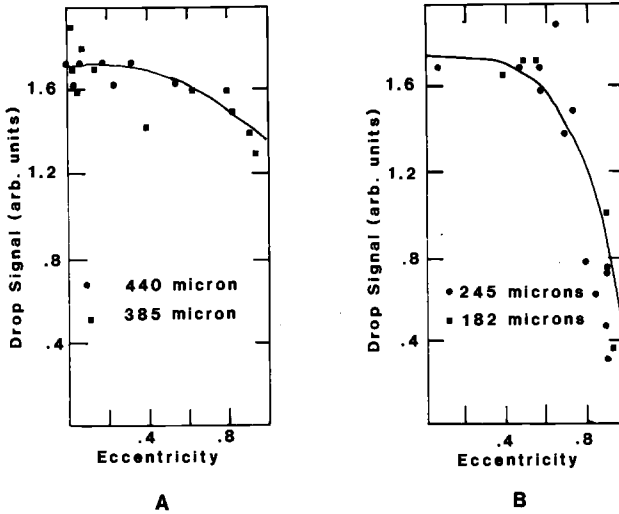


FIG. 8—Eccentricity data for (a) water and (b) mineral oil.

$R_a$  = wire resistance at ambient temperature;

$k_w$  = thermal conductivity the hot-wire; and

$k_f$  = thermal conductivity of the fluid.

This expression is derived by considering the longitudinal heat conduction to be the major contribution to heat loss [8,9]. Such an expression shows that a constant longitudinal temperature distribution is a reasonably good approximation for  $l/d > 600$  [8]. For the case of the probes used in this work, the length-to-diameter ratio ( $l/d$ ) is approximately 200. Thus, analytically one expects a significant range of temperature with respect to the longitudinal position of the wire, and, in turn, an influence on the calibration curve will result.

Figure 9 is a plot of the corrected electronic pulse as a function of the longitudinal position along the wire using water droplets. Two corrections were applied to the data appearing in this plot. First, a correction was made to adjust the pulse with respect to the droplet size. Only droplets between 55 and 70  $\mu\text{m}$  were used to minimize such a correction. Second, the data were corrected for the effects due to eccentricity as previously explained. Only droplets with  $0 < \epsilon < 0.8$  were considered.

Before comparing these data with theory, Eq. 2 was recast as

$$y = A_4 - A_3 \cosh[A_2(Z - A_1)] \quad (3)$$

where  $A_i$  are to be chosen by a nonlinear least-squares grid search program [10]. The solid curve shown in Fig. 9 is the best fit to such an analysis.  $A_1$  is introduced because it is experimentally more convenient to measure  $Z$  with respect to one end support of the wire than from the middle as was the case for Eq. 2. Comparing

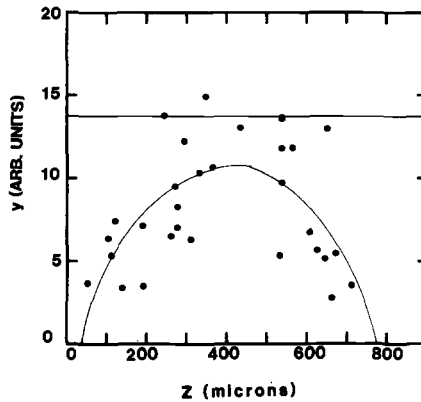


FIG. 9—Data showing the relation of the droplet signal with respect to longitudinal position. The solid curve is a least-squared fit of Eq 3 to the data. The horizontal line represents  $T_{\infty}$ .

Eqs. 2 and 3, it can be shown that

$$A_2 = 1/l_c$$

$$A_3/A_4 = 1/\cosh(l/2l_c)$$

$$y = \frac{1}{A_4} \left[ \frac{T - T_f}{T_{\infty} - T_f} \right]$$

$$A_1 = \frac{l}{2}$$

and

$$Z = z + A_1$$

Thus, plotting  $y$  versus  $Z$  is equivalent to plotting  $T$  versus  $z$ . Not only does the data reveal the effects of the longitudinal position on the calibration curve, but, in addition, the data appear to be a measure of the relative temperature distribution of the hot-wire itself. These results are consistent with a similar  $l/d$  ratio described in Ref. 8, although the present data do reveal a larger degree of scatter which is not fully understood at this time. The details of the hot-wire/support interface will also affect the longitudinal heat conduction and thus affects the longitudinal temperature distribution.

#### Calibration Curve

The incorporation of the effects due to eccentricity and the longitudinal, wire temperature distribution into the calibration is extremely important. Figure 6 is a plot of the droplet signal versus droplet diameter for water. The scatter depicted by the error bars must be carefully considered. It is due to eccentric collisions,

longitudinal effects, combinations of the two, and perhaps other effects which have not yet been identified. All of these effects occur statistically under real spray conditions, and it is important that no data points be discarded because they may seem "extreme." The "calibration curve" is a line which must be selected from this array of points in such a way that it represents the best statistical line possible. Because of the degree of scatter, it is important that as large a data sample be used as is reasonably practical.

Because eccentricity has a larger influence for a liquid such as mineral oil (in comparison to water), a separate calibration curve is needed. Hence, a separate calibration curve has been generated for use with oils. It does not necessarily mean a new calibration curve is needed for all materials, but the user must be aware of these effects. Certainly, knowing the surface tension is important when measuring nonaqueous liquid sprays.

### Data Analysis

Table 1 shows the size range of the 14 bins used for the standard DC-2A. A logarithmic increase in bin size has been used in order to maintain a constant percentage of error in each bin. However, the user can specify bin sizes to meet a specific need provided that the selected bin sizes fall within the overall size range of the instrument. The 14th bin can only be specified as representing droplets over a given size, since drops larger than bin 13 will always go into bin 14.

One may apply a generalized expression for the mean diameter

$$D_{pq}^{p-q} = \frac{\sum n_i D_i^p}{\sum n_i D_i^q} \quad (4)$$

where

$n_i$  = number of droplets per unit volume of gas in the  $i^{\text{th}}$  size class, and  
 $D_i$  = representative size of the  $i^{\text{th}}$  bin.

We usually find that the geometric midpoint of the size range is sufficient, but one could preferentially use the volume midpoint diameter or area midpoint diameter if desired for a value of  $D_i$ .  $p$  and  $q$  are integers referring to different mean values. The DC-2A has 14 bins so that  $i$  runs from 1 to 14. The number density is computed from the raw data, using a different sample volume,  $V_i$  for each size bin (Fig. 10). The sample volume of the bin  $i$  is expressed by

$$V_i = vtl(D_i + d) \quad (5)$$

where

$v$  = flow velocity,  
 $t$  = corrected time, and  
 $l$  = effective length.

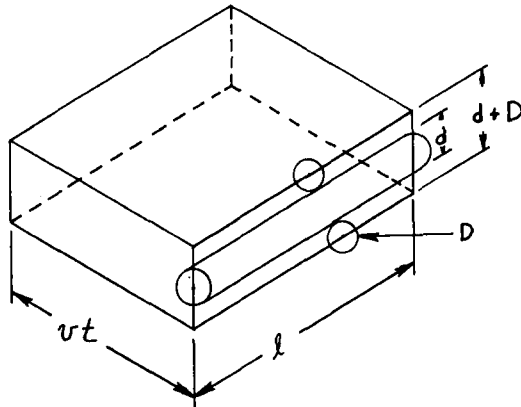


FIG. 10—Geometry of droplet interacting with wire showing how the capture volume is derived.

Combining Eqs. 4 and 5, one can write

$$D_{pq}^{p-q} = \frac{\sum_{i=1}^{14} (N_i K_i / (D_i + d)) D_i^p}{\sum_{i=1}^{14} (N_i K_i / (D_i + d)) D_i^q} \quad (6)$$

where

$K_i$  = aerodynamic correction factor (Table 1), and

$N_i$  = number of droplets counted in the  $i^{\text{th}}$  bin.

Various median diameters can be also obtained by treating the raw data in a similar manner.

### Applications, Advantages, and Limitations

Hot-wire technology has been used to investigate droplet distributions in a variety of applications. The DC-2A and its predecessor, the DC-2, have been used to obtain in situ measurements in demister towers, scrubbers, and other process facilities. With a cable length of 5.4 m (18 ft), ducts as large as 8.5 m (28 ft) across have been studied. Taking data at several locations, the cross-sectional character of droplet flow through a duct can be determined, in addition to measuring the total mass flow and liquid concentration.

Other areas where the DC-2A has been successfully used involve the measurements of demister efficiencies by several demister manufacturers and the characterization of a variety of liquid aerosol generators varying from medical nebulizers with a Sauter mean diameter ( $SMD = D_{32}$ ) on the order of  $5 \mu\text{m}$  to coarse spray nozzles with SMDs of several hundred microns. The technique has been also shown to be sensitive to a wide variety of liquids; notably water, oils, insecticides, and hydrochloric acid.

Attractive user features built into the DC-2A include:

1. No delicate alignment of the probe is needed, and the device can be operated by nontechnical personnel. Data are collected by pushing one button.
2. The instrument package is small and light weight, making it field portable.
3. A printer and printer interface are available as options.
4. Battery operation is available.

The hot-wire approach used in the DC-2A has been shown to yield accurate measurements for such statistical values as the Sauter mean diameter, volume mean diameter, volume median diameter, liquid volume flow rate, and liquid concentration. These characterizations of liquid aerosols have been specified by a majority of users. The calibration curve, as shown in Fig. 6, has been selected in order to optimize the accuracy of the DC-2A for obtaining these various "volume" dependent parameters.

### *Acknowledgments*

This work has been supported in part by the Department of the Army under contract No. DAMD17-82-C-2042, by the EPA under contracts 68-02-2111 and 68-02-1309 and by internal research funding of KLD Associates.

### **References**

- [1] Goldschmidt, V. W., *Two-Phase Flow in a Two-Dimensional Turbulent Set*, Ph.D. thesis in Mechanical Engineering, Syracuse University, University Microfilm 65-7968, 1965.
- [2] Medeck, H., Kaufman, M., and Magnus, D. E., "Design, Development, and Field Test of a Droplet Measuring Device," EPA-650/2-75-018, Environmental Protection Agency, Feb. 1975.
- [3] Medeck, H., Wu, K. C., and Magnus, D. E., "Development of Droplet Sizing for the Evaluation of Scrubbing Systems," EPA-600/7-79-166, Environmental Protection Agency, July 1979.
- [4] Magnus, D. E., Medeck, H., and Wu, K. C., "Sensing of Droplet Size and Concentration in Pollution Control Equipment," 4th Joint Conference on Sensing of Environmental Pollutants, Paper 161, American Chemical Society, 1978.
- [5] Magnus, D. E., and Mahler, D. S., "An In-Situ Liquid Droplet Sizing System," in *EPA Proceedings: Advances in Particle Sampling and Measurement*, EPA-600/9-004 Environmental Protection Agency, Jan. 1980, p. 302.
- [6] Zalosh, R. G. and Bajpai, S. N., "The Effect of Water Fogs on the Deliberate Ignition of Hydrogen," EPRI NP-2637 Environmental Protection Research Institute, Nov. 1982.
- [7] Dorman, R. G., "Filtration," Chapter 8 in *Aerosol Science*, C. N. David, Ed., Academic Press, New York, 1966.
- [8] Champagne, F. H., Sleicher, C. A., and Wehrmann, O. H., "Turbulence Measurements with Inclined Hot-Wires, Part 1. Heat Transfer Experiments with Inclined Hot-Wire," *Journal of Fluid Mechanics*, Vol. 28, No. 153, 1967.
- [9] Bradshaw, P., *An Introduction to Turbulence and Its Measurement*, Chapter 5, Pergamon Press, New York, 1975.
- [10] Bevington, P. R., *Data Reduction and Error Analysis for the Physical Sciences*, McGraw-Hill, New York, 1969.

# Closure

Norman Chigier<sup>1</sup>

## Comparative Measurements Using Different Particle Size Instruments

---

**REFERENCE:** Chigier, N., "Comparative Measurements Using Different Particle Size Instruments," *Liquid Particle Size Measurement Techniques*, ASTM STP 848, J. M. Tishkoff, R. D. Ingebo, and J. B. Kennedy, Eds., American Society for Testing and Materials, 1984, pp. 169–186.

**ABSTRACT:** This paper discusses the measurement and comparison of particle size and velocity measurements in sprays. The general nature of sprays and the development of standard, consistent research sprays are described. The instruments considered in this paper are: pulsed laser photography, holography, television, and cinematography; laser anemometry and interferometry using visibility, peak amplitude, and intensity ratioing; and laser diffraction. Calibration is by graticule, reticle, powders with known size distributions in liquid cells, monosize sprays, and, eventually, standard sprays. Statistical analyses including spatial and temporal long-time averaging as well as high-frequency response time histories with conditional sampling are examined. Previous attempts at comparing instruments, the making of simultaneous or consecutive measurements with similar types and different types of imaging, interferometric, and diffraction instruments are reviewed. A program of calibration and experiments for comparing and assessing different instruments is presented.

**KEY WORDS:** particle size instruments, measurements in sprays, laser diagnostic techniques

Interest in making measurements of size and velocity distributions in sprays is growing rapidly in the combustion, chemical process, pharmaceutical, and agricultural industries. Overall dimensions of different sprays vary from on the order of one millimetre to tens of metres, but the particle size of interest is predominantly in the supermicron range, between 10 and 500  $\mu\text{m}$ . Many of the processes involve evaporation and chemical reaction resulting in a progressive reduction in particle diameter.

The understanding and knowledge of the particle and fluid dynamics of spray structure is scant, and the science of sprays is in an early stage of development. Insufficient thought, attention, and research have been devoted to the nature of sprays. Many factors must be taken into account: the complexities of hydro-

<sup>1</sup>William J. Brown, professor, Department of Mechanical Engineering, Carnegie-Mellon University, Pittsburgh, PA 15213.

dynamic breakup of liquid films, particle and fluid mechanics, and the interaction of particles injected into turbulent confined gas flows. Heat and mass transfer and chemical reaction result in temperature, velocity, gas concentration, particle size, and particle velocity fields with high degrees of inhomogeneity. Large-scale variations occur in each quantity as a function of both space and time.

A prerequisite for the development, calibration, and testing of any measuring instrument for utilization in sprays is a prior assessment of the principal characteristics of the spray and the factors likely to affect the particular quantity that is to be measured. If, for example, measurements are restricted to particle size and velocity, it will soon become apparent that this is a formidable task for which there is currently no adequate instrument (or set of instruments).

Recently several reviews [1-4] have been made of individual instruments or groups of instruments used for particle size and velocity measurements in sprays. Experience is being gained both by research investigators in laboratories and users in industry. There is an alarmingly large number of disillusioned purchasers of commercial instruments who are finding that they have greatly underestimated the experience, time, and effort required by the user and that they have overestimated the capability of any one particular instrument.

This paper discusses the next stage—the comparison of different instruments. A few attempts have been made by a few investigators to make measurements with more than one instrument. Round-robin tests have been carried out in which research nozzles have been passed around to different investigators to make comparative tests in different laboratories with the same type (or sometimes another type) of instrument. The results to date are extremely discouraging as there is little agreement among the various groups.

Before undertaking a responsible and serious comparison of instruments the following preconditions need to be satisfied:

1. Research atomizers and nozzles must be manufactured and handled with particular care in order to produce consistent, continuous (unless pulsed), and axisymmetric sprays.
2. Liquid and gas supply systems must be free of extraneous pulsations and instabilities. Fluid properties must remain constant by maintaining constant temperature conditions.
3. The environment in the spray chamber must be controlled so that constant temperature and flow patterns are maintained.
4. Each optical, electronic processing, and computing component of each instrument must be debugged, and then the system as a whole must be calibrated.
5. The investigator needs to make an initial assessment of the region in the spray under investigation; measurement volume, frequency of large scale variations, particle size, and velocity ranges should all be considered.
6. Records need to be maintained of all factors that may initially or subsequently affect the results: fluid supply pressures, flow rates, and temperatures; environmental temperatures, and pressures influencing flow fields; location of

instrument traversing mechanisms; measurement volume dimensions, periods of, and intervals between, recording; and laser light power and other components of the instrument that could change during the course of the measurements.

7. Each instrument system must be calibrated prior to and subsequent to each set of measurements.

This paper discusses the nature of sprays, measurement systems, statistical analyses, and comparative measurements. A program for making a set of comparative measurements is presented.

### **Nature of Sprays**

Sprays almost invariably will be unstable, nonsteady, turbulent, and poly-disperse. Instabilities arise in the injection and supply lines of spray material and atomizing fluid. Pulsations from pumps, fans, and blowers are transmitted with the fluids. Hydrodynamic instabilities are inherent in wave propagation and breakup of liquid films. High shear rates and velocity gradients are associated with high turbulence intensities in both liquid and gaseous shear zones causing sporadic and random tearing and perforation of liquid sheets leading to non-uniform ligament and drop formation. Nonuniformities in fluid injection flow rates cause pulsations and spitting (periodic bursts). Rapid transitions from bulk liquid flow to particle-laden turbulent jets result in the clustering of particles by large eddy structures formed in shear and entrainment regions of the turbulent jet.

### **Standard and Consistent Sprays**

Before making a detailed analysis of a particular spray, great care must be taken to ensure that, globally, the spray remains consistent. Any uncontrolled variations in supply pressure or flow rate of liquid or atomizing fluid will cause changes in the spray. Hence supply pressures must be continuously monitored and controlled throughout the test period. Any changes in flow geometry due to changes in the nozzle or long time accumulation of deposits or corrosion in narrow passageways will cause changes in spray characteristics. Small burrs or deformations to nozzle tips have been shown to cause significant changes to sprays. Liquid films are deflected by protrusions or dents that have dimensions comparable to the thickness of liquid films (0.5 mm). The physical properties (viscosity, density, surface tension) of fluids must be maintained constant—these properties are all functions of temperature so that fluid temperatures must be also held constant.

The boundary conditions for the spray need to be maintained constant and clearly specified. The presence of chamber walls affects pressure variations and hence flow fields, recirculation zones, and entrainment rates of air into the spray. Drafts or convective flow currents in the vicinity of the spray can deflect the sprays and cause asymmetries. The smaller droplets are very sensitive to evaporation, and small changes in ambient gas temperature can cause significant changes in the population of small drops.

From a measurement point of view, it is convenient to study sprays that are symmetric about the spray axis. This requires symmetrical flow through the nozzle and the removal of all forces that can deflect the spray and result in asymmetry. In turbulent jets the flow is only axisymmetric on the average. Individual eddies and drops may readily cross the axis without recognizing it as a real boundary.

Swirling flows can be easily generated in fluid supply lines and nozzles either by design or by default — resulting in tangential velocity components for particles and fluid in the spray. Turbulence is inherently 3-D, and jet flows have regions of isotropy where velocity fluctuations have the same magnitudes in the axial, radial, and tangential directions. In sprays and jets the flow is often assumed to be 2-D with no significant motion in the tangential direction. This assumption must be proved for each particular spray by measurement and demonstration that the tangential velocity component is at least one order of magnitude less than the radial and axial velocity components.

Maintenance of fluid flow continuity (no pulsations), symmetry about the spray axis, control of the supply fluid's physical properties, control of the ambient pressure, temperature, and entrainment flow fields are all necessary and essential prerequisites for comparative spray studies. It is futile to compare instruments if the particle size and velocity phenomena are not maintained constant during individual and related measurements.

### Measurements in Sprays

Accurate measurement of physical quantities such as particle size and velocity can be ensured only if there are recognized and well-established standards against which measuring instruments can be calibrated. At first thought it might seem that the measurement of particle size should pose no major problems, since all that is required is measurement of a one-dimensional length scale, and there is a wide variety of instruments for accurate measurement of length. In sprays, interest is mainly focused on determining size distributions in the super-micron range between 10 and 500  $\mu\text{m}$ . Most sprays have large numbers of small particles ( $<10 \mu\text{m}$ ), and it is also difficult to avoid generating several very large particles. A more comprehensive range for spray studies, therefore, would be from say 0.1 to 2000  $\mu\text{m}$ . In sprays where vaporization or reaction is taking place, the smaller particles ( $<10 \mu\text{m}$ ) will evaporate or react very quickly and readily. Therefore, in many practical polydisperse sprays with normal distributions there is much less interest in accurate determination of both size and number of the lower range of particle sizes. Large particles (above 1 mm) can be readily "seen" and measured. The large particles often pose major problems because their large diameter, low surface to volume ratio, and high momentum are not catered for within the dimensions of the reaction chamber. Frequently these particles are deposited on walls or emitted from the system in an incompletely evaporated or unreacted status. In examining problems of deposition, fouling, corrosion, and emission of pollutants,

accurate measurement of the number and size of large particles with averaging over long time periods is necessary.

When, considering sprays introduced into reaction chambers, the system has the requirements that (1) evaporation and reaction must be completed within the confines of the chamber and (2) there should be no deposition on walls. The initial boundary conditions for the spray can be specified by measurement of the size, velocity, and direction of all particles crossing the entrance plane. Size, velocity, and angle of flight correlations are necessary since most sprays are polydisperse with nonuniform velocities and nonuniform injection angles. Momentum, velocity components and drag coefficients need to be determined in order to calculate trajectories of single particles.

In setting out to measure size distributions, thought needs to be given to the extent to which it is necessary to measure the size of all particles in the system. As particle size decreases, numbers of particles increase exponentially. Since there may be little interest in determining the characteristics of the fog or mists associated with sprays, the lower particle size range is often ignored. For the cases when it is of special interest and importance, the philosophy and technique of measurement may have to be changed for determination of large number densities ( $10^{10}$  particles/cm<sup>3</sup>) in the submicron (0.001 to 1  $\mu\text{m}$ ) range. Since visible light is on the order of 1  $\mu\text{m}$ , changing focus from the supermicron to the submicron size range prevents the utilization of many optical instruments.

Before attempting to measure the characteristics of a particular spray several pertinent questions need to be addressed. Bearing in mind that the effort and expense associated with the measurement is directly related to the accuracy and number of particles to be measured as well as the measurement volume and time, initial decisions based on the ultimate requirements and usefulness of the data can result in very large differences in the planning approach, selection of techniques, and making of the measurements. For example, the numbers of particles that require to be counted, per cubic metres, in a practical spray may vary from  $10^4$  to  $10^{100}$  if the lowest size to be measured is reduced from 10 to 0.01  $\mu\text{m}$ .

The prescribed or desired measurement volume and time are also related to size and the number of particles. Decisions on measurement volume and time must be related to the type of atomizer, nature, and overall dimensions of the spray. A pulsating diesel spray emerges from a nozzle with diameter on the order of 200  $\mu\text{m}$  and has an overall length of several centimetres. In a heavy fuel oil utility boiler for electricity generation, 15 tons of liquid per hour are injected into a combustion chamber where spray and flame lengths are on the order of 20 m. In large diameter rotary kilns in cement and chemical processing plants, spray lengths may even reach the order of 50 m. Despite these very large differences in the total length scale of the sprays, the particle size ranges do not change significantly and are not directly related to spray volume. Instrument requirements for dealing with microscopic or large-scale fields of view are radically different in concept, scope, and dimensions.

The effects of the invasion of sprays by light guides and fiber optics need to be studied and tested. These techniques may be the only recourse in large-dimension high-density sprays, but it must be proved that they have little effect on accuracy of measurements in the measurement volume in which particles enter from an undisturbed upstream flow. Since photography is the most accurate and reliable method of measurement, it is generally used as a "calibration" for other measuring devices.

### Light Sources

Laser light sources are now being used in almost all optical particle sizing techniques. For imaging techniques, pulsed ruby and neodymium-yag lasers provide high intensities (megawatts) and short pulses (nanoseconds). All particle and fluid flow patterns therefore can be "frozen" in time. Excellent contrast and resolution down to 5  $\mu\text{m}$  can be attained. The contrast obtained with high-powered lasers improves the capability of differentiating between in-and-out of focus drops. Double pulses with variable time intervals (microseconds) between pulses are being used for velocity and angle of flight determination of individual drops. The total number of laser pulses per second is still restricted to approximately ten. It seems unlikely that pulse repetition rates of milliseconds or microseconds will be attainable for high-frequency response turbulent measurement. The current repetition rates of 100 ms allow the accumulation of data for probability density function, mean velocity, and variance determinations.

For laser anemometry, interferometry, and diffraction particle sizing, continuous wave, (CW) lasers are used. Low powered helium-neon lasers (15 mW) are used in dilute sprays and high signal-to-noise systems. For dense sprays, for spray widths greater than 10 cm, or for sprays in the presence of extraneous light and radiation interference, argon-ion lasers (4 W) increase the signal to noise ratio. Measurements can be made in systems with light obscuration of the order of 50%.

### Calibration

Calibration devices for particle sizing include: graticules—2-D circular opaque dots or spots on transparent slides; reticles (or masks)—2-D circular holes in opaque film on transparent slides; 3-D solid particles attached to rotating transparent disks; powders, latex spheres and glass beads of known size distribution in liquid flowing through transparent columns; monosize single and multiple streams of drops generated by piezoelectric crystals; and monosize sprays produced by various spray generators. None of these devices is adequate for the calibration of instruments designed to make measurements in polydisperse sprays. Standard polydisperse sprays with controlled and maintained size and velocity distributions have not yet been designed. The range of standard sprays would need to include the drop sizes, spacing velocities, and number densities commonly encountered in sprays. Effects of high light obscuration (90%) and

multiple scattering in high density ( $10^{10}/\text{cm}^3$  and above) sprays need to be accounted for by testing and calibration.

### **Unsteady State**

The classical approach towards studying unsteady turbulent flows has been to impose the concept of quasi-steadiness on the flow. By the process of long-time averaging for various points in an Eulerian frame of reference, "pictures" of stream lines and mean velocity distributions have been drawn. These "constructed pictures" may have some relationship to long-time exposure photographs, but visual observation, short time (milliseconds and nanoseconds) exposure photography and high-speed (10 000 frames/s) cinematography reveal different structures for eddies and flow patterns according to the viewing and exposure time. Ensemble averaging of random short exposure (nanoseconds) photographs yields radically different flow patterns than those determined by classical long-time viewing and analysis. Despite the paucity of available information there should be, in principle, more interest in attempting to measure the histories of individual particles travelling with erratic trajectories through gas flow fields having large variations in temperature and concentration. It is the rate of evaporation and reaction of individual particles that determines the net rate of evaporation and reaction of the system as a whole. It is a nontrivial mathematical and measurement problem to relate long-time averaged "point" measurements in the Eulerian reference frame to particle trajectories in the Lagrangian reference frame for turbulent flows with a wide frequency spectrum. Understanding the fluid dynamics of turbulent flow has been limited by the capabilities of the instrumentation. Pitot pressure impact tubes, hot wire anemometers, and suction probes for particle and gas analysis have been placed at fixed positions in flow fields for long time (minutes) averaging. By contrast, studies of atmospheric turbulence and weather patterns have traditionally focused attention on movements and trajectories of parcels, packages, and clouds of fluids as seen by individuals or arrays of instruments at fixed locations. Developments in recent years in optical engineering, signal processing, data acquisition, and analysis have already changed and will continue to change the capabilities of instrumentation measuring smaller scales of turbulence. High frequency (10 kHz and above) response instrumentation is currently available for measuring continuous time histories of quantities such as velocity and temperature by hot wires. Laser anemometry and interferometry make individual measurements of particles crossing fringes in the measurement volume in  $1 \mu\text{s}$ . Inadequate or uncontrolled seeding arrival of particles in the measurement volume results in random time between data (TBD). Current limitations in electronic signal processing, data transfer, and analysis reduce the possible (but very difficult) net data acquisition rates from 1 MHz to 1 kHz. Developments are already under way to increase data acquisition and analysis rates by reducing measurement volumes, controlling arrival times of particles and increasing signal-to-noise ratios in signal processing and microprocessors.

Arrays of high-frequency response probes simultaneously measuring histories in real time are already yielding dimensions and shapes of large eddy coherent structures and convection velocities which correspond and agree with data recorded by high-speed cine visualization and frame by frame analysis. The relatively new field of conditional sampling [5] uses ensemble averaging of time histories in which discrete intermittent events, such as passage of a large eddy, are detected, averaged, and analyzed to yield dimensions, shapes, and velocities of discrete fluid dynamic structures. Leading edge and trailing edge contours of eddies have been already determined, and it is already feasible to use 3-D arrays to yield 3-D structural information.

### Statistical Analyses

A professional statistical analysis of sprays would take into account the nature of the spray, its changes in space and time, the specific measurement volumes, and the accuracy of measurement. Samples that are statistically representative of the ensemble need to be designated, and a range of spatial and temporal averaging techniques needs to be employed. In order that the study can be statistically "responsible" much information is required in attempting to relate changes of particle size and velocity in space and time to dependent variable changes. Progressive changes of individual input parameters such as pressures, flow rates, and nozzle geometry need to be separated and assessed for their independent or dependent influence on specific spray characteristics. In much of the published literature on sprays, there has been inadequate control of input parameters so that some conclusions about one-to-one relationships between pressure change and Sauter mean diameter (SMD) gloss over other important parameters of which there is neither knowledge nor control. Sprays are not more complex than many biological, geological, and atmospheric phenomena where sophisticated statistical techniques have yielded important clues and information on phenomena that are not directly measurable.

It is common to use "indiscriminate" time averaging to specify velocity and size without regard to fundamental requirements and specifications of the adequate quantities of data necessary for even elementary statistical analyses. In order that a sample of particle sizes or velocities can be considered statistically significant, information is required on the frequency and nature of expected changes during the sampling period. Events in a specific sampling volume need to be related to the spray as a whole, and statistical relations and correlations between specific sampling volumes and global sprays need to be demonstrated.

Judgments and decisions need to be made about each aspect of the measurement: type of instrument, measurement volumes, periods of measurement, intervals between measurements, and correlations with measurements made by other instruments. It is now generally recognized that SMD provides insufficient information and that size distributions also need to be measured. Counting millions of particles at each measuring point for several hours would yield vast quantities of information which would be accepted as being statistically adequate.

Yet storage and analysis of this quantity of data are neither cost effective nor necessary. The specified time for averaging in turbulent flow varies according to the frequency of variations and must be sufficiently long so that the time averaged quantity would not change if additional time was devoted to further averaging. Investigators normally rely on a "feel" for the frequency variations in fixing times for averaging as they proceed with measurements through a particular flow field. Without a frequency analysis it is difficult to ascertain when the odd event is likely to arrive.

SMD is often chosen as the representative diameter since it represents average surface to volume ratio and should be related to surface dependent phenomena such as heat and mass transfer. But because there is no simple relationship between drop size and heat and mass transfer phenomena, computer modelers and predictors seek information and data on size distribution [5] and probability density functions of all measurable quantities in the flow field. It is common to smooth data and force data to fit Gaussian, normalized, or multi-exponent parametric size distribution functions. Huge quantities of small particles are ignored, and insufficient time is allocated to measure all the large particles. Yet from the point of view of damage and deposition on surfaces or emission of pollutants, the "abnormal" relatively infrequent oversized particle may be of prime importance, requiring detection and possibly elimination.

Discrimination needs to be exercised in averaging. More emphasis needs to be directed towards accurate evaluation of the large-particle-size tail of size distribution curves. Particular efforts must be made in searching for and counting the larger drops. Sizes of measurement volumes and times for averaging could be increased by filtering, that is, focussing attention on drops above a certain threshold size (100  $\mu\text{m}$ ). Separate analyses could be carried out for large and small sizes using the type of differentiation between large (macro) and small (micro) length scales for eddies in turbulent flows.

Examination of high-speed cine films and analyses by laser anemometer-interferometer will yield representative time histories from which the frequency and nature of bursts can be assessed. This information, aside from providing descriptions of the physical nature of the particle and flow fields, can be used as a guide for the determination of the appropriate averages.

### **Size Measurements with More Than One Instrument**

If it were possible to accurately measure particle size in a spray with one instrument, it would be unnecessary to use others. The state of the art of metrology is well advanced so that the measurement of the diameter of a drop, at first thought, would be considered to be relatively trivial. Despite the very considerable cost and time expended over several decades on measurement of drop sizes in sprays, no one technique is considered to be "the best," and no one set of measurements can be considered to be generally reliable or applicable. The problems in measurement are associated with measurement of the spatial and temporal distribution of the spray and not with the measurement of any one

particular drop, the diameter and velocity of which can be measured with relative ease.

The relatively recent attempts at making measurements with more than one instrument have highlighted the particular problems, limitations, and inaccuracies of each of the different experimental techniques. When attempting to make comparative measurements with different instruments it soon becomes apparent that each instrument is based upon a different physical principle for measurement. The measurement volumes vary from "points" ( $1 \text{ mm}^3$ ) within the spray to the spray as a whole. Averaging periods vary from instantaneous (nanoseconds) to long (minutes); averaging may be spatial, temporal, or both. Differences in results can be due to differences in statistical analyses as well as to differences in measuring individual drop sizes.

Accuracy is assessed by direct comparison with a standard. The standard of length is fundamental to metrology and physics—it is well established to an extremely high degree of accuracy. In attempting to measure the size of a drop moving within a spray, the initial problems are associated with identification, tagging, and "freezing" so that the drop to be measured can be compared with a standard. As electronic signal processors, microprocessors, and computers are added to the instrumentation, all these elements need to be "debugged" to assure that inaccuracies are not generated by the processing system. The fact that two instruments give the same result is not necessarily proof that both measurements are correct. Inaccuracies common to both instruments may be recorded. The only way to determine accuracy is by direct comparison with a recognized standard or by comparison with an instrument that has been calibrated against a recognized standard. This again points to the need for a standard spray.

A clear distinction needs to be made between repeatability and accuracy. The fact that the same instrument can repeatedly provide the same results is not an indication of accuracy. It simply means that no change has occurred in the spray, the instrument, or the data recording and analysis system. In a turbulent spray, repeatability should be only attainable for long-time averaged global characteristics such as spray angle, SMD, time averaged size and velocity distributions, and probability density functions. Repeatability can be only expected if the phenomenon is steady and nonvariant with time. In a spray, all conditions vary with time in a random turbulent manner. Quasi-steadiness needs to be proven at each location by demonstrating that the particular phenomenon does not change with time within the specified space and time limitations. Reduction of the measuring time and volume leads to a transition from the quasi-steady to the unsteady state. In the unsteady state special provision must be made to measure variation as a function of time.

One of the major practical problems in making measurements in sprays is the lack of a priori information on the frequency of change within the particular measurement volume. Many turbulent flow systems have been "well characterized" by meticulous and painstaking long-time averaged measurement of local conditions. Measurements of mean velocity distributions have been

repeated by many different investigators in many different jet flows by a number of different instruments, all yielding, in a nondimensionalized form, essentially the same results. The more recent studies of turbulence characteristics using high-frequency response probes such as hot-wire anemometers have revealed the enormous variations occurring as a function of time during the time averaging process of taking measurements. The insights derived from conditional sampling of time varying phenomena are radically different from the picture shown by stream lines, derived from mean velocity measurements, in turbulent flows.

The most effective comparison would be to make measurements with different instruments simultaneously. The size of instruments, differences in measurement volumes, and conflicting invasive requirements makes simultaneous measurements with more than one instrument difficult. If measurements are made consecutively, separate independent monitoring must ensure that conditions within the measurement volume are "identical" (on the average).

### **Previous Attempts at Comparing Instruments**

In the development of all imaging techniques, the standard practice is to traverse a graticule (2-D dots of known size) across the depth of field. For determination of in-out-focus, a threshold light density gradient at the edge of the image is established, and thereby the boundaries of the measurement volume become known. The depth of field varies, increasing progressively, with drop size. If a means could be found for attaching 3-D particles of known size to a transparent slide, it would be preferable to calibrate with 3-D rather than 2-D particles. After calibration by graticule, the imaging system itself becomes a calibration system for other particle size measuring systems.

In the development of holographic, television, and cinematographic techniques, it is standard practice to check out the system as a whole by direct comparison with photography and/or directly with a graticule.

### **Comparison of Different Imaging Techniques**

Since most imaging systems have the light source and transmitting optics on one side of the spray with receiving optics and recording systems on the other side, it is generally not feasible to make simultaneous measurements with different imaging instruments. Measurements must be made sequentially with each instrument. High magnification double pulsed laser photography is the most reliable and accurate method of simultaneously measuring particle sizes and velocities. Repetition rates are dependent on time taken to change photographic film. The spray nozzle needs to be traversed in the axial and radial direction for determination of distributions in space.

Holography has the advantage of freezing a 3-D slice of the spray. The measurement volume is a cylinder with length equal to the total width of the spray at the particular axial station and with diameter equal to that of the laser beam (1 to 10 mm). All particles within the measurement volume at the time of the laser

pulse are recorded instantaneously (20 ns). Subsequent reconstruction of the hologram, by moving in and out of focus, yields planes (fields) of view in locations similar to those that can be measured by photography. A direct comparison between photography and holography would show the differences in recording all drops in the total 3-D measurement volume, as recorded on the hologram, with interrupted 2-D (plane) instantaneous measurements made over a total long (minutes or hours) time period to cover the same 3-D volume captured by the hologram. These measurements are not directly comparable and cannot be expected to yield the same results. Repeated holograms need to be made for time averaging. For both photography and holography, long time averages of drop sizes and velocities, in principle, should be the same, but significant differences may arise due to the differences in measurement and statistical analysis techniques. Such a comparison would be highly informative as to the temporal nature of the spray. Separate analyses of the instantaneous photographs and holograms would yield probability density functions and variance as well as direct visualization of ligaments, drop spacing, coalescence, clustering, voids, and particle and eddy shapes.

Image analysis of film negatives, film positives, and reconstructed holograms is essentially the same. Manual analysis is tedious and costly and requires visual examination of each record. Automatic image analysis by optical viewing of records (Quantimet) has been used successfully [6], but prior visual scanning is still required to eliminate bulk liquid, ligaments, and film grain images which should be treated as background noise. Analog information from optical viewing is converted to digital output for subsequent analysis. Major developments are being made to replace photographic and holographic film recording by direct digital recording on diode arrays. Optical and electronic image analysis is a subject of intense activity in the fields of optical engineering, electronics, and aerospace. Significant improvements in quality, accuracy, overall effectiveness of data recording and analysis systems, and reductions in cost can be expected in the next few years.

Recording by television camera allows immediate and direct automatic analysis of each individual record on the screen. Images are removed from the screen after analysis so that TBD is dependent upon time required to analyze all particles on the screen. Separate filming of the screen provides a record for subsequent analysis. Very significant improvements in times required for recording, analysis, and overall measurement have been achieved by replacing photographic with television recording. Direct digital recording will further enhance these improvements.

The special advantage of cinematography is the rapid recording rate which allows a reconstruction, by viewing, of the dynamic events. By focussing on the nozzle exit, the liquid film, the global spray, or small measurement volumes, the dynamic changes in liquid film formation and breakup, macro-scale changes of spray boundaries, breakup region, and large eddy structures, as well as trajectories of individual drops can be seen, visualized, and analyzed over a range

of space and time frames. Events in the Lagrangian frame of reference are revealed. Specific regions or drops can be preferentially visualized by tagging methods. For example, injection of fluorescent dye into the bulk liquid allows individual drops to be visualized when illuminated by a pulsed laser. This provides information on individual trajectories of drops within the spray. These can be radically different from trajectories of drops in isolation.

With current technology, it is feasible to measure trajectories and the rate of change of diameter of individual drops evaporating in a dense spray. It may even be possible, and certainly well worth striving for, to measure gradients of density (temperature) within boundary layers of drops moving through the spray by coupling interferometry with cinematography. Such information is of vital importance in the formulation of models and testing of computer predictions of spray structure.

Each imaging technique provides different information and has special advantages. A series of consecutive measurements by photography, holography, television, and cinematography on a section of a single "standard" spray would reveal a great deal of useful information on the nature and dynamics of that particular spray. By studying several different types of sprays, more general conclusions could be made about sprays and their common and distinguishing features.

### **Interferometry and Anemometry**

The extension of standard laser anemometry to particle sizing using single particle signal processors allows simultaneous measurement of the size and velocity of individual particles. Recording times ( $1 \mu\text{s}$ ) are dependent on particle velocity (10 m/s), number of fringes (10) and fringe spacing ( $5 \mu\text{m}$ ). If no time was lost in signal processing a digital recording rate of 1 MHz would be possible only if a continuous stream line of individual particles with  $10 \mu\text{m}$  spacings passes through the measurement volume. In practice, arrival times, particle velocities, and particle angles of flight vary over a wide range, almost at random. Controlling the arrival of particles into the measurement volume could be achieved by electric and magnetic fields acting on charged particles, but this would be an unacceptable interference to the spray. Measurements are not permitted when more than one particle is in the measurement volume. Since measurements are validated by an initial measurement across five fringes and a subsequent measurement over ten fringes, as the number density of particles and turbulence increases, the data rejection rate due to nonvalidation can become very large. A prior assessment of number density and turbulence would assist in making decisions on measurement volumes and validation criteria.

A single color anemometer provides only one velocity component. Velocity in the axial direction is usually dominant but, depending on interaction with air streams, radial (in the first instance), and even tangential components may well be significant. Only if the radial and tangential components were measured and

shown to be negligible compared to the axial component can the assumption of a single axial velocity component be valid.

In principle, a laser anemometer system requires no calibration provided that every component is functioning without deviation from the design criteria. In practice, there are many possible sources of error so that separate debugging of the optical, recording, signal processing, and computing components of the system is needed. The overall system must be tested by obtaining agreement between the independently measured speed of rotation of an element on a rotating disk and the computer printout of velocity measured by laser doppler anemometry (LDA). Periodic checking of the system with a rotating disk will ensure that no decay or change occurs in any part of the system.

Particle sizing by interferometry has been tested under a variety of conditions in sprays. Visibility has been demonstrated, both theoretically and experimentally, to be a measure of particle size within restricted and specified conditions. Measurements near maximum visibility (small particle diameters) are prone to error due to insufficient gradient of the visibility curve. Measurements near zero visibility are prone to error due to ambiguities in subsequent cycles of the visibility curve. Measurements are restricted to specific values of the ratio of the particle diameter to fringe spacing ( $<10$ ). A fringe spacing of  $5 \mu\text{m}$  is particularly convenient for velocity measurement but restricts visibility measurements to particles with diameters less than  $50 \mu\text{m}$ . To accommodate larger drops, fringe spacing needs to be increased. This is obtained by reducing the beam crossing angle which leads to increases in the length of the measurement volume. Compromises need to be made to satisfy the separate and different requirements of particle size compared to velocity measurement by the same set of fringes. It has been only recently recognized that fringe contrast and hence visibility are reduced by particles crossing the fringes, a further potential (and clearly unavoidable) source of error.

Direct measurement of peak amplitude or pedestal amplitude can be readily made from the Doppler burst by a signal processor. Signal amplitudes progressively increase with increasing drop diameter. For particles crossing the center of the measurement volume, particle size can be measured by prior calibration using particles of known size attached to rotating disks traversing the center of the measurement volume. There should be no change in background illumination or in the measurement system, between calibration and measurement. Particles crossing fringes near the edges (off the center line) have reduced amplitude due to reduced light intensity within the measurement volume associated with the Gaussian distribution of laser beams. This spatial ambiguity is reduced by off axis collection (effectively reducing the length of the measurement volume) or by clipping the Gaussian wings of laser beams to yield beams or both and hence measurement volumes with more uniform light intensity distributions. In addition to peak amplitudes the shape of the Gaussian signal can be measured by high-frequency digital analysis to yield further information on particle shape, particle location within the measurement volume, and particle diameter. Combining the

information from separate peak amplitudes and amplitude ratios (visibility) yields more information, but further development work is still required before a laser interferometer-anemometer instrument is commercially available for accurate simultaneous measurement of particle size and velocity.

### Laser Diffraction

For a rapid (minutes) analysis of the global characteristics of a spray, the laser diffraction particle sizer is currently one of the more effective, simplest, and reliable instruments that is commercially available. For many industrial applications where the relative fineness or coarseness of a spray is quantified in terms of SMD and exponents in a size distribution equation, the laser diffraction instrument with its associated microprocessor yields computer printouts of the desired information. Learning to use the instrument is relatively easy (3 days) and little knowledge of the fundamental principles of the instrument is required for operation. The laser diffraction instrument, however, does have basic limitations which need to be recognized.

The ring diodes are sensitive to changes in ambient conditions: the presence of fluorescent lights, sunlight, reflected light, or flames are all sensed by the diodes. Particular care must be taken to shield the diodes from background radiation or to at least ensure that no change in background radiation occurs during a set of comparative tests. When making measurements in flames, it may be possible to use additional sensors to monitor radiation from all sources other than the diffracted laser light and then to account for this in the software of the computer program.

The presence of density gradients arising from temperature or concentration gradients within the fluid containing the particles to be measured results in deflection of the laser beam (beam steering). A small deflection of the laser beam is first sensed by the inner ring diode which normally detects the largest (500  $\mu\text{m}$ ) particle sizes. Introduction of the laser diffraction instrument into a field in which there are temperature or gas concentration gradients but no particles present, yields a size distribution. The smaller the beam steering, the larger are the particles that are "measured." It is necessary, therefore, to ensure that no density gradients, sufficient to cause beam deflection onto the inner diodes, are present in the measurement volume. In turbulent flows, random beam steering over a range of frequencies will result in spurious signals detected by the innermost diodes. Since many particle size measurements are made in sprays where evaporation and reaction are the direct cause of density and refractive index changes in the gas field, this is a serious limitation. An independent measure of beam deflection is required to ensure that it is not being detected by the inner ring diode. By providing additional sensors for measuring beam deflection, it may be possible to account for this in the computer software.

In high-density sprays, multiple scattering affects the size measurements. This can be simply tested by progressively increasing the concentration of powder with

a known size distribution in a liquid test cell. As the light obscuration increases above 40%, there is a progressive decrease in the measured SMD. This can be accounted for by introducing correction factors for light obscuration levels between 40 and 80%. Introduction of light guides (tubes or fiber optics) into the spray reduces the field of view and hence the light obscuration, but the guides cause interference to the spray. It can be argued that disturbances from light guides are mainly downstream and that flow fields in the measurement volume are unaffected by the disturbance. The volume between the ends of the light guides may be considered as a jet orifice. No change occurs within the potential core formed by the jet passing through the "orifice." In high-density sprays, introduction of light guides into the spray, which reduces the obscuration, is preferable to making measurements with high obscuration. Reduction in size and aerodynamic streamlining of the light guides minimizes the disturbance to the spray.

A size distribution function must be chosen. The corresponding parameters are calculated by comparing the Fourier transform of the measured forward light scatter distribution with the "chosen" distribution function. For data with normal or Gaussian distributions, two or three parameters are sufficient to describe the distribution. For sprays which have multi-modal distributions or where special attention is focused on the larger sizes, this force fitting of data is inappropriate. Attempting to use the laser diffraction instrument in a monosize spray reveals the limitations of attempting to fit the measured data to a prescribed distribution function. The more recent model of the laser diffraction instrument performs a deconvolution analysis of the measured intensity to extract the spray's size distribution without relying on a specified size distribution function ("model independent").

The laser diffraction detection system has 30 concentric annular diodes. The area of these diodes progressively increases from the inner to the outer ring. The rapid increase in diode area compensates for the rapid decrease in scattered light intensity away from the central detector. The computer averages adjacent detectors so that the 30 detectors operate as 15 pairs. A major redesign of the detection system could lead to substantial increase in accuracy and capability of the instrument. For example, linear and annular arrays of detectors could be used to test for symmetry and focus on larger or smaller particles to provide more details of particular sections of the size distribution, for example, large particle size tail. A control system would activate different sections of the diode array. Separate tests could be made of background illumination and beam steering, and discrimination logic could be introduced to account for these effects.

The measurement volume of the laser diffraction instrument is governed by the laser beam diameter (9 mm) and the width of the spray at the particular axial station of measurement. A line-of-sight average is made of all particles within the laser beam. Spatial resolution is governed by the dimensions of the spray and the number of "passes" that can be made by the laser beam as it is traversed through the spray.

Tomography yields spatial information from line-of-sight measurements by varying the location and crossing angle of the laser beam. Reducing the laser beam diameter to 3 mm, traversing across the spray, and varying the angle of approach yields a series of line-of-sight measurements for a particular axial station. Using the Abel transformation, signal processing, and computational techniques developed in medical X-ray brain and body tomographic scanning, variations in size distribution across the spray can be determined. Testing of the accuracy of the tomographic system can be made by direct comparison with photographic and holographic measurements of size distribution.

## Conclusions

Setting out to make comparative measurements with different instruments has highlighted the fundamental problems of making accurate size and velocity measurements in turbulent polydisperse sprays. The ultimate objective is that data should be independent of the particular instrument used to make the measurements. Then comparative measurements would be redundant.

A very considerable amount of effort and cost has been expended, over several decades, to design, develop, manufacture, and test instruments for particle size measurement. Among the imaging, interferometric, and diffraction instruments cited in this paper, all have limitations that can result in significant errors and inaccuracies. The differences in measurement volumes and statistical averaging procedures between individual instruments excludes direct verification of absolute accuracy. No direct comparison can be made between time-averaged and spatially-averaged data or between single particle and cloud counting systems.

A testing and assessment project has been initiated at Carnegie-Mellon University. A series of simultaneous (where possible) and sequential measurements on sections of standard sprays will be made using pulsed laser photography, holography, cinematography, interferometry (visibility, peak amplitude), and diffraction. Special efforts will be made to control injection and ambient conditions to prevent extraneous pulsations, temperature, and fluid flow changes within the atomizer supply system and the spray chamber. Calibrations using graticules, reticles, fibers, and particles on rotating disks, powders in flowing liquid cells, and monosize sprays will be carried out prior and subsequent to each series of measurements.

Dimensions of measurement volumes, time periods of measurement, and TBD, will be accurately determined and recorded. Spatial and temporal averaging will be performed on raw data taking into account the frequency and nature of variations as recorded by cinematography. Rather than attempting to force "agreement" between data, each set of data will be related to the particular instrument and measurement conditions.

The final "picture" emerging from this set of experiments will reflect the combination (rather than the comparison) of information from all instruments. The composite structure of the spray will be revealed by various combinations of

the information determined by each instrument. Individual instruments will be considered as components of a hybrid instrument. Assessment of the limitations and inaccuracies of current instruments will be made. Recommendations for further development will be made to instrument manufacturers.

### *Acknowledgments*

Contributions to this research are currently being made by grants from DOE (PETC), ARO, AFOSR, and NASA Lewis. A team of engineers, technicians, Ph.D., Masters, and undergraduate students is presently working in the Combustion Laboratory in the Department of Mechanical Engineering at Carnegie-Mellon University on this research. Particular thanks to Patricia Meyer (Ph.D. student) for reviewing and Eunice Hench (secretary) for typing this manuscript.

### **References**

- [1] Chigier, N., *Progress in Energy and Combustion Science*, Vol. 9, 1983, pp. 155-177.
- [2] Chigier, N., *Combustion and Flame*, Vol. 51, 1983, pp. 127-139.
- [3] Weiner, B. B., in *Particle Sizing*, Wiley, New York, 1982.
- [4] Holve, D. J., *Journal of Energy*, American Institute of Aeronautics and Astronautics, Vol. 4, 1980, pp. 176-183.
- [5] Libby, P. A., Chigier, N., and Larue, J. C., *Progress in Energy and Combustion Science*, Vol. 8, 1982, pp. 203-231.
- [6] Yule, A. J., Chigier, N., and Cox, N. W., *Particle Size Analysis*. M. J. Groves, Ed. Heyden Press, London, 1978, pp. 61-73.
- [7] Simmons, H. C. and Harding, C. F., "Some Effects of Using Water as a Test Fluid in Fuel Nozzle Spray Analysis." American Society of Mechanical Engineers, 80-GT-90, 1980, pp. 1-6.
- [8] Azzopardi, B. J., *International Journal of Heat Mass Transactions*, Vol. 22, 1979, pp. 1245-1279.

# Summary

## Summary

---

The following papers present reviews of several different techniques used to determine the drop size of sprays under various conditions and for certain applications. The main drop size measurement techniques that are discussed are; light scattering, resonance light scattering, laser-video imaging, collection of drops on glass plates, and drop interaction with a hot wire. The usefulness of the various techniques is demonstrated by the writers who cite a wide variety of applications in the field of liquid atomization. Also, new developments of various techniques are presented, and improvements over past approaches to measurement of drop size are demonstrated.

The paper by Bachalo presents an overview of drop size measurement problems encountered in the application of measurement techniques to the investigation of agricultural sprays, liquid fuel spray combustion, the atmospheric study of cloud droplets and icing research, and the design of industrial equipment such as spray scrubbers. General requirements for the selection of a drop-size measuring instrument for a particular application are discussed with emphasis being placed on instrument capability in covering a wide drop-size range while providing good resolution and accuracy. The desirability of nonintrusive techniques and systems having automated data acquisition and processing are recommended. Light-scattering and imaging techniques are compared in terms of their relative advantages and disadvantages. The writer concludes that careful selection of a measurement technique must be made on the basis of application requirements in order to obtain drop-size data that can be used to satisfactorily characterize a spray. To do this, nine criteria of instrument capability are listed, and it is emphasized that no single instrument can be expected to meet all of the nine requirements. In the final selection of a technique, the weighing of the cost of the instrument in dollars and the time needed to learn how to obtain and process the data must be also considered. Finally, the writer concludes that "it is normal for manufacturers to expound the capabilities and virtues of their instruments and overlook the limitations."

An improved light-scattering technique is discussed in the paper by Rizk and Lefebvre. The original technique was used to measure Sauter mean diameter,  $D_{32}$ , whereas the improved technique yields not only mean drop diameter data but also drop size distribution data. To accomplish this, the light intensity profile used to measure mean drop size is converted into an energy distribution which is then related to drop-size distribution. Values of  $D_{32}$  show fairly good agreement with those determined by an imaging or photographic technique. Also, the drop-size

distribution calculated from energy distribution was found to agree well with both the particle size distribution of a standard calibration reticle and the drop-size distribution measured with a Malvern light-scattering instrument. Although the authors neglect discussing how they deal with background light when there is no spray in the light path and it is not clear how a light energy distribution curve is obtained from a relative light intensity curve, the authors' improved technique does show a marked improvement in usefulness over that of their original light-scattering technique.

In the paper by Dodge and Cerwin, the modification of a forward light-scattering technique is discussed in terms of extending the applicability of the Malvern instrument to the measurement of drop size of fuel sprays evaporating in high-temperature air with high-thermal gradients and high levels of background light such as that produced by flame radiation. Light distribution from a spray is "corrected" and Sauter mean drop diameter,  $D_{32}$ , is determined from the Rosin-Rammler distribution. Actually, the correction is made by recomputing a light distribution based on the outer 24 channels of the 30 channel detector so that the "corrected" light distribution "follows the shape expected for the scattering from a spray." Errors inherent in such a correction "increase with the number of detector signals which have to be ignored." By means of the modified technique, the usefulness of the Malvern instrument has been substantially extended by the writers to include drop-size measurements of evaporating sprays at distances relatively close to the atomizer with air temperatures and pressures as high as 700 K and 586 kPa. However, farther downstream from the nozzle the technique proved ineffective due to the high concentration of vapor. Also, attempts to apply the technique as a method of discriminating against background radiation produced by the flame did not produce "reasonable data under these conditions."

The survey type of paper written by Ferrenberg covers the state of the art of fuel spray investigations involving rocket combustors, discusses various droplet measurement techniques, and presents droplet sizing interferometry data. The writer emphasizes the importance of measuring gas velocity profiles in combustors in order to determine droplet velocity relative to gas velocity. Also, he points up limitations of previously applied techniques of measuring fuel drop size in rocket combustor studies and discusses the need for collecting temporal drop-size data rather than spatial drop-size data, since the former is more applicable to computer modeling atomization and other rocket combustion processes. An interferometric technique, which yields temporal drop-size data, is discussed, and an improved version employing principals of both signal visibility and peak intensity appears to be quite promising in providing drop-size data for a more dense concentration of droplets.

A review of resonance light scattering as a means of obtaining ultrahigh resolution sizing of 5 to 50- $\mu\text{m}$ -diameter liquid drops is presented by Lettieri and Jenkins. The status of this technique is reviewed from the beginning of the theory of the resonance phenomenon in light scattered from dielectric spheres up to the present. The review also addresses the usefulness of resonance to experimentally

determine the size of evaporating and nonevaporating drops as well as the mean drop size of "growing" aerosol drops. Finally, resonance light scattering from aspherical drops is briefly discussed, since very few theoretical or experimental studies have been made on this subject. Most investigations involving the technique of resonance light scattering have been made with individually levitated liquid drops. However, a reference is cited in which light-scattering resonances were obtained with a narrow size distribution aerosol of "growing" water droplets. The mean drop size was measured as a function of time. This technique appears only to be valid if the percent variation in drop size is quite narrow, that is, between 0.6 and 2.4%.

A description of a laser-video imaging system employing "computer vision algorithms to reduce the effects of shading and to segment candidate drops from each image" is presented by Oberdier. Pulsed-laser illumination of fuel sprays producing droplet images are stored on magnetic video disks and analyzed with an image processor and minicomputer. Various methods of pattern recognition are considered to determine drop size and to reject those outside of the sample volume. The shading of video droplet images due to films on windows and instrument nonuniformities required four image processing steps, that is, restoration, segmentation, feature extraction, and classification of in-focus and out-of-focus drop images. For image restoration, the Log-Sobel edge enhancement method and shading estimation by ensemble averaging appeared attractive. It was found that "the use of ensemble averaging of multiple images to estimate a shading function followed by the normalization of each image by that function works well on the images tested." Finally it is stated that "edge enhancement of log-compressed images using the Sobel operator is promising but needs more testing."

The paper by Popa and Varde presents drop-size distribution data for diesel No. 2 fuel atomized in a chamber at atmospheric pressure with very high fuel pressures. The fuel injection system was specially designed to operate at fuel pressures up to 150 MPa (22 050 psig). When fuel pressure was increased from 50 to 140 MPa, the Sauter mean diameter,  $D_{32}$ , decreased from 26.5 to 17.5  $\mu\text{m}$  with a 0.19 mm orifice-diameter fuel nozzle. Fuel flow rate was 4.5 to 9 g/s. The technique used to obtain drop-size data consisted of collecting fuel drops on glass plates treated with a surface modifier, photographing the collected drops, and measuring them with an image analyzer. Automation in the analysis process gave accurate measurement of a large number of drops including those having a diameter as small as 0.5  $\mu\text{m}$ . A good discussion of this method of measurement is given in the paper, and the drop size data are compared with that obtained for the same test conditions by using direct photography of the spray and also by collecting the drops and freezing them in liquid nitrogen. The results obtained with the three methods showed that values of  $D_{32}$  agreed within  $\pm 5\%$ .

A review of the usefulness of the hot-wire technique in obtaining drop diameter data for sprays is discussed by Mahler and Magnus in terms of advantages, limitations, and applications of the technique in comparison with other tech-

niques. The writers address methods of calibration, factors affecting drop and wire interaction, and calculations of mean drop size, volume concentrations, and flow rates. Calibration is achieved by determining the size of a drop photographed while contacting a constant temperature, 5- $\mu\text{m}$ -diameter platinum hot-wire sensor and then correlating drop diameter with the measured electronic pulse occurring from the droplet and wire interaction. Factors are discussed that introduce errors in spray analysis with the hot-wire technique, such as, aerodynamic effects on small drops, eccentric collision effects for various liquids, and wire temperature distribution effects. The method of analyzing drop-size data obtained with the hot-wire technique is also described. Applications of the technique to in situ drop size measurements of sprays in demister towers and scrubbers and sprays produced by liquid aerosol generators are discussed. Features such as simplicity of design and operation, light weight, and battery operation are given as some of the advantages of the hot-wire technique as compared with other techniques.

In the paper by Simmons, instruments that are commercially available for measuring liquid particle size are discussed from the standpoint of matching user requirements with instrument capabilities and characteristics. The characteristics of imaging or photographic techniques and nonimaging or light-scattering techniques are contrasted and the advantages in some cases of using both techniques is brought by the writer. Commercial instruments are available to cover the entire size range of general interest in spray investigations although some may have a limited range. If drop-size distribution is to be determined, an instrument that is not based on an assumed size distribution is to be preferred, and the choice of a size class interval often requires further investigation. Instruments are available that will give either spatial or temporal size distribution data. The choice usually depends on the type of data required in the study. Drop-size measurement accuracy is generally not clearly stated by instrument manufacturers nor are the users' requirements of accuracy. Calibration checks are more frequently needed than anticipated by instrument designers, and there is generally insufficient data available to predict the useful life of an instrument. Also, cost aspects of equipment usage need to be investigated more thoroughly by both instrument manufacturers and users of the equipment. Finally, the writer emphasizes the current need for better communication between potential users and particle size measurement instrument manufacturers, particularly in terms of the scope and needs inherent in the application of the instrument to liquid spray studies.

The emphasis of Hirleman's review is on particle sizing by optical nonimaging instruments that will measure liquid particle diameters greater than 1  $\mu\text{m}$  and fall within the class of multiparticle analyzers or that of single particle counters (SPC). The theoretical basis, performance characteristics and calibration considerations for the various methods in each class are discussed. Also, the writer addresses the three subjects of laser diffraction ensemble techniques, cross-beam dual-scattering interferometric SPC, and finally single beam SPC based on the measurement of partial light-scattering cross sections of the particles. Various

problems such as multiple scattering effects due to a high number density of particles or due to a varying refractive index produced by evaporation or thermal gradients are discussed and possible corrections are suggested. Calibration standards for optical nonimaging instruments are discussed, that is, polystyrene latex spheres, glass microspheres, photo-mask reticles, droplet generators, and spray nozzles capable of producing a standard polydisperse spray. The writer stresses the need for both size and concentration standards of measurement. He refutes the view that laser diffraction instruments might not require calibration. Finally, it is pointed up that, in attempting to reconcile drop size data obtained with various instruments, the characteristics of each instrument is very important and whether the technique yields spatial or temporal data must be known before making the comparison.

In discussing droplet characteristics determined with conventional and holographic imaging techniques, Thompson points up the satisfaction of actually seeing drop images that are directly recorded and stored by imaging techniques of drop measurement as compared with results obtained with indirect nonimaging methods. Comments are made concerning conventional imaging methods using both one and two-lens systems, with both incoherent and coherent light. The problem of determining the exact image plane and magnification with a single lens imaging technique is pointed up as a cause of size measurement error. The use of the two-lens method removes this error which is inherent in the single lens system. In discussing holographic methods, the writer concentrates on the inline far-field method of producing holograms that contain information on both the cross-sectional geometry of each particle and its position. The major limitation of the far-field holographic method results from the use of transmitted light by which particles are transilluminated. Although the method can not be used with scattered or reflected light, limited success can be achieved with the use of a separate reference beam. Finally, it is suggested that holography "might well provide an input for calibration of other methods."

A review of techniques used to determine the size and velocity of liquid particles in spray analysis studies is presented by Chigier. Pulsed laser photography, holography, TV, and cinematography are discussed as well as laser diffraction, laser anemometry, and interferometry using visibility, peak amplitude, and intensity rationing. Methods of instrument calibration and statistical analysis are examined. Previous comparisons of imaging, interferometric, and diffraction instruments are also reviewed. Those who select a commercially available instrument are warned against over estimating its capability and under estimating the experience, time, and effort required to effectively use it. Also, it is noted that it is difficult to compare the measurement of drop size obtained with different instruments due to the erratic nature of spray formation caused by hydrodynamic and aerodynamic instabilities. Since it is generally not feasible to make simultaneous measurements with different instruments, the writer suggests that a spray generator is needed which will reliably and continually reproduce a polydisperse standard spray drop-size distribution for instrument calibration. Finally the writer

discusses a project to simultaneously, "where possible," and sequentially obtain "measurements of sections of standard sprays . . . using pulsed laser photography, cinematography, interferometry (visibility, peak amplitude), and diffraction." The results will be a combination of information rather than a direct comparison of instruments, and "an assessment of the limitations and inaccuracies of current instruments will be made."

*Robert D. Ingebo*

NASA Lewis Research Center,  
Cleveland, Ohio 44135; symposium  
cochairman and coeditor.

# Index

## A

Aerodynamic force, 8  
 Aerosol, 98  
 Anemometry, 174, 175, 181  
 ASTM Standard E 799-81, 26, 29, 85, 87

## B

Bachalo, W. D., 5

## C

Calibration (*see also* Standard reference materials), 49, 51, 156, 175  
 Cerwin, S. A., 72  
 Chigier, N. A., 169  
 Condensation, 11

## D

Diffraction (*see also* Measurement techniques), 38, 174  
 Dodge, L. G., 72  
 Doppler burst, 91, 182  
 Drag coefficients, 173  
 Droplets  
   Aspherical, 105  
   Evaporating, 102  
   Levitated, 100  
   Nonevaporating, 101  
 Drop size distribution, 23, 26  
   Rosin-Rammler, 26, 68, 77  
   Spatial, 14, 19, 29, 30, 185  
   Temporal, 14, 19, 29, 30, 185

Drop velocity (*see also* LDV), 15, 18  
 DSI (*see also* Measurement techniques), 91, 93  
 Visibility/intensity, 94

## E

Energy distribution, 62

## F

Ferrenberg, A. J., 82  
 Fringe spacing, 47

## G

Gas-phase velocity (*see also* Anemometry), 20  
 Glass beads (*see also* SRM's), 174

## H

Hirleman, E. D., 35  
 Holography (*see also* Measurement techniques), 18

## I

Ice formation, 10, 11  
 Image analysis, 123, 179  
   Electronic, 180  
   Optical, 180  
   Quantimet, 141, 142  
   Restoration, 131  
   Vicom, 129  
 Ingebo, R. D., 91, 194  
 Injectors  
   Coaxial, 84

Diesel fuel, 139  
 Electronic, 140  
 High pressure, 137, 139  
 Propellant, 84  
 Interferometry (*see* Measurement techniques)  
 Intrusive (*see* Sampling techniques)

**J**

Jenkins, W. D., 98

**L**

Latex spheres (*see also* Standard reference materials), 174  
 LDV (*see also* Measurement techniques), 10, 12  
 Lefebvre, A. H., 61  
 Lettieri, T. R., 98  
 Light scattering (*see* Measurement techniques)  
 Light sources, 174  
 Liquid water content, 14, 15

**M**

Magnus, D. E., 153  
 Malvern instrument, 40, 44, 70, 72, 79  
 Mean diameter, 42, 91, 163  
   SMD, 7, 28, 42, 62, 77, 85, 148, 155, 165, 176, 178  
 Measurement techniques, 14, 23, 138, 172  
   Hot wax, 88, 138  
   Hot wire probe, 19, 153  
   Imaging, 13, 17, 23, 30, 85, 11, 179  
     Cinematography, 193  
     Direct photography, 112, 193  
     Holography, 18, 117, 185  
     Laser video, 125  
     Single lens, 112  
     Two lens, 115  
   Impact, 138  
   Interferometry, 16, 47, 91, 93, 174, 181, 192

Laser doppler velocimeter, 23, 47  
 Light scattering, 9, 15, 63  
 Single particle counter, 36, 37, 46, 192  
 Meteorology (*see also* Ice formation), 177

**N**

Nonintrusive (*see* Sampling techniques)  
 Number density, 12, 14, 19, 181

**O**

Oberdier, L. M., 123

**P**

Polarization ratio, 99  
 Popa, D. M., 137

**R**

Rain, 11  
 Reference frame  
   Eulerian, 175  
   Lagrangian, 175  
 Resonant light scattering (*see also* Measurement techniques), 98  
 Rizk, N. K., 61  
 Rosin-Rammler (*see* Drop size distribution)  
 Round robin tests, 170

**S**

Sampling techniques  
   Batch, 35, 36  
   Collection plate, 140  
   Intrusive, 23  
   Nonintrusive, 10, 14, 16, 23  
 Scrubbers, 12  
 Simon, H. C., 22  
 Single particle counter (SPC), 38  
 SMD (*see* Mean diameter)

## Sprays

- Burning, 25, 77
- Diesel, 137, 173
- Evaporating, 74
- Heavy fuel, 9
- Herbicides, 7
- Icing (*see* Ice formation)
- Insecticides, 7
- Liquid fuel, 8
- Molten wax, 23, 138
- Monodisperse, 13, 49, 50, 174
- Natural, 11, 171
- Polydisperse, 49, 51, 173
- Slurry, 8
- Standard reference materials (SRM's),  
13, 171

- Glass beads, 50, 174
- Graticules, 174
- Polystyrene spheres, 50, 52, 174
- Reticules, 50, 69
- Surface modifier, 140

## T

- Thompson, B. J., 111
- Thresholding technique, 141
- Tishkoff, J. M., 1
- Tomography, 185
- Turbulence, 181

## V

- Varda, K. S., 137



ISBN 0-8031-0227-5